CZECH TECHNICAL UNIVERSITY IN PRAGUE
ZIKOVA 4, 166 35 PRAGUE 6, CZECHOSLOVAKIA

INIS-mf--13201

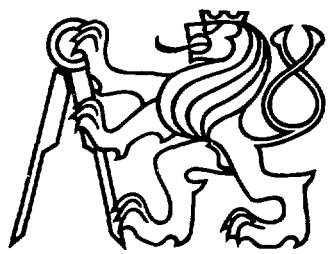

WORKSHOP 92

PRAGUE, JANUARY 20 - 24, 1992

PART B

Physical and Chemical Properties of Materials - Material Engineering - Physics - Physical Electronics and Optics - Communications - Measurements of Physical Quantities - Power Electronics - Architecture and Planning, Regeneration - Environmental Engineering - Power Engineering - Energy Savings

CZECH TECHNICAL UNIVERSITY IN PRAGUE
ZIKOVA 4, 166 35 PRAGUE 6, CZECHOSLOVAKIA

WORKSHOP 92

PRAGUE, JANUARY 20 - 24, 1992

PART B

Physical and Chemical Properties of Materials - Material Engineering - Physics - Physical Electronics and Optics - Communications - Measurements of Physical Quantities - Power Electronics - Architecture and Planning, Regeneration - Environmental Engineering - Power Engineering - Energy Savings

CONTENTS

1. PHYSICAL AND CHEMICAL PROPERTIES OF MATERIALS

2. MATERIAL ENGINEERING

3. PHYSICS

4. PHYSICAL ELECTRONICS AND OPTICS

5. COMMUNICATIONS

6. MEASUREMENT OF PHYSICAL QUANTITIES

7. POWER ELECTROTECHNICS

8. ARCHITECTURE, TOWN PLANNING, REGENERATION

9. ENVIRONMENTAL ENGINEERING

10. POWER ENGINEERING

11. ENERGY SAVING

Section 1

PHYSICAL AND CHEMICAL PROPERTIES OF MATERIALS

HARD MAGNETIC MATERIAL MEASUREMENT SYSTEM

T. Jakl and P. Kašpar

Department of Measurement of CTU, Technická 2, 16627, Praha 6

Key words: magnetic measurement, hard magnetic materials, automatic measurement systems

The development of solid magnetic materials determines the construction of many apparatues, especially electrical rotary machines. Many special devices and tools are necessary for magnetic material measurement (magnetic field intensity measurement device, electric integrator, magnetic yoke, power current source for the yoke ...). Measuring correctly, computing results correctly, determining scales and correcting results demand experience and lengthy ong concentration. The whole measurement and the computing of results could be completed by computer-controlled automatic measurement system and could bring some advantages. Our department has been interested in magnetic measurement since 1945. Many of special devices have been made to order. Cooperation between our department and Electrical Machines Research Institute in Brno has continued since 1985. The computer-controlled automatic magnetic measurement system we developed for the Research Institute is the topic of this paper.

The computer controlled hard magnetic material measurement system consists of a magnetic field intensity measurement device, two magnetic induction measurement devices (integrators), a magnetizing current controller with voltage output,a voltage/current power converter,a two-channel voltmeter with logical outputs and inputs,a computer (16 bit machine) with built-in monochrome display, built-in disk drivers and a built-in real time unit, printer and plotter. The current controller and the voltmeter are controlled via IEEE 488 bus.

Software can be used whit any power voltage/current converter with DC input form -10 Volts to +10 Volts, can be used with a magnetizing yoke or solenoid which are suitable for power voltage/current converter and software parameters or can be simply changed for any converter and any yoke or solenoid. Software is compatible with either a magnetic field intensity probe or field intensity measurement device with integrator. The voltage corresponding to zero value of magnetic field intensity is automatically measured in the second case and is computed into results. The software has a buildin feedback control of magnetic field intensity. There are eight measurement programs with changeable parameters, Hall probe calibration according to integrator, measuring coil calibration according to magnetic field intensity with Hall probe, integrator calibration according to other integrator and integrator calibration according to mutual inductance standard. Values of magnetic field intensity and magnetic flux density which are measured simultaneously by two-channel voltmeter, and the sample number which represents time between starting of measurement and the current sample ("timecode") are saved into the memory. The sample selection is made and only the sample which is different enough from the previous sample is saved into memory. This selection speeds up the consequent computing of results. The software enables the archivation of either only the measurement parameters or both the measurement parameters and the results with short commentary.

The largest and the most complicated is the computing part of the software. The computing part can:

- manually find and display any sample with "timecode",
- find the maximal values of magnetic flux density, magnetic field intensity, magnetic polarization and the minimal ones,
- find compute and the maximal product of magnetic field density and magnetic field intensity,
- manually correct errors resulting from integrator drift and correct similar ones,
- automatically correct offset of results so that the absolute value of the minimal magnetic flux density equals to the value of the maximal one, and manually add any offset to all magnetic flux density samples,
- automatically correct results to prevent influence of difference between measurement coil area and magnetic material area,
- edit resulting graph (axis moving, scale changing, drawing of several parts of final curve, adding comments),
- draw final graph on the plotter,
- make hardcopy on the printer.

The two-channel voltmeter and the consequent computing are precise enough to use the magnetic density measurement device precision and the magnetic field intensity measurement device precision.

This research has been conducted at the Department of Measurement and has not been supported by any grant. We ask for the grant support now,in order to be able to continue our research.

EQUIPMENT FOR PIXE ANALYSIS WITH EXTERNAL BEAM

J.Král, J.Voltr, R.Salomonovič, T.Bačíková

Dept. of Physical Electronics, CTU (Faculty of Nuclear Science and Physical Engineering), V Holešovičkách 2, 180 00 Praha 8

Key words: Ion beam equipment, PIXE, external proton beam

The multi-element analytical method PIXE is based on an energy analysis of characteristic X-rays induced by ion beam bombardment of the analyzed specimen. Bombarding ions are usually protons in the MeV energy range. Using the semiconductor detector and multi-channel analyzer, PIXE offers a quick, simultaneous and practically nondestructive determination of the elements from Na to U in a very small samples (<mg) with a low detection limit (typically of the order of about 10^{-6}). The method is performed usually in a high vacuum. However, PIXE analysis with the use of external beam extracted from the accelerator vacuum to the atmosphere (helium, nitrogen or air; pressure less or equal to 1 atm.) may be preferred in some cases. PIXE with the external beam may be used for the analysis of specimens strongly outgasing particularly during ion bombardment.The gas cooling effect may prevent heat - sensitive samples from damage. The ionization of the gas by ion beam in front of the specimen removes the charge of insulating specimens. Working even without any target chamber, conducting analysis in the laboratory atmosphere, manipulation of the specimen is easier and even bulky specimens may be analyzed /1/,/2/.

During the past decade equipment for analyses with energetic light ions has been constructed and built up in the ion beam laboratory of the Dept. of Physical Electronics, Faculty of Nuclear Science and Physical Engineering, CTU, using the ion beam from the 2.5 MV Van de Graaff accelerator of the Nuclear Center, Charles University /3/,/4/.Recently some modification and improvement of the equipment has been done for external beam PIXE analyses. The task consists of several items: exit window, measurement of the beam charge during analysis, adjustment of the beam on exit, gas system for the target chamber,and a protective system for a fast disconnecting ion beam line from the accelerator. A relevant question is the influence of the exit window and gas on the analyzing ion beam parameters.

The exit window uses a Kapton foil (7.5μm), stuck on aluminum ring, fastened and sealed to the exit insert. The exit insert may be connected and sealed to the vacuum ion beam inlet of the PIXE chamber, as a gate of the ion beam from vacuum to the PIXE chamber. It is easy to install or remove it when the PIXE chamber is open.

For ion beam charge measurement, the spectrometry of protons backscattered on the exit foil is used. A thin aluminum layer is vapor-deposited on the Kapton foil to yield a well-separated peak in the RBS spectrum, detected by an auxiliary surface barrier detector. The area of the aluminum RBS-peak collected simultaneously with the PIXE spectrum is proportional to the corresponding integral charge of the proton beam.In front of the foil there is a removable restricting tantalum aperture to define position and cross section of the ion beam at the foil. The beam position at the exit is adjusted by two perpendicular steerering magnets on the line.

Pressure in the PIXE-chamber should be either the ambient one or lower. To work at lower pressure, gas is admitted through a dosing needle valve with simultaneous pumping of the chamber. In the pressure range of about 10^1 to 10^4 Pa (in air) the automatic gas dosing valve in a feedback with Pirani vacuum gauge is used.

To protect the accelerator in the case of an exit foil rupture a protective system has been constructed. It consists of two fast-closing flaps, spring loaded and starting to close by a signal derived from pressure enhancement near the exit window, measured by the Penning vacuum gauge. One of the flaps is situated near the exit window assembly, the other is at the beginning of the analyzing channel, near the switching magnet of the accelerator.

With pressure low enough in the PIXE chamber it is possible to work even without the exit foil. The acceptable pressure depends on the size of the used apertures.

The exit window assembly might also be connected behind the chamber, instead of the Faraday cup. In such an arrangement it would be possible to have the external beam completely outside the equipment, in the laboratory atmosphere.

Together with the constructional modifications of the equipment the question of energy losses and straggling of ion beam due to the foil and gas has also been followed using both computer simulation and RBS measurements. The data obtained will be used in evaluation of the spectra from PIXE with external beam.

The presented modifications have been designed, constructed and arranged on the equipment. Tests of the modified equipment are being carried out to verify its functions.

References

[1] E.T. Williams: PIXE Analysis with External Beams: Systems and Applications. Nucl.Instrum.Meth.Phys.Res. B3 (1984), 211.

[2] S.A.E. Johansson, J.L. Campbell: PIXE, a Novel Technique for Elemental Analysis. John Wiley & Sons, Chichester 1988.

[3] M. Setvák, Z. Hůlek, J. Voltr, Z. Hába, R. Salomonovič, A. Šíbl and J. Král, Proc. EPM 87, (Akademie, Berlin 1987).

[4] Z. Hůlek, Z. Češpíro, R. Salomonovič, M.Setvák and J. Voltr, Vacuum 41 (1990), 1853.

This research has been conducted at the Department of Physical Electronics, Faculty of Nuclear Science and Physical Engineering as a part of the research project "PIXE Equipment with External Proton Beam" and has been supported by Czech Technical University grant No. 8058.

X-RAYS DIFFRACTION ANALYSIS OF STRESS FIELD

Nikolaj Ganev and Ivo Kraus

Faculty of Nuclear Science and Physical Engineering, Břehová 7, 115 19 Praha 1

Key words: X-rays analysis, Al-alloys

Recently we have been witnessing a growth of interest in the surface qualities of solids. However, this fact isn't surprising, when we realize that any interaction with material is being realized over its free surface. Surface layers can influence in a decisive way the employment of the whole volume of material. Surface layers are primarily important in procedures of brittle and fatique fracture and so on.

Among considerations about the technical application of solids much attention is payed to residual stresses in surface layers effected by mechanical, thermic or thermo-chemical treatment. The most reliable way of measurement of these stresses is a nondestructive X-ray diffraction method.

Until recently in X-ray diffraction measurements of stress in polycristalline materials we held from the conception of a uniform state of stress in the whole volume irradiated by the X-rays. In practice, however, we quite often confronted fields of stresses very much non-uniform, both vertically to the surface and in the surface. The issue of X-rays measurements of non-uniform residual stresses became important only recently. Knowledge of the distribution of residual stresses in surface layers enables one :

- to predict the operational security of products
- to choose a surface material treatment to make a protective stress layer near the surface, preventing the spead of cracks corrosion influence.

X-rays tensometry becomes an effective means in the new system of quality control of industrial production, the principle of this control being that the checking of finished products must be replace by the control of technological procedures.

The aim of our research was to obtain basic information on the distribution of residual stresses resulting from turning, polishing after the turning and shot peening in the surface layers of Al-alloys (CSN 424201). The results obtained are thus a contribution to the complex analyses of how the plastic deformation of the Al-Cu-Mg alloy surface affects its strength characteristics.

Non-destructive X-ray diffraction technique was used to ascertain the lattice strains in Al crystals at selected points of the worked surface of notched test bars. Owing to the large size of crystals the diffraction lines were not continuous. This drawback was eliminated by the Debye-Scherrer method arranged for back-reflection photographic recording, so that during the experiment both the specimen and the cassette could rotate, the reference substance being Ag-powder. The lattice strains were determined by means of TiKα, CrKα and CuKα radiations, which have different effective penetration depths in the investigated alloy.

The results of performed measurements entitle us to make the following conclusions:
- The state of macroscopic residual stresses is non-homogeneous; the stress gradient in turned and in polished samples is of the opposite sign then in the shot peened sample.
- Polishing of the turned samples did not lead to significant changes of residual

macroscopic stresses.
- The shot-peening residual stresses are in all cases exclusively compressive.
- At the same time as the state of of macroscopic residual stresses, the state of microscopic stress in direction from surface to depth is non-homogeneous as well.
- Polishing of turned samples raised the decrease of microscopic stress by about 30%.

References

[1] I.Kraus: X-ray analysis of non-uniform stress fields, Academia, Praha 1990.

[2] N.Ganev and I.Kraus: X-ray study of residual stress depth distribution in Al-alloys, In: "Thirteenth european crystallographic meeting"(Book of abstracts), Trieste 1991.

[3] N.Ganev and I.Kraus: Analysis of residual stress distribution in Al-alloys surface layers, In: "Application of diffraction methods in material science and engineering:(Book of contributions), Herlàny 1991.

This research has been conducted at the Department of Solid State Engineering as a part of the research project "X-ray analysis of non-uniform stress fields".

NEUTRON DIFFRACTION STUDY OF $Pr_{1-x}Sr_xMnO_3$ PEROVSKITES

M.Dlouhá, Z.Jirák**, K.Knížek**,S.Vratislav**

*Faculty of Nuclear Sciences and Physical Engineering, Břehová 7, 115 19 Praha 1,
**Institute of Physics, 162 00 Praha 6

Key words: neutron diffraction, perovskites, crystal structure, magnetic ordering

Structure analysis and magnetic ordering of mixed manganese oxide systems can be very successfully performed by neutron diffraction.

Mixed manganese oxide perovskites with coexisting Mn^{3+} and Mn^{4+} ions have received a great deal of attention both in fundamental and applied solid state chemistry. The most studied systems are the lanthanum based-manganites $La_{1-x}Ax(Mn_{1-x}, Mn_x)O_3(A = Ca^{2+}, Sr^{2+}, Ba^{2+}$ or $Pb^{2+})$ which for $0.25 \leq x \leq 0.5$ are ferromagnets with metallic conductivity and Curie temperature as high as 370 K. Stability of these oxides even above $1000°C$, appreciable electronic conductivity and electrocatalytic properties for the reduction of oxygen make them suitable candidates for cathode materials in the high temperature solid state fuel cells. Similar properties and potential applications are expected for related rare-earth manganites $Pr_{1-x}A_xMnO_3$ and $Nd_{1-x}A_xMnO_3$. The present study deals namely with the $Pr_{1-x}Sr_xMnO_3$ series and has been carried out as complement of our previous investigation of systems $Pr_{1-x}Ca_xMnO_3$ $(0 \leq x \leq 1)$ /1/ and $Pr_{1-x}Ba_xMnO_3$ $(0 \leq x \leq 0.4)$ /2/.

The knowledge of structural details helps to understand magnetism in the mixed manganese oxides. In $Pr_{1-x}Sr_xMnO_3$ each of the four composition regions observed is connected with certain Mn^{3+}, Mn^{4+} valence distribution which need not to be ideally oriented as the structure usually allow for the existence of extra holes or electrons. Both the valence ordering and the presence of extra carriers substantially influence magnetic interactions between magnetic spins. As a consequence diverse magnetic structures are observed at low temperatures. In most cases their occurance can be explained by an interplay of the possible interaction between nearest cations, namely the superexchange and the double exchange. As far as the presently investigated system $Pr_{1-x}Sr_xMnO_3$ is concerned, the size of the doping cation is intermediate between Ca^{2+} and Ba^{2+} ions.

Polycrystalline samples up to strontium content x=0.5 were prepared. The phase analysis and determination of the lattice parameters at room, low and high temperature were caried out on a diffractometer DRON-3. Complete determination of the crystal structure for x=0.1, 0.3 and 0.5 samples was achieved by the powder neutron diffraction (λ=0.1362 nm) on the KSN-2 diffractometer situated at the 15 MW reactor LVR-15 in Řež near Prague. The diffraction patterns recorded were refined using the standard Rietveld analysis procedure. In addition, neutron diffraction patterns at selected low temperatures (down to 5 K) were recorded in order to determine the magnetic properties.

Positional parameters of all atoms, the Debye-Waller temperature factors, distances and angles in MnO_6 octahedra and magnetic moments at helium temperature were determined on the basis of our neutron diffraction experiments. For x=0.1 both in the room and helium temperature the MnO_6 octahedra are tetragonally elongated with longer Mn-O bond in a, b plane. The Mn-O bonds are isometric for x=0.3. In the sample x=0.5

at room temperature the MnO_6 octahedra is deformed (angles $O_I - Mn - O_{II} = 93^o$) with one Mn-O bound shorter. The structure for x=0.5 at helium temperature is monoclinic and was not refined. For x=0.1 the magnetic structure is canted. The satured magnetic values of μ_F and μ_{AF} are equal. μ_F lies on the z-axis and μ_{AF} lies on the y-axis. This implies that the resulting magnetic moment is oriented approximately along the body diagonal direction [011] and [0-11] in alternal layers. For x=0.3 a simple ferromagnetism with magnetic moment in x-axis occurs. Magnetic behaviour of sample x=0.5 is complex. Below T_c=200 K the ferromagnetic ordering occurs and it turns into a complicated antiferromagnetic arrangement below the temperature of the above mentioned phase transition. The antiferromagnetic structure is of type CE with manganese moments oriented along the x-axis. Observed magnetic moments for Mn^{3+} and Mn^{4+} are nearly equal.

Structural and magnetic behaviour of the$Pr_{1-x}Sr_xMnO_3$ series display features of the previously investigated sytems $Pr_{1-x}Ca_xMnO_3$ and $Pr_{1-x}Ba_xMnO_3$. In the whole single phase perovskite range ($0 \leq x \leq 0.5$) the Sr doped samples are of Pbnm symmetry. At the Mn rich side a more pronounced orthorhombic deformation due to the cooperative Jahn-Teller effect occurs. The Pbnm structure in $Pr_{1-x}Sr_xMnO_3$ persists down to low temperature. The sample x=0.3 undergoes at 160 K a transition to a phase with markedly shortened c-axis ($c/\sqrt{2}$:(a+b)/2=0.975). Magnetic ordering in $Pr_{1-x}Sr_xMnO_3$ imitates the behaviour in the Ba series observed change with x from the layer-type antiferromagnetism to pure ferromagnetism. An interesting property of ferromagnetic manganites is the occurrence of metallic conductivity. Like in the Ba series, the $Pr_{1-x}Sr_xMnO_3$ systems exhibit for x=0.3-0.4 a transition from the activated type to the degerate type of conductivity. It occurs at temperatures 20-60 K below the ferromagnetic Curie points. The present study shows that large MnO_6 distortions which might stabilize manganese $d\tau$ orbitals and influence the character of change carriers are not necessary for the occurrence of metallic conductivity in the ferromagnetic manganites.

References

[1] Z.Jirák, S.Krupička, Z.Simša, M.Dlouhá, S.Vratislav: JMMM 53(1985)153-166;

[2] Z.Jirák, S.Vratislav, J.Zajíček: Phys.stat.sol.(a) 52(1979)K39

This research has been conducted at the Department of Solid State Engineering as a part of the research project "Structure and texture analysis by neutron diffraction".

EFFECT OF RADIATION ON THE REACTIVITY OF MIXED OXIDES

M.Pospíšil and M.Martykán

Department of Nuclear Chemistry FJFI,CTU,Břehová 7,115 19 Praha 1

Key words: reduction reactivity, mixed oxides,ionizing radiation

In previous papers /1/,/2/ the effects of genesis and conditions of preparation on the reactivity of various two-component oxide catalysts during their hydrogen reduction have been studied.Different physicochemical properties as well as differences in reduction kinetics were observed with nickel and zinc mixed oxides of various compositions prepared either by thermal decomposition of crystalline nitrates of both metals or by calcination of coprecipitated basic carbonates /3/. With the same system containing an incorporated radionuclide 65Zn, a decrease or, in contrast an increase in the reduction rate was found, depending on the specific activity /4/. The aim of the present work was to investigate the properties and hydrogen reduction reactivity of two analogous systems of mixed inverse genesis and their influencing by preirradiation with gamma rays (328 kGy and 3,7 MGy doses) and accelerated electrons (4 MeV, 500 kGy dose). One series of mixed oxides of various composition was prepared by calcination of precursors containing basic Ni-carbonate and Zn-nitrate /series N/, whereas the precursors of the second series consist of basic Zn- carbonate and Ni-nitrate /series Z/.

From the chemical and thermal analysis follows, that in series N the nickel oxides of variable composition (from $NiO_{1,33}$ to $NiO_{1,5}$) are present, whereas in series Z the stoichiometry of NiO remains unchanged over the whole range of composition. In contrast with series Z, the irradiation of oxides of series N results, in all cases, in a pronounced increase in the amount of super-stoichiometric oxygen, which can be attributed not only to the shift of equilibrium between various forms of sorbed oxygen in favour of the strongly bound ionogenic form, but also to the subsequent chemisorption onto the new centres generated by irradiation. The dissociative chemisorption of molecular oxygen takes place not only on the predominant $Ni^{2+} - Ni^{2+}$centres of NiO, but also on the mixed centres according to: $Ni^{2+} - Zn^{+} + O_2 = Ni^{3+} - Zn^{2+} + O^{2-}$, so that in some composition regions the oxygen chemisorption is enhanced. The different mutual interaction of components in both systems compared is further evident from the magnitude of specific surface areas and their non-additivity, from the dependences of this parameter on composition and from the different changes of the lattice parameter of the cubic NiO with increasing content of ZnO. A higher reactivity of the mixed oxides of series N manifests itself by a high reduction rates in the temperature region 290- 440°C, where only the samples with an excess of NiO in series Z are reduced by a measurable rate. From the comparison of theoretical and experimental weight losses as well as from the X-ray diffraction of reduction products it follows, that partial reduction of ZnO takes place in different composition regions of both series and a new metallic alloy phase is formed. The reduction of nickel oxide is mostly affected by the second component in the region of homogeneous solid solution, i.e. up to 25-30 wt% ZnO. A probable mechanism of the interaction of ZnO with stoichio-metric nickel oxide /series Z/ on the one hand and with the nonstoichiometric one /series N / on

the other hand, determining different dependences of the rate of reduction on composition. was given.

The effect of pre-irradiation on the reduction kinetics of mixed oxides can be expressed by the formula X $V_{max}(\%) = 100 * (V^{+}_{max} - V_{max})/V_{max}$, where V^{+}_{max} is the maximum reduction rate of irradiated samples and V_{max} is the same quantity for the original samples. Pre-irradiation manifests itself by a negative effect in the region of excess NiO in series N, as a result of the increasing concentration of strongly bound ionogenic oxygen.The reduction rate is controlled by the slow donor chemisorption of hydrogen and reduction proceeds slower in comparison with the unirradiated samples.With increasing content of the second component the negative effect of radiation is counteracted by the competing positive effect i.e. by the stabilization of non-equilibrium charge or point defects on the biographic lattice perturbations. The presence of quasi-free electrons increases the reactivity of the interface so that the decomposition processes, including reduction, are thus accelerated and the inversion of radiation effect takes place. References.

[1] M.Pospíšil, J.Topinka: Coll. Czech. Chem. Commun. 51,2098 (1986).

[2] M.Pospíšil: J. Ther. Anal. 29,49 (1991),

[3] M. Pospíšil, J.Cabicar: Coll. Czech. Chem. Commun. 38,2016 (1973).

[4] M.Pospíšil, J.Cabicar: Coll. Czech. Chem. Commun.39,3056 (1974).

This research has been conducted at the Department of Nuclear Chemistry,Faculty of Nuclear Science and Physical Engineering as a part of the research project "Radiation Catalysis".

USE OF NUCLEAR CHEMISTRY METHODS IN STUDY OF HYDROGENATION

R. Kudláček

Department of Nuclear Chemistry FJFI, Břehová 7, Praha 1

Key words: isotope effects, irradiation, catalysis, hydrogenation

Hydrogenation of organic compounds, catalysed by various metals on carrier, which is carried out in liquid phase, proceeds among three phases - gaseous hydrogen, liquid compound or its solution and surface of solid catalyst. In each phase it is possible to make any changes, which are based on the nuclear chemistry methods. Gaseous hydrogen can be replaced and connected with nonradioactive deuterium, the solvent light water is replaced by stable heavy water. The surface the catalyst or its carrier may be modified by ionizing gamma-radiation or electrons.

The replacement of protium by deuterium above all changes the character of catalytic centres, which are created as a result of the interaction between hydrogen and reduced nickel.It was found, that the past reduction for a certain time is necessary for activation of the catalyst by hydrogen (deuterium).

The rate of hydrogenation, proceeding in solution of heavy water, is influenced by changing the dissociation degree of hydrogenated substrate and the sorbed amount of the dissociated form of molecules.

Ionizing radiation can be applied either on the catalytic precursor or on the pure carrier before the preparation of the catalyst. In the first case the experimentally established effect is not greater then the error of measurement.In the second case a very significant increase of the quantity of active centres is observed as a result of the influencing on the irradiated surface. The first stage of preparation of catalyst, i.e. the process of the deposition precipitation is therefore also affected and modified.

The above described effects are studied in our laboratory on the model reaction of the hydrogenation of the maleic acid, soluted in water. The modification of the carrier is also studied and applied on the industrial catalyst employed for the hydrogenation of oils and fatty acids. The interest is concentrated on two kinds of catalyst, partly on the standard technological nickel catalyst supported on the elutriated silica, partly on the newly developed type of nickel-zinc oxide, carried on the same material.

With respect to the fact that these changes are not very great, the measurement of the kinetics of reaction must be performed very carefully. For this purpose it is necessary to develope a suitable method of measurement of the course of reaction or to improve the contemporary one from the point of view of these differences. At present it is also very important to apply the effective method of mathematical calculation of the kinetic parameters. From the testing of many models of kinetics of hydrogen consuming if followed, that the hydrogenation of neutral and alcaline solutions of maleic acid and of oil may be described by a model of reaction of the first order, whereas the hydrogenation of acide solution of maleic acid and fatty acid proceeds as reaction of zero order with desactivation of catalyst proceeding also with a zero order/1/.From the time dependance of consumption of hydrogen can be estimated the selectivity of hydrogenation of oil.

For the measurement of difference between the reaction rate in light and heavy water in the dependence on the pH of solution, it is necessary to change the acidity in the increments, which are smaller then the discrepancy between dissociation of acid in both solvents. This dependence is very different on the nickel catalyst as compared with and nickel-zinc oxide catalyst. The study of this isotope solution effect proved the priority sorption of negative acid ions on zinc oxide microzones. The above-mentioned significant difference leads to five times higher velocity of hydrogenation of fatty acid on catalyst with zinc oxide/2/. In the hydrogenation of oil the priority sorption of organic molecules causes the increase of selectivity/3/. With the change of ratio of nickel and zinc the determination of catalyst for any kind of hydrogenation can be changed. This new type of catalyst has similar propertis as the catalyst of foreign origin/4/, especially for the winterisation and partial hydrogenation.

For studing the first stage of preparation of the mixed catalyst, the method of irradiation of carrier was chosen and the properties of nickel catalyst were compared with the nickel-zinc oxide samples. With the gamma irradiated nickel castalyst the activity increases, whereas in the case of mixed nickel-zinc oxide catalyst the rate of hydrogenation decreases. The irradiation of the carrier of the same samples by acclerated electrons leads to the opposite effects. From this findingit can be concluded that the first stage of preparation of mixed samples must be different in comparison with the nickel catalyst.

References.

[1] Kudláček R., Cmolík J.: Fatt Sc. Tech. in press.

[2] Kudláček R.,Cmolík J.: Pat. applic. PV 2342 - 90, 14.5.1990.

[3] Kudláček R., Cmolík J.:Fatt. Sci. Techn., in press.

[4] Kudláček R.: 29. conference on technology and analysis of fatty, Skalský dvůr 1991.

[5] Kudláček R., Faiereisl P.: Coll. Czech. Chem. Commun. in press.

This research has been conducted at the Department of Nuclear Chemistry, Faculty of Nuclear Science and Physical Engineering as a part of the research project "Radiation Catalysis"

COMPOSITE ION-EXCHANGERS, THEIR DEVELOPMENT AND USE

F.Šebesta, A. Motl, J. John

Faculty of Nuclear Science and Physical Engineering, CTU,
Břehová 7, 115 19 Praha 1

Key words: composite ion-exchangers, radioanalytical application, radioactive wastes treatment, inorganic ion-exchangers.

Inorganic ion-exchangers are sparingly soluble inorganic compounds which are capable of exchanging cations or anions from the solution under contact with the exchanger. When compared with the synthetic organic ion-exchangers they exhibit a broad variety of more advantageous properties, e.g. higher thermal and radiation stability, often good chemical stability even in strongly acid media, quick kinetics of ion-exchange and their high selectivity for the capture of certain ions. Among the disadvantages can be listed namely their unsuitable granulometric and mechanical properties which limit their use in column applications. Various procedures of improving these properties have been proposed in literature one of them being the preparation of composite ion-exchangers.

In our laboratory a method of preparation of composite inorganic-organic ion-exchangers using modified polyacrylonitrile (PAN) as a binding polymer for the inorganic active component has been proposed/1/. The use of a PAN-based organic binding polymer has a number of advantages given by the relatively easy modification of its physico-chemical properties (hydrophylity, porosity, mechanical strength). These properties can be modified by the degree of cross-linking of the polymer, the use of suitable co-polymers or by changing the composition and temperature of the coagulation bath.An active component can be embedded in the resin even as colloidal or very fine particles which enhances the practically achievable capacity considerably. The final product can be shaped as grains, beads, fibres, felt, fabric, membranes, tubing, etc. Any polymer of acrylonitrile produced industrially can be used for the preparation of sorbents, including PAN textile fibre wastes.

The proposed method can be ..pplied on most of the inorganic ion-exchangers known. In our laboratory we have by now synthesized composite ion-exchangers with following active components: ammonium molybdophosphate (AMP-PAN), potassium-nickel hexacyanoferrate (NiFC-PAN), sodium titanate (NaTiO-PAN), manganese dioxide (MnO-PAN), magnesium dioxide (MgO-PAN), barium sulphate activated by calcium (Ba[Ca]SO_4-PAN) and synthetical mordenit or zeolite.

These exchangers were developed and tested for selective separation and concentration of radionuclides from environmental samples and for their removal from the liquid radioactive wastes produced in the operation and decommissioning of nuclear power plants. Their use is not limited only to radiochemical applications - they can be utilized in many other concentrating and separating procedures.

Laboratory test comparing the properties such as kinetics of ion-exchange on such composite ion-exchangers have shown that these properties are not influenced by the presence of the binding polymer/2/. The content of active component in composite exchanger can be varied in a very broad range depending on the application foreseen.

In this way the mechanical and granulometric properties of the prepared ion-exchanger can be modified to fit the respective application.

Lately the above described ion-exchangers have been successfully used in the following applications:

- concentration of radiocaesium from fresh and sea water for the radioanalytical determination of the concentration of 137Cs and 134Cs in these waters.
- for the separation of radiocaesium from neutral and alkaline solutions (where AMP-PAN ion-exchanger is unstable) NiFC-PAN composite ion-exchanger was tested. Among the applications the concentration of radiocaesium from milk and urine is of the highest importance.
- for the concentration of radiocobalt from ground and surface waters MnO-PAN and NaTiO-PAN ion-exchangers have been successfully tested.
- $Ba(Ca)SO_4$-PAN composite ion-exchanger was successfully applied for selective collection of radium from mining waters.
- removal of radiocaesium/3/ and radiostrontium from the water from the long-term storage pool of spent nuclear fuel (LTSP) from NPP A-1 in Jaslovské Bohunice.
- removal of radiocaesium, radiostrontium and radiocobalt from the water from biological shielding from NPP A-1/3/.
- removal of radiocaesium, radiocobalt and radiomanganese from radioactive wastes from NPP Krško, Yugoslavia/4/.
- removal of radium from waste acid underground leaching solutions from uranium mines at Hamr, CSFR.

Based on the experiments described a project for the pilot plant verification of the possibility of lowering the activity of water from the LTSP of NPP A-1 was proposed and accepted by the Federal Committee of the Environment (FVŽP) of CSFR/5/. Last but not least a method for recovery of 137Cs from radioactive wastes for the production of radiation sources was developed/6/.

References:

[1] Šebesta, F.: Exchanger composed from an active component and a binding organic matrix and the way of its production. Czech Patent AO 273369 (PV 4523-88)

[2] Šebesta, F., Štefula, V.: J. Radioanal. Nucl. Chem., Articles, 140, 1990, 15 - 21

[3] Šebesta, F., Motl, A.: Reports from the Economical Agreement between FJFI and VJE Trnava in 1988-1990, Faculty of Nuclear Science and Physical Engineering, CTU, Praha

[4] Šebesta, F., Motl, A.: Testing of composite inorganic-organic ion-exchangers for the treatment of liquid radioactive wastes from NPP Krško, Faculty of Nuclear Science and Physical Engineering, CTU, Praha 1991, 41 pp.

[5] Project of FVŽP CSFR No C1.6.1.01, Praha 1991

[6] Šebesta, F., Motl, A., Pražský, M., Adámek, A., Binka, J.: 137Cs recovery from liquid radioactive wastes. In: Proceedings of abstracts of 12. International Radiochemical Conference, Mariánské Lázně, May 1990, p. 91

This research has been conducted at the Department of Nuclear Chemistry as a part of research contracts for various industrial enterprises and has not been supported by any grant.

DEVELOPMENT OF HIGH CONDUCTIVE POLYMERIC COMPOSITE

V. Bouda, J. Lipták, V. Márová, F. Polena

Faculty of Electrical Eng. CTU, Technická 2, 166 27 Praha 6

Key words: conductive plastics, carbon black, free volume

INTRODUCTION. The conductivity of carbon black (CB) filled composites jumps by as much as ten orders in magnitude at the percolation threshold at about 2.5 Vol% of CB. The problem rises how the dispersed spherical primary particles of CB form the conductive network at such a low concentration. According to Miyasaka [1] CB particles begin to coagulate and form a network when the interfacial excess energy introduced by CB particles into the polymer reaches a universal critical value. Our free volume concept uses an universal critical volume fraction.

A NEW MODEL OF FREE VOLUME DISTRIBUTION IN SOLID STATE. The free volume can be thought of as the difference $v\text{-}v_0$ between the total volume v and the actual volume v_0 occupied by atoms and molecules. The viscosity of ordinary liquids at different temperatures can be related to the free volume fraction f, equal to $(v\text{-}v_0)/v$, by the well-known WLF equation. It applies approximately to most polymers and implies that the free-volume fraction fg for all polymers is approximately the same at the glass transition temperature T_g, 2.5 % [2]. The direct measurements of the free volume as the difference between volumes of amorphous and crystalline states gives the mean value $f_g = 11.3\%$ [2]. Our theory of the transition of the liquid state towards the crystalline or glassy states based on the existence of molecular clusters tries to explain the difference [3,4]. These aggregates of molecules can exist as solids or liquids [4]. A liquid of the total volume V consists of two parts:

$$V = V_{Cl-L} + V_a \tag{1}$$

where V_{Cl-L} is the volume of clusters in the liquid state (melt), V_a is the amorphous rest. When cooling down below the melting point Tm to the temperature of potential crystallization, a new paracrystalline structure of higher density rises inside the clusters and their volume decreases to V_{Cl}. The excess free volume $\delta V_{Cl} = V_{Cl-l} - V_{Cl}$ is expelled outside the sample in the case of crystallization and the total volume of sample decreases. In the case of amorphous materials the excess free volume remains inside the sample in the amorphous rest in a form of stable holes ineffective for the molecular motion. The total volume

$$V = V_{Cl} + \delta V_{Cl} + V_a \tag{2}$$

Because $\delta V_{Cl} = f.V_{Cl}$ and $\delta V_a = f.V_a$,

$$V_a = (V - V_{Cl} - f.V_{Cl}).f \tag{3}$$

Introducing the volume fraction of clusters $k = V_{Cl}/V$,

$$\delta V_a/V = f_{ef} = (1 - k - k.f).f \tag{4}$$

The effective free volume f_{ef} has the thermoactivated character important for molecular movements in the amorphous rest and thus for the mutual movement of the clusters.

Spherical clusters may be taken at the temperature Tm as "dense random packed". According to Bernal's theory [2] their volume fraction k = 0.63. Substituting this k and the above-mentioned free volume f = 0.113 for eq. /4/ we obtain f_{ef} = 3.38%. When cooling down far below the temperature T_m, the thermal contraction of amorphous rest causes the rearrangement of clusters to the denser configuration. We suppose that the glass transition is just the end of the rearrangement of clusters in the moment of their formation in a superlattice. It is known that the triclinic or monoclinic lattices of spheres have their volume fraction k = 0.711. In this case eq. /4/ yields the f_{ef} = 2.36%. This is the new molecular interpretation of the free volume at glass transition derived from the WLF equation.

RESULTS AND DISCUSSION. The activation energy 125 kJ.mol^{-1} of the CB network forming process has been calculated from the conductivity measurements during an isothermal annealing of the composite in the melted state [5]. This value is typical for the thermally activated process of the stress relaxation of polymers. It means that the CB network is created in the thermoactivated part of the free volume f_{ef} situated in the amorphous rest among the clusters which is a perfect continuum favorable for percolation. The accomplishing of the free volume fef filling by the CB particles represents the percolation threshold in this model. Its value lies between 2.36 and 3.38% depending on the processing temperature between the T_g and the T_m. This value corresponds well to the experimentally stated equilibrium percolation thresholds /1/. All these facts mean that *the percolation threshold is an iso-free volume state.* The idea is in harmony with the iso-interfacial energy state in the theory of Miyasaka /1/.

Our experiments show that the cooling rate from the melt influences seriously the CB network. The changes in conductivity (more than five orders of magnitude) can not be related to the changes in crystal size or degree of crystallinity (10-15 %) measured by WAXS and DTA /5/. A possible cause may be the dilatation of the amorphous rest with the CB network during the transition of clusters towards the solid state. This process of elimination is the essence of the new technology.

CONCLUSION. The theory leads to a new technology of high conductive CB composites. The experimental work has been started in cooperation with TU Berlin, firm DEGUSSA, A.G. Hanau and TIU Neratovice.

References:

[1] Miyasaka, K. at al, J. of Material Sci. 17 (1982) 1610-1616

[2] Haward, R. N., The Physics of Glassy Polymers. London 1973

[3] Bouda, V., Polymer Degradation and Stabil. 24 (1989) 319-326

[4] Berry, R. S., Scientific American, August 1990, p. 50-56

[5] Bouda, V., Seminar Polymer Physics, TU Berlin 1991

This research has been conducted at the Department of Mechanics and Materials Science as a part of the research project "Polymers for electronics" No.IV-7-4/04 (3215) and has been supported by the Individual Mobility Grant 1990-91 Tempus No.IMG-CZT-0062-90.

CRYSTALLIZATION OF "TUNABLE" SUBSTRATE OE MATERIALS

J. Venkrbec, Z.Čečil*, V.Rosická**, J.Kohout**, J.Sedláček*, Z.Kodejš***, P.Pacák****

*Fac. Electr. Eng., CTU,16627 Praha 6; **Inst. of Radioelectronics;
**Inst. of Inorganic Chem.-both Prague, Czechoslovak Acad. Sci.

Key words: Optoelectronic Crystals, Crystal Growth - from Solutions, Semiconductor Materials - III-V, Solid Solutions.

In principle it is possible to solve a lattice matching problem in four known ways:

1. modifying a given substrate by a compositional epi-layer grading - high technology is needed, e.g. MBE, MOCVD etc.;
2. modifying an epi-layer composition, possessing 3-, 4-, or even 5 components, which brings inevitably further difficulties;
3. direct growth of bulk substrate crystals with a lattice parameter demanded - TSS (Ternary Solid Solutions) are promising, but to keep a lattice parameter constant throughout the significant part of such a crystal is an uphill battle and, up to now, not successfully solved; though it is highly asked;
4. combining the above-mentioned ways.

This work can partially contribute to the third way by the application of two original and simple theories [1,2]:

- CAM-S (A Crystallization Method Providing Composition Autocontrol in Situ).This method enables the performance of all necessary procedures, i.e. especially: synthesis, a molten-solution zone (MSZ) creation, horizontal zoning with a vibrational stirring (VS) and a consequent crystal growth, all in situ [1].
- COM-S (Calculation Method of Optimal Molten-Solution Composition), which can determine a more stable region for a successful crystallization in some of three-components systems [2]-part 4.1. It is based on Td (thermodynamic) models of phase diagrams (PD).

All the above mentioned have brought about the new way for growing bulk TSS crystalline ingots possessing an a-priori chosen and calculated lattice parameter "a" which is at the same time kept constant throughout the significant part of these grown ingots. Moreover, this implies a "tuning" possibility of main parameters resulting from "a".

This way is based on two approaches:
- The modification of CAM-S by COM-S.
- The acceleration of the whole process by a VS, [1] pg.19.

The last one enables one to receive response much earlier, notably at the MSZ growth (compare $\approx$ 1 mm/day [3] with 2.5 mm/h in this case [4]). VS also facilitates operative corrections in Td (thermodynamic) calculations and in process parameters, which play a remarkable role mainly in an establishing innovative techniques, new materials etc. - It saves time properly, and it can bring even a new insight to growth processes (e.g. the virtual elimination of buoyancy-driven convection etc.).

These approaches are illustrated by particular RESULTSobtained on the last three TSS

($Ga_xIn_{1-x}Sb$) ingots which were grown. Ingots, bearing a mosaic structure and having $x \approx 0.95$, were about 125 mm long, with a cross section of ≈ 0.43 cm^2. The "a" was measured by the Debye - Sherrer method in 6 places along all ingots with a period of about 25 mm, which corresponds to 5 parts. The "a"-values being measured on the first 4 places (corresponding to $\approx$ 75 mm of the ingot length) were taken into the consideration next [4].

The maximal deviation in the "a"-values achieved on these 4 places at the "A" ingot was 0.114% , whereas (after further improvements) the "a"-values stayed really constant (!) on places 1+2 and 3+4 ($\approx$ 25 mm each) at the both ingots "B" and "C". The deviation of "a"-values between pairs of these places, i.e. the difference 2-3 (corresponding to 25 mm), did not exceed 0.033% ! (0.2pm) at either ingot. All samples of these last two ingots were quite homogeneous. Measured data were fully successful in a "Back Scattering Method" too. These results compared e.g.with [3,5] look highly promising.

DTA/DSC measurements were simultaneously fulfilled to correct the data for fitting with the calculated phase diagram.

These facts proven above and supplemented by studies on the melt growth of InSb with the VS - (see [6]) - enable the subsequent CONCLUSIONS:

- The VS being adequately applied (which necessitates a thorough study) could contribute to a relatively fast MS crystallization of TSS. The ultrasonic vibrations with powers e.g. from 30 to 90 W were used in [6], while the energy of low-frequency VS being introduced into the MSZ was less than 10 mJ in these experiments.
- It seems this work has contributed to one of the successful ways of how to grow TSS crystals of some materials, with the a-priori chosen and calculated composition which is kept constant throughout the prevailing part of the whole ingot,from a MSZ homogeneous bulk. Though ingots possess mosaic structure and their characterization was modest only, the remarkable constancy of "a" having been reached is, at least on this type of TSS, the best. (It is caused by Td peculiarities of the modified CAM-S.) Further study and improvements are required [7].

References:

[1] Venkrbec. J., Sci. Rept. Res. Inst. Electr. Commun., B27 (Tohoku Univ., Sendai, 1975) 11-21.

[2] Venkrbec. J., J. Crystal Growth, 48 (1980) 611-20.

[3] Bischopink G. and Benz K.W.,J.Crystal Growth,97 (1989) 245-53.

[4] Venkrbec J. and Sedláček J., A Laboratory Equipment for a Molten-Solution Crystallization of Semiconductors, in Proc. and Coll. Abstr.:"Workshop on Development of Mater. Sci. in Research and Education" (Czechoslovak Assoc. for Crystal Growth, Gabčíkovo, Sept. 1991), 114 - in Czech.

[5] Fuh Shyang Juang and Yun Kuin Su, Prog. Crystal Growth Charact., 20 (1990) 285-312.

[6] Hayakawa Y.and Kumagawa M., Crystal Res. Technol., 20 (1985)3.

[7] Venkrbec,J. et al.,Novel Approaches to Crystal Growth of Bulk Ternary Solid Solutions, J. Crystal Growth, submited.

This research has been conducted at the Dept. of Mech. and Mater. as a part of the research project " Crystallization of Bulk and "Tunable" TTR based on III-V Semiconductors; (Calculation and 3-D State Diagrams Construction on PC, Modelling and Application Incl.) and has been supported by the Dept. from Instit. Sources.

THE INFLUENCE OF DEFORMATION RATE ON RECRYSTALLIZATION KINETICS

P. Zuna and P. Čížek

Faculty of Mechanical Engineering CTU in Prague Technická 4, 166 07 Praha 6

Key words: Dynamic, metadynamic, static, Recrystallization, precipitation, hot deformation, substructure

In the present work recrystallization in model alloys FeNi36, FeNi36NbC and austenitic stainless steel 08Cr18Ni11Ti (17247) after hot deformation is studied. The main aim of the study was to deepen knowledge of the influence of minority phases and high deformation rate on recrystallization processes in the above-mentioned materials.

Deformation by forging was applied with deformations 30 or 50% at temperatures 950 and 1050°C. Two deformation rates $5.10^2 s^{-1}$ and $3.10^3 s^{-1}$ were used. Hot deformation was followed by annealing at deformation temperatures either immediately without intermediate cooling in water or with it. Quantitative metallographic analysis with the use of light and transmission electron microscopy was utilized.

During analysis of obtained results one had to take into consideration that in the case of model alloy FeNi36 no interaction between recrystallization and precipitation occurs and consequently recrystallization is not slowed down by precipitates. In the model alloy FeNi36NbC and also in the steel 17247 on the other hand, interaction between recrystallization and precipitation processes must be accounted.

In these two alloys under hot working conditions with lower deformation rate dynamic recrystallization proceeds slower than in model alloy FeNi36 because of the effect of fine precipitates. Metadynamic and static recrystallization during annealing are slowed down by precipitates too.

If annealing is applied immediately after deformation (without intermediate cooling), metadynamic and static recrystallization develop faster in comparison with the case when samples are quickly cooled after deformation and then reheated to the annealing temperature. It is caused by the fact that in the latter case more precipitates can be formed. If the full recrystallization of this steel (under these conditions) is to occur we have to apply annealing immediately after hot deformation without intermediate cooling.

Application of a higher deformation rate leads to faster development of both dynamic and metadynamic or static softening processes in comparison with the case of lower rate of deformation. Dislocation substructure study confirmed that wider dynamic softening applies in this case and precipitation processes are more intensive as well. The increased intensity of precipitation is accompanied by faster coarsening of precipitation particles therefore fine particles of precipitate slow down softening processes for a shorter time.

The fact that in the investigated range of deformation rates intensity of dynamic recrystallization increases with increasing deformation rate seems not to correspond to data presented in literature. But this disagreement is only apparent. The fact mentioned above can be explained by the occurrence of considerable adiabatic heating during the application of high deformation rates. The influence of adiabatic temperature rise predominates that of deformation rate increase and more intensive dynamic

recrystallization occurs. With high deformation rate are closely connected changes in dislocation substructure too.

Many available literature data suppose that some limit value of Zener-Hollomon parameter exists. Below this value dynamic recrystallization develops and above it the only softening mechanism is dynamic recovery.

In our study, in spite of the very high value of Zener-Hollomon parameter used, intensive dynamic recrystallization occurs. That is why we came to the conclusion that under hot deformation conditions with deformation rates in the range of $10^2.10^3 s^{-1}$ the criterion of a limit Zener-Hollomon parameter value mentioned in literature cannot be used.

Alloy:	FeNi36	FeNi36NbC	17247
C	0,004	0,070	0,075
Mn	0,18	-	1,4
Si	0,16	-	0,62
P	0,005	0,005	0,02
S	0,005	0,005	0,006
Cr	0,020	-	17,8
Ni	36,6	37,0	11,1
Mo	0,1	-	0,034
Ti	-	-	0,30
Nb	0,007	0,11	-
Cu	-	-	0,15

Tab 1. Chemical Constitution of Studied Alloys

This research has been conducted at the Department of Materials Science, Faculty of Mechanical Engineering CTU in Prague.

MICROMECHANICS

P. Neužil, V. Jurka and S. Charvát*

TESLA-VÚST, Microel. div., Novodvorská 994, 142 21 Praha 4 *FEE, CTU, dep. of Microelectronics (ext. postgrd. student)

Key words : micromechanics, pressure meter, tensometric membrane, micromotor, electrostatic motor.

In our work we concentrated into two topics - micro pressure meters and micromotors. Both devices were fabricated by applying of micromachining.

The first one - micro pressure meter (in fact there were a family of similar sensors - accelerometers, slopemeters, meters of vibrations) was based on a piezoresistive phenomenon of boron doped silicon. There were four resistors connected into the Wheaston bridge. Three of them were on the solid support and the fourth one was at the movable part of sensor - silicon membrane. Material of piezoresistors was polycrystaline silicon (poly-Si). The main feature was that it had been a planar type of sensor formed by single-side processing so the sensor did not need any special support. and the membrane diameter was 100 m. The second advantage was about 13.000 such sensors at one 3" wafer.

The process flow was as follows: The silicon wafer was covered by LPCVD silicon nitride (which protected silicon against the oxidation), wafer was patterned and windows in nitride were opened - here would be membranes. Silicon dioxide was grown in these areas in wet oxidation ambient. Oxide was etched off by BOE (Buffered Oxide Etchant) and next oxide was grown. Oxide thickness was computed by SUPREME II so we obtained the planar structure (except the "birds beaks"). The second oxide acted as a sacrificial layer. Now silicon nitride were removed and polycrystaline silicon was deposited with thickness of 1 m. Ion implantation of phosphorus was used for defining the base conductivity of poly-Si. This layer was patterned and the etch holes were opened to remove the sacrificial layer (fig. 1). Piezoresistors were defined by high dose implantation of boron. This high dose was needed for lowering of temperature dependence of the piezoresistance coefficient [1]. Now the polycrystaline silicon was underetched by BOE (approximately 8 hours) through the etching holes, the sacrificial layer was removed and silicon membrane was created (fig. 2). For filling of these holes, wafer was covered with 0.5 μm of PECVD silicon nitride. As the work pressure during PECVD deposition was 0.3 torr and entrances to the cavity under silicon membrane was shut in that time, the residual pressure within the cavity is lower than 0.3 torr. In comparison with normal pressure, we can assumed, that the inner pressure is zero, so this pressure meter is an absolute one. After silicon nitride covering the wafer the contact holes were opened, aluminium was sputtered, etched and sintered.

The second one - electrostatic motor. It was fabricated again from poly-Si. The main idea of the process flow were similar to the previous one. The rotor diameter was 120 μm and its thickness was 2 μm. The distance between movable and static parts was 3 μm.

These devices, current trends of their development and the other sensors (e.g. ISFETs) will be presented at the workshop.

Reference:

[1] Y. Kanda: A Graphical Representation of the Piezoresistance Coefficients in Silicon, IEEE Trans. of El. Devices, Vol. ED-29, No. 1, 1982.

This research project in micromechanics has been supported by TESLA - VÚST.

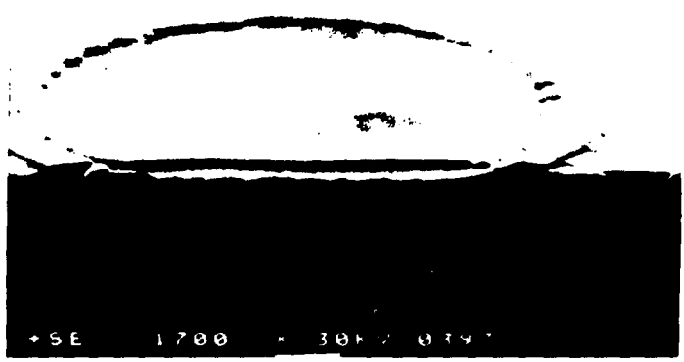

Section 2

MATERIAL ENGINEERING

STRUCTURE AND FAILURE MECHANISM OF POLYAMIDE COMPOSITE

V.Zilvar, J.Steidl and Z.Kořínek

Faculty of Mechanical Engineering, Karlovo n. 13, 12135 Praha

Key words : Polyamide 6, glass fibres, microstructure, annealing, water absorption and desorption, strength, ductility

Mechanical properties, failure mechanism and fractografic features of polymer composites are strongly influenced by microstucture, e.g. crystallinity, the crystal perfection, the fibre length, the orientation, the volume fraction, the fibre matrix interface, the testing conditions, namely temperature, enviroment and the type of loading. The objective of our paper is to show possible effects of matrix supermolecular structure /1/, annealing /2/ and water absorption-desorption process /3/ on the mechanical properties and failure of short glass fibre composites with polyamide 6 matrix.

The toughness of polyamide 6 (PA-6) can be increased by a slight crosslinking or branching of the molecules while partly suppressing crystallization, and also by modification with rubbers. The high ductility of the polyamide matrix has no favourable effect on their resistance to the growth of sharp cracks unless a satisfactory interfacial adhesion is also secured. With PA-6 not modified by rubber, the matrix ductility contributes little to the ductility of the composite below T_g. At temperature above T_g the fibres are stripped easily due to a loss of adhesion in the microregions where the matrix contracts because of its great plasticity. The pull-out energy is low. Rubber-modified composite retains a high adhesion strength even above T_g and preferential shearing destruction of the matrix occurs without a full detachment of the fibres.

The tensile strength of PA-6 composite reaches its maximum at annealing temperatures between 145° and 200°C. On the other hand, the notched impact energy decreases with increasing annealing temperature. The principal effects of annealing on the mechanical behaviour of composite are consistent with changes in the supermolecular structure of a matrix material as revealed by X-ray scattering and DSC. For example, the polyamide matrix material undergoes the most intensive crystal lattice transformation at annealing temperatures, at which mechanical properties of both a composite and the matrix material change substantially. A strong perfection of the semicrystalline matrix material has been observed in the annealling range of 110-145°C. The greatest changes in mechanical properties of a composite correspond to the annealing temperature range where an intensive perfection of the matrix material occurs. A higher degree of the matrix perfection results in a higher brittleness of the matrix but also in a probably stronger matrix-fibre adhesion in a composite. The fracture mechanism of a composite annealed at lower temperatures is different from that annealed at higher temperatures (from about 110° to 200°C)as identified by SEM.

An investigation of irreversible changes in PA-6 glass fibre composites caused by water absorption-desorption process has been initiated by the fact that polyamide composites can be subjected to extremes in hygrothermal conditions during long-term applications.

Two commercially available PA-6 composites with 30% of glass fibres have been used in our experiments in order to show the influence of the PA-6 matrix type on the

absorption-desorption process. The differences in molecular and supermolecular structures and content of low molecular weight admixtures result in substantialy different mechanical behaviour of both matrices. Prior to the structural and mechanical testing, the specimens were subjected to the water absorption at various periods of time at 20°C. The time dependency of water desorption was measured at 20°C and at 30% of relative humidity and/or by drying at 80°C. The water effect on composites was compared with the behaviour of the neat PA-6 matrix of the same hygrothermal history.

The effect of water absorption-desorption process on fibre-matrix adhesion and the fracture morphology of matrix has been studied by the scanning electron microscope on fracture surfaces after notched impact tests. The structural interpretation is based on differential scanning calorimetry and X-ray diffraction measurements. Water treatment leads to changes in crystallinity and crystal perfection in dependency on the PA-6 matrix type used in a composite. These irreversible changes in the matrix supermolecular structure influence the fibre-matrix interaction. It is supposed that T_g reduction that progresses with increasing amount of absorbed water is of primary importance for the additional improvement of the matrix supermolecular structure. It results in microvolume changes and consequently in a loss of fibre-matrix adhesion after water desorption. The loss of fibre-matrix adhesion is apparently more pronounced in a composite with higher water extractable portion. Therefore, we conclude that the amount of water "extractables" strongly contributes to the loss of fibre-matrix adhesion after water desorption and to unfavourable changes of some mechanical properties. Fibre orientation and fibre-matrix adhesion are shown to be important for the different longitudinal and transversal dimensional changes of specimens caused by absorption-desorption process.

References

[1] V.Zilvar,Z.Kořínek and J.Steidl: Microstructure and Impact Behaviour of Injection Moulded Glass Fibre reinforced Polyamide 6.In: Durability of Polymer Based Composites Systems. A.H. Cardon and G.Verchery /Eds./.Elsevier, London 1991 , p.218.

[2] J.Steidl, Z. Kořínek and V. Zilvar : Effect of Annealing on Mechanical Behaviour of Short Fibre Composites With Semicrystalline Polymer Matrix.In : Composites.S.W. Tsai and G.S.Springer /Eds./.SAMPE, Covina, U.S.A.,1991,p. 12 I.

[3] J.Steidl, V.Zilvar and Z.Kořínek :Water Absorption and Desorption Effect on Polyamide 6 Composites. In : Microphenomena in Advanced Composites. G.Marom and M.D.Wagner /Eds./ Israel, 1992 (in preparation).

This research has been conducted at the Faculty of Mechanical Engineering as a part of the research project "Mechanics of Polymer Composites" and has been supported by CTU grant No. 8009.æ

EXPERIMENTAL AND NUMERICAL INVESTIGATION OF POLYMER COMPOSITES

M. Černý

Klokner Institute, CTU, Šolínova 7,166 08 Praha 6

Key words: composites, experiments, numerical analysis

Experiments

Long-term behaviour of composite materials plays an important role in the analysis of composite structures. An experimental investigation of such phenomena cannot be carried out without difficulties connected with the load application process, measuring displacements and forces. The most important long-term experiments are creep and relaxation tests, where constant loads or strains, respectively, are applied at the origin of time and response of composite material is measured according to relations

$$\sigma = \sigma_0 \,.\, h(t) \quad \epsilon = \epsilon_0 \,.\, h(t)$$

where h(t) denotes the Heaviside function.

Creep tests of polypropylene Mosten have been carried out on the special equipment of Klokner Institute. The samples of polypropylene have been loaded by the instant load during 2 min interval. Loading time was about 2000 hours for each sample. Displacements resp. strains have been measured during the entire whole time interval. Stress level was 15 MPa.

Relaxation tests of polypropylene Mosten have been carried out on the testing machine with constant rate of strain. At the origin of loading process the maximum load 2000 N has been reached with the rate of 20 mm.min^{-1}. Forces have been measured during the time interval. Some results of the experiments are included in following table.

creep test* [strains (10^{-2})]			**relaxation test** [forces (N)]		
time (h)	sample 1	sample 2	time (h)	sample 1	sample 2
0	0	0	0	2000	2000
0.25	0.55	0.5	0.33	1760	1760
1	0.95	0.85	0.66	1700	1700
48	2.14	1.76	1	1640	1640
312	3.16	3.04	5	1450	1450
480	3.43	3.44	10	1290	1260
720	3.82	3.84	24	1140	1090
1896	4.37	4.37	100	1010	1010

* the difference between total and elastic part of strain has been measured

Numerical analysis

A numerical analysis of composite structures can be effected by introducing of layers with oriented characteristics. For complete analysis the finite element method is advantegous. The bending part of shell element stiffness matrix can be found from the Mindlin theory. Problems occur in derivation of higher-order elements as the number of nodes increases. For triangular element with three nodes in the corners only linear approximation can be used. Consider the linear approximation of rotations of the Mindlin

normal Φ about the axis and quadratic approximation of displacements. It can be included in the relationship

$$\Phi_x = \sum L_i \Phi_{xi} \ , \ \Phi_y = \sum L_i \Phi_{yi} \ , \ w = \sum N_i . w_i$$

where L_i denotes the linear approximation functions and N_i quadratic approximation functions. To eliminate node on the boundary where the function of displacements is defined, we get from the analogy with beam deflection in the mid-node of the side i-j :

$$w_k = (1/2)(w_i + w_j) + (1/8) l_{ij} (\Phi_{sj} - \Phi_{si})$$

where Φ_s denotes rotation of the Mindlin normal and l_{ij} the length of the side i-j. The rotation Φ_{sj} can be transformed into directions x and y according to relation

$$\Phi_{sj} = -\Phi_{xj} . \cos\tau + \Phi_{yj} . \sin\tau$$

where τ denotes the angle between directions s and x. Therefore

$$w_k = (1/2)(w_i + w_j) + (1/8) y_{ij} (\Phi_{xj} - \Phi_{xi}) + x_{ij} (\Phi_{yj} - \Phi_{yi})$$

matrix $[B_s]$ can be obtained from the relationship

$$\{\tau\} = \begin{vmatrix} \Phi_y & + & \frac{\delta w}{\delta x} \\ -\Phi_y & + & \frac{\delta w}{\delta y} \end{vmatrix}$$

Stiffness matrix of the element can be evaluated from the equation

$$[K] = \int_A [B_b]^T [D_b] [B_b] \, dx \, dy + \int_{k_A} [B_s]^T [D_s] [B_s] \, dx \, dy$$

where k denotes the shear correction factor and matrix $[B_b]$ can be found from linear relation curvatures displacements in an usual way. Explicit form of matrix $[B_s]$ is of following form

$$[B_b] = \begin{vmatrix} 0 & 0 & L_{1x} & 0 & L_{2x} & 0 & 0 & L_{3x} \\ 0 & -L_{1y} & 0 & 0 & 0 & 0 & -L_{3y} & 0 \\ 0 & -L_{1x} & L_{1y} & 0 & -L_{2y} & 0 & -L_{3x} & -L_{3y} \end{vmatrix}$$

Relationship concerning the stiffness matrix can be transformed into triangular coordinate system p - r

$$[K] = 2A \int_0^1 \int_0^{1-r} [B_b]^T [D_b] [B_b] \, dp \, dr + 2A_0 k \int_0^1 \int_0^{1-r} [B_s]^T [D_s] [B_s] \, dp \, dr$$

Stiffness matrix [K] can be evaluated by the Gauss integration scheme in 3 points.

References:

[1] Černý M.:A Numerical Analysis of Composite Vessels in: Composite Structures, ed.C.Bord, Paris 1988,

[2] Černý M.: Composite Shells for TV Tower Prague, AIPC Symposium "Mixed Structures including New Materials ",Proceedings, Brussels 1990

This research has been conducted at the Klokner Institute as a part of the research project "Mechanics of polymer composites" and has been supported by CTU grant No. 8009

ACRYLATE DISPERSIONS AND REPAIRS OF CONCRETE

V.Pumpr

Klokner Institute, CTU, Šolínova 7, 166 08 Praha 6

Key words: repair of concrete, acrylate dispersion, polymercement compositions

The repairs of concrete and reinforced concrete constructions constitute an up-to-date problem of the building industry in all advanced countries where reinforced concrete became a prevailing construction material after the Second World War .

If we confine the term "repair" to the complementing of missing or removed lots of concrete by new material, then we can define the repair as the coating of the pretreated surface of the old concrete with the repair material.The purpose of the repair may be to renew or to increase the load-carrying capacity of the construction (i.e. the constructional repair) or to prevent the corrosion of the reinforcement or to restore the desirable esthetic appearance of the construction (i.e. the cosmetic repair).

Generally it can be said that the ultimate requirement is that the repair material which must prove to be (from a long-term point of view) an appropriate bond with the original concrete. A long-term bond depends on a number of properties of the repair material as well as on the concrete repaired. Plum /1/ institutes for the quantification of the cooperation of the repair material the term "repair function" which has the following form for the esthetic repairs :

$$\epsilon = k_3 p_b (1 + \phi r)/E_r \qquad (1)$$

where ϵ- thermal or moisture expansion of the repair material, k_3- coefficient given by the size of the damaged spot (place),p_b- adhesion of the repair material to the undercoat material, ϕr - coefficient of creep, E_r- modulus of elasticity.

The relation (1) can be interpreted as the maximum tolerable degree of expansion which can be proved by a given repair material with a certain value of adhesion to the coatground. The relation of the tolerable expansion to the expectable expansion (the failure factor τ) expresses according to Plum for the given atmospheric and temperature conditions the efficiency or effectiveness of the repair. Generally it is desirable that this factor be greater than 2. Values smaller than 1 signal that, in the conditions given, the repair is very likely to fail.

In Czechoslovakia, in recent years cement mortars modified with the domestic acrylate dispersions of the trademark SOKRAT have been widely used for repairs of reinforced concrete and concrete constructions. The information and experience with their use published up to now show their good applicability, but the procurable results are usually limited to the rigidity parametres of the materials, the adhesion to the coatground was sporadically tested in situ. There is practically no information available on the influence of the domestic dispersions on the volume behaviour of the polymercement compositions which could help to evaluate the suitability of these repair materials in the sense of the above listed criteria.

Therefore, the work carried out in the Klokner Institute of the Czech Technical University in Prague was in the first phase directed to verify the influence of the addition

of the domestic styren-acrylate dispersion SOKRAT 2804 on some properties of the model polymercement compositions. Definitely it was the matter of determination of compression strength during bending after 3 and 28 days on beams 4x4x16 cm according to the Czechoslovak standard ČSN 72 2117, additionary, the shrinkage (expansion) during the hardening was measured and also the expansibility due to temperature and moisture was determined on matured bodies. On top of that, the influence of the addition of acrylate on the beginning and the completion of setting and on the standard density of cement paste according to ČSN 72 2115 was determined. For the tests, the model fine-grained mixtures with a content of dispersion 0; 2,5; 5,7; 10 and 12,5 % related to the weight of cement was used.

The results obtained show that the addition of the dispersion had a considerable liquefying effect accompanied, of course, by retardation of setting and undesirable frithing up of mortars. Mechanical strength in the case of identical curing of mortars was influenced negatively; only in the case of moist curing was it ascertained that an increase of tensile strength during bending took place, namely in the case of dispersion contents 12,5% by about 37%.

The influence on volume behaviour during setting and hardening is negligible, the coefficient of thermal expansivity is substantially unaffected and values found are in the range of tabulary given values $12.10^{-6}(K^{-1})/2/$. Volume changes during changes of moisture are increased to a certain extent by the addition of dispersion.

This information shows that if during further stages of the experimental work the favorable influence of the SOKRAT 2804 dispersion on the adhesion of modified mortars or, as the case may be, on further properties, will be confirmed, polymercement mortars on the base of this domestic styrenacrylate dispersion can have good prospects in the field of repairs of reinforced concrete and concrete constructions, especially of cosmetic character, where their economic, technological and hygienic advantages, as compared to polymerconcretes, can assert themselves significantly.

References:

[1] The Structural Engineer,68,1990,No.17.,pp.337-345,

[2] Hořejší J.,Šafka J.: Statické tabulky (Static tables), SNTL Praha 1987, p. 180.

This research has been conducted at the Klokner Institute as a part of the research project " Diagnostics and improving of the serviceability of engineering structures" and has been supported by CTU grant No. 8060.

EFFECT OF DISCONTINUITIES IN NON-HOMOGENEOUS MATERIALS

V. Weiss

Faculty of Civil Engineering, CTU, Thákurova 7, 166 29 Praha 6

Key words: Concrete, discontinuitiy, filling, stiffness, strength.

Investigating the mechanical behaviour of non-homogeneous materials, the contained hollow discontinuities induce (particularly at structure cracks tips) even at low load levels high stress and strain concentrations and, simultaneously, present internal shifts. Thus a very compliant system is formed where a great portion of deformations of the body proceeds, whereas other parts of the body behave like rather stiff regions and their contribution to average deformation of the body is relatively low.

This mechanism for concrete was clearly demonstrated by DANTU using reflexive photoelasticimetry under compression, and by the author, under bending, when a dense array of shifts inclined approximately at +45° to the direction of the main tension stress on the tension face was observed far before structure cracks appeared.

If discontinuities in a non-homogeneous material are filled by a solid substance and sufficient cooperation is assured with the basic material then resulting properties of the material can be estimated using mixture laws. A great change occurs when the substance stuffing the discontinuities has approximately the same stiffness as the basic material or one of its phases. Then stress and strain concentrations as well as shifts are completely or at least substantially excluded and further development of discontinuities is blocked, so the mobility of overstressed regions is strongly limited, the material behaves under loading almost linearly and its resulting stiffness Er is dramatically increased according to the formula

$$E_r = E_0(1 + \sum_i A_i k_i p_i) \qquad (1)$$

where E_0- denotes the initial stiffness of the original material without fillings, i- determination of the type of structural discontinuities, A- constant depending on material properties, size and configuration of discontinuities, k- the stress concentration factor at structural discontinuities, p- the volume content of structure discontinuities. Subsequently, a corresponding marked gain in strength is to be noted.

The described improvement of both basic mechanical properties was revealed by experiments. The tested cement concrete with a natural humidity had the Young modulus 20,5 GPa at room temperature and 25,5 GPa at -196°C, due to freezing of the water in fine pores. Otherwise, the Young's modulus for the fully wet state, when all hollow discontinuities including great structure cracks were completely soaked by water, reached at -196°C the value of 47,6 GPa (!) whereas its increase at frequent negative temperatures did not exceed 30% [1]. This surprising result consists of the behaviour of ice which Young's modulus is about 3 GPa at frequent negative temperatures but rapidly increases at cryogenic temperatures to 10,8 GPa. This value is in the range of Young's modulus of cement stone (10 to 15 GPa) which forms one of the solid phases in concrete. Calculating the possible effect according to the principle of simple superposition, the Young's modulus

of the fully saturated concrete here should reach 127 % of the basic value of 20,5 GPa. The real value of 232 % of the mentioned basic value clearly testifies the homogenization of concrete due to filling of structure cracks and other greater voids by a substance of approximately the same stiffness as the cement stone in concrete . The stress-strain diagram of this fully wet concrete at -196°C was almost linear up to the highest loads and the ultimate stress exceeded 250 % of the basic cube strength at room temperature.

Another proof of the described phenomenon was made by R. BAREŠ on polymer concretes of following compositions:

A - 150 parts of sand and 16 parts of furane resin

B - 150 parts of sand and 24 parts of resin

C - like sub A but subsequently impregnated by 8 parts resin to fill the inherent structure cracks by the same matrix.

The strength of the quite dense material B was 126 - 132 % compared to that one of the porous material A but, regarding the healed material C, its strength increased up to the values of 205 - 220 %. The corresponding Young's moduli B vs. A and C vs. A reached the values of 115 % or 148 %, respectively.

The behaviour of polymer-impregnated cement concretes can form the third proof of this discovery. The impregnation of structure cracks and other voids by organic monomers, e.g. by MMA, leads to a full straightening of the stress-strain diagram and to the enhancement of the Young's modulus up to 170 - 200 % and of the strength up to several times higher values. Young's modules of PMMA in bulk is only 2 - 4 GPa but, according to L. CZARNECKI, it is several times higher at interfaces, i.e. in very narrow structure cracks completely, due to the more perfect orientation of the molecular structure. Thus, it is comparable here with that one of the cement stone, similarly like in the first example described above.

More detailed data about the experimental work are published elsewhere /2/.

An application for a discovery presenting the described effect was recently delivered to our Federal Office for Inventions /3/.

The formulated principles enable one to look for new ways of how to improve mechanical properties of further non-homogenous materials.

References:

[1] VOVES, B.: Influence of very low temperatures on materials for prestressed concrete (in Czech). Stavebnícky časopis, 1986, 34, pp. 837-849.

[2] WEISS, V.: Effect of discontinuities in the structure on stiffness and strength of non-homogenous materials. In: BMC-3, Elsevier, London et New York 1991 (pp.481-7).

[3] WEISS, V., VOVES, B. and BAREŠ, R.A., Stiffness and strength of non-homogenous material with filling of structure discontinuities (in Czech). Discovery Application No. 49-90, Office for Discoveries and Inventions, Praha, December 1990.

The research has been performed at the Departement of Concrete Structures and Bridges as a part of the research project "Concretes with macromolecular components" and supported by the Faculty of Civil Engineering, CTU grant No. 1116 .

PHYSICAL AND MECHANICAL PROPERTIES OF SHOTCRETE

T. Klečka and J. Dohnálek

Klokner Institute, CTU, Šolínova 7, 166 08 Praha 6

Key words: shotcrete, properties of shotcrete, acceleratives, tunnel structures

Shotcrete is concrete which is transported to the site by a high-pressure hose or pipe, is propelled by spraying and its setting is fast. Shotcrete technology is rapidly expanding, especially in tunnelling where it became part of the so-called "New Austrian Tunnelling Method" the technical and economic parametres of which are qualifying it as the most progressive tunnelling method. In ČSFR this new progressive technology is expected to be widely applied in the construction of the subway or of the Strahov tunnel. One characteristic of shotcrete technology is that both domestic and foreign technical literature barely provide specific experimental results describing the physical and mechanical properties of shotcrete depending especially on the components used, or the process of their application and curing. The likely cause for this is the relatively high cost of such experiments, as the testing samples are not obtained in the traditional way of pouring the concrete into moulds - the samples are cut out or drilled out from larger pre-sprayed samples. The information on the specific values of the modulus of elasticity, the values of shrinking and creep is hardly available.

The proposal of the experimental program was based on the basic request to describe the physical and mechanical properties of shotcrete in the initial stage of setting and hardening in the greatest detail possible. This conforms to the logic of the new Austrian method, where shotcrete serves mainly as a temporary lining exposed to certain rock pressures right from the very start. Due to certain technical limits laboratory samples were used in the initial stages with the provision that later on, when the larger samples from the real shotcrete have been cut into smaller testing samples, these will be used for real shotcrete tests so that both laboratory and real shotcrete tests will have been carried out. Firstly a number of laboratory tests were carried out to determine the best type and dose of the accelerator, as well as the most suitable type of domestic cement and the optimum amount of water. After optimalization of the recipe the current machine technology was used directly under the ground at the Strahov tunnel construction site to spray the samples into wooden moulds of 600 x 600 x 200 mm with their bottom sides opened. From these, smaller samples were drilled or cut out for further tests. The time curve of bending under tension strength and tensile strength on laboratory samples of 40x40x160 mm:

- according to the recipe used in situ
- with ash added
- with siliceous fly ash added
- with the Ostrava SVPC 325 sulphate-resistant cement

Compression strength tested on cubes and prisms 1,3,7,14 and 28 days old. Bending under tension strength at 1,3,7,14 and 28 days. Both big 100x100x400 mm prisms and smaller

40x40x160 mm bodies were to be tested. 100x100x400 mm prisms at 1,3,7,14 and 28 days were tested for the modulus of elasticity and deformability. Shrinking and creep of concrete on small 40x40x160 mm prisms.

Next, a relatively extensive experimental program was started to follow the process of sulphate corrosion using samples cut out from blocks of shotcrete made in situ and using also various lab-made samples. The spraying was carried out in the so-called dry technology, i.e. when water is added to the dry mix directly in the nozzle.

Results of the physical and mechanical tests of the testing samples cut out from shotcrete made in situ show that concrete compactness defined by its volume mass and depending largely on the technology of spraying or processing of the concrete mix significantly influences velocity of shotcrete strength growth, so that besides the quality of the accelerator used it may become an important factor enabling a significant growth of strength after 1 - 3 days. The spraying technology with its resulting concrete compactness substantially influences the values of the elasticity and deformability modulus in the early stages of 1 - 3 days. In the subsequent stages these moduli depend less on spraying technology because their values largely result from the quality and dose of the aggregates used in the concrete mix. The volume change tests clearly sustained the generally known fact of the strong shrinking tendency of shotcrete. The final shrinking values are 4 to 6 times higher than those of the conventional compact concrete. The scope of the experiments we carried out is relatively narrow, due to the amount of work involved. It is highly desirable to continue in these experiments in reasonable scope and establish the influence of change of various technological factors onto the resulting physical and mechanical parametres of shotcrete. As the shotcrete technology could be applied in Prague, it is necessary to predict the influence of sulphate water on shotcrete. The results obtained can be used for significant optimization of the stress analysis of the shotcrete tunnel lining.

This research has been conducted at the Klokner Institute as a part of the research project " Technology of shotcrete used in tunnelling" and has been supported by CTU grant No. 8061.

THE PROPERTIES OF WELDS IN HIGH STRENGTH STAINLESS STEEL

K.Macek, J.Janovec

Department of Materials Science, School of Mechanical Engineering CTU, Karlovo n. 13, 121 35 Praha 2

Key words : maraging steel, weldability, fracture behaviour

In the past decade we investigated extensively the physical metallurgical properties of dual phase martensitic-austenitic age - hardenable steels /1,2/. These Cr- Ni- Mo- Ti- Al steels present a suitable corrosion- resistant alternative to the classical ultra-high strength Ni- Co- Mo- Ti- Al maraging steels. Intended applications in nuclear-power stations ruled out cobalt as an alloying element. The change in alloying base caused a definite increase of the volume fraction of austenite (up to 10% in as-quenched state). However, the microstructure is free of delta ferrite. Further analyses of the phase constitution led to the minor correction of the well-known Schaeffler plot /1/ and to a new findings related to precipitation hardening and corrosion resistance of those steels /2/.

The most promising type 02Cr10Ni10Mo2TiAl of high strength stainless (HSS) steel is contemporarily being manufactured in POLDI Kladno works with trade mark AKHM. This alloy in age- hardened state achieves yield a strength of $R_p0,2$ = 1450 - 1650 MPa and possesses a fracture toughness of K_IC= 50 - 70 $MPa.m_{1/2}$.

In recent years we solved some welding problems and post-weld heat treatment. We performed welded joints by different processes: metal-inert-gas (MIG), submerged arc (PT) and electron beam (EP) welding. A remelted and drawn base material of the following chemical composition (in wt.%): 0,011% C, 10,80% Cr, 10,30% Ni, 2,31% Mo, 1,01% Ti, 0,35% Mn, 0,23% Si, 0,05% P and 0,01% S was used as a filler metal for MIG and PT processes The thickness of welded sheets was 28 mm. Optimalization of welding parameters was based on structural analyses of weld area and of heat affected zone (HAZ).

Post-weld heat treatment consisted of austenitizing at 930° C, 1h and quenching in water. Test specimens were then machined and aged or intercritically annealed for 3h followed by air cooling. After aging at 520° C maximum strength but minimum toughness were obtained. Averaging at 560° C gave optimum strength and toughness. During intercritical annealing at 650° C partial austenitization took place that favorized toughness for account of strength. Some welded joints were just air cooled and given no post-weld heat treatment.

The results of tensile tests, related to optimum post-weld heat treated specimens, are shown in Fig.1. EP-welds attained highest strength, but also the high ratio of yield strength to ultimate strength $R_p0,2/R_m$. This ratio accompanied with relatively low ductility (elongation to fracture of 7-16%) is the warning signal of declined toughness. Experimentally measured values of yield strength for EP-welds were fitted to the relation /3/

$$R_p0,2(T) = R_p0,2(20°C).1,745.exp(-0,019(273+T)) \quad (1)$$

however within the low temperature range definite discrepancy was detected. Therefore we expressed this temperature dependence in the form

$$logR_p0,2 = a + b.T^{-1} \quad (2)$$

where the both constants a= 2,48 - 2,78 and b= 29,4 - 33,8 depend on the post-weld heat treatment.

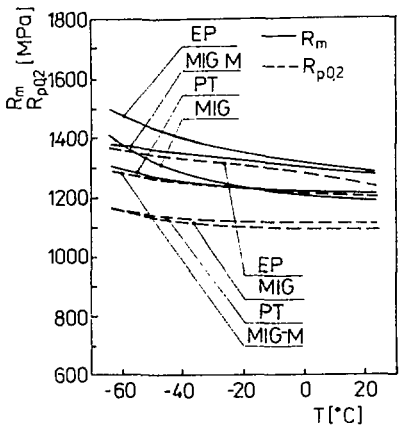

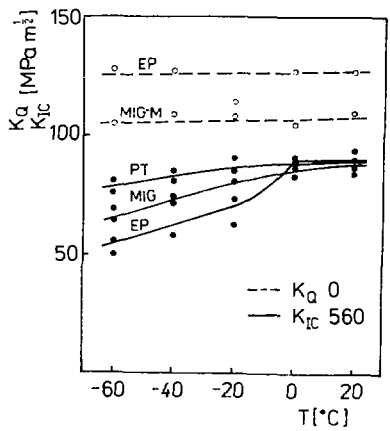

Fig.1 Strength vs test Fig.2 Fracture toughness vs temperature test temperature

Fracture toughness $K_{IC}(K_{IJ})$, critical crack-opening displacement and J-integral were determined according to CSN 420347-8 and ASTM STP 813-81. Then K_{IJ} and critical length cc of model crack were converted into inner and surface weld defects with actual geometry /4/.

The comparision of fracture toughness of welded joints produced by different processes *revealed (Fig.2) that the best results were obtained for EP-welds without any heat* treatment (K_QO). By contrast, EP-welds are least suitable for age-hardening even at optimum aging temperature($K_{IC}560$).

Conclusions: HSS steel of the type 02Cr10Ni10Mo2TiAl is fairly weldable by various welding processes. Mechanical properties and microstructure of weld metal and HAZ are comparable with these of base material. Welded joints may be put into service without post-weld heat treatment. Further studies of relationship between structure and toughness are required mainly for EP-welds.

References K.Macek,

[1] J.Pluhar, J.Cejp, J.Janovec, J.Sasko: Kovove materialy 24, 1986, s.54.

[2] K.Macek, J.Pluhar, J.Cejp: Materials Sci. Eng. 100, 1988, s.153.

[3] R.A.Mulford a kol: Metallug. Trans. 7A, 1976, s.1183.

[4] J.Janovec: Acta Polytechnica, 16(II,4), 1990, s.5.

This research has been conducted at Department of Mater. Sci. as a registered research project No.2104(1986) and No.2042(1991)æ

ESTIMATION OF LOAD IN CLOSED-DIE FORGING

J.Čermák

Department of Forming, Casting and Welding, CTU, Technická 4, 16607 Praha 6

Key words: Closed-die forging, forging load, temperature, flow stress, strain rate, flashgap, crank press, computer

The overall design of a forging process requires the selection of adequate forging machine among the machines available in a particular forge shop for each operation.

This selection is determined by the following three groups of factors:

1. Characteristics of the material to be forged: flow stress, temperature, strain rate, degree of deformation.
2. Characteristics of the forged part: shape, size, weight, drafts, geometrical complexity, number of preforming operations.
3. The size of production lot.

Any forging machine has its own characteristics as load and energy capacity, single (press) or multi-blow (hammer) availability, stiffness, ram velocity under load, production rate, availability of ejectors, etc.

Forging load and deformation energy are the basic characteristics according to which the size of given forging machine is chosen.

In this contribution I have concentrated on press forging. Mechanical presses are commonly classified with respect to their nominal load capacity. But it must be emphasized here that it is always necessary to calculate both the forging load and the deformation energy. Blow energy is taken from the flywheel and if the need of energy is too high, the flywheel may slow down to such an extent that there is insufficient energy to carry on forging.

If any method of calculation the forging load is to be reasonably accurate it must take into account all the following factors:

- the material flow stress, taking into account temperature and strain rate.
- the friction value
- the flashgap dimensions
- some factor which accounts for the forging shape, especially the width/thickness ratio

I have written software to calculate forging load for press forging to enable the quick choice of the press size. The program is written in FORTRAN on an IBM PC running under MS DOS system.

According to requirements mentioned above it was divided into four main blocks: material properties, forging dimensions, flashgap dimensions and methods of calculation. The way of using this program is interactive. The user is guided by the instructions appearing on the screen. The system is opened and may be extended in the number of *material data or methods of load calculation.*

The material is characterized by its flow stress kp that represents the resistance of a metal to plastic deformation. This value if known may be given directly from the keyboard.

If not a special data file was prepared where each material is enclosed by its mark or denomination (combinations of letters and/or digits) and its value of tensile strength R_{mt} is calculate according to given temperature T.

The influence of strain rate fist is expressed as

$$k_p = R_{mt} . n_{fist} \tag{1}$$

where

$$n_fist = (fist/0.02) * *(0.217.T_H * *1.83) T_H = (T + 273)/(T_{melt} + 273) \tag{2}$$

If the data for given material are not included the value of Rmt is calculated for low carbon steels according to their tensile strength Rm for room temperature and forging temperature.

The forging is described by its principal dimensions (diameter, height), weight and the shape difficulty coefficient. It is also possible for a axisymetrical forging of round shape to use a special procedure where the shape of forging is codified by the coordinates of its axial section and appropriate radii.

The flashgap dimensions may be also given directly from the keyboard. If the user is not sure about the correct value another special procedure was prepared according to four different sources. One of them is based on the data used in forging shop SKODA Mlada Boleslav, manufacturer of passenger cars.

Three different methods are at disposal for the calculation of forging load .The first one is very simple, just for quick estimation, derived from the chart published by firm EUMUCO. The second one is that used by our manufacturer of forging presses SMERAL BRNO, derived again from the given chart. The third most complex one, was proposed by A. Thomas and is used by Drop Forging Research Association, now Materials Forming Technology. This method differentiates among the forgings with external flashgap only and with both internal and external ones.

After the estimation or calculation of load is finished the following possibilities are given:

1) choice of another method
2) change of input data
3) repeating the same method with another shape difficulty factor
4) end

After the end the special file PROTOCOL.RTL of results with all our attempts is created and we can make its copy.

Instead of this program several others for calculation of load and energy are at disposal, again according to different authors.

References

[1] Čermák J.: CAP in Closed Die Forging. 1st International Conference on Research and Design of Metal Forming Machines. Beijing, China, May 22 ö 26, 1989.

[2] Čermák J.: Engineering methods of calculation in metal forming. (in Czech). Strojárská ročenka 1989. Alfa Bratislava 1989.

[3] Čermák J.: Using of computer technique in die-forging. (in Czech). Sborník přednášek z konference "Progresivní metody zápustkového kování". Agrozet Zetor. Brno, 2. ö 3.6.1987

This research has been conducted at the Department of Forming, Casting and Welding, Faculty of Mechanical Engineering.

X-RAY ANALYSIS OF RESIDUAL STRESSES INDUCED IN STEEL DURING LASER SURFACE MELTING AND ALLOYING

R. Králová

Faculty of Nuclear Science and Physical Engineering of CTU, 115 19 Prague 1

Key words: x-ray diffraction, residual stresses, laser treatment

One of the most important ways how to control the physical properties of the surface layers is the use of a thermal treatment which has a character of a programmable heating, melting and cooling. The use of lasers is very advantageous in this respect. They allow for application of such a thermal treatment which is sharply confined in space and time, so that the interior of the sample remains unperturbed.

The use of the laser radiation in the regime of melting (power density about 10^5-$10^6 W cm^{-2}$) leads to the appearance of residual stresses in the remelted layer, which are a consequence of large temperature gradients and structural and volume changes. The magnitude and sign of the residual stresses depend on the number of factors like: type of material, density of laser power, scanning velocity, etc.

When an other chemical element is added into the melted track a cladding is created which differs from the substrate in the chemical composition and mechanical properties. The distribution along the depth coordinate, of the alloying element concentration can be either very homogeneous in the melted volume, or it can depend significantly on the depth. This space distribution depends upon which temperature regime is chosen.

The residual stresses created in the course of the laser treatment vary strongly along the surface and depend also strongly on the depth below the surface. In particular, from this reason it is very advantageous to utilize the x-ray diffraction technique which enables one to describe the residual stress field "point by point".

The materials studied were a carbon steel 11375. The specimens were grounded, annealed for 3h at 650°C in hydrogen and subsequently cooled very slowly to the temperature of 150°C. A continuous CO_2 laser with maximum power of 2kW was used in the regime of surface melting and surface alloying with 13.96% of Cr. The distribution of residual stresses was determined by x-ray tenzometric method [1], irradiation CrK-alpha, irradiated area about 4.4 mm^2. The calculation of stresses from the measured lattice strain was made using {211} diffraction line, neglecting effect of elastic anisotropy.

Longitudinal residual stresses σ_L parallel to the direction of displacement (track) and transverse stresses σ_T perpendicular to the direction of the displacement were measured. The following results were obtained:

1. The application of the laser in the regime of surface melting resulted in a series of tracks with the displacement of the tracks 0.8 mm, laser beam diameter about 1 mm, scanning velocity 12.5 mm/s. The depth distribution of σ_L and σ_T was measured. Three levels of stresses are observed: at the depth below the surface (0-500) μm: σ_L=350 MPa, σ_T=250 MPa, (500-800)μm: σ_L=290 MPa, σ_T=150 MPa, (800-1200) μm: σ_L=150 MPa, σ_T=50 MPa. In agreement with [2] these three ranges correspond to the melt zone, heat affected zone and substrate, respectively. The positive values of residual stresses

indicate the prevailing influence of the temperature effect above the microstructural transformation in the remelted zone [2].

2. Specimens with individual tracks of surface melting. The scanning velocity of individual tracks: 1...4.2mm/s, 2...8.3mm/s, 3...12.8mm/s, 4...25mm/s, 5...50mm/s. The dependence of residual stresses L on the scanning velocity was found. These stresses develop from positive values at small velocities (1,2) to compressive stresses (3,4,5) which reach the maximum value at the scanning velocity of 25 mm/s (fig. 1).
3. The dependence of σ_L on the depth below the surface was measured at five points of alloying specimen. The compressive stresses reach the value of about 1000 MPa at maximum. At the depth of 550 μm they change into the tensile stresses of approximately 100 MPa. Also at this depth a considerable decrease of the width of {211} diffraction line is observed. The development of σT in depth is quite similar.

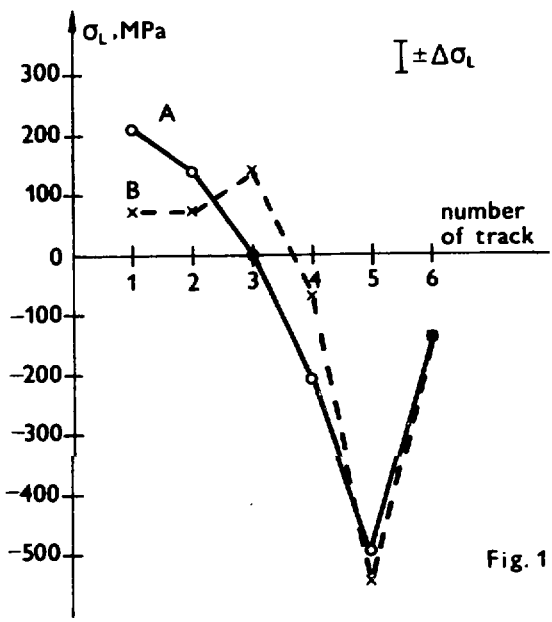

Fig. 1

References

[1] I. Kraus, V. V. Trofimov: Rentgenová tensometrie, Academia Praha 1988.

[2] M. M. James, D. S. Gnamamuthu: Laser Process Materials, Symp. 1984.

DETERMINATION OF SURFACE FILMS AND LAYERS QUALITY

I.Kvasnička , I.Nedbal** , R.Novák**

* Fac. of Mech.Engn., CTU, Technická 4,166 07 Praha 6
* Fac. of Nucl.Sci.and Phys.Engn.,CTU, Křemencova 10, 110 00 Praha 1

Key words: surface layer, thin film, residual stress, fatigue,acoustic emission, X-ray analysis

The solution of the task was realized in three laboratories in the following specific directions:

1. The measurement of surface layers and coatings composition, structure, thickness, internal stresses and adhesion presents one important part of the study of degradation processes caused by coating exposition to external mechanical or thermal stresses. Our work was aimed at the study of two non-destructive diagnostics methods: x-ray analysis and acoustic emission analysis.

   For measurement of TiN, TiC and Ti(C,N) single and multilayer coatings, prepared by PVD or CVD methods, we studied and improved the method of both quantitative and qualitative phase analysis, which enables for example thickness measurement both single and multilayer coatings, determination of layers sequence and measurement of chemical composition of TiN and Ti(N,C) coatings. Our work was also aimed at the the estimation of the correction of prefered orientation and macroscopic stresses influence.

   The degradation of ceramic coatings during the exposure to high temperature was studied by analysis of acoustic emission signals. For this analysis we used a statistical approach, i.e. from a large number of recorded data the average values of chosen parameters were evaluated. For example, according to the distributions of the acoustic events vs. frequency or maximum amplitude was it possible to differentiate several ways of coatings delamination. We also prepared the necessary electronics and software equipment for future recording and analysis of signals from single acoustic emission event.

2. The second research object was aimed to determine application and limitations of the new technique based on ultrasound propagation along the surface.

   The essence of the device (in patent procedure) is that a transmitter of defined ultrasonic pulses and a receiver are fixed in a holder in a steady spacing. The transmitted pulse induces a stress wave in investigated surface and this wave is transformed by the receiver into an electric signal. This signal is further adapted and evaluated in a special device. The amplitude, the number of counts above threshold level etc. are parameters of monitored signal that are in correlation with the surface residual stresses.

   The function of the device mentioned above was checked out during determination of residual stresses in flat samples of AlCu4Mg1 alloy last year. Various stress field were generated by face milling, grinding and shot peening. The results obtained indicated the possibilty to judge the kind and magnitude of the surface residual stresses thanks to the well chosen parameters of acousto-ultrasonic technique.

The realiability and reproducibilty of measurements demand checking of the limit factors, e.g. surface roughness and bearing ratio, type of microstructure, texture, grain size etc.The starting observations were carried out using two sets of experimental samples:

- flat carbon steel samples with rather different surface roughness for the study of interaction between front surface and the probe.The possible influence of residual stresses was eliminated by annealing of test samples in vacuum
- flat tool steel samples, heat treated to obtain different microstructures.

Determination of the factors studied (incl. measurment of residual stresses by classical method) could not be finished before the dedline of the WORKSHOP 92 articles.

3. In the third field the initial experiments were carried out to prove the method for the study of fatigue behaviour of the film/substrate interface. The steel fatigue specimens with a Cr films on one side (Cr implanted with N^2) were tested in a special device (SF-TEST) being developed at the Dept.of Materials FJFI. Fracture analysis of the form and path of cracks (using SEM JSM-840A) led to these conclusions:

   - The used coating technology created film with very good adhesion to the substrate. The homogenity of the interface was not significantly damaged by the cyclic loading in order of 10^6 cycles.
   - The gradual rise of the network of cleavage cracks in the film was observed. The character of the first stage of failure led to the working hypothesis about the unfavourable influence of Cr thin film to the fatigue behaviour of the modified surfaces. The cleavage microcracks may be effective as stress concentrations that shorten the time before fatigue cracks initiation in an important way.

   The possibilities of the SEM detailed study of mechanism of coatings fracture during so-called "scratch test" were also observed. First results proved that it will be useful to develop a testing method for detection of coating film resistance against the local *contact failure and the decohesion from the substrat material.*

   Information gained from these experiments will be used for the proposal of the experimental programme in 1992.

This research has been conducted at the Department of Physics and at the Department of Machining of the Faculty of Mechanical Engineering and at the Department of Materials of the Faculty of Nuclear Science and Physical Engineering as a part of the research project "Diagnostics of subsurface layers and thin coatings on real bodies" and has been supported by Czech Technical University grant No.8001.æ

NEUTRON TEXTURE ANALYSIS OF ZIRCALOY-4 TUBES

M.Dlouhá and S.Vratislav

Faculty of Nuclear Sciences and Physical Engineering, Břehová 7, 115 19 Praha 1

Key words: neutron diffraction, texture analysis, Zircaloy-4 tubes, inversion pole figures

In recent years neutron diffraction texture analysis has been extensively used in material research/1/.

The application of the neutron diffraction method in texture analysis is associated with the absorption and scattering characteristics of thermal neutrons. The high penetration of neutrons through the majority of materials together with high area sections of the neutron beams (up to 10^3 mm^3) make it possible to irradiate large specimen volumes. Therefore, inhomogenity of the texture, large grains and the beam penetration through specimens cause no major problems in relation to neutrons. In comparison with X-ray or electron diffraction, neutrons are not sensitive to the surface layers and so it is possible to obtain an information from the internal parts of the measured specimens by means of nondestructive way. The large differences in penetration are indicated by the half thickness values which vary in the range from 3 to 70 mm for neutrons and from 0.0021 to 0.053 mm for X-rays, respectively. Therefore, the neutron diffraction method can provide the great accuracy pole figure data, which are required in the three-dimensional orientation distribution function (ODF) determination. Information on average texture provided by neutrons is most profitable in studies of correlation between texture and anisotropy of some physical properties(like elasticity/2/, plasticity, magnetocrystalline energy/3/, corrosity).

The present study deals with the texture analysis of the Zircalyo-4 tube specimens. The type and the form of the texture were investigated under different conditions of the tensile tests. One consequence of the termomechanical proccesing of zirconium-based alloy components for nuclear application is the development of a strong preferred crystallographic orientation or texture. A great deal of work has concentrated on understanding the effect of texture-induced anisotropy on the mechanical properties of zirconium alloys. The quantification of texture is important for two reason. First, the definition of texture by tubing suppliers and fuel element vendors is an essential part of the quality control process. Secondly, the ability to correlate mechanical properties with the texture of the material is necessary. This study follows with our previous investigations of zirconium materials/4/.

Measured specimens were cut out from the initial Zircaloy-4 tube materials under three different angles which are given by the tube axis and the specimen bar axis direction, respectively ($\alpha = 0°, 22°, 90°$). Tensile tests of these bars were examined at 20° and 310°C /5/. After tensile tests the texture analysis was provided by means of the inversion pole figure method. Neutron diffraction data was recorded on the KSN-2 diffractometer located at the research reactor LVR-15 in Řež near Prague. The texture goniometer TG-1/6/ was used for the angle position determination specimens in the monochromatic neutron beam. Neutron diffraction patterns was recorded in the 2Θ angle range from (100) to (114) diffraction lines of zirconium. Neutron data were processed by means of the profile

analysis method. Results of the inversion pole figure method are given in the form of the main texture characteristics, i.e. pole figure density phkl,texture index Ji, and texture f^i-coefficient, where h,k,l - Miller indices, i=N,T,L-the axes in the specimen coordinate system . All these values were determined for three N,T,L directions. By means of our results we could determine the directional dependence of the p_{hkl}, J_i and f_i on the α in the L-T plane of the N,T,L coordinate system of samples.

With respect to the results which we have obtained following conclusion were given:

- The crystallite basal pole are preferentially oriented parallel to the radial tube direction. The orientation seems to be independent on different tensile test conditions.
- The tensile strength oriented parallel to the tube axis do not affect the original tube texture.
- The largest texture changes occur when the tensile strength is directed near parallel to the transversal direction of a tube.
- The tensile test temperature increase from the room temperature to 310°C leads to the decrease of the texture sharpness.

All results and their analysis are given in our publication which is in print in "Kovové materiály"/7/. References

[1] H.J.Bunge: Zeischrift fšr Metellkunde 76(1985)457;

[2] S.Vratislav, M.Dlouhá, J.Jeřábek, L.Kalvoda: Kovové materiály 22(1984)733;

[3] S.Vratislav, M.Dlouhá, L.Kalvoda, A. Zidek, E.Chudčjová: Metallurgical Journal 43(1988)594;

[4] M.Dlouhá, L.Kalvoda, S.Vratislav, J.Marek: Kovové materiály 27(1989)152;

[5] J.Cejp,B.Cech:Acta polytechnica Práce CVUT v Praze 4(1988)9;

[6] M.Dlouhá,J.Jeřábek.S.Vratislav: Jaderná energie 29(1983)73

[7] S. Vratislav, M.Dlouhá,L.Kalvoda, B.Cech: Kovové materiály (1991) - in press

This research has been conducted at the Department of solid state engineering as a part of research project "Structure and texture analysis by neutron diffraction".æ

Section 3

PHYSICS

NON–LINEAR MODELS IN QUANTUM PHYSICS

K.Košťál and B.Rudolf

Department of Physics K202, CTU, Technická 4, 166 07 Praha 6

Key words : Stochastic mechanics, non–linear Schrödinger equation

The research carried out at the Department of Physics of the Faculty of Mechanical engineering has been concerned with the construction and investigation of non–linear terms in the generalized Schrödinger equation.

Previously, a stochastic model of non–relativistic random functions was constructed [1,2]. The equations of motion obtained in this model for a system of N particles yield the following generalized Schrödinger equation

$$\frac{ih}{2\pi}\frac{\partial\Phi}{\partial t} = -\sum_{k=1}^{N}\frac{h^2}{8\pi^2 m_k}\Delta_k\Phi + V\Phi + \Theta\Phi\ln(\bar{\Phi}\Phi)$$

satisfied by a complex function Φ; V denotes the total potential energy of the system, h the Planck's constant, k the particle's index number, m_k the mass of the k-th particle, Θ is a parameter. In addition to the quantum–mechanical motion, the model involves also the termal motion of particles, which is represented by the non–linear logarithmic term.

For stationary states of systems basic relations of thermodynamics including the second and the third principle were derived. Moreover, it was proved, that the parameter Θ depends on thermodynamic temperature T of the system and that for sufficiently large temperatures $\Theta = KT$.

The method which enables the expression of different terms appearing in the general evolution equations obtained for our stochastic model of random motion was used to extend them by further terms. First, the additional term was introduced which represents the deceleration of a particle caused by a force proportional to its velocity. In this case, the resultant generalised Schrödinger equation (for one particle) is as follows

$$\frac{ih}{2\pi}\frac{\partial\Phi}{\partial t} = -\frac{h^2}{8\pi^2 m}\Delta\Phi + V\Phi + (\beta\ln\Phi + \bar{\beta}\ln\bar{\Phi})\,,$$

where $\beta = \Theta - ib$ and b is a positive constant.

For this equation the Liapounoff functional

$$H \approx \int_{R^3}\left[-\frac{h^2}{8\pi^2 m}\bar{\Phi}\Delta\Phi + V\bar{\Phi}\Phi + \Theta\bar{\Phi}\Phi\ln\bar{\Phi}\Phi\right]\,\mathrm{d}x_1\mathrm{d}x_2\mathrm{d}x_3$$

was found, where x_1 , x_2 , x_3 are the orthogonal cartesian coordinates of the particle.

Since

$$\frac{\mathrm{d}H}{dt} = -\frac{4\pi bm}{h}\int\bar{\Phi}\Phi < v >^2\,\mathrm{d}x_1\mathrm{d}x_2\mathrm{d}x_3 \quad \leq 0\quad ,$$

H is a non–increasing function of time t. The orthogonal cartesian components of the particle's local mean velocity $< v >$ in this case are given by

$$< v_j >= \frac{ih}{4\pi m}\left[\frac{1}{\bar{\Phi}}\frac{\partial\bar{\Phi}}{\partial x_j} - \frac{1}{\Phi}\frac{\partial\Phi}{\partial x_j}\right] \quad , \quad j = 1,2,3 \; .$$

Consequently, the Liapounoff functional can be used to define the equilibrium probability distributions of the particle's coordinates. The density $f = \Phi\bar{\Phi}$ of every equilibrium distribution corresponds to such function Φ, for which the Liapounoff functional assumes its minimum value. It has been proved, moreover, that every equilibrium distribution, if it exists, defines a stationary state for which $< v > = 0$. Such stationary states were found previously [2,3] and the Liapounoff functional, as expressed for those states, was interpreted in terms of the energy of the system and the entropy of the stationary probability distribution.

Some of the new results can be specified for the classical limit ($h \to 0$). It was proved that in this limit, there exists only one equilibrium distribution which is identical with the single stationary solution of the equations of motion for which the condition $< v > = 0$ is satisfied. In this case, the probability distribution of particle's coordinates corresponds to the Boltzmann distribution if we set $\Theta = kT$, where k is Boltzmann's constant.

Further additional terms depending on the particle's local mean velocity, namely terms corresponding to Lorentz magnetic force, were introduced in our model. In this case the evolution equations satisfied by the probability density f were obtained. However, the form of these equations is such, that is impossible to transform them into a generalised Schrödinger equation, since no complex function Φ with convenient properties can be constructed. On the other hand, the Liapounoff functional has been found even in this case whose derivative dH/dt is given by the same expression as above. Accordingly, the properties of the equilibrium distribution are the same as in the absence of magnetic field.

References:

[1] K.Košťál: Generalization of the Schrödinger equation based on a stochastic model of motion, Acta Polytechnica – Práce ČVUT v Praze (1982) 65-76.

[2] K.Košťál: Stochastic mechanics based on differentiable random functions. In: "Selected Topics in Mathematical Physics and Quantum Field Theory", World Scientific, Singapore (1990) 251-264.

[3] K.Košťál, B.Rudolf: Stochastický model pohybu částic zahrnující jejich tepelný i kvantově-mechanický pohyb, Výzkumná zpráva dílčího úkolu SPZV I-2-3/6, Praha 1987.

This research has been conducted at the Department of Physics, Faculty of Mechanical Engineering as a part of the research project "Non-linear models in quantum physics" and has been supported by CTU grant No.8002.

A REMARK ON FINITE DIFFERENCE ELECTRODYNAMICS

J. Kafka

Faculty of Nuclear Sciences and Physical Engineering, Břehová 7, 115 19 Praha 1 - Staré Město

Key words: differential equations of the electromagnetic field, numerical solution, application to electrical engieneering

Under "Finite difference physics" we shall understand a theory, in which the laws of physics (mainly of classical physics) are formulated in the form of finite difference equations or any equivalent discretized form suitable for the numerical solution of the respective (ordinary or partial) differential equations.

First of all, we shall shortly describe the discretization process. First of all, we have to state the law of physics governing the natural phenomena under consideration. This law of physics has to be formulated in its integral form {in the case under consideration, the Maxwell equations in their integral form (four simultaneous equations in total)}.

As a second step, we are dividing the body under consideration (in general, a domain containing one or several bodies immerged either in vacuum or in a medium of deliberate permittivity and magnetic permeability) into a set of "elementary domains". Here we have to differentiate two cases:

1. If the main terms in the integral formulation of the law of physics are volume integrals, as e. g. in the case of heat conduction, then we are simply dividing the definiton domain of our differential equation by three families of mutually ortogonal planes into a set of "bricks". In more general cases, the planes need not to be orthogonal or we can take curved surfaces instead of planes (in the presented paper, we shall need cylindrical coordinates in order to describe the cylindrically or axially symetrical case).

2. If the main terms in the integral formulation of the law of physics are surface integrals (as is e. g. in our case of the electromagnetic field), then we cannot content ourselves with the above -mentioned "bricks", but we have to design a set of meshes in every above mentioned plane or curved surface. Let us restrict our choice to three families of orthogonal planes for a while. Let us choose one plane parallel to the xy coordinate plane and a second plane parallel to the yz coordinate plane. They are intersecting in a line parallel to the y axis. On this line, we draw points shifted from one by another half step length. The odd points will serve as centers of meshes drawn in the plane parallel to the yz plane, the even points will serve as centers of meshes drawn in the plane parallel to the xy plane. The resulting meshes are interlaced as to form a kind of a chain (the neighbouring links of which are mutually perpendicular).

As a third step, we are applying the law of physics in its integral form to the newly generated meshes. The meshes in one plane are used for calculating the electromotive force, the perpendicular meshes are used for calculating the magnetomotive force. In the general three-dimensional case (which will not be treated here), we have to design six sets of meshes in total, three of them being shifted by a half step from the preceding three sets of meshes.

Now, let us concentrate on two-dimensional cases. Let us take the **E** vector as the basic quantity. Then only one component, namely E_z is different from zero. For practical reasons, the cylindrically symmetrical case is more important. Here, only the tangential component of the **E** vector is different from zero and the lines of force of this vector are circles drawn in parallel planes and their centers lie on a common axis. This scheme can be used for calculating for example the inductive heating of axially symmetrical bodies (e. g. when hardening or melting those bodies)

N. B. the presented method allows, especially in the two-dimensional case, the designing irregular meshes and the designing of locally subdivided nets for the application of the finite-difference method.

The formulations of problems and many useful hints have been given to the author by the late Docent Ing. Zdeněk Ryska and by the late Ing. Hanuš Topinka.

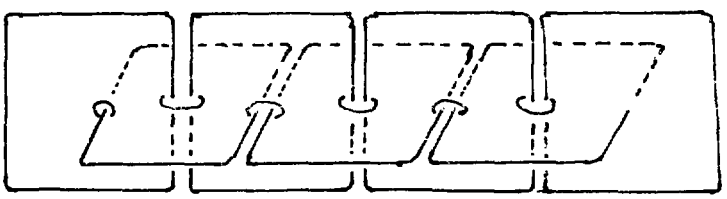

Fig. 1 The chain of meshes. The meshes in the vertical plane are well suited for the calculation of $\int Es\, ds$; the meshes in the horizontal plane are well suited for the calculation of $\int Hs\, ds$.

This research has been conducted at the Departemnt of mathematics of the Faculty of Nucear Sciences and of Physical Engineering of the Czech Technical University , for some period under the heading of the research project "Microwave integrated circuits" and in the previous year has not been supported by a grant.

INSTRUMENTATION AND TECHNIQUES FOR THE MEASUREMENT OF NEUTRONS AND RADON WITH ITS PROGENY

*Z. Janout, A. Gosman, Č. Jech+, S. Pospíšil, B. Sopko, Z. Češpíro, E. Havránková, D. Houšová ++, J. Jursík +++, J. Koníček, I. Mácha, T. Vašek, M. Vobecký**

Faculty of Nuclear Science and Physical Engineering, CTU, Břehová 7, 115 19 Praha 1, +Institute of Physical Chemistry and Electrochemistry, Czech. Ac. of Sciences, Dolejškova 3, 180 00 Praha 8, ++Institute of Dental Research, Vinohradská 48, 120 60 Praha 2, +++Ekotronika, spol. s r.o., Náchodská 754, 193 00 Praha 9, *Inst. of Nuclear Chemistry and Biochemistry, Czech. Ac. of Sciences, Vídeňská 1083, 142 20 Praha 4

Key words: Si semiconductor detectors, neutron detectors, radon 222, daughter products, tracer techniques, labelling, tooth, slow neutrons, neutron capture therapy

The PN junction Si diode can operate as a detector of heavy charged particles,if reverse bias is applied. For the detection of neutrons the detector has to be completed by a converter where a nuclear interaction takes place. Electronics for signal processing is then practically the same for detection of alpha particles or neutrons [1].This is the unification idea through the presented experimental project. The manufacture of the Si detectors needed as well as their utilizations for a) development of the new type slow neutron detector, b) measurement of radon and its daughter products in the environment, c) surface labelling of solids with radon and its progeny, were the main aims of the project.

a) **Si diode as a small detector of slow neutrons.** PN junction Si diode produced on nondislocation FZ silicon N type material with resistivity 1300–2500 Ωcm by means of planar technology [2] is used as a surface barrier detector. The ^{6}LiF-converter is utilized. As main construction materials Al and polyethylene were used. Overall dimensions were chosen less than 17mm and, basically, they are limited only by the dimensions of the Si-wafer used. Efficiency of the detector for thermal neutrons is selectable approximately in the range between 0.1% and 1% . Slow, resonance and fast neutron contributions can be estimated by means of Cd, Au and B filters, respectively. Efficiency of the Si detector for different components of external gamma radiation depends on detector bias. There are the following advantages [3] of the described detector : -low sensitivity for gamma-rays and fast neutrons, -the well known 1/v dependence of efficiency for detection of slow and resonance neutrons, -long term stability of the detection parameters, -rugged mechanical construction,-low voltage applied bias,-almost isotropic dependence of slow neutron detection efficiency.

b) **Radon and its progeny.** Most of the effort was devoted to the development of techniques for measuring of Rn and its decay products. For the technique developed earlier, which is based on *collection of Rn decay products on a filter* and measuring the collected activity at certain time intervals, more precise simple procedures for determination of low volume RaA, RaB and RaC activities in air were devised [4]. Alpha activity deposited on the filter is measured by means of the Si detector. Volume activities can be then obtained from the derived equations which include the pumping throughput, filtering efficiency, detection efficiency and the decay constants. Three practical procedures, which differ

slightly in the statistical precision of results, were proposed. Equivalent volume activity of Rn on the 200 Bq/m^3 level can be determined with 4% relative error. Separation of the RaA and RaC contributions by means of alpha spectroscopy was investigated. The second method for measurement of Rn (in ambient air and samples of air from soil) consists of *continously collecting the created Rn decay products directly on Si detector entrance window from a chamber using an electrostatic field.* Efficiency of collection and from this ensuing increase of Rn detection sensitivity was determined. A procedure for primary calibrations of Rn measurement techniques was devised. It is based on a precise measurement of an Rn sample which has been implanted into a metal foil and release of the Rn by heat treatment into the Rn measuring chamber. Diverse *portable instruments* with variety of detectors (Si detector, Lucas chamber, BGO scintillator) were constructed, modified and tested for instantaneous measurement as well as for continuous long term investigations of Rn variations. The obtained data can be stored into the memory and consequently transferred onto the PC.

c) **Radon labelling**. A simple procedure has been developed which makes it possible to introduce atoms of Rn 222 and its decay products into surface layers of solid specimens exploiting the recoil during alpha decay of Ra 226 from a thin layered source [5]. Decay curves and depth distribution of the implanted activity has been determined. This surface layer labelling technique has been applied to the study of the abrasivity of various tooth pastes in tooth brushing simulation experiments.

Conclusions: a) The described neutron detector can be used in the following applications: -thermal and slow neutron flux measurement and monitoring, especially in tissue-equivalent and in strongly moderating surroundings, -as a detector for fast neutron Bonner spectrometry, -neutronography, -for boron neutron capture therapy. b) Variety of methods related to the Rn and its progeny were proposed and tested. The electrostatic collection of the radon and thoron products makes it possible to measure their extremely low activities in environment. c) Radon surface layer labelling technique can be applied in different fields of material science. d) It was established that detection structures produced on Si surface by means of planar technology are very promising for nuclear instrumentation and inexpensive. It is proposed that this project be continued toward the design and production of smallest detectors and the more complex detection structures.

References:

[1] S. Pospíšil et al: Device for impulse indication, measurement and checking of ionizing radiation (in Czech), cs. patent AO 263 601, Praha 1989.

[2] B.Sopko et al: Application of planar technology on silicon with high resistivity (in Czech), 2nd Sci.Conf.of EF STU, Bratislava, 1990, p. 25.

[3] S.Pospíšil et al: Small detector of thermal neutrons (in Czech), Abstr. of the Conf. IAA 91, ČSFR, VTEI ÚJV Řež, p.29-31.

[4] Z. Janout , S. Pospíšil: Measurement of Rn progeny in air by means of pumping through a filter (in Czech), Acta Polytechnica-Práce ČVUT v Praze, 19(IV,3)1991, p.1-16.

[5] Č.Jech, A.Gosman: A simple technique for surface labelling of solids with Rn 222 and its shortlived decay products, submitted to the J. Radioanal. Nucl. Chem., Letters.

This research has been carried out at the Department of Physics FNSPE CTU as a part of the research project "Correlation and resonance effects in atomic nuclei" and has been supported by CTU grant No.8054.

PROTON NON-RUTHERFORD ELASTIC SCATTERING CROSS SECTION

R Salomonovič

Dept. of Physical Electronics, Faculty of Nuclear Science and Physical Engineering
CTU, V Holešovičkách 2, 180 00 Prague 8

Key words: protons, resonant scattering, ion beam analysis

A simple, one run method for the determination of the non-Rutherford scattering cross section for scattering of MeV protons on light elements is presented. The main purpose of the present investigations is to obtain cross section data at different scattering angles. The angular and energetic dependence of the cross section are useful for backscattering analysis of light elements.

In the past twenty years the proton scattering spectrometry has been widely used in several applications as a powerful analytical tool for quantitative sample analysis namely for concentration and depth profiling of component elements. In comparison with 4He ion backscattering, the higher non-Rutherford scattering cross sections of the light elements leads to higher sensitivity of a MeV proton beam probes and longer proton range in the target material is also an advantage. On the other hand, the poorer depth resolution and lower mass resolution are the disadvantages of protons used as projectiles.

For the evaluation of the non-Rutherford backscattering cross section a simple procedure can be used. It may be applied for any light element from which a bulk solid target can be formed. The monoelemental target is the most suitable, the bielemental structure of known composition (like TiN or BN) is acceptable too, but there may be some difficulties (background or interference of the yields from other elements). At first a common spectrum of the sample at known parameters is collected. From accurate energetic calibration the energy width ϵ of one channel is obtained. Using stopping power [1] of the sample material along the ingoing and outgoing path, one can calculate the thickness δ of a slab at the depth t from which projectiles are scattered into a energy interval ϵ located at an energy E_1 (i.e. into one channel) in the energy spectrum. Our computer program prepares data files which consist of proton energies just before scattering for all slabs, the depth t, thickness δ of these slabs and energy of outgoing detected protons. From these data one can easily derive the scattering cross section as a function of primary energy using common formula:

$$\sigma(E_0^i) = H^i/(\Omega N \delta^i [\cos\Theta_1]^{-1})$$

where $\sigma(E_0^i)$ is the proton scattering cross section at the energy E_0^i, H^i is the spectrum height of the i-th channel, corresponding to the energy E_1^i, Q, Ω, N are charge, solid detector angle and target density, Θ_1 is the incident angle. The shape of this function is influenced by the energy straggling and multiple scattering. Their role is not significant in surface region. So it was necessary to measure the same sample at several different proton energies to compile a non-influenced curve for the whole energetic scale.

The backscattering measurements were carried out on a 2.5 MeV Van de Graaff accelerator at Charles University Prague on the ion beam probe [2] built at the Technical University of Prague. The primary beam energy calibration was performed with reactions $^{27}Al(p,\tau)^{28}Si$ (resonance at E_p = 991.91 keV) and $^{58}Ni(p,\tau)^{59}Cu$ (resonance at E_p = 1843.45 keV). The collimation system prepared a beam with 1 - 2 mm in diameter and current intensity about 10^{-8} A. The measurements were carried out at a set of lab scattering angles Θ from 170 to 130 degrees. For every Θ, measurements were performed at the energies E_p = 1660, 1720 and 2030 keV with the same charge dose 15 μC. The precise calibration of the energy - channels relation was ensured using C, O, Mn, In and Bi peak centroids obtained from special calibration target at several different laboratory angles. The silicon wafer was used as a target and the result is compared with earlier published data [3].

The angular distribution of scattering cross section in combination with certain values of the primary energy provides some interesting features for light element analysis. Several measurements of light element profiles and surface impurities analysis using non-Rutherford scattering of protons have been done, one of them also in our laboratory [4].

References:

[1] H. H. Andersen and J.F. Ziegler, Hydrogen Stopping Powers and Ranges in all Elements (Pergamon Press, New York, 1977).

[2] M. Setvák, Z. Hůlek, J. Voltr, Z. Hába, R. Salomonovič, A. Šíbl and J. Král, Proc EPM 87, (Akademie, Berlin 1987).

[3] E. Rauhala, Nucl. Instr. and Meth. B12 (1985) 447.

[4] Z. Hůlek, Z. Češpíro, R. Salomonovič, M.Setvák and J. Voltr, Vacuum vol.41 (1990) 1853.

IMPULSE SOUND FIELD IN A ROOM

Zdeněk Kyncl

Faculty of Electronical Engineering CTU, Department of Physics,
Technická 2, 166 27 Prague 6

Key words: Sound Field, Impulse Response, Acoustic Coefficient

Let a sound impulse wave be emitted from a source in the room. The resultant sound field in the room is created by the superposition of the emitted impulse wave and the response of the room. The influence of the room on the impulse sound field is discussed in this paper . The analysis is based on the impulse room statistics published in [1]. For analysis of an impulsive sound pressure is used the Fourier transform. The squared Fourier transform modulus is named the Quadratic Spectrum

$$Q(f) = \left| \int_0^\infty p(t) \exp(-j2\pi f t) \mathrm{d}t \right|^2 \tag{1}$$

The relative contribution of the room impulse response to the resultant sound field at the point located by the radius vector r can be expressed by the Relative Quadratic Spectrum

$$q(\mathbf{r}, f) = Q_r(\mathbf{r}, f) \; / \; Q_e(\mathbf{r}, f) \tag{2}$$

where Q_e and Q_r are the quadratic spectra of the emitted impulse and the impulse response, respectively. For an overall evaluation of the response we use the mean spatial value of the response quadratic spectrum $< Q_r(f) >$ in the room. The relative spectral contribution of the room impulse response to the sound field can be characterised by an Acoustic Coefficient

$$< \epsilon(f) >= E_r(f) \; / \; E_e(f) \tag{3}$$

where $E_e(f)$ is the spectral density of the acoustic energy emitted by the impulse source, and $E_r(f)$ is the spectral density of the acoustic energy emitted into the room by all walls during the whole response process. For the acoustic coefficient the following formula is valid [1]

$$< \epsilon(f) >= S \; < Q_r(f) > \; / \; [\, 2 \, \check{C} \, c \, E_e(f)] \tag{4}$$

where S is the surface of the room. After introducing the Normalised Quadratic Spectrum

$$\epsilon(\mathbf{r}, f) = S \, Q_r(\mathbf{r}, f) \; / \; [\, 2 \, \check{C} \, c \, E_e(f)] \tag{5}$$

the acoustic coefficient can be expressed as

$$< \epsilon(f) >= V_0^{-1} \int \int_{(V_0)} \int \epsilon(\mathbf{r}, f) \, \mathrm{d}V \tag{6}$$

where V_0 is volume of the room. According this formula the acoustic coefficient can be measured by using a reference source of a short spherical impulse wave [2],[3]. Normalised spectrum can be evaluated according to formula

$$\epsilon(\mathbf{r}, f) = S \, q_r(\mathbf{r}, f) \, [16\pi r^2]^{-1} \tag{7}$$

where r is the distance between the source and the microphone.

Let $Q(\mathbf{r}, f)$ be the quadratic spectrum of the resultant sound pressure given by superposition of the emitted impulse and the room response. For an overall spectral characterisation of a sound field at the distance r from the source a mean spherical value can be used

$$< Q(r, f) > = (4\pi r^2)^{-1} \int_{S(r)} \int Q(\mathbf{r}, f)\, \mathrm{d}S \tag{8}$$

where $S(r)$ is the integrating spherical surface around the source. Then

$$< Q(r, f) > = \text{Ç}c\,[(8\pi r^2)^{-1} + 2 < \epsilon(f) > S^{-1}]\, E_e(f)\,. \tag{9}$$

Spherical mean relative quadratic spectrum of the total sound pressure at the distance r from the source is then

$$< q(r, f) > = < Q(r, f) > / Q_e(r, f) = 1 + 16\pi r^2 < \epsilon(f) > S^{-1}\,. \tag{10}$$

Let us express the Sound Pressure Exposure at the position $\mathbf{r}$

$$b(\mathbf{r}) = \int_0^\infty p^2(\mathbf{r}, t)\mathrm{d}t = 2 \int_0^\infty Q(\mathbf{r}, f)\, \mathrm{d}f\,. \tag{11}$$

Owing to [9] the frequency band value of the mean spherical sound pressure exposure at the distance r from the source can be predicted by formula

$$< b_B(r) > = \text{Ç}c\,[(4\pi r^2)^{-1} + 4 < \epsilon > S^{-1}]\, W_B \tag{12}$$

where

$$W_B = \int_{f_1}^{f_2} E_e(f)\, \mathrm{d}f \tag{13}$$

is the band acoustic energy emitted by the impulse source.

Described analysis enables evaluation of the sound energy emitted by an impulse source. Let us analyze the sound pressure in a number of different positions $\mathbf{r}_k$ in the room. If the acoustic coefficient of the room is known then the spectral density of the emitted energy can be evaluated according to formula

$$E_e(f) = (\text{Ç}c)^{-1} < Q(\mathbf{r}_k, f)\,[(8\pi r_k^2)^{-1} + 2 < \epsilon(f) > S^{-1}]^{-1} > \,. \tag{14}$$

Band acoustic energy emitted by the impulse source can be evaluated by integrating according to (13).

References:

[1] Kyncl Z.: New Concept of Impulse Statistics Analysis of Room Acoustics, Acoustics Letters, London, Vol. 3 (1980), No. 11, 200-207.

[2] Kyncl Z.: Impulse Response Method of Sound Absorptivity Measurement in Enclosures, 8th Colloquium on Acoustics, Budapest 1982, 1981-1986.

[3] Kyncl Z.: Acoustical Diffusivity Diagnostics by an Impulse Response Digital Processing, Proc. 6th FASE Symposium, Sopron 1986, 115-18.

This research has been conducted at the Faculty of Electrotechnical Engineering ČVUT as a part of the research project "Interaction of an Impulse Sound Field with Structures" and has been supported by ČVUT grant No.3029.

THE INTERRUPTED Z-PINCH FILAMENTARY STRUCTURE

Kubeš P., Kravárik J., Hakr J., Píchal J., Kulhánek P.

Czech Technical University, Dpt. of Physics, Technická 2, 166 27 Praha 6, Czechoslovakia

Key words: z-pinch, filamentary structure, discharge stability

1) Introduction

The longitudinal z-pinch is a type of high-current discharge (kA÷MA), characterized by the cylindrical symmetry and plasma compression due to its own magnetic field (typical is e.g. the coaxial gun plasma focus or the vacuum spark with cylindrical symmetry). For more detailed information see [1, 2,3].

2) Experimental Apparatus and Diagnostic Methods

The z-pinch had been formed in the discharge between two cone-shape electrodes (top angle 90° and diameter 10 mm each, interelectrode distance 10 mm) placed in the glass vacuum chamber filled with air under 5 kPa pressure. The energy source used the condenser battery was charged to a voltage of 18 kV and the discharge current reached its maximum (40 kA) after 1 μs.

Assuming the cylindrical geometry in the plasma layer surrounding the z-pinch, the results of the Michelson interferometry enabled the discharge evolution study as well as the electron density calculations.

The Michelson interferometry results were not applicable for calculations of the electron density gradient's mean value in the small inhomogeneity regions characterized by large gradient changes, therefore the schlieren method with the variable diameter of the focal point disk screen was used [4].

Both methods, the Michelson interferometry and the schlieren method, comprise a ruby laser switched in the Q – regime as the light source. The laser light pulse length was 40 ns, but due to the synchronisation and the delay of the light pulse from the discharge ignition, there was a possiblity to get a series of experiments. The experiments were carried out every 100 ns in the 1 μs time interval after the discharge ignition, the results being registrated with a camera. During every discharge there was only one shot taken, but the sequence of measurements was very well acceptable for the discharge evolution study due to the good repeatibility discharge.

3) Results

During the 0.5 μs time interval after the discharge ignition, the boundary between plasma and neutral gas creates the shock ionisation wave. Later this shock wave distintcly separates from the plasma region The shock wave velocity is 10^4 m/s.

The densest part of the discharge – the z-pinch – has cylindrical shape with the diameter about 3 mm during the first 200÷300 ns after the discharge ignition. Later, by discharge current some 20 kA, the z-pinch breaks in its central part, where the current channel is largest and the electric and magnetic fields relatively weak, into two parts off. Their ends connected with the electrodes turn to the plasma jets throwing plasma in opposite directions towards the discharge centre, where collisions of plasma flows result in the

increase of the plasma density. The temperature and number of particles in this region are probably the main factors influencing the z-pinch dynamics.

Both plasma flows from the jets as well as the discharge central region have filamentary structure. The filaments are in both flows visible near the electrodes only (in the pinch area) and are orientated parallel with the electric field. Their orientation in the central region is fortuitous and they seem to congregate in the centre of this region. Every filament has the length of $1 \div 3$ mm, diameter about 10 μm and electron density $(6 \div 9) \times 10^{24}$ m^{-3}.

The electron density function increases from the shock wave outer boundary ($\approx 5 \times 10^{23}$ m^{-3}) towards the pinch approximately as $1/r$ function. The electron density on the pinch pinch boundary rises from 2×10^{24} m^{-3} at 200 ns after discharge ignition to 8×10^{24} m^{-3} at 500 ns and later seems to be constant.

There are no interferometric contours at the interferograms of the plasma flows and the discharge centre, hence there is no possibility of direct electron density calculations. In this case the density lower limit can be defined by the particle density in the neighbourhood of the current layer.

4) Conclusion

Experimental results suggest further speculations.

Important information is the electron density distribution in the current channel. Its character seems to be caused by the plasma transport from the discharge boundary towards the discharge centre initiated by the magnetic forces created by the discharge electric current. The magnetic force seems to push plasma into the plasma jet region, where the plasma radial velocity changes into the axial one. This assumption will be verified by computer modelling.

Further interesting result is the filamentary structure of the plasma flow and its stability. The stability condition could be connected with the plasma transport suggested in the previous paragraph.

We take the existence and the orientation of filaments in the discharge central region as the most spectacular result. Are they created due to the plasma flow filaments or are they the result of the plasma flows collision?

The further study will be concentrated on the plasma flow spectroscopic study and the plasma flows effects caused by the electrode shape.

References:

[1] Meierovitch B. F.: Uspechi fizitcheskich nauk 149, 1989, 221

[2] Janjkov B. B.: Fizika plazmy 17, 1991, 521

[3] Vichrev V. V., Braginskij S. I.: Voprosy teorii plazmy 10, Moskva, Atomizdat 1980, p. 243

[4] Kubeš P. et al.: Czech. J. Phys. B 35, 1985, 155

This research has been conducted at the Department of Physics and up to this time has not been included in any research project.

ATOMIC PHYSICS OF SYSTEMS WITH EXTREME PARAMETERS

L. Drska, M. Sinor and J. Vondrasek

Faculty of Nuclear Sciences and Physical Engineering, CTU, Břehová 7, 115 19 Praha 1

Key words: Atomic structure, Average atom model, EOS, transport coefficients, stopping power

The updated version of the microphysics subpackage of the MIRIAM code [1], a general code for simulation of pulsed systems with high energy densities, includes the consistent description of the high-Z ion physics based on Thomas-Fermi Corrected / Self Consistent field Average Atom Model (TFC/SCAAM) approaches. The programs of this subpackage have been applied to calculate the equation of state, thermal and electric conductivity of dense systems and energy losses of fast ions in non-ideal plasmas.

Average Atom Model: In the ion-sphere average atom model (AAM) a nucleus of charge Ze is located at the center of a spherical cavity with radius R_0 determined by the ion number density. The density of bound and free electrons inside the sphere is restricted by the neutrality condition.

In the implemented ion-sphere AAM several approximations are introduced: 1) Spherical symmetry of the system is supposed. 2) The exchange and correlation effects are evaluated in the local density approximation. 3) Approximate treating of band structure is used. 4) Free electrons are taken in the semiclassical approximations. 5) Relativistic effects are described in the first order of the perturbation theory.

On the basis of the density functional theory it can be shown that for the system outlined above, having temperature T and chemical potential μ, there exists a functional of density having an absolute minimum in the state of LTE. The variation of this functional with respect to the distribution functions of electrons and wave functions yields the set of one-particle Schrödinger-like equations that are solved self-consistently with the above mentioned restriction on the charge neutrality of the ion sphere and results in obtaining of the average ionization state, density of bound and free electrons, etc. Using these data thermodynamic characteristics can be calculated. Detailed description of this model with selected results can be found in [2]. Fig.1 shows one of these results.

Interaction of ions and electrons in cluster model approximation. For mutual interaction of ions and electrons in the plasma cluster model with two types of clusters are used: 1) The cluster of ions consists of N randomly distributed ion spheres with radius R_0 in positions $\{R_j,\ j = 1,...,N\}$. 2) The cluster of free electrons is formed by free electrons distributed in ion spheres that have the same positions as in the case of ion cluster. Model for the interaction of clusters is defined by potential of interaction between: 1) ion cluster and ion clusters, 2) ion cluster and free electron clusters, 3) free electron cluster and free electron clusters.

Introducing the structure factor $S(k)$ for description of the average ion distribution in the cluster we can find the average potential energy of the ion cluster in the field of ion clusters associated with one ion sphere and analogical quantity for electron cluster in the field of electron clusters.

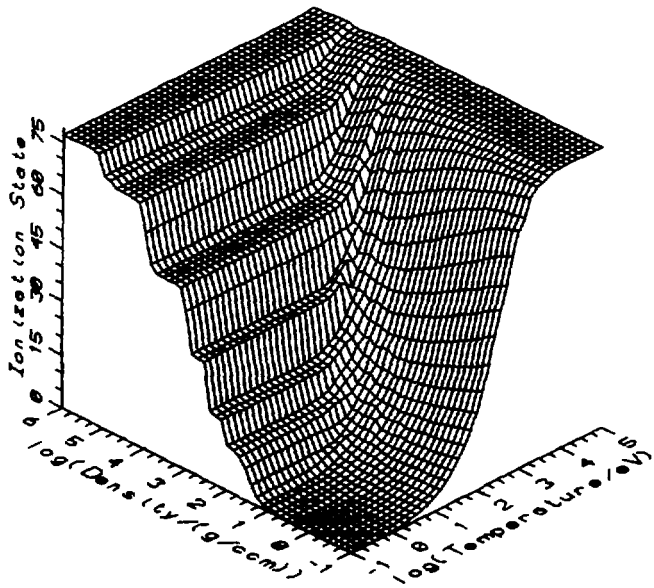

Fig. 1 Average ionization state of gold

Kinetic theory of ions and free electrons in the plasma: The atomic structure data obtained by SCAAM and the cluster interaction model are used in the formulation of the kinetic equations. BBGKY equations hierarchy is truncated after the 2/nd equation. This procedure gives the transport equation with collision integral in the modified (extended) Balescu-Lenard form. The collision integral can be transformed in the Landau-like form. In this expression formulas for stopping power and diffusion coefficients can be localized. Electron transport coefficients (thermal and electrical conductivity) are obtained from the solution of the stationary linearized kinetic equation [3].

The results for the conduction coefficients and stopping power of ions in plasmas are presented in [4].

References:

[1] L. Drska, R. Liska, M. Sinor and J. Vondrasek: Miriam package development: new results. In: Laser Interaction with Matter, p.360, G. Velarde et al., eds.. World Scientific, Singapore 1989.

[2] L. Drska and M. Sinor: Average Atom Model and EOS Calculations: DFT Approach. Laser and Particle Beams, to be published (1992).

[3] L. Drska and J. Vondrasek: Some aspects of the unified model of non-ideal high-parameter plasmas: electron EOS and conduction coefficients. Laser and Particle Beams 7, (1989), 237.

[4] L. Drska, M. Sinor and J. Vondrasek: Self-Consistent AA Model and Calculation of Atomic Characteristics of Systems with Extreme Parameters. Laser and Particle Beams, to be published (1992).

This research has been conducted at the Department of Physical Electronics of the Fac. Nucl. Sci. & Phys. Eng. as a part of the research project "SUPER" and has been supported by an IBM Academic Initiative grant.

BREAKDOWN VOLTAGE OF THE SURFACE GLOW DISCHARGE

S. Pekárek, J. Rosenkranz

CTU, Faculty of Electronical Engineering, Technická 2, 166 27 Prague 6

Key words: Glow discharge, Surface discharge, Breakdown voltage, Plasma display, Configuration of electrodes

During the past few years, work on development of gas discharge displays (GDD) has progressed rapidly. One of the modifications of the GDD involves the use of so-called surface discharge, that is the discharge between anode and cathode laying side by side on the same substrate [1,2].

An important electrical parameter which determines conditions for driving electronic circuit of the GDD is breakdown voltage. This voltage for nonhomogeneous electric field can be expressed as [3]:

$$\int_{Ui}^{Ub} \mu \, dU = \ln(1 + 1 / \Gamma)$$

where μ is the electron multiplication factor along the flux line and Γ is the coefficient of the secondary emission.

The electron multiplication factor is therefore influenced by the electric field distribution. This breakdown voltage depends upon the configuration of electrodes and geometry of the discharge chamber.

The breakdown voltage for the surface glow discharge in a small volume was studied experimentally. The schematic view of the discharge chamber is shown in Fig.1.

The gap between anode A and cathode C is denoted as g, cathode width is denoted as w and symbol d is used for the distance between low and upper glass desks which create the discharge chamber. The electrode configuration which was screen printed with nickel paste ESL 2555 is shown in Fig.2.

On the left side of this figure nine segments of cathodes can be seen which are situated in different distances around the square anodes. These cathode segments have a width of 1 and 2 mm. On the right side of this figure three are six segments of cathodes which are situated perpendicularly to the common anode. The distances among cathode segments and anode are given in Tab. 1.

The breakdown voltage was measured in penning mixture Ne-Ar (99,5 : 0,5%) for various filling pressures and gaps. The data collected are shown in figs 3 and 4.

Breakdown voltage as a function of product p.g (torr.mm) for segments which are oriented perpendicularly to the anode (see Fig. 1 - right side) for distance between lower and upper glass desk d=0,8 mm is shown in Fig. 3.

Breakdown voltage as a function of ratio of the cathode segment width and anode - cathode gap g for distance d=1,4mm is shown in Fig. 4.

From this figure it is seen that with the increasing value of the ratio (w/g) the breakdown voltage diminishes to the certain constant value. It is also obvious that the breakdown voltage reaches its minimal value if the gap between anode and cathode equals or is smaller than the cathode segment width.

A proper choice of the anode - cathode gap plays an important role for obtaining the minimum value of breakdown voltage and this diminishes the demands for driving electronic of GDD.

References:

[1] Munisamy anandan, 1981, IEEE Trans. on El. Devices, Vol. ED-28, No. 9, 1035-1042

[2] Yukio Okamoto, 1983, IEEE Trans. on El. Devices, Vol. ED-30, No. 8, 904-907

[3] J. R. Acton, Cold Cathode Discharge Tubes, London 1963

This research has been conducted at the Department Physics as a part of the research project "Plasma Displays" and has been supported by Tesla Holešovice.

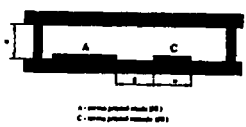

Fig. 1. DISCHARGE CHAMBER

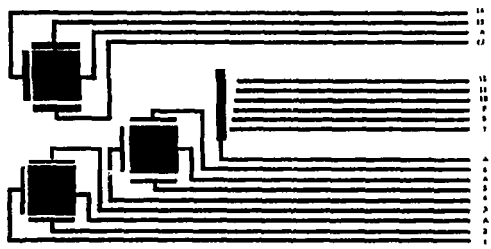

Fig. 2. ELECTRODE CONFIGURATION

Segment N°	1	2	3	4	5	6	7	8
g [mm]	0.79	0.53	0.96	1.17	1.63	1.38	0.79	1.02
Segment N°	9	10	11	12	13	14	15	
g [mm]	1.21	1.39	1.59	1.80	1.59	1.20	1.37	

TABLE 1

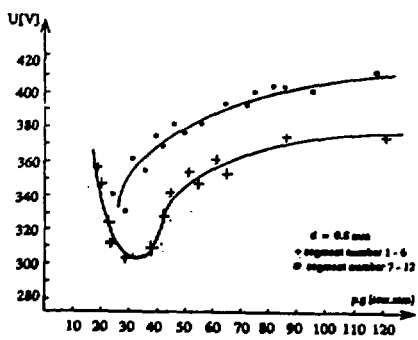

Fig. 3.: Breakdown voltage versus (p.g)

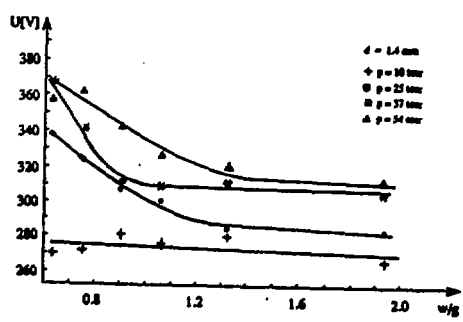

Fig. 4.: Breakdown voltage versus (w/g)

ELECTROMAGNETIC PLASMA LAUNCHERS

J. Maloch

Faculty of Electronical Engineering, Czech Technical University, Technicka 2, 166 27 Prague 6

Key words: accelereation, plasma accelerators

The theory and design of plasma accelerators working under atmospheric pressure scored big advances in recent years. The modification of these accelerators, that can be used as ultraspeed propulsion systems, are often called electromagnetic plasma launchers (EML).

The solid body acceleration basic equations for linear type of EML are

$$d/dt\,[\,L(x)I\,] + RI + Q/C_0 = 0 \tag{1}$$

$$d/dt\,(\,mv\,) = F_I + F_P \tag{2}$$

$F_I = (1/2)\,L_1 I^2$; $F_P = \frac{P_0 S}{(1+Sx/V_0)}$

$L(x) = L_0 + L_1 x$; $R = R_0 + R_p$; $m = m_p + m_0 + m_1 x$

where x is the distance of the centre of mass from the discharge initiation point, I is the discharge current, R_0 is the resistance and L_0 the inductivity of the power supplies, R_p is the constant plasma resistance, Q is the charge and C_0 the capacitance of the capacitor battery, L_1 is the inductivity of the unit electrode length, F_I is the electromagnetic force, F_P is the pressure force, m_p is the initial mass of the plasma cluster, m_0 is the mass of the accelerated solid body, m_1 is the mass of the air in the accelerator per unit electrode length, S is the electrode cross section area, P_0 is the initial pressure and V_0 is the initial volume.

The schematic diagram of the accelerator is shown in Figure 1. Supposing the solid body acceleration is only caused by electromagnetic force, the equation (2) can be rewritten in the form :

$$d/dt\,(\,mv\,) = (1/2)\,L_1 I^2 \tag{3}$$

and one obtains [1] for velocity

$$v(t) = \frac{p(t)}{[\,(m_p + m_0)^2 + 2m_1\pi(t)\,]^{0.5}} \tag{4}$$

$$p(t) = \int_0^t (1/2) L_1 I^2\,dt \;;\; \pi(t) = \int_0^t p(t)\,dt \tag{5}$$

The acceleration process can be also influenced by the pressure force F_P caused by a wire explosion at the moment of the discharge ignition. Considering the fact that no exact data for plasma temperature after the explosion are known the isothermic behaviour of the plasma is supposed. For the case when the solid body acceleration is caused by the pressure force F_P only, the equation (2) has the form

$d/dt\,(\,mv\,) = \frac{P_0 S}{(1+Sx/V_0)}$

and the velocity is

$v(x) = \frac{(2P_0V_0)^{0.5}}{m_p+m_0+m_1x}[(m_p + m_0 - m_1V_0/S)\ \ln(1 + Sx/V_0) + m_1x]^{0.5}$

In fact the pressure and electromagnetic forces do not occur separatively. The theoretical analysis mentioned above was also tested experimentally. The measured (curve 1) and calculated (curve 2) path characteristics of velocity for differrent values of solid body mass and condenser battery capacitance $C_O = 1,77.10^{-4}\ F$ and voltage $U_0 = 10^4\ V$ in Figure 2 ($F_I > 0$; $F_P = 0$) and Figure 3 ($F_P > 0$; $F_I > 0$).

The accelerating process for small values of condenser battery capacitance is mostly caused by the pressure force F_P, but with an increase of the condenser battery capacitance the electromagnetic force begins to be the most important one.

The output velocity for different capacitances and the existence of both forces F_I, F_P can be at the distance of 1 m about 4000 m/s.

References:

[1] Kulhanek P., Maloch J., Valenta R.: Acta Phys.Slov.37 (1987), 130.

[2] Uzel M., Kulhanek P., Maloch J.: Acta Phys.Slov.39 (1989), 129.

[3] Maloch J., Kulhanek P., Pichal J.: Acta Phys.Slov. (in print)

This research has been conducted at the Departement of Physics, Faculty of Electronic Engineering.

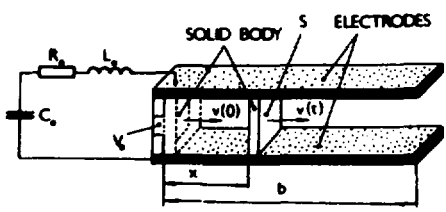

Figure 1.

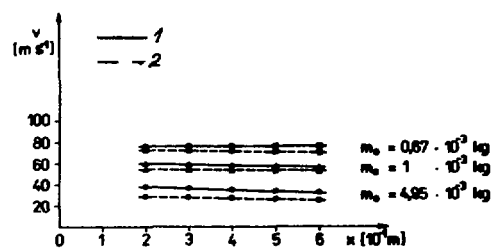

Figure 2.

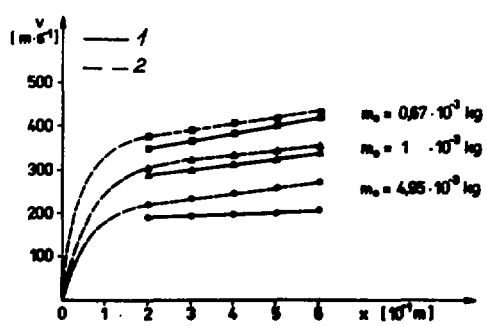

Figure 3.

Section 4

PHYSICAL ELECTRONICS AND OPTICS

THE MAGNETRON PLASMA OPTICAL DIAGNOSTICS

F. Hanitz, J. Lego, S. Pekárek, J. Rosenkranz

Dpt. of Physics, Electrotechnical faculty CTU, Technická 2, 166 27 Prague 6.

Key words: Magnetron, discharge plasma, deposition process, optical diagnostics

The basic parameters of the planar magnetron discharge plasma used for titanium thin films deposition were studied. The magnetron filling gas was argon. For the plasma parameters determination the spectroscopic methods were applied. The obtained spectra in the range 390 ÷ 450 nm (the gas pressure 0,1 ÷ 2,5 Pa, the magnetic coil current 1,4 ÷ 2,6 A, the discharge current 0,4 ÷ 1,8 A) were used for the selection of the suitable neutral argon, ionized argon and neutral titanium spectral lines.

For the electron temperature determination the method of the dependence of the spectral line intensities on the excitation potential used. It was found, that the electron temperature differs for different ranges of the excitation potential. The temperature 0,48 eV was evaluated from the ionized argon line intenzities (excitation potential 19,7 ÷ 22,6 eV). This temperature is independent of the discharge parameters. The temperatures evaluated from the neutral titanium line intensities (excitational potential 3,1 ÷ 5,7 eV) are given in the Tab. I.

Tab. I.

	p=0.1 Pa			p=0.5			p=2.5		
	1,4	2,0	2,6	1,4	2,0	2,6	1,4	2,0	2,6
1,8	-	0,615	0,602	-	0,594	0,594	0,604	0,605	0,598
1,6	0,608	0,602	0,612	0,583	0,584	0,599	0,599	0,618	0,590
1,4	0,611	0,611	0,622	0,590	0,595	0,601	0,597	0,611	0,595
1,2	0,614	0,616	0,620	0,600	0,605	0,604	0,599	0,585	0,587
1,0	0,624	0,615	0,626	0,601	0,608	0,604	0,600	0,561	0,579
0,8	0,618	0,631	0,622	0,615	0,617	0,596	-	0,561	0,576
0,6	0,633	0,637	0,650	0,611	0,601	0,612	-	-	-
0,4	0,650	0,658	0,644	0,628	0,636	0,622	-	-	-

These values are significantly higher and depend weakly on the discharge parameters (especially on the discharge current). The neutral argon lines were not used for the temperature determination because of the narrow range of the excitation potential. The thermodynamics nonequilibrium is caused by the magnetic electron trap, necessary for the discharge existence at such a low pressure [1].

The values of both temperatures mentioned above are rather small for the ionization degree explanation, using the ionized and neutral argon line intenzities, and corresponding to the measured line intensities. Corresponding to the measured line intensities in LTE the effective ionization temperature was established (See Tab. II.). This temperature depends practically on the pressure only.

For the determination of the titanium atom concentration in the discharge, it is necessary to know the ionization degree both for titanium and argon. For titanium ionization degree the temperature determined from titanium lines and for argon ionization degree the effective ionization temperature were used, with respect to different

temperatures in the region of the titanium ionization potential (6,84 eV) and argon ionization potential (15,76 eV).

Tab. II.

	p=0.1 Pa			p=0.5			p=2.5		
	1,4	2,0	2,6	1,4	2,0	2,6	1,4	2,0	2,6
0,4	0,786	0,781	0,782	0,838	0,828	0,822	-	-	-
0,6	0,790	0,782	0,783	0,839	0,826	0,826	-	-	-
0,8	0,791	0,783	0,783	0,840	0,827	0,827	-	0,894	0,873
1,0	0,794	0,787	0,786	0,843	0,829	0,829	0,895	0,889	0,873
1,2	0,793	0,786	0,788	0,843	0,832	0,832	0,896	0,892	0,890
1,4	0,793	0,788	0,789	0,846	0,834	0,834	0,896	0,899	0,891
1,6	0,797	0,790	0,790	0,844	0,833	0,833	0,896	0,903	0,892
1,4	-	0,799	0,790	-	0,836	0,836	0,896	0,900	0,894

The rate of the titanium and argon neutral atoms can be calculated from the rates of the neutral titanium and argon line intensities. Using the ionization degrees the rate of the titanium and argon total concentration can be calculated too. Knowing the pressure, the total concentration of the titanium atoms can be calculated. (See Tab. III.)

Tab. III.

	p=0.1 Pa			p=0.5			p=2.5		
	1,4	2,0	2,6	1,4	2,0	2,6	1,4	2,0	2,6
0,4	1,162	0,927	0,304	7,008	5,619	4,646	-	-	-
0,6	1,606	1,267	1,239	8,052	5,684	6,327	-	-	-
0,8	1,895	1,734	1,175	9,950	8,772	6,785	-	8,406	34,47
1,0	2,740	1,827	1,662	10,75	10,49	9,113	17,22	34,10	48,97
1,2	3,095	2,286	2,042	12,87	11,29	10,72	23,49	54,01	64,06
1,4	3,652	2,547	2,443	12,20	12,12	11,36	64,25	81,47	77,99
1,6	3,743	2,620	2,568	13,65	12,55	13,86	73,30	98,64	76,22
1,4	-	3,667	2,660	-	15,67	14,23	82,90	84,84	93,29

Comparing the total titanium atoms concentration with the measured deposition rate, the mean velocity of the titanium atoms near the substate can be obtained. This velocity (approximately 10^4 m/s) is in a good agreement with [2].

Conclusion : The basic parameters influencing the thin film properties (i. e. the total titanium atoms concentration and the mean velocity of their moving to the substrate) can be obtained from the measured spectral line intensities of the neutral titanium, neutral argon and ionized argon.

References:

[1] Vosen J. L., Kern W.: Thin Film Processes, Academic Press 1978.

[2] Musil J., Vyskočil J.: Tenké vrstvy nitridu titanu, Studie ČSAV 1989 Academia Praha

This research has been conducted at the Department of Physics of the Electrotechnical Faculty as the research project "The Optical Diagnostics" through Czech Technical University grant No 8036.

USE OF OPTOELECTRONIC DEVICES IN DOSIMETRY

L.Musílek and A.Dařícková

Faculty of Nuclear Sciences and Physical Engineering, CTU, Břehová 7, 115 19 Praha 1

Key words: Radiation effects, dosimetry, gamma radiation, neutron radiation, optoelectronic devices, photo-couplers, glass fibres, fibre light guides.

The radiation damage of semiconductor devices has been studied for many years for the purposes of their use in nuclear industry, cosmic space, military instrumentation and sometimes also dosimetry. In the recent period optoelectronic devices have started to replace "classical" electronics in some applications and therefore also interest in their radiation damage has started to grow. Our research has also turned to this area, and has not only intended to study the extent of damage by radiation doses but its possible usefulness for dosimetry too. The optoelectronic system consists generally of three main parts: a light emitter, a light guide and a light receiver. Ionizing radiation doses usually cause the degradation of all three components. Therefore changes of both only one part and all the system may be investigated (e.g. [1], [2], [3]). Our research has concerned photo-couplers, with the irradiation of the whole system and separate parts too, and glass light guides, where neither emitter nor detector has been irradiated.

If a photo-coupler is placed into a radiation field, all three basic parts degrade and contribute to the decrease of one of the basic parameters, the current transfer ratio (CTR). We have used Czechoslovak photo-couplers made by Tesla Blatná, from which the type WK 164 12 has appeared to be the most promising for dosimetric purposes. Therefore the following results are those obtained with this type of photo-coupler.

Dose response for gamma radiation (Co 60 in air) is not very dramatic and a slow decrease of CTR is registred in the range of tens and hundréds Gy (half of the original CTR value is reached at 500Gy). These are radiation sensitivities which might be very useful for some radiation technologies. The sensitivity to fast neutrons (Cf 252 and fast spectrum of IBR-2 reactor) is much more pronounced and a tissue dose of 0,5Gy is easily detectable, i.e., such a device is suitable for accidental fast neutron dosimetry. The fading of the response is negligible at room temperatures. In comparison with most semiconductor devices used as dosimeters, low temperature dependence in the region of interest is profitable, being from -10°C to +40°C lower than 5%. On the other hand the dose dependence is not linear (but the formula proposed in [4] for the radiation degradation of LED light output may be used for linearization). Nonuniformity of the properties of various pieces is still another complicating factor which needs the selection of photo-couplers.

Irradiation of LEDs and phototransistors gives some evidence about the contribution of various parts of the device to the overall degradation. The decrease of LED light output represents approx. 2/3 of the response, but the contribution of phototransistor and light guide also is not negligible.

Photo-couplers are quite sensitive electronic devices - especially to fast neutron radiation - and care must be taken if they are used in instruments designed to work in neutron radiation fields. On the other hand they offer a simple possibility for monitoring

fast neutron doses in the range of tenths Gy to hundreds Gy and gamma doses in the range of hundreds Gy to tens kGy.

Another possibility how to get a dosimeter for the dose range of tenth Gy and higher is to use only a light guide and to evaluate the formation of colour centres by irradiation. Therefore we have studied the response of various glass optical fibres to gamma and neutron radiation.

Material for waveguides must fulfil not only dosimetric requirements but also optical (suitable refraction indexes) and mechanical (good flexibility and fracture-resisting). From each standpoint we have tried a few various fibres. The first one has been made of dosimetric Al–P (alumino-phosphate) glass cladded by Kovar glass. The dosimetric qualities of this glass are good, doses (Co 60 in air) of the order of 0,1Gy are easily measurable and fading is low. On the other hand the fibre is relatively fragile and its manipulation is delicate. Better mechanical properties have been observed at GI (gradient index) fibre made of silicon doped by GeO_2 and P_2O_5 cladded by polymer. Dosimetric properties are similar to Al–P glass.

The sensitivity to fast neutrons has been measured for GI fibre and it has been found to be approximately 25 times lower than the sensitivity to gamma-radiation. This type of fibre seems to be the most promising for integrating dosimetry of gamma radiation. Another type, PCS (polymer cladded silica) fibre gives a well – pronounced response to Cherenkov radiation, being irradiated by high dose rates (of the order of Gy per minute).

For further studies both photo-couplers and GI and PCS fibres may be recommended. These types of dosimeters are a matter of interest for instance for nuclear industry and radiation therapy. Cooperation with the Dukovany nuclear power plant has started not long ago and some fibres were placed into the boxes of the primary circuit.

References:

[1] M.Šandera et. al.: Radioisotopy (ÚVVVR Praha) 24 (1983) 383.

[2] F.Paic et al.: Nucl. Instr. Meth. 205 (1983) 385.

[3] K.Yasuda et al.: Phys. stat. sol. (a) 88 (1985) 389.

[4] L.W.Aukermann, M.F.Miles and M.McColl: IEEE Trans. Nucl. Sci NS-13 (1966) 174.

This research has been conducted at the Department of Dosimetry and Application of Ionizing Radiation as a part of the research project "Radiation damage of optoelectronic devices and their dosimetric use" and has been supported by Czech Technical University grant No. 8052.

NEW MICROTRON IN OPERATION AT FJFI CTU, PRAGUE

M. Vognar, Č. Šimáně, P. Malinský

Faculty of Nuclear Physics and Physical Engineering CTU, Břehová 7, 115 19 Praha 1

Key words: Microtron, gamma-n neutron sources, activation analysis, electron optics, electron accelerators

In November 1990 the first internal electron beam was accelerated in the new microtron MT 25, which replaced the previous MT 22,for more than 10 years in use in the microtron laboratory and dismantled in January 1990. The main parts of the new accelerator having been manufactured and tested already, the assembling could start immediately. The most significant difference between the old and the new microtron, designed and developed in close collaboration with JINR Dubna, consists of the omission of the acceleration chamber, the acceleration taking place between the pole pieces of the vacuum tight iron magnetic yoke with magnetization coils accomodated inside [1]. The major advantage of this so called chamberless microtron is the complete removal of all for checking inaccessible vacuum joints and in easy access to the acceleration space by lifting the roof of the magnetic yoke enabling at the same time an uncomplicated exchange of the only rubber sealing in the microtron if dammaged by radiation. For complete description of the new microtron see [2]. On this place only the main features are mentioned.

A new adjustable high stability DC supply up to 400 A at 12 V was developed for the main magnet, alimented from 50 c/s distribution network, which eliminated the old one fed from a 400 c/s rotary convertor, left for alimentation of HF generator only. Another current supply of the DC pulsed type, less power consuming, is in the final state of development.

The HF system from the old microtron was used, however seriously modified by matching the wave guide line to the European standard and substituting the ferrite isolator for a circulator. The matching of pulsed magnetron HF generator to the resonant acceleration cavity was improved considerably and operaration stability increased as a result of these modifications.

In order that the output electron energy could be varied in large limits, a new extraction system was developed. Although based on the same principle as that in JINR, an entirely different solution of the driving mechanism for the telescopic iron output channel has been adopted, enabling the withdrawal of electrons tangentionally from the 8. to the 25. orbit. Thus, the energy can be varied in 0,6 MeV steps from 5 to 15 MeV or in steps of 1 MeV from 8 to 25 MeV with the use of two types in interchangeable resonant cavities

In the initial period of operation 7 μA internal target electron current from the 17. orbit was obtained immediately, which raised successively up to 17 μA. These assembling of the external electron guide lines started in the first half of 1991. This transport system comprises two magnetic dipoles, one of them as an integral part of the internal extracting system and deflecting the beam from all selecteable orbits to a fixed direction, the second deflecting the beam to three experimental posts for electron, bremsstrahlung and neutron irradiations. The transverse dimensions of the beam passing through evacuated 50 mm ID tubes must remain within internal openings of all deflecting and focusing

elements and are controlled by the main quadrupole doublet inserted between the two dipoles. Additional two quadrupole doublets are available for the control of the spot size and beam divergence on the target when placed on the final sections of the electron guides. Before having been installed, all deflecting or focusing elements were submitted to precise measurements of magnetic field distribution from which their optical parameters were calculated. The coincidence with design parameters was found to be satisfactory. The initial set of magnetic current values for all possible energies and beam paths was calculated by special programm before starting the experiments with real beam. The initially supposed beam positioning system along the transport line had to be omitted because of lack of funds in the last years. Thus, the tuning of the whole transport system became very difficult and one had to proceed by succesive adding of individual components which proved to be a very tedious procedure, during which the microtron had to be filled with air and high vacuum restored again many times. The performance of the whole transport system in the most difficult configuration, represented by the 4 m total path length leading to the neutron irradiation post, with two deflections and 30 mm guide tube ID at the end, was tested with electrons from the 14. and 24. orbits. The currents in optical elements giving the best results were close to those calculated before.

An unexpected decrease of the electron current from higher orbits was observed probably due to some magnetic field inhomogeneities not supposed before. The real magnetic field configuration, especially the required homogeneity could not be tested because the lack of a precise magnetometer. The field has to be corrected experimentally by correction coils, which again is a time consuming procedure.

Several convertors have been prepared for measurements of neutron yield from gamma-n reactions in Pb, U, D_2O and in their combinations. The Pb and U convertors are water cooled. Calculations of neutron yields from Pb and U convertors in combination with D_2O or Be convertors on the base of monochromatic cross sections data were performed as well, to enable a comparison with the results of the measurements, which started at the end of November when the whole microtron installation was put into operation at the output energy of 22 MeV. For the moment the results of the neutron measurements are not available and will be presented at the Workshop 92.

References:

[1] M. Vognar, A. G. Bělov, Č. Šimáně, V. N. Pokrovskij: Electromagnet for an electron accelerator, CSFR Patent 239494, PV 5538-84.

[2] Č. Šimáně, M. Vognar, R. Černý: Internal Research Report SPZV, III-9-1/08, FJFI CTU, 1991.

This research has been conducted at the Central microtron laboratory, from 1991 at the Chair of Nuclear Dosimetry and Application of Radioisotopes of the Faculty of Nuclear Physics and Physical Engineering, under research project III-9-1/08 of the State plan of research and under project numbers 4025 and 4026 KDAIZ FJFI and has also been supported by Czech Technical University grant No. 8053.

QUANTUM NONDEMOLITION MEASUREMENT OF THE PHOTON NUMBER

V.Sochor, G. Lončar*, I. Paulička*, J. Zhang***

* Faculty of Nuclear Science & Physical Engineering, CTU, Břehová 7, 115 19 Prague 1
** Department of Optical Engineering, Xian Institute of Technology, P.R.China

Key words: Nonlinear optics, Optical Kerr effect, Fibre optics, Optical fibre interferometer

An experiment of quantum nondemolition (QND) measurement of the photon number using only one single-mode optical fibre is reported in this paper. Two beams with different wavelength counter-propagate in a single-mode optical fibre and interact with each other in optical Kerr medium. The value of optical Kerr constant is measured by means of this scheme. A relationship between quantum nondemolition measurement and direct detection of the photon number is obtained.

In QND measurement the photon number is detected without disturbing its free motion state. The QND detection was first proposed to be used in overcoming the quantum limit in detecting gravitational waves [1, 2], but recently the relationship with quantum optics has been established.

The experimental configuration overcomes the instability [3] of the interferometer sensitivity and the temperature compensation which should be considered in Mach-Zehnder interferometer. This configuration can also be used in measuring the optical Kerr coefficient nk of silica fibres.

A 1.06 μm cw YAG laser beam which serves as a signal light propagates counter-directionally to a probe beam of He-Ne laser at 0.6328 m in an optical single-mode silica fibre. Used fibre is an optical Kerr medium with a length of 300 m. The YAG signal beam is chopped with a frequency of 540 Hz so that the photon number can be measured by means of lock-in amplifier. A prism is used to separate two different wavelengths. The power of YAG laser is 11.5 mW at the output of the fibre while the probe He-Ne laser power is about 100 μW. A polarizer and a quarter wave plate are set in front of one input end of the fibre to obtain the probe beam with a circular polarization state. A phase retarder is placed at the opposite end of the fibre to convert the output probe beam to a linearly polarized state. The prism does not change the polarization of both probe and signal beams. This linearly polarized infrared beam modulated by the chopper with a duty ratio of 0.5 is coupled into the fibre in the direction opposite to that of probe light. These two optical signals interact in the Kerr medium.

A silica optical fibre can be considered as a linear optical medium when transmitting low optical power. But when the high power is coupled into the fibre, the refractive index of the fibre is not a constant any more due to the optical Kerr effect being modulated by the intensity of the signal and it can be expressed as :

$$n = n_0 + n_k P_s / A_e \qquad (1)$$

where n_0 - refractive index of the core of the fibre, n_k - Kerr constant of the fibre, P_s - intensity of signal light, A_e - effective area of the fibre core.

Modulated refractive index of the medium will cause modulation of the phase of the probe wave and produce a phase shift. The phase shift of the probe beam can be derived from the intensity changes of He-Ne laser beam detected by a lock-in amplifier. When YAG laser signal is blocked the phase change of the probe beam is zero. Obviously, this change is caused by the Kerr effect. The optical Kerr coefficient can be given by the relation:

$$n_k = cA_e\delta\Theta / \Omega_p L P_s \tag{2}$$

where c - vacuum velocity of light, $\delta\Theta$ - phase shift of the probe light, Ω_p - frequency of the probe wave, L - interaction length.

The value of nk calculated by equation (2) is 4.8×10^{-20} m^2/W, which is close to results published by other authors [4, 5, 6]. The photon number of the signal wave can also be obtained from this phase shift of the probe beam. The theoretical relationship between the signal photon number and the probe phase shift is expressed:

$$N_s = \pi\, c\, A_e\, \delta\Theta / \Omega_p\Omega_s\, h\, f_m\, L\, n_k \tag{3}$$

N_s - signal photon number per modulated pulse, Ω_s - frequency of the signal wave, h - Planck constant, f_m - chop frequency of signal.

In the experiment the modulated signal with power of 11.5 mW leads to a phase shift of the probe beam of 25.6 mrad, then the photon number of the signal wave per pulse is calculated as 5.63×10^{13}. This photon number is obtained nondemolitionally without changing the free motion state of the signal beam. The output power of the signal beam was also detected demolitionally using a power meter. By changing the power of signal light the correlation was established between the QND measurement of the photon number and the direct detection of the photon number. The results obtained by these two methods are in a good agreement.

In this experiment, the photon number of the signal wave is detected nondemolitionally. The classical relationship between the QND measurement and the direct detection of the signal photon number is established. This one-single-mode fibre scheme has a lower noise output than two fibre configuration proposed in [1] and there is no need of the temperature compensation.

References:

[1] Caves C.M., Thorne K.S., Drever R.W.P., Sandberg V.D., Zimmerman M.: Rev. Mod. Phys., 52(1980), 341.

[2] Milbutn G.J., Walls D.F.: Phys. Rev. A, 28(1983), 2065.

[3] Imoto N., Watkins S., Sasak Y.: Opt. Comm., 61(1987), 159.

[4] Paulička I., Sochor V.: Proc. Int. Conf. "Applied Optics '91", Prague 1991, pp. 191.

[5] Davison A., White I. H.: Opt. Lett., 14(1989), 802.

[6] Mikhailov A. V., Wabnitz S.: Opt. Lett., 15(1990), 1055.

This research has been conducted at the Department of Physical Electronics, Faculty of Nuclear Science & Physical Engineering, CTU Prague as a part of the research project "4012 - Guided optical waves" and has been supported by CTU grant No. 8055.

OPTICAL FIBER SECURITY SYSTEM WITH HIGH SENSITIVITY

M.Khodl, A.Gabrovski , V.Sochor, J.Resl, J.Pavel, P.Horák, P.Peterka

Department of Physical Electronics, Czech Technical University
V Holešovičkách 2, 180 00 Praha 8

Key words: fiber optics, interferometer, speckle pattern, coherent graininess, sensor, security system

The primary aim of our grant is the investigation of speckle pattern generated by intermodal coupling in optical fibers and the use of notions for design of sensitive security systems for the environment. The emphasis is placed on those areas where simple electromagnetic detectors and infrared detectors are not sufficient, particularly to the large surface regions or outdoor protection. In the following the simplified model of investigated system is described:

The output radiation from the multimode optical fibre when projected to the screen produces a random system of speckles with different intensity - a so called coherent radiation speckle pattern. On the assumption of the closed steady-state system (without environmental influences, without variations of laser dynamics etc.) composed of an ideal laser, an optical fiber, firmly placed detector in space (a system of detectors) and an electrical circuit, the speckle pattern is constant in time and its spatial distribution is also stationary (The whole speckle pattern changes its linear dimension proportionally to the distance between the fibre and screen, unlike the coherent graininess appearing when the laser light is scattered on rough surface.). It is possible to describe this steady-state by the equation of intensity distribution:

$$I(x,y,z) = \left| \sum_{m=1}^{N} a_m E_m(x,y,z) \exp(i\,[\,\Phi_m(x,y,z) - \Omega t\,]) \right|^2 \qquad (1)$$

where a_m is the polarization unit vector, E_m the amplitude, Φ_m the phase of the m-th mode and Ω is the angular frequency.

When an external disturbance changes the dimension or shape of the optical fibre, the guided mode acquires a phase shift which is different for each mode because of their different paths. The system is then open and time varying. Thus, the task is to detect the dependence of intensity changes in individual points of speckle pattern with respect to mechanical changes of the fibre (direct deformation of fibre, deformation caused by vibration of environment etc.).

Let $\delta\,\Phi_m$ is phase shift of the m-th mode in consequence of above changes. Then equation including a phase change will have this form:

$$I(x,y,z) = \left| \sum_{m=1}^{N} a_m E_m(x,y,z) \exp(i\,[\,\Phi_m(x,y,z) - \Omega t\,]) + i\,\delta\,\Phi_m(t) \right|^2 \qquad (2)$$

This equation describes a modal noise at multimode optical fibre communication. The optimum size and density of the speckle pattern can be reached by proper selection of the fibre parameters and radiation wavelength (e.g. low density can be reached using the single-mode fibre working under the cutoff wavelength).

Experimental part: the experiment was implemented with samples of optical fibres from the test production of ÚCHSKM ČSAV. All these fibres used in experiments were nonstandard. Finally, the optical fibre T675/P157 was chosen as optimal for experimentation a with gas-laser as a source. This is a gradient fibre with average core diameter 147 μm and with attenuation about 4dB/km on He-Ne wavelength. 15m fibre samples were used in the experiments. The position of fibre was tested in three modifications: casted into concrete brick (a), placed between non-flexible basis and flexible cover plane (b), placed between two layers of hard rubber (c).

Detector is composed of three fototransistors (Fig.). Their signal is AC coupled to the sum-amplifier after trimming up the amplification. Then it passes through four band-pass filters. The maximum signal level is expected in the range of 10-2000 Hz according to the ref.[1]. The band transmittivity center frequencies of the individual filters are 10, 100, 1000 and 10000 Hz. The values 10 and 10000 Hz are served only for check of proper range selection (small changes of voltage were expected in the band of 10000 Hz, the measurement precision was limited by fluctuation of laser radiation intensity in the range of 30 Hz).

High sensibility to mechanical distortion of the fibre and to the mechanical vibrations induced by a person walking in the surroundings where the sensing fibres are located has been proved by these experiments. The arrangements (b) and (c) have been working successfully. Arrangement (a) was not suitable, because of the too small elasticity coefficient of concrete brick used. The investigated system showed high sensitivity to individual events: it was able to detect the dropping of a 100 mg mass from the height of 1m.

A succeeding experiment was proposed in accordance to analog filter measurements. Digital filtering equipment of the output signal by 12 bit A/D converter with maximum sampling frequency 60,000 s^{-1} has been prepared. The obtained signal will be computer processed (FFT).

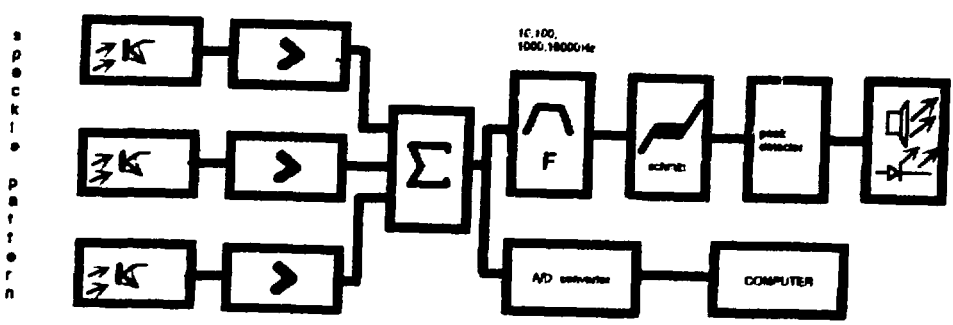

References:

[1] Chung-yee Leung, Cheng-hao Huang and I-fan Chang, "Optical Fiber Security system: a field test report", SPIE vol. 838 Fiber Optic and Laser Sensors V(1987), p. 365-371.

[2] John Markus,"Modern Electronic Circuits Reference Manual, McGraw-Hill.

This research has been conducted at the Department of Physical Electonics as a part of research project "Optical Fiber Security System with high sensitivity" and has been supported by Czech Technical University grant No. 8056.

COMPUTER GENERATED HOLOGRAMS

R. Houha, T. Jerie, P. Fiala, and J. Růžek

FNSPI, CTU, Břehová 7, 115 17 Praha 1

Key words: Holography, diffractive optics, computer generated holograms, binary holograms

1. Introduction

Holographic optical elements (HOE), e.g. elements transforming optical, IR and UV wavefronts by means of diffraction by quasiperiodic structure can be considered an important part of optics. The elements of the above-mentioned type are usable in general optics (phase correctors), as parts of optical processors (spatial filters, spectral analysers), mechanical engineering (beam shaping elements for laser cutting and marking) and laser technology (*focussing elements, wavefront transformers*).

Synthesized HOEs are superior to the optically recorded ones especially in generating wavefronts of a very complex shape and in spectral regions where the optical recording is rather complicated or simply impossible.

For these reasons synthesized HOEs are within the field of interest in all developed countries.

The generation of synthesized HOE can be divided in two parts:

a) Theoretical - computation and coding of the requested diffractive pattern

b) Experimental - physical recording of the synthesized HOE.

2. Objective and selected approach

Our project covers both the theoretical and the experimental part of the problem.

The design of the artificial interference pattern consists of the optimizing of the requested diffraction pattern using available degrees of freedom and in the coding of the optimized pattern. In optimizing the process we used technique of slightly distorting the input data to reduce the spatial bandwidth to be coded. In coding we concerned some kinds of binary coding for the sake of simplicity of their recording by available experimental means. The general interest is not only in obtaining the requested image or wavefront transformation but also in high diffraction efficiency of the synthesized HOE. Because the diffraction efficiency of usual synthesized amplitude HOEs is only several percent we tried to find out ways of converting such amplitude HOEs to the phase ones in order to increase efficiency. Because we are interested also in HOEs usable for IR and UV light it is impossible to use volume recording materials. That is the reason why we concentrated on relief photoresists gratings and especially on the ways of converting a thin hologram to the relief one.

3. Conclusions

The binary Lee holograms of simple objects have been designed and the influence of the limited dynamic range of the recording media on the quality of reconstructed image has been studied. The optimization of the input data has been carried out with the help of a computer-simulated one dimensional reconstruction.

To improve the possibilities of recording more complex grayscale synthesized HOEs we worked out the concept and design of the optical head for the eight channel optical plotter with dot size of about 1m. This recorder is prepared in cooperation with UTIA ČSAV.

In the experimental part of the research the following work has been done:

- Development of new technology for the production of the silver halide material intended for direct recording of the thin amplitude gratings by an optical plotter.
- Generation of binary holograms by a photographically reducing diffraction pattern obtained by an ordinary XY plotter.
- Introductory experiments with diffraction gratings recorded in photoresist.
- Verification of the production process based on converting the amplitude or phase grating to the relief photoresist grating.

This research has been conducted at Faculty of Nuclear Sciences and Physical Enginnering and has been supported by Czech Technical University grant No. 8057.

RED LUMINESCENCE OF Hg_2Cl_2 SINGLE CRYSTALS

Zdeněk Bryknar, Anna Koňáková, Pavel Jiroušek

Czech Technical University, Břehová 7, 115 19 Praha 1

Key words: luminescence, mercurous chloride, emission spectrum, excitation spectrum, thermally stimulated luminescence, exciton

Optical properties of Hg_2X_2 (X = Cl, Br, I) crystals have been widely investigated in the last decade because of their strong birefringence, good transparency in infrared spectral region, strong acousto-optic effect, and other interesting anisotropic physical properties. Therefore they are very convenient for the fabrication different of optical elements as polarizators, acousto-optic modulators, etc. However, mercurous halides decompose into Hg and HgX_2 under their irradiation with ultraviolet (UV) light at room temperature (RT). These structural defects are present in virgin crystals as well, and their concentration depends strongly on the quality of crystals. Some of these defects have luminescence [1] and this fact can be used to check the quality of the fabricated crystals [1,2]. Bryknar et al.[2,3] suggested that luminescent centres responsible for the blue emission and green I (513 nm) are formed by neutral Hg atoms interacting strongly in excited states with the neighbouring chlorine ions, and the green II (503 nm) emission is caused by the mercury dimers.

In this work, we focused our attention mainly on the red luminescence of Hg_2Cl_2, as up to now no successful attempt to explain this emission has been made. We wished to define, whether the red emission is of an intrinsic nature or whether it belongs to the structural defects of crystals. We looked also for the emission of free excitons.

For this reason we studied the following effects on Hg_2Cl_2 single crystals: X-ray excited luminescence, glow-curve of the thermally stimulated luminescence (TSL), and emission and excitation spectra of luminescence conventionally excited by UV lamp.

The method used for the measurement of the emission spectra a thermoluminescence (TSL) can be applied only when the electrons or holes released in the course of the warm-up samples are coming from only one kind of traps. In this case the glow-curve of TSL has a simple form, relatively narrow, without superimposition of the adjacent peaks. This condition was fulfilled for our samples. The measurement was carried out as follows: the samples were irradiated with X-rays (Cu anode, 93 μA, 43 kV) for 1 h at 82 K. Then they were warmed with the nearly linear increase of temperature and a glow-curve was recorded for the 800 nm wavelength. The emission intensity $I_{GC}(T_1)$ and measured temperature T_1 were stored in a computer memory. After further irradiation of samples with X-rays at 82 K the emission spectrum $I_M(L_1,T_1)$ was recorded in the course of the sample heating at the same temperatures T_1 as above; L_1 denotes a wavelength. Hence the true spectrum I(L) of TSL referred to a constant value of TSL intensity is

$$I(L_1) = I_M(L_1,T_1)/\left[\, I_{GC}(T_1) \cdot D(L_1) \,\right] ,$$

where $D(L_1)$ is spectral sensitivity of the detection.

The excitation spectra of Hg_2Cl_2 for the red luminescence measured at 300 and 82 K have a similar structure for excitation from the bulk and from the crystal surface,

however, the main excitation bands for excitation from the surface are shifted to the longer wavelength in comparison with excitation from the bulk. This can be understood if we suppose that the centres responsible for the red emission have the origin in the structural defects arisen in crystals after irradiation with X-rays or UV light at RT. The absorption bands of such centres are superimposed with the lower energy tail of the absorption edge so that if the concentration of these defects is higher near the surface, then the excitation bands for the excitation of luminescence from the surface will be shifted to the longer wavelengths.

The emission spectra of Hg_2Cl_2 in the red spectral region remarkably depend on the wavelength of excitation light, it means that there are more than one type of structural defects with red emission. Inside of the crystal mainly the defects with emission near 810 and 1200 nm are present and, in addition, near the crystal surface the centres with emission around 900 nm were found. From these facts it can be concluded that the emission of Hg_2Cl_2 in the red spectral region has its origin in the structural defects and cannot be interpreted as emission of self- trapped-excitons. By X-ray irradiation of Hg_2Cl_2, a part of structural defects is ionized and electrons are excited to the conduction band. The electrons are then caught either on some shallow traps or by the same defects so as to emit spontaneous red luminescence. If the irradiation is performed at 82 K, then the population of these shallow traps is stable. In the course of sample heating the electrons are released from traps and they recombine with the ionized luminescence centres and TSL is observed.

The results of the Hg_2Cl_2 red luminescence measurements can be summed up as follows: a) Luminescence of Hg_2Cl_2 in the red spectral region excited either with X-ray or UV light originates from the structural defects of the crystals and it is not of the intrinsic nature. b) It was for the first time that the thermally-stimulated luminescence of Hg_2Cl_2 was observed and its emission spectrum was found in the red spectral region, as well.It is assumed that this luminescence also originates from structural defects of crystals. c) There is no emission of free excitons of Hg_2Cl_2 even at 4.2 K under strong excitation by X-ray and UV light.

References:

[1] Bryknar, M.Procio, Č.Barta: Czech. J. Phys. B37 (1987), 1301.

[2] Z.Bryknar: Cryst. Latt. Def. and Amorph. Mat. 17 (1987), 219.

[3] Z.Bryknar, Č.Barta, M.Lébl:Czech. J. Phys. B27 (1977), 808.

This research has been conducted at the Department of Solid State Engineering as a part of the research project "Photolytical processes in crystals suitable for detection of electromagnetic ra-diation and for optoelectronics".

EFFICIENT CONVERSION OF LASER LIGHT INTO SOFT X-RAYS

L. Pína, M. Kálal, V. Kmeťík, G. Lončar, I. Ulrych

Faculty of Nuclear Sciences and Physical Engineering, CTU, Břehová 7, 115 19 Prague 1

Key words: Laser, soft X-rays, plasma, conversion

Interaction experiments of intense laser pulses (wavelength 1.06 μm, intensity 10^{12}W/cm^2) with planar solid targets made from C, Al, Cu and W are described. Laser plasma created this way is characterized by a very intense emission in the X-ray region from 100 eV up to several keV. Laser light to X-ray integral conversion efficiency was measured.

INTRODUCTION

The collimated beam from a laser can be readily concentrated with the help of a lens or a mirror to a spot size whose diameter can, in principle, be as small as the wavelength of the laser radiation. In addition, pulsed lasers can deliver their energy in very short pulses. The light intensities achievable with concentrated laser light are so high, that any material which is dense enough to absorb the laser light is immediately transformed into a hot plasma.

The laser light can penetrate into the plasma only up to the so-called critical electron density n_{ec} inversely proportional to second power of the wavelength. Most of the soft X-rays are generated in an overdense region. For a shorter wavelength laser (e.g. Nd:Glass laser) the distance between the critical density and the overdense region is relatively short and the absorbed energy is effectively transported to this region.

Laser intensity dependence was studied by several authors (See e.g. Ref. [1] and [2]) giving the best integral conversion efficiencies with intensities of the order of 10^{13}W/cm^2. The most suitable pulse durations were established to be around 3 ns. It was also confirmed that using target materials with different atomic numbers will lead not only to different integral conversion efficiencies but this approach may be used to tune the peak of the emitted X-rays to the desired wavelength. This last feature is of a considerable importance from the point of X-ray lithography, X-ray microscopy, X-ray radiobiological studies and X-ray laser (XRASER) studies.

Inspite of increasing number of published measurements of laser-generated plasma X-ray properties in the soft X-ray region there still remains a lot of work to be done. Moreover, results published so far usually exhibit some variations (only partly atributable to the differencies in experimental conditions and detection techniques). The aim of our experiments was meant as a small contribution to the existing body of knowledge in this area.

EXPERIMENTAL SETUP

As a source of the laser light our facility GOLEM was used. It consists of an Nd:YAG oscillator generating laser pulses of the order of 12 ns. After preamplification these pulses can be shortened up to 3 ns using Pockell's cell optoelectrical switch. Subsequently they are spatially filtered, preamplified again and sent through the chain of amplifiers and spatial filters to the target chamber. Optical insulation of the system is enhanced with

the help of one Faraday rotator and two polarizers. In our experiments laser pulse duration was 5 ns and the energy of pulses was in the range of 0.5 – 5 Joules. These parameters, together with the focal spot diameter of approximately 80 μm, provided intensities in the range of $(0.2-2)\times10^{13}$ W/cm^2. Planar targets made from C, Al, Cu and W were mounted on the rotating holder inside the target chamber which was equipped with the diagnostics of the incoming laser light (PIN diodes) and emitted X-rays (X-ray PIN diodes).

RESULTS

The highest conversion efficiency obtained in this experiment was 0.36 (for tungsten target). Notice, that the laser plasma as a source with characteristic dimensions about 100 μm emits 108W of power in the soft X-ray spectral region during a laser pulse.

A comparison of results with those obtained by MPQ group shown reasonable agreement. The differences observed can be atributed partially to slight variations in experimental conditions (laser wavelength, pulse duration and laser intensity on the target) and partially to differences in X-ray detectors used for these measurements (non-identical ranges of detection).

CONCLUSIONS

Laser generated plasmas are a very powerful soft X-ray source compared with other laboratory based soft X-ray sources. In this paper we have described our investigation of the X-ray conversion efficiency of C, Al, Cu and W planar targets in the range of 0.1 – 10 keV. Our experimental conditions were near optimal. Measured values are close to those published by other groups. So far we have measured the X-ray signals integrated over the region 0.1-10 keV. Our next step is to perform measurements of X-ray spectra using our especially designed 1-D CCD arrays as on-line detectors.

REFERENCES

[1] R. Sigel, K. Eidman, F. Lavarenne, and R.F. Schmalz: Conversion of laser light into soft x rays, Phys. Fluids B 2 (1), 199 (1990)

[2] Guang-ming Zen et al: High repetitive plasma x-ray source produced by a zigzag slab laser, J.Appl.Phys.67(8), 3597 (1990)

This research has been conducted at the Faculty of Nuclear Sciences and Physical Engineering as a part of the research project "Interaction of High-power Laser Beams with Matter" and has been supported by CTU as the research project No. 4010.

NONLINEAR OPTICS, OPTICAL PHASE CONJUGATION

P. Hříbek, I.Richter*, P.Peka***

*Faculty of Nuclear Sciences and Physical Engineering, CTU, Břehová 7, 11519 Prague 1
** Present address: Fritz-Haber Institute, Faraday Weg. 4-6, Berlin 33

Key words: photorefractive devices, optical phase conjugation, optical information processing

In the past years, optical data storage and real-time optical data processing operations have been demostrated in photorefractive materials such as lithium niobate ($LiNbO_3$), potassium niobate ($KNbO_3$), barium titanate ($BaTiO_3$), strontium barium niobate (SBN), bismuth silicon oxide ($Bi_{12}SiO_{20}$), bismuth germanium oxide ($Bi_{12}GeO_{20}$), bismuth titanium oxide ($Bi_{12}TiO_{20}$) and others. These crystals are known to be attractive for dynamic holography experiments and phase conjugation. Specific application of phase conjugation to nondestructive testing, image processing, imaging through phase-disturbing media, aberration cancellation, different types of interferometers, novelty filters, frequency and phase locking of several lasers, associative memories, optical data processing, and many other applications in the different fields of applied physics has already been demonstrated [1]. For these applications the precise knowledge of the specific properties of these crystals, and the physical proceses involved in such crystals, as well as spatial-frequency response of the recording parameters and polarisation properties of photorefractive diffraction are important.

Nonlinear optical properties of BGO and BTO sillenite crystals had been intensively studied in the degenerate two-wave mixing (DTWM) and degenerate four-wave mixing (DFWM) proceses and properties of $BaTiO_3$ single crystal in the self-pumped phase conjugation (SPPC) regime was observed.

Attention was directed to the energy conversion and diffraction efficiency at DTWM and especially to the PC reflectivity at DFWM at sillenite BGO and BTO. The influence of the optical activity to the diffraction efficiency, phase-conjugated (PC) reflectivity and polarisations of interacted waves was considered in the case of small interaction angles. Theoretical analysis based on the results of the dynamic theory of Kukhtarev at al. [2] was made. Theoretical results were verified experimentally. The measurements showed 34of the dynamic grating realised by DTWM with BGO in external electric field. The possibility of the generation of PC wave was observed. The maximum PC reflectivity obtained was 1.1%.

On the basis of the theoretical and experimental results obtained the main physical parameters as r14 (electrooptic coefficient) and N0 (concentration of the traps) of BGO was determined. The results obtained are $r_{14}=(1.36\pm0.03)\times10^{-12}$ m/V and $N_0=1.04\times10^{22}$ m^{-3}.

We studied the energy exchange between the beams in DTWM geometry in dependence on the angle of turning øof the crystal BTO rotated around the [110] axis, in relation to the structure of the interference field created by the waves participating in the process of self-diffraction.

The [110] cut of the crystal corresponded to the traditional geometry of interaction of light waves with these crystals. The vector of the holographic grating q and the light

induced electric field connected with it lay in the plane of cut [110]. The results showed that the deflection from the canonical geometry of the experiment (ϕ=0; $\pi/2$) as the result of the rotation of the crystal leads to an increase in the energy exchange between the beams. The piezoelectric effect and photoelastic properties of the medium together with electro-optical mechanism of the recording of the hologram make it possible to clarify a series of DTWM experiments carried out in crystal. Results of the experiments fit the Kukhtarev's theory closely for both lineary polarised and circular polarised interacting beams [3].

One of the most important effects in photorefractive crystals is self-pumped phase conjugation process (SPPC) [4]. In recent years, SPPC process in $BaTiO_3$ has been intensively studied. Up to now several different theories of this effect have been published and the role of TWM, FWM, and stimulated diffusion scattering, as well as that of transmittion and reflection gratings have been discussed. However no one theory can satisfactorily explain all of the effects observed in the SPPC process.

We concentrated on an experimental study of the SPPC process to help elucidate its physical mechanism. The SPPC reflection (SPPCR) from $BaTiO_3$ single crystal as a function of the angle of incidence, beam entrance position, pump power and pump beam diameter were measured. Measurements showed that the different types of SPPCR's (stable and unstable SPPCR, pulsations and oscillations) can be obtained from a $BaTiO_3$ crystal only by changing the laser pump beam entrance position in the c axis direction of the $BaTiO_3$ crystal or changing the angle of incidence of the pump beam. Selecting the optimal pump geometry of the $BaTiO_3$ we can generate just one of these SPPCR's. The maximum stable PC reflectivities obtained for the He-Ne laser beam, argon-ion laser beam (514.5 nm), and He-Cd laser beam were 72 %, 50 %, and 21 %, respectively. The build-up time of SPPC emision process in this experiment was also measured. By elections of right geometry it is possible to minimize the build up time of the stable SPPCR's.

On the basis of the results obtained the experimental conditions for stable SPPCR were determined, and two original applications were implemented. The multicolour imaging and through the SPPCR controlled photorefractive ring generator.

References:

[1] Photorefractive Materials and Their Applications I, Eds. P.Günter, J.P.Huignard, (Springer-Verlag, Berlin-Heidelberg, 1988).

[2] N.V.Kukhtarev et al., Ferroelectrics 22, 949 (1979).

[3] N.V.Kukhtarev, T.I.Semenec, P.Hříbek, Ferroelectrics Letters 13, 29 (1991).

[4] J.Feinberg, Optics Letters 7, 486 (1982)

This research has been conducted at the Department of Physical Electronics as a part of the research project "Nonlinear Optics" and has been supported by the Czech Technical University, Faculty of Nuclear Sciences and Physical Engineering.

BARIUM BORATE PICOSECOND OPTICAL PARAMETRIC OSCILLATOR

V. Kubecek, Y. Takagi, K. Yoshihara* and G.C. Reali+*

Faculty of Nuclear Science, CTU, Brehova 7, 115 19 Praha 1
*Institute for Molecular Science, Myodaiji, Okazaki 444, Japan
+Dept. of Electronics, University of Pavia, 271 00 Pavia, Italy

Key words: Optical parametric oscillator, synchronous pumping, Nd:YAG laser

Pulsed, passive negative feedback mode-locked (PNFM) solid state lasers have demonstrated very good performances in generating long trains of very short and energetic pulses in several crystalline Nd:doped materials [1,2]. PNFM is implemented by inserting a GaAs platelet into the cavity of an actively passively mode-locked laser. Two-photon absorption induced self-defocusing,which limits the intracavity intensity close to the saturable absorber saturation threshold, produces an optimum compression of the circulating pulse and delays the gain depletion, stretching the pulse train by several tens of roundtrips. For example, in Nd:YAG, trains of 50 to more than 100 pulses, depending upon the operating conditions, with 10-μJ/pulse energy and 10-ps time duration, are generated. This makes PNFM Nd:YAG a strong candidate as a synchronous pump for the generation of ultrashort pulses.

We report here, we believe for the first time, the results of the operation of an optical parametric oscillator (OPO) based on the use of a beta-barium borate (BBO) crystal and synchronously pumped by the third harmonic of a PNFM Nd:YAG laser [3].A pulse train from the PNFM YAG oscillator having a duration of 500 ns and energy of 1 mJ was amplified by using three Nd:YAG amplifiers, and a third harmonic was generated by using two KDP type-II crystals with a 15% efficiency to the maximum energy of 2 mJ at wavelength of 0.355 μm. The 0.355-μm beam with a single pulse duration of 8 ps was focused into a type-I, 5 x 7 mm^2 and 7-mm-long BBO crystal cut at phase matching angle of 31 deg.The pump beam diameter in the nonlinear crystal was 300 μm. Noncollinear pumping geometry, similar to the one recently reported by Laenen et al.[4] and by other groups , was used. Single resonant oscillation of the signal wave between 0.407 and O.690 μm (the available reflectivity of our mirrors) was achieved. This corresponds to an idler wave tunability between 2.8 and 0.72 μm. The pump threshold for the OPO operation was 150 μJ, corresponding to the pump power density of 330 MW/cm^2. The optical parametric oscillator build-up time from 50 ns (pump energy 2 times above threshold) to 350 ns (near threshold) was measured. Pulse duration was measured at the signal wavelength of 0.6 μm by using a streak camera with resolution of 1.8 ps. The pulsewidth was found to be 3.1 ps.

We have demonstrated a singularcy resonant optical parametric oscillator synchronously pumped by the third harmonic of a passive negative feedback mode-locked Nd:YAG laser. Such a source of widely tunable picosecond light pulses can find applications in spectroscopy, measurement of properties of optical fibers e.t.c.

References:

[1] A. Del Corno, G. Gabetta, G. C. Reali, V. Kubecek and J. Marek, Opt. Lett. 15, 734, (1990)

[2] A. Agnesi, J.-C. Diels, P.Di Trapani, V. Kubecek, J. Marek, G C. Reali and C. Y. Yeh, Ultrafast Phenomena VII, Springer Series in Chemical Physics, Vol.53, p. 38 (1990)

[3] V.Kubecek, Y. Takagi, K. Yoshihara and G.C. Reali, in Technical Digest on Conferemce on Lasers and Electro-Optics CLEO'91 (Optical Society of America , Washington D.C. 1991) paper CThR10

[4] R. Laenen, H. Graener, and A. Lauberau, Opt. Commun. 77, 226 (1990)

This research has been conducted partially at the Department of Physical Electronics , Faculty of Nuclear Science and Physical Engineering CTU as a part of the research project no. 4018 "Quasicontinuous and pulsed solid state lasers", at the Department of Electronics, University of Pavia, Italy and at the Institute of Molecular Science, Myodaiji, Okazaki, Japan.

MULTIWAVELENGTH MODE-LOCKING OF SOLID STATE LASERS USING A FREQUENCY- DOUBLING NONLINEAR MIRROR

K.A. Stankov, V. Kubecek ,K. Hamal, H. Jelinkova and I.Prochazka*

Faculty of Nuclear Science, CTU, Brehova 7, 115 19 Praha 1
*Laser Laboratorium, W-3400 Gottingen, Germany

Key words: Mode-locking, nonlinear mirror,second harmonic generation, Nd:YAP, Er:YAP,

Locking the phases of the longitudinal modes of a laser remains still the most widespread technique for generating ultrashort laser pulses and recent developments have proved the big potential of this technique. To give an example, the colliding-pulse mode-locking (CPM) technique is unsurpassed with respect to generation of the shortest pulses directly from a laser and the soliton laser and additive mode-locking also feature subpicosecond pulse generation. The negative feedback in passively mode-locked lasers provides reproducible ultrashort pulses, down to several hundreds femtosecond.

With respect to the brief overview of the mode-locking technique developments given above, the mode-locking technique based on intracavity frequency doubling offers new capabilities for generation of ultrashort laser pulses. A frequency doubler inside the cavity, together with an output mirror with high reflectivity at the second harmonic, forms a nonlinear mirror, whose reflectivity at the fundamental wavelength can either increase or decrease when the input light intensity increases. When the phase condition facilitate increasing reflectivity, the device can be used as a passive mode-locker [1].

In this report we investigate the attractive potential of the second harmonic nonlinear mirror to mode-lock lasers at quite different wavelengths. Using a single 30° -cut $LiIO_3$ frequency-doubler, mode-locking at the 1.064 μm, 1.08 μm and 1.34 μm transitions of pulsed laser with Nd-doped crystals was achieved. Pulses as short as 20, 40, and 15 ps at the corresponding wavelengths were obtained. Mode-locking was achieved also in Er:YAP laser at 1.66 μm wavelength with pulse durations of 450 ps. A comparative analysis of the mode-locking performance at the different wavelength is presented, indicating that the minimum pulse duration is determined by the limited number of round-trips only. The laser configuration was the following: As a gain media we used a flashlamp pumped Nd:YAG laser crystal, lasing at 1.064 μm and b-cut Nd:YAP, Er:YAP crystals, generating at 1.08 μm, 1.34 μm and 1.66 μm wavelengths. The frequency doubler was a 20 mm long $LiIO_3$ crystal angle phasematchable at all four wavelengths. The laser cavity was formed by the dielectric dichroic mirrors. In all cases the end cavity mirror was a total reflector at the fundamental, the output dichroic mirror was total reflector at the second harmonic and had 20%-24% reflectivity at the fundamental.

Mode-locking was achieved using the procedure described in [2]. We observed reproducible satellite free pulse trains. Streak camera measurements of the pulse duration were performed at the second-harmonic wavelengths. The measurements at the beginning and at the end of the pulse train revealed pulse shortening, from 40 ps down to 15 ps in the case of 1.34 μm operation. The laser exhibited two-threshold operation, typical

for saturable-absorber mode-locking as well [3]. Mode-locking at 1.08 μm, 1.064 μm and 1.66 μm wavelength was obtained by replacing the laser crystal and the cavity mirrors. The observed pulse trains ranged in durations from 200 ns (1.06 μm, 1.08 μm) to 500 ns (1.34 μm). In case of shorter trains the reduced number of round-trips in the pulse train development of shorter pulses.

As compared to the operation at 1.064 and 1.08 μm, the longer pulse train development at 1 .34 μm due to lower gain favours the pulse shortening as a result from the compression action of the nonlinear mirror [4,5].

In this experiment we have demonstrated the advantage of the nonlinear mirror to operate as a mode-locker in different spectral regions. This technique features all-solid-state implementation and readily available second harmonic output. It can provide mode-locking in all spectral regions for which suitable nonlinear crystals exist [6].

References:

[1] K.A. Stankov, Appl. Phys. B45, 191 (1988)

[2] K.A. Stankov, Opt. Lett.14, 359 (1989)

[3] G.H.C. New, Proc. IEEE 67, 380 (1979)

[4] K.A. Stankov, V. Kubecek and K. Hamal, Opt. Lett.16, 505 (1991)

[5] K.A. Stankov, V. Kubecek and K. Hamal, IEEE J.Quantum Electron.27, 2135 (1991)

[6] K.A. Stankov, V. Kubecek, K. Hamal, H. Jelinkova and I.Prochazka, Proc. EQEC'91, Edinburgh, paper OITh6.

This research has been conducted at the Department of Physical Electronics, Faculty of Nuclear Science and Physical Engineering as a part of research projects no. 4014 " Picosecond Lasers" and no. 4018 " Quasicontinuous and pulsed solid state lasers".

SINGLE PHOTON RANGING SYSTEMS FOR SPACEBORN ALTIMETRY AND ATMOSPHERE MONITORING

I. Prochazka, K. Hamal, S. Pershin ***

* Faculty of Nuclear Science and Physical Engineering, CTU
Brehova 7, 115 19 Prague 1
** Space Research Institute, Moscow, USSR

Keywords : altimeter, single photon detection, lidar

We are reporting on a novel design of a spaceborn altimeter based on a single photon detection technique and a laser diode pulser as a transmitter. The MARS 94 mission [1] will carry, among others, the balloon probe experiment. The balloon with the scientific cargo in the gondole underneath will drift in the Mars atmosphere , its altitude will range from zero, in the night time, up to 5 km at noon. The accurate gondole altitude will be determined by compact altimeter described below.

As a transmitter, the integrated laser diode pulser LD91 is used. It delivers uniform, fast risetime pulses at 880 nanometers wavelength 100 nanoseconds long with the energy of 2 microJoules at the repetition rates up to 25 kHz. The receiver consists of a Single Photon Avalanche Diode detector package , its operating voltage is controlled by a newly designed circuit in a wide temperature range from down to -60 Centigrade. The diode aperture is partially matched to the laser aperture, its quantum efficiency reaches 20 %. The transmitter and receiver share the same optics of 40mm aperture, the optical path is separated by a thin film polariser plate. The bandpass filter 5 nanometers / 60% in front of the detector along with the limited field of view, the adjustable range gate electronics and the data processing software permit the single photon ranging on the single photon detection level even in the daytime. The altimeter electronics consists of a flying time counter, the programmable range gate generator, the control logic and interface to the board computer.

The extensive ground tests of the experimental sample of the altimeter has been carried out. The ranging precision of meters within the ranges of 0-2.5 km has been obtained both day/night time and using the optics aperture of 17 mm only. Employing the full 40 mm aperture optics of the final version, the full range will be guaranteed. The altimeter described above outranged the microwave and Nd YAG systems by low weight, low power consumption and the compact design.

The application of the LIDAR is well known since the sixties. However, the availability of low cost semiconductor laser diodes together with the fast development of the single photon detection techniques is opening new perspectives in LIDAR applications. On the basis of the original space born altimeter for MARS 94 balloon probe mission we developed the laser ranging system capable of monitoring the atmosphere within the range of a few kilometers [2]. The system is expected to be implemeted into the "Small Mars Station" to be deployed to Mars in the mid-nineties. The system is detecting the photons backscattered in the atmosphere from the transmitted laser pulse. The system is operating on a single photon detection level with the high repetition rate.

The system is employing the integrated semiconductor laser pulser delivering 90 nanosecond pulses at 850 nanometers having an energy of 2 microJoules at the repetition rate 5 kHz. The standard TV lens optics of diameters ranging within 9 to 25 millimeters have been used as a transmitter and receiver in the first experiment. The special design Single Photon Avalanche Diode operating in an active quenching mode has been used as a returned signal detector. The 9 nanometers wide bandpass filter has been used in daylight measurements. To increase the signal to noise ratio, the diode aperture has been matched to the laser output. The system electronics consists of the time interval meter, range gate electronics and the interface to the computer to collect and analyze the data. The results of the atmospheric monitoring experiments will be presented. The following parameters may be monitored : the atmospheric visibility, the aerosol content, the fog, the clouds height & range and others. The mass, dimensions and price of such a system make it attractive for mobile, air and space born remote sensing applications. The excellent stability of both the laser transmitter and the single photon detector permits one to calibrate the receiver sensitivity to high accuracy and thus to use the system as a precise visibility and surface reflectivity sensor. The applications of a visibility sensor in automated meteo stations, traffic safety, air and ship safety systems seem to be quite promising. Application air and space-born remote sensing is under consideration in agriculture, geology, large area forest monitoring, soil humidity and radioactive Cesium dust monitoring.

References:

[1] S.Pershin, V.Linkin, V.Makarov, I.Prochazka, K.Hamal, Spaceborn Laser Altimeter Based on the Single Photon Detection, technical digest of the Conference on Lasers and Electro Optics, CLEO 91, Baltimore, May 1991

[2] I.Prochazka, K.Hamal, S.Pershin, Capabilities of Single Photon Detection in LIDAR for Atmospheric Studies, International Symposium on Radars and Lidars in Planetology, Cannes, France, Sept. 1991

This research has been funded by the foreign contract No. 409690 with the Space Research Institute, Moscow, USSR.

ADVANCED CONTROL AND SAFETY SYSTEM OF NUCLEAR REACTOR

K.Matějka, P.Hiršl, J.Fleischhans, T.Šejba, M.Kropík, D.Pičmann

Faculty of Nuclear Sciences and Physical Engineering (FNSPE), Department of Nuclear Reactors, CTU, Břehová 7, 115 19 Praha 1

Key words : experimental reactor, nuclear safety, control system, reliability of hardware and software

The training nuclear reactor 'VR-1' in CTU was built between 1985 to 1988. Physical start up occurred in December 1990. The reactor is equipped with a microcomputer based control system, which was developed in FNSPE and built with components available in Czechoslovakia around 1985 [1]. The advanced nuclear reactor control system (ANRCS) [3], based-on-up to date electronic components, should improve operational reliability and nuclear safety.

Nuclear reactor control systems are usually built on analog principles. Input signals from sensors are processed by analog circuits. These circuits check the operational state of the reactor, produce control signals for the rods and break the emergency chain when operating conditions are exceeded. Emergency chains are built as a chain of relays, which usually cut off the power holding the rods up, thus causing the rods to fall and the chain reaction in the reactor to stop. To ensure reasonable operational reliability, for the shut down of the reactor, it is necessary to have agreement among independent channels. We speak about the logic of the emergency chain, which is usually 2/3. This means that two out of three independent control channels must break the emergency chain in order to shut down the reactor. There were no available control systems for experimental reactors on our market at the time this reactor was built. The decision was made to develop a new microprocessor based control system for such reactors. The present control system satisfies the requirements of the Czechoslovakian Nuclear Agency. It was necessary for the development and production of the control system to use only components and equipment available in Czechoslovakia or the rest of Eastern Europe. The technology used in this control system seems obsolete today. Now, it is possible to get the latest components and equipment in our country. We have decided to develop an advanced control system using such components and equipment. We also want to use up to date methods of computer supported design and development of electronic circuits and software. We are developing our ANRCS according to not only Czechoslovakian nuclear safety requirements, but also to IAEA, IEEE and IEC requirements for such equipment.

Now we want to briefly describe our control system project. Measurement of the neutron flux is accomplished by four independent measuring channels. Each channel receives pulses or current (according to neutron flux). The analog part of the channel converts this input signal to a frequency, which is then measured and processed by the computer part of the channel. From the input data the microcomputer calculates the power (N), period (V) and deviation from setup power (D). This data is sent (serial communication) to the next stage of the control system. The measuring channels have the possibility of shutting down the chain reaction in the reactor. When N, P or D is too

high, a channel breaks the emergency chain. The emergency chain for measuring channels is built in the 2/3 logic.

Four fully independent safety channels check the maximum power of the reactor and other important parameters. When N or V exceeds setup values, the safety channel breaks the safety chain (logic 2/3)

Two communication channels form the next stage of the control system. These channels receive data from measuring and safety channels, compare their values, and calculate control actions for the control and safety rods. These communication channels can also break the emergency chain when unexpected deviations occur between data from different channels (hardware or software problems are expected). The emergency chain for communication channels is built in the 1/2 logic.

To ensure high reliability of the microcomputers, they were designed using a CAD system for developing printed circuits. It is desirable for the microcomputers used to be single board microcomputers in order to limit relatively unreliable connectors and long computer bus wires. To fit the whole microcomputer on a small single board it is necessary to use a high performance microprocessor (microcontroller) with integrated peripheries (ZILOG Z280, NEC V25). All hardware should undergo complete independent testing by the Czechoslovakian Nuclear Agency. To ensure galvanic separation of all microcomputers (high degree of independence) used in ANRCS and to avoid electromagnetic disturbance, light guides were selected for the serial communication lines.

High level languages (probably C) should be used for development of the software for ANRCS. The use of high level languages was formerly excluded because of the low executive power of microcomputers with the I8080A microprocessor [2]. The new microcomputers should be 5 to 10 times faster then the I8080A based one. The use of high level languages provides programs, that are more readable, shorter and easier to understand. Measuring and safety channels should be based on different types of microprocessors (Z280 and V25) with different instruction sets. In this way the development of the software for measuring and safety channels would be done by different tools and the nuclear safety should increase.

This new nuclear reactor control system should be developed by 1992 and installed in 1993. Now, the hardware for the safety channels and serial communication cards has been developed and is being tested. Other hardware is being designed now. Suitable tools for the development of the software has been found. We believe that our ANRCS will contribute to an increase in nuclear safety, operational reliability and the comfort of work within a reactor.

References:

[1] Matějka, Hirši, Lněnička: Contribution to the control system conception ..., FNSPE 1984,

[2] Šejba: Description of the control program ..., FNSPE 1991,

[3] Kropík :ANRCS, FNSPE 1991.

This research has been supported by Department of Nuclear Reactors, FNSPE CTU.

Section 5

COMMUNICATIONS

CONTRIBUTION TO THE THEORY OF PIEZOELECTRICAL TRANSDUCER

*Z. Škvor, F. Kadlec *, A.M. Bruneau, P. Lotton ***

* Faculty of Electronical Engineering CTU, Prague ** Acoustics Laboratory C.N.R.S., University du Maine, France

Key words: Tranducer piezoelectrical, Transducer electrostatic, Analogy electromechanical, Piezopolymer.

The piezoelectric properties of piezopolymer materials are suitable for experimental acoustics, applied acoustics and electroacoustics in the broad frequency range from the infrasonic frequencies to the ultrasonic area in such applications as low-weight vibration sensors, accelerometers, pressure and force sensors, hydrophones, sonars, loudspeakers, microphones, headphones etc.

The piezoelectric transducer in a cylindrical form, developed during the research work, presents a new modification of the spiral electrostatic transducer /1/, /2/. It consists of one or more piezopolymer mono-axially oriented diaphragms with a thickness between 9 and 25 μm. It can be used at sonic and ultrasonic frequencies as a loudspeaker, microphone or headphone. The cylindrically-shaped piezopolymer diaphragm of diameter $2R$, thickness h and width b can be described by the pair of piezoelectrical equations

$$S_1 = s_{11}^E T_1 + d_{31} E_3, \tag{1}$$

$$D_3 = d_{31} T_1 + e_{33}^T E_3, \tag{2}$$

where S_1 and T_1 are strain and stress in the angular direction 1, respectively, E_3 and D_3 are the intesity of electrical field and the induction in the radial direction 3, respectively, and s_{11}^E , d_{31}, e_{33}^T are the piezoelectrical constants (compliance coefficient, piezoelectrical coefficient and permitivity). The electrical field acting in the radial direction 3 provokes the strain S_1 and the stress T_1 in the angular direction 1. The radial displacement of the diaphragm is $S_1 R$ and the simplified electromechanical equation in phasor for the unit of length of a thin cylindrically shaped piezopolymer diaphragm is as follows

$$-\omega^2 \hat{\xi} \rho + /(R^2.s_{11}^E) + \hat{T}_3(a)/h + \hat{T}_3(b)/h = d_{31} \hat{E}_3/(R.s_{11}^E), \tag{3}$$

where ρ is diaphragm density and $T_3(a), T_3(b)$ respectively, are the tensions corresponding to the acoustical load acting on both sides of the diaphragm. The theoretical description and modelling were based on the electroacoustic and electromechanical analogies of systems with distributed elements /3/.

The measurements were carried out on the small-sized piezoelectrical tranducer as earcanal - insert earphone "loudspeaker or microphone" of outer diameter $11mm$ and height $15mm$. A cylindrically-shaped diaphragm of the length $15mm$ was turned onto the central cylindrical template each turn separated from the following turn by means of a plastic spacer. Each side of the diaphragm was loaded by the acoustical impedance of a slit of thickness $H = 60\mu m$. The mechanical impedance according to /3/ acting on the diaphragm is

$$\hat{Z}^2 = j r^o c^o 2\pi R H N.[-\cot kb + 1/(kb)], \tag{4}$$

where $N = 5$ is the number of turns and k is the wave number. The resistance due to viscous losses in a slit is /3/

$$R_m = 8\mu\pi RbN/H, \tag{5}$$

where μ is the dynamic viscosity of air. The equivalent circuit of the transducer, loaded at the one side by the cavity V_x and at the other side open to the free field, is shown in Fig.:

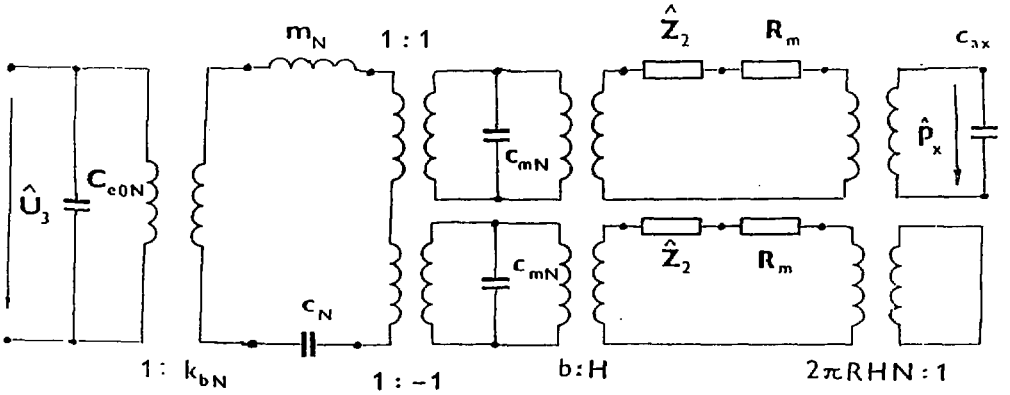

where U_3 is the input voltage, kbN is the tranducer factor, Ce_{ON} is the transducer capacitance, c_N is the compliance of the slits, mN is the mass of the diaphragm, c^{mN} is the compliance of the slit, c_{ax} is the compliance of the output cavity of volume V_x, and p_x is the acoustic pressure. The experiments confirmed that the transducer functioned as expected and were in accordance with the theory /4/. The transducer is suitable for many applications in applied electronics, telecommunications, medicine, active noise control etc. The main results will be reported in publications /5/, /6/.

References:

[1] U.S. Patent appl. 3,850.447, CS Patent appl. 1449574, Škvor Z.: Spiral Transducer.

[2] Škvor Z.: Piezoelectrical Transducer with Piezopolymer Diaphragm (patent applied for 1991).

[3] Škvor Z.: Vibrating Systems and Their Equivalent Circuits. Studies in Electrical and Electronic Eng. 40, Elsevier Publ. Comp. Inc., Amsterdam-Oxford-New York-Tokyo, 1991.

[4] Lotton P.: De la modélisation des transducteurs électrostatiques et piézoelectriques en spiral. Rapport de stage D.E.A. d'Acoustique Appliquée, FEL Prague, Laboratoire d'Acoustique, Université du Maine, 1991.

[5] Kadlec F., Škvor Z.: Ultrasonic Transducers and Their Design, to be published.

[6] Škvor Z.: Trasducteurs électromécaniques et électroacoustiques et leurs circuits équivalents. Invited paper, 2eme Congres Francais d'Acoustique, April 1992, Arcachon, to be published.

This research has been conducted at the Department of Radioelectronics as a part of the research project "Generation and evaluation of acoustic fields in fluids and solid state in a wide frequency range" and has been supported by Czech Technical University grant No.8043.

ELEMENTS AND METHODS OF OPTICAL INFORMATION PROCESSING

E. Kostal, M. Klima, K. Ludvik, M. Bernas, J. Hozman

Dept.of Radioelectronics, Faculty of Electrical Engineering CTU, Technicka 2, 16627 Praha 6

Key words: Optical information processing, optical sensors, optical spatial modulators, acoustooptics

We have analyzed the fundamental applications of particular kinds of optical spatial modulators and sensors based upon solid state technology. The main idea for the present project period has been a fast signal processing system for radiosignals for example radar, channelised receiver, spectrum analyser, correlators etc.

An optical spatial modulator and an optical panoramatic sensor are fundamental blocks of optical information processing systems. The first part of our work has concentrated on a new type of pyroelectric optical sensor. Based upon our previous results we have designed and partially experimentally verified a panoramatic sensor model. Particular elements of sensor are supposed to be commuted by an addressable multiplexor created in amorphous silicon layer attached to pyroelectric substrate [1]. The sensor function has been computationally proved by model analysis which has been focused esp. on a TFT and pyroelectric element descriptions and relevant system model. As pyroelectric substrate material a lithium tantalate has been assumed. In this first stage we have used a linearized model of TFT. A possible array topological structure was designed and patented. System voltage responsivity has been derived in explicit expressions.

$$R_V = \frac{\eta.p.A.R.\omega}{G_T\sqrt{(1+\omega^2\tau_T^2)(1+\omega^2\tau_E^2)}} \cdot \frac{1}{\sqrt{1+(\frac{4\pi^2n^2k}{\omega})^2}} \qquad (1)$$

Several scanning structures have been suggested - shift register, array and CCD type. The last one, based upon a dark current accumulation is patented.

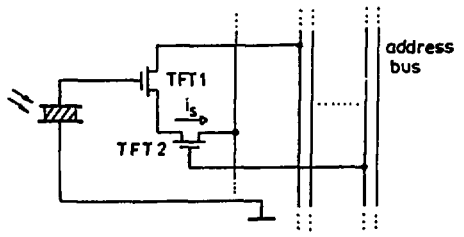

Fig.1.: Array scanning structure

Experimentally, the isolated thin film transistors on passive substrate (silicon) were prepared including required masks and for planned sensor experiments too. We achieved following parameters: $R_{on} = 10k\Omega$, $R_{off} = 100G\Omega$.

The most important contribution of this part of work is a model expression for thin film transistor based upon amorphous silicon layer. The experiment was devoted to proving the

manufacturing technology of TFT either on the passive substrate or active pyroelectric single crystal cut. Experimental works have been performed as a joint activity together with Research Institute VUST and Institute of Physics Academy of Sciences.

In the field of optical spatial modulators the effort has been concentrated on bulk acoustooptic units. The activity was based upon the results of previous research tasks. One of the most important acoustooptic unit applications is a signal correlation unit.

A theoretical part has been devoted to an influence of input additive noise on a result signal to noise ratio of correlation unit output signal. The model has been based upon a definition of correlation integral and has been implemented on a personal computer. The additive noise level varied in the presence of a constant input signal in order to achieve an output signal to noise ratio 2:1. This analysis has been done for various materials of piezoelectric transducer - interaction element bonding. Based upon this model a thickness of bonding layer has been optimized from the point of view of maximum system resistance against an input additive noise. The system noise resistance is plotted in [2] as a function of thickness up to 20 microns. For most suitable bonding materials an optimum thickness is approx. 5 microns. For electromechanical conversion analysis a Mason model of piezoelectric transducer has been used and particular parts - transducer, bonding layer etc. - bave been described by cascade matrices to express a transfer function. By means of this transfer function an output correlation peak has been evaluated for various bonding layer thicknesses and materials.

Experimental part has been mostly devoted to an experimental model of simple correlation signal processing unit based upon a mercurous chloride with slow shear acoustic wave 347 m/sec in direction [110]. As a test signal a rectangular radioimpulse was applied; reference image function has been created by a narrow slit (1 mm width). An output correlation peak has been evaluated.

The last part of a spatial modulator topics is a study and investigation of new materials suitable for acoustooptic applications. In cooperation with the Institute of Physics we are continuing in this field and after mercurous and lead halides we will study mixed halides single crystals or mixed tungstates. At present a theoretical study is being performed According to our previous experience based on pure mercurous halides and lead halides we expect very good optical and acoustooptical properties of the above mentioned-single crystallic materials.

References:

[1] E.Kostal, M.Klima, Karel Ludvik: The proposed self-scanned array IR sensor based upon pyroelements, Proc. of 25th Annual Int. Carnahan Conference on Security Technology, Taipei 1991

[2] E.Kostal, M.Klima, K.Ludvik, M.Bernas, J.Hozman, Research Report of CTU grant No.8042 for year 1991, is to be published

[3] Kostal E. et al, Panoramatic pyroelectric sensor of radiation, Pat.Appl. PV 6893 - 90

This research has been conducted at the Department of Radioelectronics as a part of the research project "Elements and methods of optical information processing" and has been supported by CTU grant No.8042.

THE COMPUTER AIDED MICROWAVE MEASUREMENT AND DESIGN SYSTEM.

K. Hoffmann, Z Škvor, P.Hudec

During last several years there have been ,various CAD systems developed for analysis and synthesis of high-frequency and microwave circuits, mainly in USA. Engineers in research laboratories and students at universities have received top efficient tools, that enable complex design, analysis, synthesis and optimization of both linear and nonlinear circuits. In case of professional application these CAD systems can significantly accelerate design of new appliances and reduce development expenses. University students quickly acquire professional skills if these systems are used in education.

In modern design and research laboratories these CAD systems are implemented together with CAM systems, used for both measurement of designed circuits and input data. In a frequency band above 2 GHz only a complex computer-aided measurement system can provide data with necessary precision. CAM systems use complicated correction methods , that can eliminate most measurement errors.

Up to now there has been no CAD and CAM system like this in Czechoslovakia, except for very simple ones,the main reasons begin very high prices of such foreign systems and unfavorable license policy. But even in the case of entire releasing of commercial restrictions, customers can obtain only a closed system. They do not know used formulas and have no possibility to develop it or to adapt it to their special demands.

Our research group started work on these problems already four years ago. As a basis of CAM system we have set together a computer-controlled microwave workplace for measurements in 2 to 18 GHz frequency band. We have also developed a special test fixture for measuring of microwave transistors and diods. With our measurement system and fixture we are able to get data with the same accuracy, as is usual in top-equipped European laboratories. In Czechoslovakia the system is unique in that we use it both for our own research work and for our partners from industry. We have carried out a large set of comparative measurements at the University of Roma. The results show that our test fixture provide in some parameters better results, than the test fixture produced by the firm Intercontinental Microwave, which is supposed to be the best one in the world. In case we have the possibility to finish the design of the fixture and to finish work on the new correction method, we would have the possibility to reach the top of this fieldat least at the European level.

Two years ago we have started work on a microwave CAD system. Last year we finished the first version of the FELMIC programme, designed for PC-AT implementation. The programme has been already used in research laboratories of the Radio Research Institute in Opocinek, where it serves for design and optimization of both active and passive circuits up to 20 GHz. This year we have developed a new and more powerful version MICAN. This version will be implemented in Tesla Hloubetin and in the Research Institute 060 in Prague. Many different high frequency circuits have already been modelled and practically designed, some of them have already been produced in large series. Within the faculty we use both CAD systems with a great success in subjects "Microwave Integrated Circuits", " Active Microwave Circuits" and "CAD in High-Frequency Technique".

In the future we plan to substantially extend both systems and to create a complex CAD and CAM workstation for microwave measurements and design up to 100 GHz. It corresponds to the most recent development efforts in a microwave field in the world and is of a great interest to our partners from other research laboratories and industry.

OPTOELECTRICAL SENSORS FOR NON-CONTACT DISTANCE MEASUREMENT

J. Velebil

Faculty of Electrical Eng., CTU, Technická 2, 166 27 Praha 6

Key words: Optical triangulation, Position Sensing Detector

There is increasing number of applications in the use of electro-optical instruments to measure angle, distance, height, centering, surface and other parameters, related to position sensing. The principal advantage of electro-optical methods is non-contact measurement. Therefore an object to be measured is not affected by a measuring system. Distance measurement is usually performed by optical triangulation. Fig. 1 shows the principle of the method.

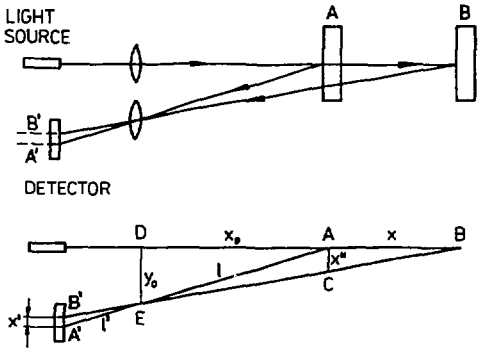

Fig. 1

A collimated beam of light hits the surface of an object. The light is reflected back through a lens to a point on the surface of the position sensitive detector. The position of the light spot on the detector surface corresponds to the distance to the object. If the distance is altered, the light spot on the detector surface will be displaced, thus indicating a change in distance. The relationship between movement of the light spot x' and object movement x is (from Fig. 1):

$$x' = \frac{x}{x + x_0} \cdot \frac{l'}{l.y_0} \tag{1}$$

As the dependance /1/ is not linear, the method is suitable for measurement with offset x_0, which is several times greater then measured displacement x.

Position sensitive detector is the most important part of the system. There are several methods to optically measure the position of an object. CCD image sensors can be used for this purpose. These devices have some disadvantages, i.e., the detection speed is limited by the scanning and the real time measurement is impossible. There are another solid

state devices, emploing "Lateral Photo Effect", known as Position Sensitive Detectors (PSD)[1]. This PSD has following advantages compared with scanning type detectors:

- there is no dead area on the sensitive surface, therefore, continuous position information is available
- position resolution is not limited by the light spot size, precise focusing is not required
- operating circuit is simple

In this work the development of an opto-electrical sensor for non-contact distance measurement is presented. The sensor employs a linear lateral photo effect PSD, developed by Tesla Vakuová technika. An IR high radiant LED is used as a light source. A speciall attention was paid to the design of operating circuitry. Due to dramatical decrease of optical power as a result of difussion type reflection, the light modulation is applied together with synchronous detection and following digital filtration of the signal. The digital data processing and the control of other functions (calibration, serial data output, LED display) is performed by a single chip microcomputer. As the reflectance of different surfaces varies significantly, an optical feedback control is applied to maintain the total generated photoelectric current constant. As a result, the position resolutin is almost constant for varies types of reflective surfaces. Typical parameters of the sensor:

Offset	$200\,mm$
Measuring range	$-50\,mm$, $+50\,mm$
Position resolution	$1mm$ (*0.1 mm with aditional digital filtration*)
Linearity	$1.5\,\%$(*after linearization*)

The sensor is especially useful for shape and dimension inspection, for position detection of moving parts and for varies application in idustrial automation. There is intention to develop another sensor of this type with higher modulation frequency and analog output signal for non-contact vibration analysis.

References:

[1] H.J.Woltring: Single- and dual-axis lateral photodetectors of rectangular shape, IEEE Trans. Electron Devices ED-22 (1975), 581-590.

This research has been conducted at the Department of measurement as a part of the research project "Non-contact measuring methods"

COMPUTER CONTROLLED COMPENSATION FERROMETER

V. Havlíček , M. Mikulec , P. Uhlíř and I. Zemánek

Dept. of Circuit Theory, CTU, Technická 2, 166 27 Praha 6

Key words: Single sheet tester, digital control, compensation method, iteration process

In electrical steel sheets testing there is a general tendency to replace the standardised measurement in the Epstein frame by the measurement in yokes. In the Dept. of Circuit Theory of CTU an original compensation method has been developed to solve the problems bound with these single sheet testers (SST). This method has been used for construction of four types of SSTs for testing of strips and sheets and of one on-line measuring device /1/. All these devices were successfully tested in the Iron and Steel Research Institute in Dobrá (ČSFR) and they are also used in the industry. The compensation method was verified also in U.K. /2/ .For the next extention of this method in our country and especially in the exterior it was necessary to continue in research work on problems of the compensation method accuracy and of the optimisation of the computer control system used.

The investigation of the SSTs accuracy /3/ has shown that in the device using the compensation method it is mostly dependent on the efficiency of the feedback loop which is formed by a supplementary winding, a power amplifier and a Rogowski-Chattock potentiometer (RCP) as a sensing element. It should realize, at any time instant, a state in which the magnetomotive force (mmf) of the magnetizing winding is imposed to a certain part of the tested specimen only. The setting of this state relies on the correct measurement of the portion of the mmf along the axis of the RCP. Therefore the accuracy of this measurement has been investigated in detail. Since the RCP is only a zero state sensor in the compensation method, the magnitude of the parameter relating its linked flux to the relevant portion of the mmf is not important, i.e., no calibration is necessary.

As found /4/ the accuracy of SSTs is influenced also by an asymmetrical magnetization if a single yoke system is used. In this case additional eddy currents occur in the tested specimen in dependece on its overhang of the yoke. Because of these currents the actual value of specific power losses is increased. The measured value of these losses depends on position of the RCP, too. Theoretical and experimental results show that a double yoke system for correct measurements is necessary.

The computer controlled system has to determine the dependence $Ba = f(Ha)$ for required values of Ha. Due to a strong nonlinear properties of magnetic materials it is necessary to set all working points by a numerical iteration process. It was theoretically derived and experimentally proved that the modified regula-falsi method (discrete Newton's method) seems to be the best one /4/, /5/. Since the SST has to work usually in a hard industrial medium it is preferable to situate the standard PC system to a special room, thus, the control and measuring signals must be transmitted by a serial line. For this purpose a local control system with one-chip microcomputer communicating

with a PC through the standard RS 232 interface has been developed.

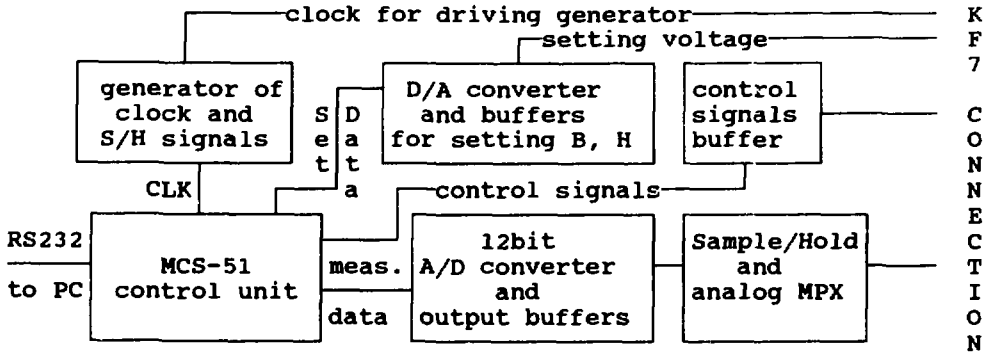

Fig. 1 Block diagram of the control system

The interface consists of three main parts, the MCS-51 control unit, driving circuits and measuring circuits. The MCS-51 control unit is used to receive commands from an IBM-PC compatible computer and to transmit the measured data into it. The commands state, how to set control signals, control reference voltage and how many samples are to be sampled. The clock signal for exciting generator (in the KF7) and for deriving the S/H signal is taken from the MCS-51 control unit. This unit is also used for obtained data preprocessing. The microprocessor computes only necessary values from the data and sends them to the PC. In this way the disadvantage of the serial line communication (relative small speed) is removed.

References.

[1] V.Havlíček and M.Mikulec: On-line Testing Device Using the Compensation Method. Physica Scripta 39, Stockholm 1989.

[2] A.J.Moses: Recent Advances in Experimental Methods for the Investigation of Silicon Iron. Physica Scripta 24, Stockholm 1988.

[3] M.Mikulec: Accuracy of Single Sheet Testers. SMM 10, Dresden 1991.

[4] V.Havlíček: Digitally Controlled Single Sheet Tester. SMM 10, Dresden 1991.

[5] I.Zemánek: The Numerical Methods for AC Magnetic Measuring. Workshop on Circuit Theory and Applications, Budapest 1991.

This research has been conducted at the Departement of Circuit Theory as a part of the research project "Design of the Compensation Ferrometer Controled by IBM PC" and has been supported by Czech Technical University grant No.8047.

PC MEASURING SYSTEMS - EVALUATION OF QUALITY

V. Haasz, P. Kocourek, M. Kubíček, S. Podolák

Faculty of Electronical Engineering CTU, Technická 2, 16627 Praha 6

Key words: measuring system, plug-in card, quality, parameter, accessories, measuring software

Introduction

The project was undertaken in cooperation between PTB Braunschweig and TU Prag, Electrotechnical Fakulty. Two departments in the Electrotechnical Faculty participated in the solution - the Dept. of Measurement and the Dept. of Computers. This report concerns the part that was solved by the Dept. of Measurement.

The problems concerning the hardware (measuring part of plug-in cards) were solved in the Dept. of Measurement. The solution of the project was aimed at the following areas:

1. The criteria of a classification of plug-in cards from the point of view of their parameters, the compiling of a database and the determination of the criteria for the objective choice of plug-in cards.
2. The classification of plug-in cards from the subjective point of view of users.

Subject experience with measurement cards

They are many ways and considerations how to choose the best PC card for our measurement. For technology centers, and when we need complex installations, it is better to contactact a specialized firm e.g. DISYS. However when we want to measure in the laboratory and often modify our own software it is better to use a card from Meilhaus or a number of other producers.

For measuring alternating waveforms it is necessary to know that the sampling circuits must be employed in the card. All card producers do not realize this. Since the sampling frequency can be set in the range of mHz up to kHz, the sampling frequency must be at least twice the signal frequency to maintain the Shannon - Kotelnik theorem. Thus a general purpose anti aliasing filter cannot be designed. The user must remember these facts. Some producers help users and these printed circuit boards are prepared with the motive of designing individual filters for each channel.

For higher accuracy of measuring waveforms it is better to select a faster card than is necessary, because one can then expect a better solution of the chain multiplexer - sampler - converter.

In order to evaluate the dynamic quality of multifunction cards we used the sinewave curve fitting method. This method is also used by HEWLETT PACKARD for AD converter testing. First, save the data from measuring a spectral clear sinusoid. Next fit the ideal sinusoid over these data, and then the difference between these two curves is the quantization noise. From its value we can calculate the number of effective bits. This number tells us how precisely we can measure. Concern for the noise and interference from the power supply of computer is very important. It depends on the method of feeding the plug-in card and the type of input amplifiers.

As a computer without software is simply lifeless material, so the multifunction card without software has no value. Four levels software support exist. Drivers for a program packages (Lab- Windows, Asyst and others) can be designated as the highest level. The next level is a basic program for data acquisition which is sent directly from the producer. Good producers also offer drivers for different languages like GW Basic, Quick Basic, Microsoft C, Turbo C and Turbo Pascal. The orientation of Borlad and Microsoft is evident. Some firms developed simple and low cost, user-friendly software specially for their cards (data acquisition, graphic, signal processing). The lowest level of software support means detailed description of control and status registers of the card. The advanced user can write his/her own special software to meet specific needs.

The program MESBASE gives fast information about data acquisition and control boards for the IBM PC XT/AT. The control program allows the user to select values of parameters in two ways. The first is the selection in the menu with fixed values of parameters. The second way uses the definition of a maximum and minimum value of a chosen parameter. As a consequence of the selection records of boards not satisfying user's demands are deleted. After every delete of a record the computer displays information about the number of remaining records in the database. The user can repeat the selection with more detailed demands and eventually get a reasonable list of boards satisfying his/her requirements.

Conslusion

The part of the task solved in the Dept. of Measurement concerns the gathering of the necessary information and their processing in the tabular form. The created database system makes possible the easy choice of plug-in cards on the basis of required technical parameters.

Borrowed plug-in cards were examined at the same time, because their other characteristics are necessary for users in addition to a cataloque of information. It is important to focus attention first of all at:

- how the sampling is solved and how many effective bits the card has by dynamic measurements
- the possibility of the choice of base address in I/O space
- how the noise level and interference of the power supply of computers is responsible for AC net.

It is a fact that most plug-in cards are designed above all, for measurement in industrial conditions (small measuring and control systems) and for the measurement of non-electrical quantities in connection with signal condition accesories and sensors. Data aquision plug-in cards can be used also for precise dynamic measurements of electrical quantities. However some problems could arise because most of the plug-in cards only have a differential and not an isolated input. For the measurement of static electrical quantities , data acquisition plug-in cards cannot achieve the parameters as the current digital multimeters (isolated inputs, normal mode rejection, effective common mode rejection, resolution). There is not the delivered software determined for this purpose, either.

RECOGNITION OF ISOLATED WORDS

J. Uhlíř, et al.

Faculty of Electrical Engineering CTU, Technická 2, 166 27 Praha 6

Key words: Speech recognition, hidden Markov models, speech enhancement

This paper summarizes the work, which was carried out in the department of Circuit Theory at the Czech Technical University, Prague last year and proposes the continuation of the research. We describe a project of automatic speech recognition system. Our aim was to design a simple speech recognition system and acquire necessary knowledge for more sophisticated systems. We will discuss the used algorithms.

The recognition system consists of several parts: Speech acquisition, the preemphasis (FIR filtration of the speech signal), the speech signal segmentation (Hamming window), the computation of autocorrelation coefficients for every segment, the normalization of the autocorrelation coefficients, the estimation of an autoregressive model, the approximation of the model by a cepstrum vector, the vector quantization (VQ) of cepstrum vectors and recognition procedure.

Speech acquisition is supported by the begin end processor which consists of a finite automaton interacting with a time and energy measuring subsystem. States of the automaton represent various positions in the analyzed utterance. Transitions between these states are controlled by the signals from the measuring subsystem. The system is able to find beginning and end of the utterance eliminating non-speech sounds produced by the speaker and random noise bursts. The phonetical knowledge used to do this is incorporated in the topology of graph of automaton transitions.

Concerning the signal analysis procedure we have chosen the LPC model order eight, for spectra estimation of speech segments. We implemented the Durbin's algorithm which produces the autoregressive coefficients that are used directly for computation of cepstrum coefficients.

In our system the observation sequence of parameter vectors is processed by a Vector Quantizer (VQ). The VQ simply maps the parameter vector space to the finite number of scalar code symbols set.

For the recognition we have chosen the most popular approach: the Hidden Markov Modelling (HMM) technique. The simple modelling led to very good results in almost every speech recognition problem. The output of the VQ, is the code symbol sequence which is from the point of view of HMM an observation sequence. These observation sequences of the same words are different not only for different speakers, but they change in two utterances of the same speaker, too.

The basic HMM is composed of a set of states and transitions between states. The HMM models the observation sequence by emitting an observation symbol in every state after a transition from the state to the other state or to itself.

Every state is described by two probabilities. The first is the probability of the transition to the next state or to itself and the other is the probability of emitting an observation symbol (code symbol) in this state. The probabilities of observation symbols are calculated for every state and each word in vocabulary. The transition probabilities and state probabilities make up matrices. The third problem of finding HMM parameters

is based on the maximum likelihood estimation. It uses a training sequence, which statistically represents one word. The process of model estimation is iteratively repeated until some convergence criteria is met.

Our recognition system is designed to recognize ten Czech digits zero to nine. It has been trained on the database which contains the Czech numbers zero to nine uttered by 50 speakers 20 females and 30 males in a quiet room. Every speaker uttered every word four times. The first utterance in normal fashion, the second well articulated, the third as a question and the fourth in an relaxed way.

The speech recognition system was developed at the Department of Circuits Theory in the last year. It was in the frame of cooperation between US West and the Faculty of Electrical Engineering of Czech Technical University in Prague, Czechoslovakia. The project has been successful and it is possible to propose the research activities which will continue the research work. Continuing the work on speech recognition systems, we want to investigate the behavior of the designed system with corrupted speech and in noisy environments, e.g.in cars as the voice-controlled dialing system or control of the voice mail by voice from the car.

The objectives of the proposed research are as follows:

1. To analyze present methods and to do some comparisons with respect to the application mentioned above.
2. To work out an effective method for cancelling undesired additive interferences in speech using iterative adaptive methods.
3. To analyze the whole system from the point of view of numerical properties and prepare the system for implementation.

Because the car noises are highly nonstationary, we suggest the aplication of iterative methods and adaptive preprocessing of the corrupted speech. The whole structure of speech recognition system can be divided into four main parts: preprocessing of an input signal (picked up by one or more microphones), noise reduction, speech recognition and knowledge based control of the first three parts.

In accordance with our experience in this area, we expect that the recognition rate of the speech recognition system can be improved only if the proper setup of all parts is designed for the specific noise environment. No general solution is available.

We are going to use noise cancelling and speech enhancement methods for an improvement of the recognition rates, recognizing the speech under real conditions.

References:

[1] Uhlíř,J.,Filčev,J.: Spectral Distance Measures for Speech Processing, ISSSE'89. Int.conference of URSI Erlangen, 1991

[2] Filčev,J.,Šedivý,J.,Uhlíř,J.: One Chip Speech Recognition System, Eurospeech 91, 2nd European Conference on Speech Communication and Technology, Genova, Italy, 1991

This research has been conducted at the Department of Circuits Theory but not supported by any grant of CTU.

THE OPTIMAL SOLVING OF GATE LOADABILITY

M. Laipert and M. Kolář** and Z. Horčík**

* Faculty of Electronical Engineering CTU, Technická 2, 16627 Praha 6
* VŠST, Hálkova 6, 46117 Liberec 1

Key words: CMOS gates output loadability, dynamical properties, optimization

The main influence on dynamical properties of CMOS integrated circuit is the capacitive load on logical gates outputs in its structure. In synchronous logical circuits it is necessary to control some tenth or hundredth of next gates inputs. When the IC works with higher clock frequency, it is necessary to minimize the delay of critical ways of exciting signal. In dependence on the number of particular loads it is necessary to select suitable types and connection methods of gates.

The linearized model of CMOS inverter was used for the determination of gate load influence on dynamics of the processed signal. In this model the effect of connecting lines capacity and resistance and of output capacity of logical gates is not considered [1]. The basical load is given as the input capacity of the P- and N-type FET from the basical inverter.

In the case of using various inverter types (with different output power) in the IC structure are the different values of gates input capacity expressed as multiples of basical load values,

$$C_I = n.c_I, \tag{1}$$

where n is the sum of basical loads of all gate inputs connected on analyzed gate output. The C_I capacity is usually the dominant part of the whole load.

Dynamical properties of IC are closely connected with signal delay on logical gates outputs. Delay on signal transition between L and H is defined by the formula

$$T_{LH} = R_H.C_O, \tag{2}$$

where R_H is resistance of closed P-type transistor in driving gate and C_O is its whole capacity load. Delay T_HL is defined similarly, in formula (2) is on place R_H used resistance R_L of N-type transistor.

It is possible to express resistances R_L and R_H of various types of inverters as 1/n-multiple of basical inverter resistance value. Next, we will suppose that ways of exciting signals are built from symmetrical inverters, where $r_H = r_L = r$.

Two basic cases, a tree exciting structure and a cascade exciting structure, are from point of view of dynamical properties practically equivalent. In next we will solve only the cascade exciting according to fig.1

Parallel placing of inverters is implemented in CMOS technology by increasing the gate area on the chip. It is possible to express various inverter areas as k-multiples of basical gate area. The inverter is characterized by its input capacity C_I and resistance R,

$$C_I = k.c_I, R = r/k, \tag{3}$$

where constant k gives the number of parallel connected basical inverters of possible equivalent realization.

According to this consideration we can express an algorithm for optimal design of logical gates load based on principle of consecutive sum of time delay in inverter structure.

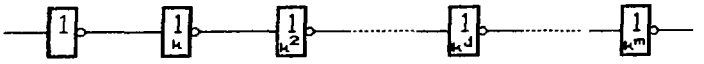

Fig.1: Inverters cascade

The delay in structure consisting of m inverters on fig.1 can be expressed as

$$T = \sum_{j=1}^{m} R_{j-1}.C_j = \sum_{j=1}^{m} \frac{r}{k_{j-1}}.k_j.c_I, \tag{4}$$

where j is the succession of the inverter in cascade. This function will be minimal, when the partial delay between particular inverters in cascade will be the same. This comes true, when all inverters of the cascade from fig.1 will be designed according to the condition $k_j = k^j$. The first inverter is considered to be a single power, because it is usually a part of the IC logical network. alln excited inputs of gates are concentrated In the last inverter of the cascade,

$$n = k_m = k^m, k = k_1 = n^1/m. \tag{5}$$

With substitution (4) into (5) and finding the minimum of this function from the condition dT/dm = 0, this resulted in relation m = ln n. Next we obtain the value of constant k, k = e, where e is base of natural logarithm.

In practical cases m and k_j are integers. Constant k_j is usually chosen as 3^j. An error is caused by rounding off constants m and k_j. As a result, of it the time delay increases in the investigated signal path.

It is possible to partly eliminate this error. Let suppose, that constants k for the first $m-2$ levels in inverter cascade are chosen as power of three. (3^j for j = 0, 1, 2,..., m-2). The last but one level of the inverter cascade has time delay given by formula

$$T1(k_{m-1}) = \frac{r}{k_{m-2}}.k_{m-1}.c_I + \frac{r}{k_{m-1}}k_m.c_I \tag{6}$$

The elimination of design error is based on finding of minimum of the time delay (6). Minimum is achieved for

$$k_{m-1} = \sqrt{(k_{m-2}.k_m)}. \tag{7}$$

The result of (7) need not be integer in all cases.

Procedure of error elimination for the exciting inverter cascade design has a common validity. It is usable for solving the problem of parameters design for inverter placed between two given gates, too.

References.

[1] M. Kolář and M. Laipert: Design of digital semicustom IC. Slaboproudý obzor, 51, 1990, No.7, pages 284-290.

THE REFERENCE CLOCK DISTRIBUTION IN THE DIGITAL NETWORK

L. Strnad

Faculty of Electrical Engineering CTU, Technická 2, 166 27 Praha 6

Key words: Digital Network, Reference Clock, Synchronization

A unique digital telecommunication network allows 64 k bit/s channels to be connected and switched. One of the means for suppressing specific errors (slips due to the time base frequency differences) is the synchronization of the clocks in the digital network. The configuration of the synchronization network and the digital network which is synchronized, need not be the same. The most used configuration of the synchronization network is hierarchical, and the method of synchronization is caled hierarichical master-slave (HMS). For this structure of the synchronization network, use of the reference clock is unavoidable. A reference clock frequency error in telecommunication networks is not to be greater than 1 .10 E -11. In other networks, such as in private branch networks (PB), local network, etc., the situation is similar, nevertheless the demands are not so strict.

Actual problems in the field of network synchronization are problems of reference clock distribution between the different networks, and problems of use of various multiplex hierarchies (synchronous or plesiochronous) within the network. It may be noted here, that so calld synchronous hierarchies (SDH) solve other problems than suppressing of errors.

By planning synchronization of digital networks in Czechoslovakia it is necessary to respect the demands of Czechoslovak telecommunications, which are summarised in the "Synchronization plan".

From the point of view of synchronization the connection of PB and other networks to the communication network can principally be made:

a) independently with plesiochronous operation between networks,

b) by synchronization of the PB network to the communication network, without slips.

For an acceptable slip rate (one slip per 1,4 day for example) between networks, the frequency error of the PB master clock after case a), is to be about $1 \cdot 10\ E^{-9}$. By using a clock with other frequency errors, or in the case of synchronization disturbance, the slip rate changes. The problems can be solved by using the controlled frequency normals or the secondary frequency standards. Within networks with multiplexes of higher orders, or different hierarchies, the problem is which part of multiplex signal is to be used to transmit reference clock. To avoid difficulties with waiting time jitter influence and other influences, the use of frequency synthetisers is suggested.

References:

[1] Příprava výstavby čs. JTS, VÚS 3-43-006-91, Oct.1991 (in Czech),

[2] Příprava a využití integrovaných systémů ... VÚS 3-43-001-90 Oct.1991 (in Czech).

LOW NOISE RECEIVER FOR REMOTE SENSING EXPERIMENTS

M.Mazánek, J.Janík, J.Macháč, Z.Pečený, J.Prokop, J.Šedivý

Department of Electromagnetic Field, CTU, Technická 2, 16627 Praha 6

Key words: remote sensing, radiometry, atmospheric transmission, high temperature superconductors, microstrip antennas

The research of the new radiocommunication services, electromagnetic compatibility, frequency management, application of remote sensing method - all need equipment for experimental work. The portable radiometers for measurement of atmospheric transmission, as different sensors in industry, for remote sensing experiments are in the centre of interests. Some results achieved on this field during the short period of the year 91 include application of the new technology, system design modeling for measurement are mentioned.

The input circuits of the communication systems, e.g. antennas, filters, resonators, made from planar high temperature superconductors (HTSC) can replace waveguide and dielectric resonator for these applications. The theory published in /1/ for microstrip antennas was applied /2/. Software for pattern, input impedance and polarization were developed . Polarization properties of different type of vegetation were studied and measured during the spring and summer 1991. Application of multispectral radiometry (X and IR band) in agriculture /3/,/4/ were verified. Methodology and a new radiometer system design for the next propagation and remote sensing experiment are prepared.

The ollowing results of the evaluation of electromagnetic field in microwave structures have been achieved: The evaluation of the reflectivity and transmissivity of various discontinuities in amicrostrip line. The analysis of rectangular waveguide-microstrip line junction and optimizing of this structure with respect to the minimal VSWR were performed using the universal code based on the method of minimal autonomous block. Using the cavity model the evaluation of a rectangular microstrip antenna input impedance and polarization with the aim to find the feeding point position were solved. Microstrip line filters and resonators were fabricated using epitaxial thin film $YBa_2Cu_3O_7$ (YBCO) on $NbYAlO_3$ substrates. Substrate 10x10mm of thickness 0.5mm were used, acthough in principle also another thicknesses are available. Filters were made without a superconducting ground plane. Because it was not possible as yet to prepare superconducting films on both sides, only a planar microstrip structure was made as superconducting. A structure consisting of two separate substrates, one for the planar structure, the second for the ground plane is also possible. Our studies include straight linear resonators with transformer, parallel-coupled bandpass filters. Software developed at the CTU were used for practical design and optimization. Cooling 77K for YBCO is already available. The package designed to minimize parasitic reactances and electromagnetic input-output coupling must be mechanically stable in the thermal cycling. Methodology and test fixture for measurements of planar HTSC structures were developed for measurement next year.

Portable "autocallibrating" radiometer at 12GHz frequency range, sensitivity 0.05K, was developed for radiometric measurements of polarization matrix for experiments in

atmospheric transmission. Similar system will be also used for multispectral radiometric remote sensing experiment in agriculture. The input switch of the radiometer is probably one critical point of the design.The designed system uses polarization switch on circular waveguide and linear polarization of the antenna. Then the thin film load orthogonal to the signal plane can be used as reference. For the portable system for the measurement in the field it is not necessary to stabilized a temperature of the load; to measure and to calibrate continuously during or in data is possible. Using the polarization switching on the input of radiometer allows the development of more complicated structures for calibrations.

Two ways to approach to real radiometric picture were studied: deconvolution of the antenna pattern and multispectral deconvolution /4/,and using a simplification that emissivity at given frequency is a linear combination of values representing observed physical parameters. The multispectral process leads to the linear problem which can be solved using Singular Value Decomposition technique.

The newly discovered HTSCs offer new possibilities for passive microwave application. It appears that using narrow microstrips allows the dielectric thickness to be reduced and thereby to reduce dielectric losses, also the inverted microstrip can be used. HTSC planar radiated arrays can be suitable especially at millimeter wavelengths and will be applicable for small low noise receivers and radiometers. Much work remains to be done. The theory of depolarization and evaluation of remote sensing data as well as software for radiometric measurement /5/ are the efficient tools in the remote sensing agriculture experiments and in the satellite Mayak experiment performed by PTT.

References:

[1] W.F.Richards and others: An improvement theory for microstrip antennas and applications, IEEE, Transactions on AP, Vol.29, No.1.,January 1981.

[2] J.Macháč: Analysis of discontinuities in waveguiding structures by MAG method, IEE Proc.Part H, Microwave antennas and propagation, to be published 1992.

[3] M.Mazánek, report HS 310297,

[4] T. Český, M.Mazánek: Evaluation of remote sensing data, ICAP, York, 1991.

[5] J.Janík: Automatic antenna test, diploma theses, CTU, 1991.

Acknowledgement:

The computation, was except for the 2D solution of a microstrip line and filters, was performed on IBM 3090 computer, thanks to the IBM Academic Initiative in Czechoslovakia.

We are deeply indebted to our co-workers at the Low Temperature Laboratory of the Institute of Physics and in PTT research institute in Prague. We wish to express our deep gratitude to Dr.Tomáš Český, the expert of European Radiocommunication Office in Copenhagen, for his advice during this work.

This research has been conducted at the Department of Electromagnetic Field in the frame of the research project: "Propagation of the electromagnetic waves in the new frequency bands" and has been supported by CTU grant No.8045 and partly by the project "Multispectral radiometry" of Ministry of Environment by contract HS 310297.

MODULATION AND CODING METHODS FOR RF TRANSMISSION

V. Žalud, Z. Šubert, J. Horevajová, B. Syrovátka, M. Ponikelský.
Department of Radioelectronics, CTU, Technická 2, 16627, Praha 6

Key words: Analog and digital modulation, Satellit receivers, Communication systems, GaAs monolithic circuits.

The team of research workers applying for the grant of Czech Technical University in Prague has been engaged in basic research and modern radiocommunication devices development for many years. In 1981 - 1985 most of the team members were working under the supervision of Dr. Václav Žalud, Associated Professor, on the state assignment P-02-128-402/08 "Application Principles of New Modulation Methods in Satellite Systems ". This assignment was successfully defended in 1986. In 1981-1989 Dr. Žalud cooperated with the TESLA VUST Praha Research Institute.This cooperation resulted in the development of several unique measuring devices for satellite television receivers measurements (FM signal generator and selective microvoltmeter for the range 0.9-1.8GHz etc.). In 1990-1991, further to this cooperation, a unique spectral analyser for satellite if range was developed. All instruments mentioned above establish the equipment basis for the workplace of the team applying for the grant in question.

During 1987-1989 Dr. Žalud cooperated with the Semiconductors Department of the TESLA VUST Research Institute in the field of microwave monolithic GaAs-based integrated circuits design. That successful cooperation resulted in the new microwave monolithic GaAs-based amplifiers design. At the beginning of 1990 the cooperation was discontinued because of TESLA VUST department reorganization.

Problems of modern modulation methods, and closely related coding have been solved by some members of the team in question, supervised by Dr. L.Subert, Associated Professor. This group also carried out a simulating experiment, which proved the possibility of digitally processed picture signal transmissions, coded in the composite form Y, R-Y, B-Y (component coding 4-2-2, discretisation speed 13.5 MHz, 8 bits per pixel, 27 MHz bandwidth on 70 MHz carrier). Signal speed reduction (216 to 40.5 MHz) was achieved by the input picture signal processing in the DPCM system to 3 bits, preserving the good quality of TV program picture at the same time. Fundamental problem consists of 8 state phase modulation and synchronous demodulation. In addition, it was necessary to design matched band passes, which met requisite group delay in the given frequency range, demanded by the multi state phase modulation. During our work on the problems we have achieved a good agreement between results simulated on computer and the experimental results, in which the subjective quality of the picture information was evaluated. The work on these problems, especially on the solution of the multi state modulation which saves the frequency bandwidth to a great extend, is being continued.

The group is also engaged in the development of technical and programming tools for the protection of the series information transmission using various types of data processing devices, which enable communication between all users. A concrete microprocessor data processing device , which controls complex sets in the urban traffic, was designed and realized.

In 1988-1991, noise characteristics in radiocommunication sets for various modulation types were investigated within the research work at the Department of Radioelectronics. From the discussion over the results, general rules for the particular modulation method utilisation have been derived. Noise properties were also treated both theoretically and experimentally not only in radiocommunications but also in other spheres.

Recently, the team of research workers applying for the grant have been engaged in treating problems both theoretical and practical ones closely related to the grant. That would guarantee the success in the solution of all tasks in the future.

This research has been conducted at the Department of Radioelectronics in recent years.

GPS SUPPORTED BY INMARSAT-3 OVERLAY

F. Vejražka and Z. Hrdina

Faculty of Electrical Engineering, CTU, Technická 2,166 27 Praha 6

Key words: satellite radionavigation, GPS, Inmarsat, DOP

CNS systems are evaluated as one of the most significant branches of a technology development because they are contributing to rescuehuman lives and to an improvement of the world energy and ecology situation.

They are an association into one unit of communication (C), navigation (N) and surveillance (S) systems which have been independent till now. A navigation part determines automatically an object's position, information on the object state is added, and they both are transferred by a communication part to a centre. The surveillance part of the CNS system ensures processing of infor- mation on position and states of objects and displays it in the centre. Information leading to a desired alteration of position or state can then be sent back to the object by the communication part of the CNS.

A person, means of transport (plane, ship, bus, truck, car of fast medical care), combine harvester, drilling platform, weapon or security system can be the mentioned objects.

Satellite CNS systems are of the greatest importance because their impact is world-wide and capable of further development.

The satellite navigation subsystem is a main element of the CNS. The satellites with known parameters C of their orbits transmit ranging signals, and on the basis of their evaluation a user assesses a position estimation. On the acceptable presuppositions a covariance matrix of estimation errors is [1]

$$P = \sigma_d^2.(C^T.C)^{-1} \tag{1}$$

where σ_d^2 is the dispersion of measured range. Rms of a radial position error ΔR is

$$rms(\Delta R) = \sqrt{E[\Delta R^2]} = \sigma_d.DOP \tag{2}$$

$$DOP = \sqrt{tr[(C^T.C)^{-1}]} \tag{3}$$

A standard deviation of measured range depends on ranging signal quality, on ionospheric refraction and on Selective Availability. It could be decreased by placing a monitor station into a point with known coordinates. This station measures its position and compares it with the real one. The corrections are computed from this comparison and they are transmitted. A user achieves radial error cut-down of the order of 10 times by processing them in his equipment. This method is named differential navigation.

The DOP factor (2) is smallest when the satellites are uniformly spread in the sky. In the existing GPS satellite navigation system moments appear when the DOP factor reaches unacceptably large values. By adding other satellites to space segment they can be diminished. It has been suggested to use the INMARSAT-3 satellites for this purpose [2]. They transmit an integrity message (GIC) only or a ranging signal of a GPS type.

We evaluate the performance of the satellite navigation system by means of (a) the uncoverage and (b) the accuracy.

The uncoverage is a probability of a situation in which navigation is impossible or the DOP is greater than its greatest admissible value DOP_max .

The accuracy R_n is determined for given probability P from error probability distribution f

$$\int_{x_1^2+..} \cdots \int_{x_n^2<R_n^2} f(x_1,...,x_n)dx_1..dx_n = P \tag{4}$$

The uncoverage and the accuracy are computed by a simulation in points of a space-time network. The time step T of points has to correspond to the spatial step α. Then supposing small values T and α we can obtain

$$T \doteq 73.1\alpha \tag{5}$$

The simulation procedure consists of computing the covariance matrix (1) and DOP assessment for each point of the space-time network. The uncoverage is a relative frequency of points with $DOP > DOP_{max}$. The average covariance matrix is calculated for points with $DOP \leq DOP_{max}$ and the accuracy R_n (4) is then obtained from it. Both values depend on a mask angle, i.e. on a minimum value of an elevation angle with which it is still possible to receive satellite signals. It is evident from the figure that in the case of addition of INMARSAT satellites to the GPS space segment the transmitting of the ranging signals together with the GIC messages is desirable. It makes the uncoverage 50 times smaller for values of the mask angle smaller than 20 degrees.

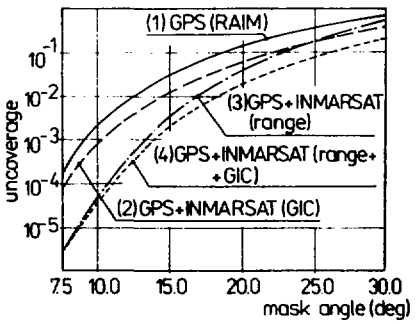

Our next CNS systems studies will be aimed at the use of this method for the GLONASS system performance assessment and at a development of differential navigation methods mentioned above [3].

References.

[1] Vejražka,F.;Hrdina,Z.;Nagle,J.: Performance of GPS supported by Inmarsat satellites. In: NAV91, Satellite Navigation. The Royal Institute of Navigation, London, 1991.

[2] Vejražka, F.: Provisional report on GPS signal coverage supported by Inmarsat-3 overlay. London, Inmarsat 1991.

[3] Obuškevič,V.: Přesná měření polohy navigačními systémy. Praha, ČVUT-FEL 1991.

This research has been conducted at the Department of Radio Engineering as a part of the research project "Signal Processing in CNS Systems" and has been supported by CTU grant No. 8044.

OPTICAL WAVEGUIDE STRUCTURES IN GLASS AND $LiNbO_3$ FORMED BY DIFFUSION TECHNIQUES

J. Schröfel, Z. Burian

Faculty of Electrical Engineering CTU,Department of Microelectronics, Technická 2, 16627 Praha 6

Key words: integrated optics, planar waveguides, diffusion technologies

Introduction For further progress in optical communication, sensor systems and several measurement equipment as well it is very important to reach also some substantial improvement of technical - economical parameters of optical structures and components for distribution and harnessing of optical radiation.The substantial part of these elements are planar(channel) waveguides made in various types of dielektrical or semiconductor substrates usually using several diffusion or thin-layer techniques [1].

Optical waveguides in glass substrates The most used technology for preparation of planar waveguides in glass substrates is based on ion-exchange cations Na^+ and K^+,which are in structures of soda-lime silicate glasses bounded rather weekly,to ions with higher polarisibility (e.g.Tl^+,Ag^+,Cs^+,Rb^+ and Li^+); these ions come from external source usually a melt of suitable salt.Process of ion exchange can also be field-assisted externally.

Side restriction of ion-exchange area made with the help of lithographical techniques , at suitable conditions,results in an exactly-defined strip layer with gradient or nearly step refraction index profile,this layer being completely surrounded by areas which have rather refraction indexes.This structure is in fact a planar analogy of optical fiber waveguide [2].

Our interest has been directed toward promising waveguides which are based on $Ag^+ \longleftrightarrow Na^+$ ion exchange in glass substrates. The objective of our research that was carried out was first of all to explain and to overcome commonly existing large optical loss of waveguides in range of used wavelengths (0.85 - 1.55μm) and then to work out preparation procedures of channel waveguides which will resemble multimode fibre waveguides concerning their dimensions and optical properties.In connection with various applications of these waveguides in structures for distribution and harnessing optical radiation or components for the same purpose, we solved also problem implementation of low-loss coupling of channel waveguides to fibre waveguides.At the same time we also studied necessary measurement methods.It has been proved that it is possible to use $Ag^+ \longleftrightarrow Na^+$ exchange in special very pure silicate glasses with high content of natrium oxide (Na_2O) and $NaNO_3/AgNO_3$ melt to obtain waveguide layers with depths 1 - 50μm and optical loss ¡0.1 dB/cm.Moreover, it follows from these experiments that combined multistage ion-exchange process with and without assistance of electrical field can be used at appropriate conditions for preparation of low-loss multimode channel optical waveguides with semicircular crossection and nearly parabolic refractive index profile.

Optical waveguides and waveguide structures in $LiNbO_3$ The first develope dmethod of channel waveguides preparation is based on thermal diffusion of titanum from thin strip-layer made on $LiNbO_3$ surface using combination of suitable lithographical and vacuum deposition techniques.Another, later method is based on $H^+ \longleftrightarrow Na^+$ ion-exchange (so called proton-exchange method).

Several problems arise in the process of preparation of these waveguides.In the case of titanium diffusion it is mainly sensitivity of resulting waveguides to optical damage and appearance another parasitic waveguides by out-diffusion of Li_2O.The main problem connected with proton-exchange waveguides is a poor parameters reproducibility [3].

Our recent research has been concerned with waveguides based on $Ti : LiNbO_3$ with a special regard to study of detailed relations between diffusion conditions (diffusion source thickness, diffusion temperature and time) and dimensions and refractive index profile and also in order to explain and eliminate out- diffusion effects.

Gained results were used to fabricate monomode channel waveguides for wave-lengths 0.85 - 1.3μm with relatively low-loss (0.5 - 0.8 dB/cm) and limited out-diffusion effects.In collaboration with RE SAV and TESLA VST these results were also used for the realization of some complex structures which are fast electrooptical modulators and switches.As to modulators some experiments of preparation structures with Mach-Zehnder interferometer have been carried out.In the case of switches our interest has been pointed at a research of a structure which is labeled X or BOA.Gained results are very promising and can be not only a good base for future work in this field but give also some application possibilities for various purposes. Conclusions We have designed and proved a multistage $Ag^+ \longleftrightarrow Na^+$ ion-exchange process carried in special silicate glasses which enables a preparation of multimode waveguides with semicircular crossection nearly parabolic refractive index-profile and optical loss less than 0.1 dB/cm in the range 0.85 - 1.55μm.As to waveguides based on $Ti : LiNbO_3$ for the same wavelength range we have gained further improvement parameters either from the point of view of optical loss (0.5 - 0.8 dB/cm) either substantial elimination of out - diffusion effects.Resulting waveguides have been used with success for preparation experimental samples of planar electrooptical modulators and switches.

References

[1] Čtyřoký,J.,Hüttel,I.,Schröfel,J.,Šimánková, L.:Integrated Optics.Praha, SNTL 1987 (in Czech).

[2] Schröfel, J.,Čtyřoký,J.,Janta,J.:Integrated optical couplers in glass substrate. 2.Lichtwellenleitertagung (RGW - offene Tagung), 30.1 -1.2.1990. Karl-Marx-Stadt, p.118-120.

[3] Čtyřoký,J.,Göring,R., Janta,J.,Karthe,W.,Rasch,A.,Rottschalk,M.,Schröfel,J.:Kybernetika, 26,1990,p.171-190.

This research has been conducted at the Department of Microelectronics as a part of the research project A 07-119-802.

APPLICATION OF FAST LIGHT IONS IN SEMICONDUCTOR DEVICE PROCESSING

P. Hazdra, M. Kejhar, J. F. V. May, P. Seidl, B. Sopko, J. Vobecký

Dept. of Microelectronics, Faculty of Electrical Engineering CTU, Technická 2, 166 27 Praha 6

Key words: lifetime control, radiation defects, semiconductor devices

Semiconductor materials show temporary and metastable changes in their electrophysical and optical properties when irradiated with elementary particles and quanta. Although apparently simple, the radiation methods found application only after many years of extensive studies. While the research is still under way, a qualitative generalized model of the radiation processes has emerged with the effective means of control of said processes defined and developed, which allows obtaining the required fairly stable changes in characteristics of semiconductor materials and structures. Radiation compensation of the semiconductor material, thin layer doping by ion bombardment, creation of radiative recombination centres, control of the photoconductivity spectra and nonequilibrium carrier lifetime, and doping by nuclear transmutation are a few examples that illustrate the importance of radiation methods to semiconductor technology.

The usual way to control the lifetime of semiconductor devices is to introduce point defects, giving rise to levels in the forbidden band gap where electrons and holes can recombine. Today these traps are introduced in a final off line processing step by high energy electron irradiation. This technique offers several advantages such as good control of charge-carrier lifetime and high reproducibility. A drawback is, however, that the electrons effect the entire bulk, since they pass straight through the devices, creating defects all along the way. By the use of light, high energy ions, this drawback can be overcome [1]. These nuclear particles are stopped within the bulk at a depth determined by their energy. They create most of the lattice damage towards the end of their range, enabling localisation of regions of high defect concentration while most of the silicon bulk is left relatively unaffected. This principle of localized lifetime killing might be favourable for the improvement of the trade-off between on state and turn-off loses of many modern power switching devices [2].

The detailed investigation of radiation defects created by fast light ions must proceed before their technological application in the process of localized lifetime tailoring. The attention must be paid especially to the influence of irradiation conditions on particular defect generation and to the determination of their electrical properties. For this purpose utilization of high sensitive electrical diagnostic methods (e.g. DLTS - Deep Level Transient Spectroscopy, I-V and C-V measurements) and various process simulators is necessary together with adequate technological support.

The intensive investigations in the field of radiation defect characterization have recently been carried out in our Department . They have been focused on the identification of the radiation defects produced in silicon by medium energy self-implantation, determination of their concentration profiles, thermal stability and the influence of implantation temperature on individual defect production [3]. Simultaneously comprehensive system of diagnostic and simulation methods (DLTS, I-V, C-V, AS,

OCVD) has been developed [4]. All these achievements make a basis for development of modern technology for localized lifetime control. This project submitted to the CTU grant agency supposes first the experimental characterization of radiation damage created by fast light ion and its comparison with radiation defects generated by other high-energy techniques. The goal of this work is the full understanding to the process of controlled introduction of point defects for local control of semiconductor microphysical parameters. All the acquired information about generated defects will be used primarily as an input for a device simulator serving as a prediction tool for optimizing the irradiation conditions taking into account required device parameters.

References:

[1] J. Vobecký, "Lokální řízení doby života ve výkonových polovodičových strukturách", Čs. čas. fyz. 41 (1991), pp.43-54

[2] D.C. Sawko, J. Bartko, "Production of Fast Switching Power Thyristors by Proton Irradiation", IEEE Trans. Nucl. Sci. NS-30(1983), pp. 1756

[3] P. Hazdra, V. Hašlar, M. Bartoš, "The influence of implantation temperature and subsequent annealing on residual implantation defects in silicon", Nucl. Instr. Meth. Phys. Res. B55(1991), pp. 637-641

[4] M. Hátle, J. Vobecký, "Infrared Observation of Gate Turn-Off Thyristor Segment Parameter Nonuniformity", IEEE Trans. Electron Devices, Vol. ED-37(1990), pp. 1169-1171

This project is supposed to be carried out at the Department of Microelectronics, Czech Technical University of Prague.

AN APPLICATION OF DEVICE SIMULATOR ON GTO THYRISTOR

J. Vobecký, M. Hátle

Dept. of Microelectronics, Faculty of Electrical Engineering CTU, Technická 2, 166 27 Praha 6

Key words: Simulation, thyristor, GTO, secondary breakdown

Contemporary semiconductor device structures have revealed the need for a better understanding of basic device behaviour. The miniaturization and complexity of devices led to a breakdown of the classical models. As a consequence numerical analysis and simulation based on comparatively fundamental differential equations has become necessary and important. This trend has been supported by the enormous progress in technology and performance of computers. Contemporary modeling of semiconductor devices has attained such a high level of sophistication that even three-dimensional transient simulations have been reported. Numerical analysis of semiconductor devices became a basic methodology of research and development engineers. However, one must not expect that people using computer programs as numerical analysis tools are specialists considering the complexity of the assumptions, algorithms and implementation details of the programs they use. Nowadays, one can utilize the support of some software firms, e.g. Technology Modeling Associates, Palo Alto, USA, in order to buy outstanding simulation tools, that are continually updated and enhanced. Unfortunately, in our case a relatively high cost of the tools mentioned makes their ordering impossible. This is why we have to survive with our own tools as well as with tools obtained thanks to close cooperation with other universities.

At present we employ a 1-D device simulator equiped with all features that most complete semiconductor device simulators have today. It was applied in original manner on problems related to high-power diodes [2] and thyristors [1]. In case of thyristors the simulation of small-signal current gains in arrangement of a real measuring circuit of Fulop's method was performed for the first time [1]. Excellent qualitative agreement with measurements, that we also dispose, was reached. Furthermore, our investigations showed excellent sensitivity of current gain's magnitude to any device and/or technological parameters. Therefore, the very efficient control of technological process based on both measurement and simulation may be established in the case of any thyristor. However, the transition from 1-D to 2-D model may enable a simulation of other technologically advanced structures that the 1-D model precludes. Another reason for the implementation of 2-D simulator suitable for true transient analysis of thyristors is the necessity to clarify the physical phenomena connected to the secondary breakdown of the GTO thyristors occuring during turning off the inductive load. The above-mentioned effect was widely published in case of transistors but negligibly for thyristors with gate turn-off capability. Nevertheless, we had already opportunity to perform a lot of experimental investigations by means of advanced optical diagnostic methods [3]. Both methods revealed that the avalanche injection or punch-through mechanism supported by the high anode voltage rise dV/dt are responsible for the destruction of the GTO subjected to the turn-off of the inductive load without snubber circuit [4]. Nevertheless, limited time resolution

of diagnostic methods used disabled the quantification the related physical phenomena that are several order of magnitudes faster compared to the mentioned time resolution. Therefore it is only the simulation that can clarify the whole effect in required details. The solution of this problem has a great potential for the power device industry because of possibility to develop the true snubberless GTO and to support the physics behind the avalanche injection switching devices. It is worth pointing out that the transient analysis of the thyristor structure is the most advanced problem from the simulation point of view. It explains why there is the lack of results obtained and why this subject is still of great scientific importance. Consequently, the justification of future financial support by the grant agenture of CTU occurs readily.

REFERENCES:

[1] M. Hátle, J. Vobecký: "A Contribution of Small-signal Current Gains Frequency Dependence Investigation to Overall Diagnostics of the GTO Thyristor: Simulation and Measurement", Proceedings of the Symposium on Materilas and Devices for Power Electronics, pp. 402-406, Florence, Italy, 1991

[2] M. Hátle, J. Vobecký: "Optical Characterization of the Carrier Distribution in Silicon Power Devices with Defined Spatial Resolution", Periodica Polytechnica ser. El. Eng. Vol.34, No.1, pp.13-20, 1990

[3] H. Bleichner, M. Rosling, J. Vobecký, M. Lundqvist, E. Nordlander, "A Comparative Study of the Carrier Distributions in Dynamically Operating GTO:s by Means of Two Optically Probed Measurement Methods, " Proceedings of Int. Symposium on Power Semicondustor Devices and Int. Circuits'90, pp. 246-251, Tokyo, Japonsko 1990

[4] H. Bleichner, M. Bakowski, J. Vobecký, M. Rosling, E. Nordlander, M. Lundqvist, and S. Berg, "A Study of Turn-Off Limitations and Failure Mechanism in GTO Thyristors by Means of 2-D Time-Resolved Optical Measurements, " submitted to Solid-State Electronics

This work is supposed to be carried out at the Department of Microelectronics, Czech Technical University of Prague.

LOW-RATE DATA TRANSMISSION OVER LONG PRODUCT LINES

J. Přibyl

Faculty of Electrical Engineering CTU, Technická 2, 166 08 Praha 6

Key words: Data transmission, product lines

The build-up of product line networks, primarily including oil lines and gas lines, envisages the construction of parallel cable circuits for the transmission of information relevant for the control and monitoring of the flow of products through the pipeline. The information of this type can be introduced into the communication subsystem in nodal points of product-conveying networks e.g. in the locations of spherical valves and compressor stations. For the operation of long-distance pipeline networks other information is necessary, too, for the safeguarding of reliability of these conveying media. This information, which characterizes for example the condition of anticorrosive protection devices of a pipeline or the changes of the tension status of pipelines routed through seismic regions, can be introduced into the communication subsystem neither in nodal points of product-conveying (because the information sources are as a rule situated in a section between two adjacent nodes with a mutual distance 40 km) nor at the information sources themselves (because of the inaccessibility of the cable communication subsystem).

The precondition for the solution of the problem of the transmission of the above-characterized information from the locations of their sources on the pipeline to the nearest nodal point of the product-conveying network is therefore the design of an economically and energetically unpretentious transmission of small data volumes over a distance equal up to one half of the distance between two adjacent nodal points (i.e. over a distance up to 20 km) or the solving of the problem of utilizing the body of the product-coveying pipeline not only for the transportation of products but also for the transmission of data signals having the above-mentioned character. Because, theoretically, a product-conveying pipeline and its anticorrosion system can be conceived as a one-conductor line against ground and mathematically modelled as transmission media with a low limit frequency of the order of tens of Hz, it should be in principle possible to make use of old telegraph transmission methods on higher level technology.

The low-speed transmission system over long-distance product-conveying pipelines designed, realized and tested by the author in realistic operating conditions can be regarded as a proof of the statements in the above paragraph. The system consists of two parts, the transmitting and receiving part. The transmitting part consists of the data signal source whose design depends upon the character of the monitored information, of a power transmitter and of a power source. The data source is connected at standard logical levels to the input of the circuit for keying the power transmitter. The power transmitter transmits current polar signal elements of the order of amperes at the modulation rate up to 50 Bd into the product conveying pipeline. The output impedance of the transmitting part is very low, corresponding to the impedance of the pipeline against ground. The power supply of the transmitting part is provided by a normal autobattery whose capacity is sufficient for fourteen days of unattended operation of the equipment.

The receiving part consists of the input circuit for automatic compensation of the permanent potential of the anticorrosive protection of the pipeline, of a selective active filter and of the output shaping circuit with level transducers to levels in compliance with CCITT Recommendations V.24/V.28 convenient for processing in further devices e.g. modems or PCs. The receiver is capable of processing signals of polar character with peak-to-peak voltage from tens of millivolts and higher what guarantees errorless transmission over distances required.

The input and output part of the receiver provides for manual setting of minimum telegraph distortion according to the existing situation. The selective active filter plays an important role in the suppression of a whole set of disturbing effects having various causes as e.g. unsufficient rectification of power supply voltages of anticorrosion protection devices, the crossings of pipelines with high voltage lines, stray currents and parallelisms with electrified railway lines. There are pretentious requirements imposed on its attenuation response as seen from the variation of measured values in Fig. 1.

The development of functional samples of the transmitting and receiving parts of the system proceeded in the years 1987 to 1991 and claimed a significant extent of experimental work in real conditions. Some results of experimental data transmission over the transit gaspipe lines of 900 mm pipe diameter are fixed in the following figures. Fig. 2 represents the variation of attenuation of data signals with modulation rate for a transmission distance of 1.2 km, Fig. 3 the variation of attenuation of data signals with distance for the modulation rate of 45 Bd.

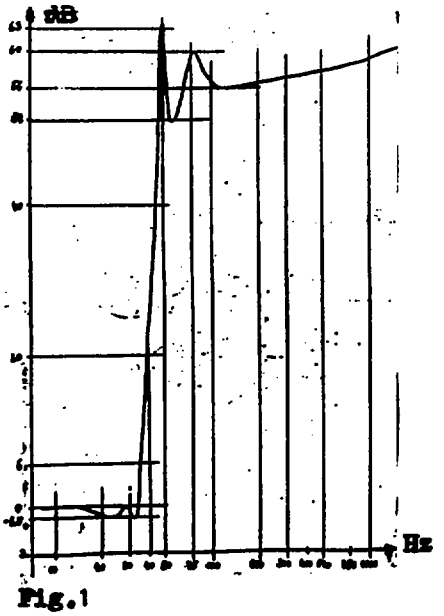

Fig.1

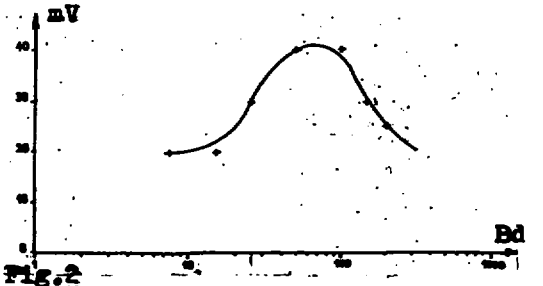

Fig.2

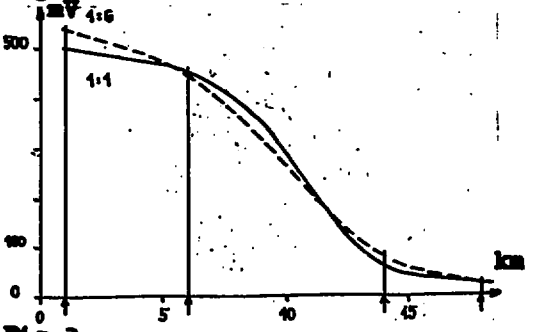

Fig.3

DESIGN OF ANALOG AND ANALOG - DIGITAL ELECTRONIC FUNCTIONAL BLOCKS

Přemek Neumann, Jiří Kadlec

Faculty of Electronical Engineering CTU, Technická 2, 166 27 Praha 6

Key words: Analog circuits, functional blocks, testing, analysis

In the period from 1970 till 1985 our research activity has been focused on the analysis of nonlinear and linearized transistor circuits including a relatively large class of these circuits. Attention has concentrated on basic one-transistor circuits on the one hand and on simple opamp structures and networks comprising several opamps on the other hand. During this period many research reports, contributions presented in journals and conferences and diploma works has been published dealing with absolute value amplifiers, logarithmic converters, RMS converters, modulators and demodulators. The aim was to acquire some experience and data making possible to synthesize hybrid integrated circuits and in the future monolithic integrated circuits as well which can implement prescribed nonlinear functions /1/. Standard laboratory equipment has been used to perform measuring and testing of these circuits. During the experimental work an insufficiency of the standard equipment occurred. As a consequence of this fact attention has been paid since 1980 to the study and development of special circuits and systems which are usable as parts of testing equipment. Our aim is to prepare equipment giving the possibility to realize repeated testing and measuring of parameters describing analog and analog-digital functional blocks. We intend to create two different testing laboratories in the future. The first one could be directed at testing basic structures and measuring their parameters yielding to data acquisition for the identification of micromodels. The second one could serve as a macromodels testing laboratory. Analog functional blocks are to be tested there predominantly with respect to the linearity of their dynamic characteristics (/2/, /3/, /4/) and threshold signal variations /5/.

During the last decade very quick development of digital techniques and networks has been accomplished, especially in the field of personal computers. Efficient digital signal processing methods applicable on analog signals has simultaneously been worked up on the large scale. To ensure adequate practical applicability of these systems technical parameters of attached both analog functional blocks and analog-digital converters have to be improved. Our recent research activities have been directed toward this goal. New technology developed for digital circuits (ASIC) represents an economically-appropriate way how to solve the above-mentioned problems. The task to be solved is to find technically-feasible realizations and to create a set of appropriate circuits usable for the system ASIC. To ensure practical implementation restrictions following from used technological procedures have to be taken into considerations.

From the available literature it follows that there are at least 27 foreign producers who are able to deliver analog and analog-digital ASIC. Only 3 of them are oriented exclusively toward the bipolar technology. The rest, that is the majority of them, produce circuits on the basis of the CMOS technology or combined one. From the economic point of view the CMOS technology seems to be preferred. In view of this fact some relations with the Department of Microelectronics have been established and by means of it with

the home producers of CMOS circuits (Tesla VÚST, Tesla Piešťany) as well. Recently-made investigations of the ASIC production yield results that there are two groups. The first group represents the ASIC consisting of some primitive structures such as diodes and different sorts of bipolar transistors. Different types of transistors (NPN, PNP) are realized with different dynamic properties, different dissipation power etc. This type of ASIC can be used quite generally. The second group comprises ASIC made almost exclusively of more complex functional blocks (e. g. Analog Devices) which are intended to be used only for special purposes. In this sense they replace formerly-used printed circuits plates. We have an idea to create "intelligent" sets of ASIC consisting of some optimal configurations of diodes, transistors, simple circuits, opamps and D/A converters giving the possibility to build systems realizing almost arbitrary conversion of analog signal to the digital one. We intend to focus our research work in this direction in the future.

References:

[1] Neumann P., Ptáčková G.: Some New Applications of Operational Networks, Proceedings of the Czech-Polish-Hungarian workshop on CT, ČSVTS FEL ČVUT, Praha 1986.

[2] Neumann P., Kadlec J.: Harmonic Distortion Measurement and Simulation, Proceedings of the Polish-Czech-Hungarian workshop on CT, Institute of Electronics, Warsaw - Zakopane 1988.

[3] Neumann P., Kadlec J.: Quick and Precise Sample and Hold Circuits, New trends in the signal processing, ČSVTS pri VVTŠ v Lipt. Mikuláši, Račkova dolina 1990 (in Czech).

[4] Neumann P. and group: Quick and Precise Analog Signal Digitalization Methods and their Possibilities, partial research report connected with HS 30 18 88, FEL ČVUT, Praha 1988 (in Czech).

[5] Kadlec J., Neumann P., Horčík Z.: Measurement of Operational Amplifier Noise Parameters, Proceedings of the workshop on circuit theory and applications, Budapest 1991.

[6] Neumann P., Kadlec J., Horčík Z.: Analysis of Properties and Synthesis of the PLL, partial research report connected with HS 30 67 89, FEL ČVUT, Praha 1990 (in Czech).

This research has been conducted at the Department of Network Theory as a part of research activity in the field of networks for signal processing.

THE RELIABILITY OF DIGITAL SWITCHING SYSTEMS

J. Novák, J. Rynt, J. Chod

CTU Faculty of Electrical Eng.,Technická 2, 166 27 Praha 6

Key words: Reliability, Temperature Map, Switching System

The Czechoslovak telecommunication network is largely analogue at present,and the electromechanical switching systems are predominant. The extensive introduction of digital switching systems with programme control is expected in the future. The reliability is closely connected with the operation of electronic digital switching systems from the equipment temperature mode point of view mainly.

Keeping reliability parameters within allowed limits given by the producer is conditioned by the strict temperature air conditioning mode in which the equipment operates. It is very important to consider that the digital switching systems are mostly located in the rooms where the electromechanical switching systems with lower temperature demands operated previously.

In order to evaluate the general processes sliping in the mentioned structures, we shall use the information from a science branch - the physics of failures. Technology parameters of any detail working in the electrical circuit are effected by the external parameters, by their limit values and waveforms. This influence evokes the degradation of technology parameters and the consequent failure of detail. The speed of degradation which is effected by many external parameters is described by Eyring's model. The speed of degradation which is effected by external temperature only we can describe by Arrhen's model. We can evidence the limitation of technology life of the semiconductor details which operate in the temperature modes which exceed the highest-allowed temperature of the semiconductor transient. The determination of temperature maps will be the origin for the solution of the reliability of the equipments, subsystems and whole system. It is not suitable to use the temperature sensors only because the space temperature distribution is very rough. The use of the thermovision camera with additional temperature sensors distributed is much better. Data collection will be performed by the personal computer PC AT.

Continuously on these bases the limitation factor of the service life of particular exchange blocks will be established by the distribution of temperature maps. The recommendations of the temperature mode changes of the critical parts of the telecommunications equipments will be the result.

The task will be compiled in the form of objected research report including drafts of recommendations for the determination of the air conditioning temperature mode and for the location of racks in the present switch rooms both for the new and present digital systems. This will be solved with respect for the minimalization of energetic power consumption with keeping of the projected service life.

THE PROJECT OF THE VIDEOTEX SYSTEM ON CTU PRAG

J. Svoboda, B. Šimák, T. Zeman, J. Houda, P. Chaloupka

Faculty of Electrical Engineering CTU, Technická 2, 166 27 Praha 6

Key words: videotex, local area network, information system

A videotex (VTX) is a modern interactive telematic service, that enables a subscriber to have access to important databases through to telephone or data networks. The videotex terminal is a relatively simple and cheap device. The subscriber can choose information selectively, make interactive transactions, send news to another participants,and change and complete information in a reserve part of the database.

A well-tried system "paper-telephone" is mainly used in practice of internal information flow. However great economical pressure to improve effectiveness of management process leads to searching for new ways. One known way is installation of a local area networks (LAN) that provide transmission of information between computers connected into the internal network of a university. This arrangement enables a very rapid information gain to any subscriber. Use of LAN like a public information means is not applicable in conditions of diverse work places of the university. The percentual prevailing type of information transmitted is "question-answer" that does not require such a speedy and powerful means asLAN is.

Another way, the goal our activity, is the design and implementation a local videotex system, that can be applied under university conditions, especially in the following application areas :

- teaching, scientific-research and administrative process management
- scientific-research and economical information distribution
- direct support of teaching process. Assumption results:
- increasing of the activity in information field
- decreasing routine administrative works
- acceleration of the informatic stream on university
- higher effectivity of the utilisation internal telefon lines
- generation of VTX applications for national VTX network on commmercial base
- cooperation of the local VTX system with LAN on CTU and connection with public VTX networks

The realization of the proposed project would significantly contribute to the improvement of effectiveness of management, scientific-research and teaching activity of CTU.

NONRECIPROCAL LOW SENSITIVITY REACTIVE FILTER STRUCTURES

P. Martinek and I. Matzner

Faculty of electrical eng., CTU, Technická 2, 166 27 Praha 6

Key words: Circuit theory, filters, active RC filters

One of the most attractive ways of designing low sensitivity RC active filters is by deriving from LC passive prototypes. The optimal design and production technique for fully hybrid integrated filters has been developed during the last period of our research. Particularly the technical level of hybrid integrated filters produced by Tesla Hradec Králové comp. has been improved by using the research results.

The latest investigation has been oriented to the development of other structures, which have achieved more general applicability not only in the field of classicall RC filters, but also for switched-capacitor filters (SC) or digital systems. These structures can be more suitable in comparison with passive ladder structures because of their sensitivity performances.

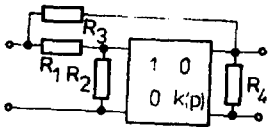

Fig.1

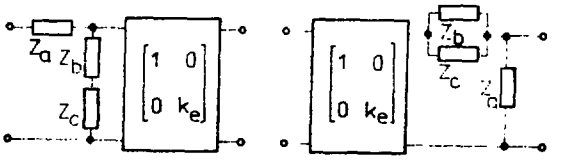

Fig.2

The obtained structures are based on the new type of functional blocks as is shown in Fig.1. The topology is the same as the Yanagisawa's NIC biquadratic cell [1]. Passive part is formed by resistors $R_1, ..., R_4$, GIC is generalised immitance converter. In this case the cascade matrix can be written in the folowing form (1) and the matrix elements poles and zeroes are on the imaginary p-axis by using of the conversion function $k(p) = p^2$ or $k(p) = 1/p^2$.

$$[A] = \begin{bmatrix} \dfrac{k(p).(G_3.R_1 + G_4.R_1) + 1 + G_2R_1}{k(p).G_3.R_1 + 1} & \dfrac{k(p).R_1}{k(p).G_3.R_1 + 1} \\ \dfrac{k(p).G_4.(1 + G_3.R_1) + G_2.(1 + G_3.R_1)}{k(p).G_3.R_1 + 1} & \dfrac{k(p).(1 + G_3.R_1)}{k(p).G_3.R_1 + 1} \end{bmatrix} \qquad (1)$$

The matrix (1) can be also presented as a matrix of equivalent circuits shown in Fig.2, where the passive part coresponds to LC cell, containing transformed immitances (R, FDNR) and GIC is defined by equivalent conversion function k_e expressed by (2).

Element-transformation corresponds with the Bruton's transformation $Z(p)W(p)$, where $W(p)$ is defined as $W(p) = p$, or $W(p) = 1/p$.

$$k_E(p) = \frac{k(p).(1 + G_3.R_1)}{k(p).G_3.R_1 + 1} \tag{2}$$

A higher-order structure can be obtained by cascade connection of presented functional blocks. It is equivalent to the passive ladder structure with inserted GIC between every two cells. Resultant circuit preserves all good performances of resistive terminated LC structure and can be frequency transformed to other types of filters (HP, BP). With respect to the character of network elements the frequency transformation concerns the GIC conversion function and loading impedances only. In comparison with the Bruton's technique based on direct transformation of LC ladder prototype the new structures provide better sensitivity properties and easier conditions for frequency transformation LP-to-BP and LP-to-HP.the described technique also gives the designer the degree of freedom to produce minimum spread/sensitivity realization. Other possibilities give suitable impedance and frequency transformation of basic structures which can be used to obtain minimum switches/minimum sensitivity SC implementation.

Nonreciprocal behaviour of the basic structure does not allow the application the design method LC ladder structures used. From this point of view considerable effort has been devoted to create a general algorithm providing efficient design technique. The result of this investigation is original algorithm [2] based on dropping of fundamental cascade partial matrixes. The recurent expressions allowing circuit elements computation have been derived by using this algorithm. A modified form of this algorithm exists for the passive ladder structure design. From this point of view, these passive structures can be regarded as a special case of general nonreciprocal network.

Real properties of described structures have been tested by concrete implementations of Cauer's filters. The standard GIC network corresponding to Antoniou two Op-Amp converter [3] have been used for practical implementation. The new filter structures have the low sensitivity to real parametres of operational amplifiers used, particularly to the gain-bandwidth product. Results of this research have been proposed for the high quality continuous-time analog filters and sampled-data switched capacitor filters synthesis. We assume these structures will be also usable in digital filter design and with respect to particular assumption in microwawe filter technique.

References:

[1] Yanagisawa,T.: RC Active Networks Using Curent Inversion Type NIC, Trans. IRE, Vol. CT-4., No.3. Sept. 1957, pp.140-144.

[2] Martinek,P., Matzner,I.: Nonreciprocal Reactive Selective Networks, will be published.

[3] Schaumann,R., Ghausi,M.,S., Laker,K.,R.: Design of Analog Filters, Prentice Hall, New Jersey, 1990.

This research has been conducted at the Department of Circuit Theory as a part of the research project "Analog and Digital Selective Networks" and has been supported by Czech Technical University grant No.8046.

Section 6

MEASUREMENT OF PHYSICAL QUANTITIES

CORRECTION OF DEAD-TIME LOSSES BASED ON COUNTING INTERVALS

J. Sabol

Faculty of Nuclear Science and Phys. Engng., Dept. of Dosimetry and Application of Ionising Radiation, Břehová 7, 115 19 Prague

Key words: Counting losses, dead-time, detector, radiation

Detection of individual particles of ionising radiation belongs to the most required type of measurements in experimental nuclear physics, dosimetry and various applications of radiations and radionuclides in science, technology, medicine etc. For this purpose pulse-detection systems are widely used. Because of their dead-time, however, a resulted count rate has to be corrected in order to obtain a true count rate.

In practice, there are two principal methods for correction of counting losses caused by the dead-time:

1. Scaler counts, accumulated during the measuring interval T, are converted into the true counts using a common relation [1]

$$N = M \,/\, T(1 - M\, d \,/\, T)$$

where M is the number of measured counts, d is the dead-time and N is the number of corrected counts.

2. A dead-time compensation circuitry in conjunction either with a ratemeter or with a scaler is used [2].

In both cases the information about the dead-time has to be known. For this purpose two-source or decaying-source methods are usually utilized [3]. The disadvantage of the mentioned approach is that the dead-time obtained from a separate measurement may differ from the actual dead-time under various experimental conditions.

The proposed method of the dead-time correction overcomes these difficulties.

The method is based on the distribution of time intervals between two adjacent detector output pulses [4, 5]. Ideally, with d = 0, the probability of occurrence of a time interval within $< t, t + dt >$ will be

$$p_t(n) = n \, \exp(-nt)$$

assuming n is a true counting rate.

Under the condition of a finite dead-time, however, a modified equation to describe the resulting time distribution has to be used

$$p_t(n, d) = n \, \exp[-n(t - d)], \;\; t \geq d$$

Integrating this distribution from T to ∞ one obtains a relation for the probability that a randomly chosen time interval will be longer or equal to T, i.e.

$$P_{\geq T}(n, d) = \exp[-n(T - d)]$$

This equation can directly be used to estimate the fraction of the number of time intervals longer or equal to T_1. If the total number of intervals and the number of intervals with a length $> T_1$ is M and M_1, respectively, it can be written

$$M_1/\ M = \exp[-n(T_1 - d)]$$

For two values T_1 and T_2, selected in such a way that $T_2 > T_1$,

$$M_1/\ M_2 = \exp[n(T_2 - T_1)]$$

from where the true count rate can be expressed as

$$n = [1/\ (T_2 - T_1)].\ \ln(M_1/\ M_2)$$

The derived formula can be used for direct evaluation of the true count rate n virtually without prior knowledge of the dead-time of a detection system.

The measuring assembly consists of the detection system with a dead-time d, and an electronic block which includes two parallel time interval discriminators and an evaluation unit performing the necessary calculations in order to obtain n. The discrimination levels T_1 and T_2 are set in such a way that satisfactory statistics with respect to M_1 and M_2 are achieved.

The selection of the time discrimination levels T_1 and T_2 is not too critical as long as T_1 is close enough to the dead-time d, e.g. $2d > T_1 > d$, and at the same time T_2 is larger than T_1, but still such that the statistically sufficient number of intervals M_2 is obtained.

The performance of the method can be assessed by the relative error r defined as

$$r = (n - n_c)/\ n$$

where n_c is the corrected count rate determined on the basis of counting the number of time intervals M_1 and M_2.

The method has been verified both experimentally and using the Monte Carlo simulations. The results have shown [6] (the relative error r can be as low as 0.1–1%) that the proposed technique is more reliable and accurate than other methods based on a separate measurement of the dead-time followed by the application of the well-known correction formula.

References:

[1] J.W.Muller Nuclear Instruments and Meths., 112(1973) 47,

[2] R.A.Todd: Review of Scientific Instrum., 51(1980) 1132,

[3] G.F.Knoll: Radiation detection and Measurement, J.Wiley and Sons, New York, 1989,

[4] J.Sabol: Radiation Prot. Dosimetry, 23(1988) 89,

[5] J.Sabol: Kernenergie 33(1990) 245,

[6] J.Sabol: Nuclear Energy (submitted for publication).

This research has been conducted at the Department of Dosi- metry of Ionising Radiation as a part of the research project "Optimization of processing and evaluation of the radiation detector response"

SATELLITE RANGING USING PICOSECOND LASERS

*K.Hamal, M.Cech, H.Jelinkova, A.Novotny, I. Prochazka**
*B.B.Baghous, Y.E.Helali, M.Y.Tawadrous ***

* Faculty of Nuclear Science and Physical Engineering CTU, Brehova 7, 115 19 Prague 1
**National Institute of Astronomy and Geophysics, Helwan, Egypt

Keywords : satellite laser ranging, picosecond laser,global ecology

Satellite laser ranging has been provided since the mid sixties. Data are used in global geodesy, geophysics, plate tectonics and recently in remote sensing for global ecology. For ecological application the European Research Satellite ERS-1 has been launched by the European Space Agency in 1991. Our group is been providing the laser ranging since 1973. In 1973-85 the satellite laser ranging systems have been constructed on four continents. Till now, our main interest has been focussed on the station located in Helwan, Egypt.

The satellite laser ranging data user's requirements are strongly expressed toward the range precision and data coverage. The laser ranging precision has been gradually improved from 1 meter in the early seventies to subcentimeter values in 1991. The main contributions to the overall budget are coming from the satellite, the atmospheric dispersion and the laser radar on the ground itself. Assuming each subsystem to be at an upto-date limit (the time interval meter plus start/stop detectors and the Global Positioning System time base), the dominant contribution to the error budget comes from the finit duration of laser pulses. The second generation of the satellite laser radars was based on Q-switch laser transmitter, which allowed one to achieve the ranging precision of up to 20 cm RMS. Exploiting the picosecond pulses we obtained the precision of 3 cm up to 7 000 km of the range.

In our Satellite Laser Station, the YAG laser transmitter consists of the passively mode-locked oscillator generating a train of 30 picoseconds long pulses, pulse selector separating the second part of the pulse train, double pass amplifier, final amplifier, second harmonic generator and the telescope. The output energy at 0.53 micrometer is 50 milliJoules contained in 3 - 5 pulses. The laser radar is operating in so-called semitrain mode with the repetition rate of 2.5 Hz. The laser has been designed and constructed on our faculty. Its main advantages are the high average power, short and stable pulses, simple operation and compact design. The systems high reliability is a key feature of the remote field operation : Sahara desert. The mean time between laser maintenance in the harsh condition is in the order of weeks or even a month, when firing inthe order of a million laser shots.

The ERS-1 satellite was launched in middle of July 1991. The laser ranging campaign at Helwan started in August 1st and lasted until December 1, 1991. The ranging precision was 28 mm on a long term average (for comparison for the Starlette satellite 22 mm, and for Lageos 28 mm , and Ajisai 34 mm precision has been obtained).

The ERS-1 satellite laser observations are organized by Deutsches Geodatisches Forschunginstitut from the Control Center in Munich. The orbit elements are distributed via BITNET network to about 20 stations on four continents and the observations are collected on a daily basis via the same channel. All the observations collected at the center allow one to define the orbit/position and thus to exploit the remote sensing apparatus on the spacecraft and to generate the orbit elements, as well. The satellite 's low orbit is very

unstable due to influence by solar activity, winds etc. During the observation campaign the orbit has been corrected several times. To be able to hit the satellite on such a rapidly changing orbit new satellite aiming and tracing proceduses had to be developed. The satellite position is computed on the station personal computer using the satellite state vectors generated in the Control Center, Germany and distributed twice a week via the information network. The orbit integration algorithm is used for this purpose, using the Earth gravity field coefficients up to the terms 22,22. The calculated prediction is improved on-site on the basis of the daily distributed time correction parameter and on the basis of the last ranging results.

The Satellite Laser Station in Helwan belonging to Czech Technical University and National Research Institute of Astronomy and Geophysics is the only one operating on the African continent. The station is contributing significantly to the international satellite laser tracking campaigns like MERIT (Monitoring of the Earth Rotation by Intercomparison Techniques) and MEDLAS-WEGENER (intensive laser tracking activity in Mediterranean are for the plate motion and tectonics studies). The quality of the data obtained has been appreciated by the international scientific community [1],[2]

References:

[1] K.Hamal, I.Prochazka, G.Kirchner, Advanced Technologies for Satellite Laser Ranging , IUGG general Assembly meeting, Vienna, August19-23,1991

[2] K.Hamal, I.Prochazka, J.Gaignebet, New Technologies in Laser Ranging for Nineties, proc. of the International Symposium on Radar and Lidar in Planetology, Cannes, France, Sept.2-4,1991

The campaign was granted under the contract number ERS-1/7831/91 provided by Deutche Geodatisches Forschung Institute together with the European Space Agency.

NEW TECHNOLOGIES IN PICOSECOND LASER RANGING FOR THE NINETIES

K.Hamal, I.Prochazka, G.Kirchner,** J. Gaignebet +*

* Faculty of Nuc Sci and Physical Engineering, CTU, Brehova 7,115 19 Prague 1
** Observatory Lustbuehel, Technical University Graz, A-8042 Graz
+ CERGA, Avenue Copernic, 06130 Grasse, France

Keywords : picosecond laser, satellite laser ranging, single photon detection, streak camera

The use of laser ranging to measure the distance of an Earth satellite is an attractive technique applied in geodesy, geophysics and others. The laser ranging precision has been improved from 1 m in the seventies to a subcentimeter values in 1991. This precision increase has been obtained mainly by shortening the transmitted laser pulse, employing the higher resolution time interval meters and applying the faster optical detectors. To meet these demands, a new laser ranging technologies have been developed, tested in the Indoor Calibration Center in Prague and implemented at the Satellite Laser Station in Helwan, Egypt and Graz, Austria.

The laser transmitter : the laser output pulses have been shortened down below 40 picoseconds, to maintain the transmitted average power and the system reliability, as well, the semitrain form of the transmitted pulse is applied. The Start photodiode & discriminator have been replaced by the fast optical switch. The single photon ranging techniques have been developed and routinely applied. In the radar receiver, the conventional photomultiplier has been replaced by specially designed Single Photon Avalanche Photodiode. Such a configuration permitted the avoidance of all the electronic amplifiers and discriminators. As a result, the system submillimeter stability has been obtained. Although dedicated for single photon ranging, the system delay variation versus return signal strength is within the 3 millimeters for the dynamical range of 1 to 30 photoelectrons of returned signal strength. The reported values of ranging precision and stability are the world's second, just following the NASA Laser Tracking network performance [1].

However, to meet the one millimeter accuracy level required by the data users for the nineties, new ranging techniques have to be applied. At present, the main contributors to the systematic error budget is the atmosphere refraction model and the target geometry. Ranging on the two wavelengths and determining the dispersion, the atmospheric refraction model may be improved. Several schemes for the generation of two wavelength pulses have been tested, the second harmonics of Nd YAG and the Raman Stokes pulse (red) and the Raman anti Stokes (blue) are expected to be the candidates for field application. The two wavelength ranging technique employing only one single photon receiver diode will be presented [2],[4].

To carry out the temporal analysis of the laser pulses reflected from satellites the specially design Modular Streak Camera has been used. We have been reporting, to our knowledge for the first time, on the temporal analysis of echoes from satellites using the picosecond laser as a transmitter and the streak camera as a receiver. The experiment was accomplished at the Satellite Laser Station Graz, employing a 0.5 meter tracking

telescope, the laser transmitter emitting 10 milliJoules, 30 picoseconds long pulses in green. To perform the temporal analysis the modular streak camera interfaced widt the IBM PC image processing system has been used. We detected the retrosignals from the geodetic satellites on the 1000-2000 km heigh orbits. To calibrate the system performance we have ranged the ground target using picosecond pulses and we determined the range with the 6 picoseconds precision RMS which corresponds to the ranging precision better than 1 millimeter [3].

References:

[1] K.Hamal,I.Prochazka, G.Kirchner, Advanced Technologies for Satellite Laser Ranging, proc. of the Scientific Session of the XXth general Assembly of the International Union of Geodesy and Geophysics, Vienna, August 19-23,1991

[2] I.Prochazka, K.Hamal, H.Jelinkova, Femtosecond Two Color Ranging to the Ground Target, technical digest of the Conference on Laser and Electro Optics, CLEO 89, Baltimore, USA, May 1989

[3] I.Prochazka, K.Hamal, G.Kirchner, M.Schelev, V.Postovalov, Circular Streak Camera for Satellite Laser Ranging, presented at the Conference on Electronics Imaging, San Jose, California, Feb.24-27,1991, published in SPIE 1358-55,1991

[4] J.Gaignebet, J.L.Hatat, K.Hamal, H.Jelinkova, I.Prochazka, Two Color Ranging on the Ground Target using 0.53um and Raman 0.68 um Pulses, technical digest of the Conference on Lasers and Electro Optics, Baltimore, USA, May 1989

This research has been partially funded by the European Space Agency grant ERS-1/7831/91 and by the Space Research Institute, Moscow, USSR, contract No. 409690 .

PRECISE SURFACE ACOUSTIC WAVE VELOCITY MEASUREMENT

R. Bálek

Czech Technical University, Technická 2, 166 27 Praha 6

Key words: Surface acoustic waves, components, velocity, aluminium overlay.

In the practical application of components with surface acoustic waves (SAW), mainly in creating interdigital transducers, it is important to know the influence of thickness of the conducting overlay, deposited on the surface of the piezoelectric substrate, on the performance of the device.

Coherent optical laser probes have been used for measurements on acoustic surface v..ve devices. The basic operation of the system has been previously describe [1, 2]. Since the probe measures both the amplitude and phase information, a scan transverse to an acoustic surface beam contains in principle a complete diffraction record of the two-dimensional field. The technique for evaluation of the velocity characteristic of the surface involves the measurement of three transverse complex field distributions spaced by a known distance. The Fourier transforms of the spatial domain represent the plane wave spectrum of the spatial distributions. The three phase values of each plane wave, separated by measured distances, are used to find the propagation constants e.g. phase velocity and angle of propagation.

The surface acoustic beam was excited by interdigital transducer (IDT) deposited on the Y-Z $LiNbO_3$ substrate. The IDT of 20 lambda aperture, lambda = 58 μm, was operating at 60 MHz. For achieving the large angle velocity profiles it was necessary to reduce the aperture by producing a secondary aperture using SAW absorber. The scans were recorded in the far field of the transducer in an approximate area of 30 x 30 mm^2.

The Al overlay was deposited by the conventional resistive heating method at an evaporation rate of 200 Å/min in a vacuum of 3.10^{-6} Torr. For thin film thicknesses, as high as 250 Å, a thickness monitor was developed to measure the overlay thickness during the evaporation process. The monitor was a photo-resistor mounted behind a glass plate which was placed directly next to the $LiNbO_3$ substrate. The resistance of the photo-resistor was increased as the light intensity on the resistor was reduced due to the increase of the Al film thickness. The monitor was calibrated by means of a Talystep. Thick overlays were measured using the Talystep after the evaporation process.

Using the probe the SAW velocity was measured at 60 MHz operating frequency over a range of angles with respect to the Z- crystal axis on an open circuit, short circuit and mass loaded Y-Z $LiNbO_3$ plate. After each, velocity and thickness measurement, the Al film was etched and a different thickness overlay was evaporated on the substrate. The velocity measurements were conducted at 24 $\pm$ 0.5°C and accuracy was $\pm$ 0.1 m/s. Since the velocity measurements were carried out over a wide range of angle the velocity change as a function of Al film thickness characteristic was not suffering by misalignment of the IDT with regard to the Z-axis.

Of specific interest is the fractional change in the SAW velocity Fig. 1 as a function of Al normalized film thickness on the virgin YZ- $LiNbO_3$ sample. In this figure it is seen that the velocity variation is slow at thin film thickness; this is the region where the Al

film is not continous and the piezoelectric substrate is not short-circuited. Once the Al film is continous there is a large drop in the SAW velocity and the sort circuited velocity is constant. The next sharp drop in the SAW velocity occurs when the substrate is mass loaded. The characteristic in Fig. 1 shows that a Y-Z $LiNbO_3$ substrate is short circuited with an Al overlay of 130 Å thickness at 60 MHz operating frequency.

References:

[1] R. De La Rue, F. F. HUMPHREYS, J. M. MASON and E. A. ASH. Proc. IEEE, vol 119, No 2, Feb 1972 pp 117

[2] R.Bálek 25. Akustická konferencia - Ultrazvuk 86 Bratislava 91/1986

This research has been conducted at the Department of Physics and up to this time has not been included in any research project.

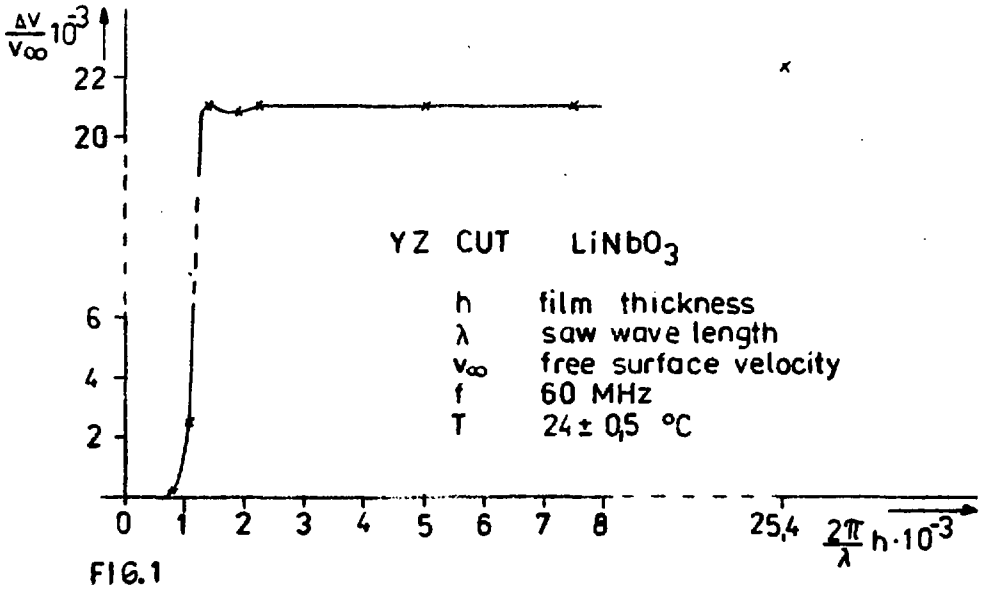

FIG.1

SOUND POWER MEASUREMENTS OF STEADY SOURCES

O.Jiříček

CTU, Faculty of Electrical Engineering, Department of Physics, Technická 2
166 27 Prague 6

Key words: Sound Power, Sound Intensity, Measuring Methods

At present, besides the sound mean square pressure level method (ISO 3740 - 3747), the method based on the determination of acoustic power flow through any surface totally enclosing the source under the test is commonly used for the determination of sound power radiated by acoustic sources.

Since intensity is power flux density, it is evident that the integral of the scalar product of the sound intensity vector and the associated elemental area vector over any surface is equal to the total power flow through this surface:

$$W = \int_S I.\,dS = \int_S I.n\,dS = \int_S I_n\,dS\,, \tag{1}$$

where I is sound intensity vector, n is the unit normal vector of the surface S corresponding to the element of surface dS and I_n is the magnitude of the vector component I normal to the surface.

If this surface encloses a finite volume, the resulting integral is equal to the total sound power radiated by sources in this volume. Normal components of sound intensity generated by steady sources operating in the environment external to S do not contribute to the surface integral. From the eq. (1) it follows that, for the purpose of sound power determination, the source is defined by the choice of the respective enveloping surface.

However, a sound intensity probe can measure only at single points in space. Thus, we need a practical procedure which enables estimation of the integral (1). Basically, there are two sampling methods:

In the first one we divide the measuring area into N subareas δS_i and in the middle of each δS_i we measure associated I_i normal to the surface. Sound power is calculated as a sum of partial power contributions:

$$W \doteq \sum_{i=1}^{N} I_i\,\delta S_i\,. \tag{2}$$

This method we refer to as Discrete Points Measurement (or Point by Point Measurement).

The second one, which is the focus of this report, is based on moving the intensity probe continuously along a linear path. Providing the steady sound field integral (1) can be written as [1]:

$$W = \int_S I_n\,dS \doteq D\int_l I_n\,dl, \tag{3}$$

where D is a width of band associated to scanning path l (dS $\approx$ Ddl). If the scanning speed is constant we can continue:

$$W \doteq D\int_0^L I_n\,dl = S/T\int_0^T I_n(t)dt\,. \tag{4}$$

$I_n(t)$ in eq. (4) means temporal variation of the normal component of sound intensity due to it's spatial variation and probe movement. The measurement method based on eq. (4) is called the Scanning Method or Sweeping Method.

In both methods the resulting estimates are affected by bias and random errors. Assuming the previous considerations, those errors depend on intensity measurement errors. In sound power measurements there is an additional error connected with chosen approximation (see eq. (2) and (4)). It is shown in [1,2] that a systematic error due to choice of scanning path might appear.

A number of measurements were carried out in order to find out whether comparison of results of two different scanning patterns may be used as a simple indicator of the validity of the respective scanning method.

Two densities of lines in a scanning pattern were used in two orientations (horizontal and vertical). The results show that the systematic error due to choice of the scanning path can be eliminated by repeating the same measurement technique, but scanning along a path rotated of 90°.

Table 1 contains a survey of results measured along a trajectory consisting of four or eight parallel lines ("4m" or "8m" respectively). Results marked "h. & v." in the table are mean values of the respective horizontal and vertical values below. This test was performed with a unique scanning speed of 0.21 m/s.

distance [m]	0.1	0.2	0.4
true value	80.6	80.0	78.5
scan 4m (h. & v.)	80.6	80.0	79.0
scan 4m horizontal	78.5	78.8	78.3
scan 4m vertical	82.0	81.0	79.6
scan 8m (h. & v.)	80.2	79.5	78.5
scan 8m horizontal	80.1	79.3	78.6
scan 8m vertical	80.3	79.6	78.5

Table 1: Dependence of measured sound power levels in dB on the distance between source and measurement surface

The difference between the single results shows that the measurement along a 4-line-trajectory is not sufficient; the latter technique is to be used. To optimize the measurement technique, influence of different scanning patterns on validity of the scanning method is to be investigated.

The following question is to be solved as well: Which difference between the resulting pair is acceptable and what is the information that the density of lines is insufficient. Without any knowledge of distribution of intensity over the measurement surface it is necessary to implement an appropriate statistical technique.

References:

[1] Bockhoff, M., Some Remarks on the Continuous Sweeping Method in Sound Power Determination. Proceedings of Inter-noise 84, New York, 1984.

[2] Jiříček, O., Analysis of some parameters determining the precision of results. Report CETIM, Senlis (France), 1991.

[3] Fahy, F.J., Sound Intensity, Elsevier Science Publishers LTD., London, 1989.

A significant part of this project was performed at CETIM, Senlis, France

MEASUREMENT OF REFLECTION COEFFICIENT USING SOUND INTENSITY

J. Bouček

CTU, Faculty of Electrical Engineering, Department of Physics, Technická 2
166 27 Prague 6

Key words: Reflection Coefficient, Sound Intensity

In a one-dimensional sound field, where a sinusoidal sound wave propagating along the positive z direction is reflected by a surface with the pressure reflection coefficient R at $z = 0$ (Fig. 1), the complex sound pressure at the point z is given by (assuming that the environment is not dissipative):

$$P(\Omega, z) = A(\Omega).[\exp(-jkz) + R(\Omega).\exp(+jkz)] , \tag{1}$$

the complex particle sound velocity is

$$U(\Omega, z) = (A(\Omega)/ @ .a_0).[\exp(-jkz) - R(\Omega).\exp(+jkz)] . \tag{2}$$

Then the reflection coefficient is

$$R(\Omega) = N . \frac{U(\Omega, z) . @ . a_0 - P(\Omega, z)}{U(\Omega, z) . @ . a_0 + P(\Omega, z)} \tag{3}$$

N denotes the phase shift caused by the distance z between the measuring point and the reflecting surface and does not influence the absolute value of R.
Furthermore,

$$R = N . \frac{1 - @ . a_0 [UP^*] / [P.P^*]}{1 + @ . a_0 [UP^*] / [P.P^*]} \tag{4}$$

Let us denote the distance between these microphones as Δr. According to Fig. 1 and eq. (1), the sound pressure P_a and P_b at the measuring points a and b, $P_a = P(\Omega, z - \Delta r/2)$, $P_b = P(\Omega, z + \Delta r/2)$ is given by

$$P_a = A . [\exp(-j.k.(z - \Delta r/2)) + R. \exp(+j.k.(z - \Delta r/2))] , \tag{5}$$

$$P_b = A . [\exp(-j.k.(z + \Delta r/2)) + R. \exp(+j.k.(z + \Delta r/2))] . \tag{6}$$

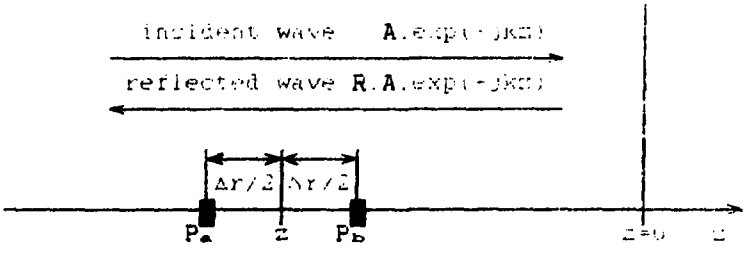

Figure 1: Reflection of the wave incident on the surface

As long as the distance $\Delta r/2$ is small compared with the wavelength, i.e. $(k.\Delta r/2) \ll 1$, the sound pressure at the point z is given by

$$P(\Omega, z) = [P_a + P_b]/2 \tag{7}$$

and the particle velocity

$$U(\Omega, z) = (j/@.a_0.k.\Delta r).[P_b - P_a] \,.\, M, \tag{8}$$

where $M = M(k.\Delta r) = (k.\Delta r)/\sin(k.\Delta r)$ is the high frequency factor correcting the underestimated value obtained by the approximating measurement technique at higher frequencies (Fig. 2).

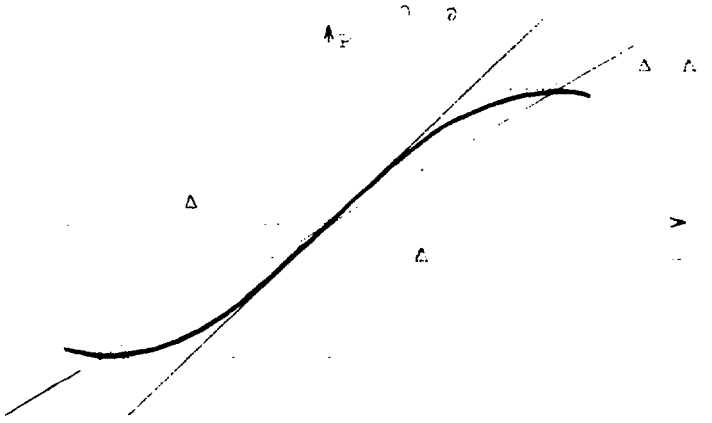

Figure 2: High frequency correction factor

Then, $R = N\,.\,(1-Q)/(1+Q)$ where

$$Q = \frac{2.M}{k.\Delta r} \cdot \frac{j.(G_{bb} - G_{aa}) - 2.\mathrm{Im}[G_{ab}]}{G_{bb} + G_{aa} + 2.\mathrm{Re}[G_{ab}]}, \tag{9}$$

G_{ij} and G_{ii} are one-sided cross-spectra and one-sided autospectra respectively.

A measuring set has been developed and results have been obtained according to the presented method. These results were compared with those measured at the same measuring set, but according to the ASTMM Standard E1050, which is the present technique used for such measurements. The high frequency factor M is not involved in the ASTMM Standard. The results obtained with the proposed method show better course at higher frequencies, while the frequency range of those obtained with the ASTMM is limited. Further investigation in comparing both methods is to be suggested, in order to develop the first one, as it enables the extension of the measuring frequency range without any change of the hardware set.

References:

[1] Munjal M.L. : Acoustics of ducts and mufflers, Wiley Interscience 1987.

[2] : Gade S. : Sound Intensity (Part I. Theory), Technical Review 3/1982, Brüel & Kjær.

[3] : ASTMM Standard E1050.

[4] Bouček, J. : Simulation of Acoustic Mufflers, Brüel & Kjær 1990.

A significant part of this project was performed at Brüel & Kjær, Denmark

ULTRASONIC TRANSDUCERS FOR IN SITU MEASURING IN ROCKS

J. Plocek, K. Malinský

Faculty of Electrical Engineering CTU, Technická 2, 166 27 Praha 6

Key words: ultrasound, transducers, geology, mining

Requirements for ultrasonic transducers used in measuring parameters of rocks in situ are:

- the transmitting (receiving) pattern as near to the omnidirectional one as possible, i.e. a broad maximum in the YX plane and no important maxima the XY plane
- long-term reliability in function underwater as transducer (with output power as near to the cavitational threshold as possible)
- dimensions suitable for application in boreholes 45-55 mm in dia
- long-term stability.

After various experiments, we found that a radially vibrating piezoelectric ring is the best solution. The transducer must be watertight, therefore we put rubber plugs in both fronts.

As the first step in construction of the transducers, we found the solution for the pressure field of a radially vibrating ring. The description of the computing procedure exceeds the extent of this short report - the technique of least squares was used as described in [1]. The result of the procedure was a system of complex linear equations. We found the solution of these equations for three cases of a finite cylinder. The pressure in far-field area was evaluated using a dimensionless ratio as

$$p(r,\Theta) = -jk\varrho c\psi(r,\Theta) = ka\varrho cu\frac{e^{-jkr}}{kr}\sum_{n=0}^{N}\frac{\bar{a}_n}{a_u}j^n P_n(\cos\Theta)$$

Computerized normalized directivity charts of the pressure amplitude for several values of ka (for the ratio $b/a = 2$) are plotted in Fig. 1. It follows from the diagrams that the approximation of the requirements for $ka = 1$ is good.

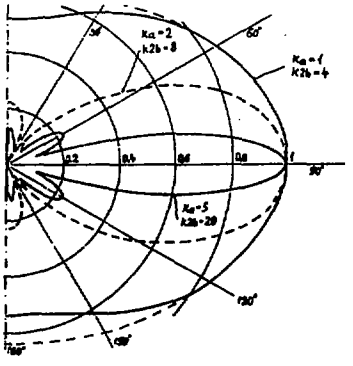

Fig. 1. Normalised directivity charts of pressure amplitude of a piezoceramic ring with plugs for ka = 1,2,5.

As a following step, a lot of practical problems concerning the construction of transducers had to be solved. First of all, we had to make the vibrating ring secure against destruction. The piezoceramic material is far less durable in pull than in pressure. We made the ring pre-stressed by using a precisely-made titanium ring. The piezoceramic ring was cooled in liquid nitrogen, the outer titanium one was heated up to several hundred degrees C (the temperature was limited by Curie temperature of the piezoceramic material) and the both rings were put together. This outer ring was also useful for the protection of the piezoceramic material against chemical and mechanical damage including the ultrasonic cavitation.

The electric supply to the inner electrode was made in a similar way. (Here there were complications due to of mechanical stress of the flexible cable during intense vibrations.) A thin-wall bronze ring was used, connected with the piezoelectric ring in the same way. The procedures described are a part of a patent pending. The receiving transducer was made in the similar way but only the outer protective ring was used. (The inner protective ring was not necessary for the inner surface of the receiver does not vibrate intensively.) The construction of the transducer is on Fig. 2.

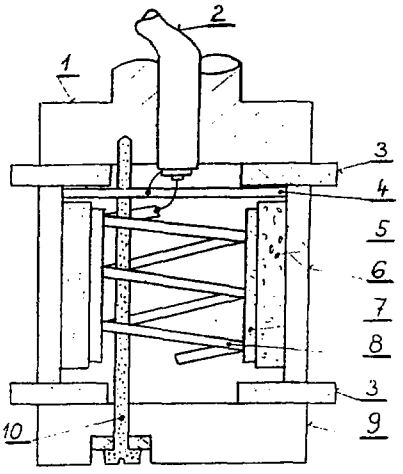

1 - cover, upper
2 - lead
3 - ring, rubber
4 - ring contact, steel
5 - ring, piezoceramic
6 - ring, titanium
7 - ring, bronze
8 - contact, spring
9 - cover, lower
10 - screw, (3 pieces altogether)

Fig. 2. The cross - section of the transducer

We tried to prove directivity charts of our transducers in a water basin. Unfortunately, it was established that the acoustical damping in the basin is practically unfulfillable but we found that the directivity of transducers may be guessed in a simple measurement in the air - despite different acoustic impedantion - and the transducers proved suitable.

The next practical test of transducers was their excitation in water up to the cavitational threshold. After these preliminary tests, the transducers were used for long-term measuring in holes in a gallery in the vicinity of a mine near Jezeří castle (North Bohemia). Initial results are quite satisfactory.

Reference:

[1] Skudrzyk E.: The Foundation of Acoustics, Springer, Vienna-N.Y., 1971.

This research has been conducted at the Department of Physics, Faculty of Electric Engineering.

CONCENTRATION OF SAND-WATER MIXTURE MEASURED BY ULTRASOUND

K. Malinský, M. Plachý

Faculty of Electrical Engineering CTU, Technická 2, 166 27 Praha 6
Institute of Hydrodynamics CSAS, Podbabská 13, 166 12 Praha 6

Key words: ultrasound, porosity, concentration, hydrodynamics, biotechnology, fluidized bed, ecology

(Preliminary report) Ultrasound was used for measuring the concentration of sand in sand-water suspension in the bioreactor with a fluidized bed, the model of which consisted of a perspex column with inner diameter 123 mm and height 3 m. The bioreactor will be used for denitrification of either potable water or wastewater using up the ability of certain microorganisms to reduce the nitrate ions to gaseous nitrogen during the metabolic process at the absence of oxygen and in the presence of a suitable donor of electrons. These microorganisms (bacteria) adhere on the sand particle surface, thus influencing the hydraulics of the system which is given by Richardson-Zaki equation u = w e exp(n), where u is superficial fluidizing velocity, w is the terminal settling velocity, e is porosity of the fluidized bed and the exponent n depends on the Reynolds number. The porosity is defined as the void to fluidized bed ratio (it equals 1 minus volume concentration). The characteristic property of a particular fluidized bed is its particle size classification along the bed height and therefore the porosity is not constant along the height of the bioreactor. The porosity of a fluidized bed is very important for a reactor project. It can be calculated when the particle size and pressure drop have been evaluated but due to the size change of bioparticles during the process and the change of hydraulic parameters, the measurement of the pressure drop cannot be done by usual methods. The use of ultrasound offers an advantage in a permissive possibility of direct and instant porosity measurements.

Instead of the ordinary X-ray method, ultrasound was used for measuring the concentration of sand in water. The acoustical impedance of bacterial bioparticles adhered to the surface of sand grains equals the acoustical impedance of water. Therefore, the acoustical properties of the fluidized bed do not depend on the amount of bacteria. During the passage of ultrasound through the mixture, an interaction of ultrasonic wave with sand particles occurs with consequent changes in sound velocity and in the attenuation of sound. The velocity proved to be the more stabile parameter (and the better measurable one) in the fluidized bed.

In velocity measurements, choosing the proper frequency is important.In the case of ultrasound in the mixture of solid particles, the frequencies whose wavelength is sufficiently longer than the characteristic particle size are to be preferred. In this case, neither velocity dispersion nor anomalous attenuation occurs. On the other hand, too low frequency does not give sufficiently accurate results. In our measurements, the frequency 1 MHz was used (the wavelength is 1.5 mm and five times exceeds the characteristic particle size). The amplitude of signal received was sufficient.

We measured the transit time of ultrasonic waves. We used the ultrasonic impulse device UIDS and a storage oscilloscope. A sufficient reproducibility of results was necessary

to achieve a sensitivity of measuring the time (velocity) changes in range of several % or less.

The transducers were mounted in perspex blocks (Fig. 1), sliding along the bioreactor to allow measuring in various places and under various hydraulic parameters. The concentration (porosity) was calculated from pressure drops.

The velocity of sound was calculated from measured transit times with respect to temperature changes and geometrical factors. The results are on Fig. 2.

Fig. 1

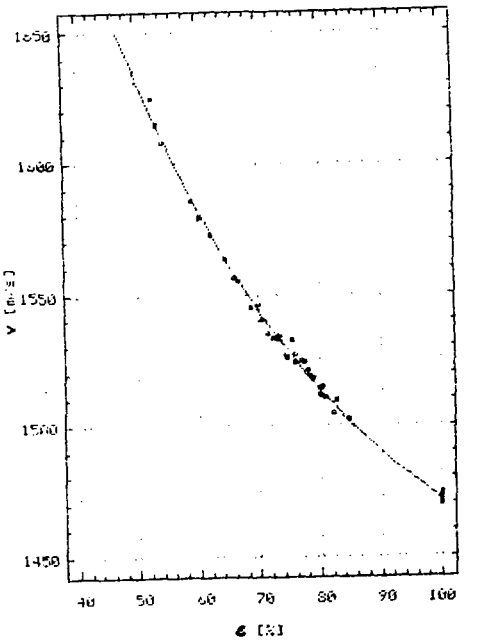

Fig. 2

Regarding the fact that the particles concerned are not exactly defined, we used the experimentally measured curve instead of results of theoretical calculations. The regression analysis gives as a result

$v = 5600 + 183\ e\ \exp(.5) - 844\ e\ \exp(.25) - 1851\ e\ \exp(.125)$,

where v is velocity of sound (m/s) and e is porosity (%).

Conclusion: Measuring velocity of ultrasonic waves is a suitable method for evaluating concentration (porosity) of sand-water mixture in a bioreactor for concentrations in the range of 20-50 % used in biotechnology.

This research has beed conducted at the Institute of Hydrodynamics, CSAS, and at the Department of Physics, Faculty of Electric Engineering, CTU

Complex Permeability Meter

K. Draxler, P. Kašpar, P. Ripka

Electrotechnical Faculty CTU, Department of Measurement Technická 2, 166 27 Praha 6

Key words: Magnetic measurements, Permeability, Measuring systems

AC complex initial permeability is an important material parameter for the design of the magnetic circuits . Operation frequency of precise magnetic devices such as current and voltage measuring transformers is still increasing, especially with the use of amorphous magnetic materials. This paper describes the computer-controlled system for measuring the complex permeability on toroidal samples at higher frequencies.

Complex permeability μ is defined by the formula [1]

$$\mu = \mu' - j\,\mu'' = \mu \exp(-j\,\delta) = \frac{B}{\mu_0 H}$$

where H is the complex value of the field strength, B complex value of the first harmonics of the flux

The sample is magnetized by the sinewave generator with power amplifier. The magnetizing current flows through the coupling capacitor C (to remove any DC component) and sensing resistor R into the primary winding of N_1 turns. The phase-sensitive detector measures the current equivalent with magnetic field strenght H and voltage induced in the measuring winding with N_2 turns. Each PSD measurement is performed twice with ortogonal references, so the amplitude and relative phase of both the voltage and the current may be calculated. The complex permeability may be then evaluated using the specimen parameters.

The current version of the instrument serves for the measurement in the production of toroidal cores at Kovohutě Rokycany plant. The system is controlled by the PC using parallel output for connection to the internal 24-bit bus (8 bits bidirectional data and 16 bit control bus). The generator frequency is programmable in small steps from 20 Hz to 20 kHz. The amplitude of the magnetization current is controlled by the 12-bit multiplying D/A converter, the serial resistor is software selectable from 1 ohm to 10 kohm. The input for the sensing resistor voltage is floating, so the single winding measurement may also be performed; transformer configuration is used when the shape of the sample requires different N_1 and N_2. In the first case, the error caused by the wire resistance may be software corrected. The gain of the voltage amplifier is programmable from 1 to 10 000.

The important part of the instrument is the software. The program written in the Turbo-Pascal language manages user-friendly communication with the operator, automatic setting of the magnetization current according to the selected field value, adaptive selection of the measuring circuit parameters for minimizing of an error, computation and archivation of the results, auto-callibration and self-diagnostic procedures. The measurement may be performed in full-automatic, semi-automatic or hand mode.

The operator has to enter the sample parameters (sample number, material, sample size) and demanded measuring conditions (excitation frequency and intensity). The program automatically calculates the average magnetic path lenght, crossection and

excitation current corresponding to demanded field intensity. The space factor may be calculated from sample size, mass and density, or entered directly.

In the automatic mode the proper value of the excitation current is adjusted while amplification of the measuring amplifiers and value of the sensing resistor are optimized for minimum error. To keep this process as short as possible, complex algorithm was used: the initial value of the excitation amplitude is estimated from the sample parameters; the proper value of the exitation current is then iteratively adjusted while maximizing serial resistor R. After the range-selection of all the amplifiers is performed, final high-resolution measurement is performed using digital filtration.

The Data Managing system allows one to print the measured data or save them on floppy disk. The records may be moved among files, browsed and sorted and printed later.

The calibration of the instrument may be performed using the resistance or capacitance normals. The amplitude and phase errors are software-corrected at each frequency. The correction table is updated according to the calibration results. Using the precise lock-in amplifier PAR 5210 the instrument accuracy was estimated as 2% in amplitude and 2 grades in phase.

Conclusion:

The described instrument was developed and built in our laboratory under the contract for the Kovohutě Rokycany plant. A laboratory version was built in cooperation with Metal research institute (VUK) Panenské Břežany also on contract basis. The latter modification is described in [2]. The measurements on standard samples from the Czechoslovak Metrological institute have shown that the error at 50 Hz was below 1% .

At the present time the new version of the instrument is being built. The target is to increase the frequency range up to 100 kHz.The software part of the instrument will be extended to be able to perform automatic measurements of the frequency characteristics and automatic calibration using coaxial resistance normals. Such an instrument would be very useful for measuring the basic parameters of amorphous magnetic cores and might be offered to producers of magnetic materials, transformers for switching power supplies and interference suppression chokes.

References:

[1] Methods of measurement of the magnetic properties of isotropic nickel-iron soft magnetic alloys. IEC publication 404, 1986.

[2] K. Draxler, P. Byron, P. Kaspar, P. Ripka, System for measuring the complex permeability Electronic Horizon (Slaboproudy obzor) 52 (1991) 177-181.

A research project for building a PC-controlled system for measuring the complex permeability for frequencies upto 100 kHz was proposed for the competition for ČVUT research grants in 1992.

Low-Noise Fluxgate Sensors

P. Ripka

Department of Measurement, Electrotechnical Faculty ČVUT
Technická 2, 166 27 Praha 6

Key words: Magnetic measurements, Magnetometer, Fluxgate sensor

Introduction:

Fluxgates are the most suitable magnetic field sensors for the measurement of DC or low-frequency AC fields in the range of 1 nT to 1 mT. They are used in space research, for geophysical prospecting, in rock magnetism, for magnetic field mapping and in magnetic variation stations. Fluxgate compasses are extensively used for aircraft and vehicle navigation [1]. Fluxgate magnetometers are used for magnetic ink sensing, location of ferromagnetic bodies, indirect current measurement, nondestruction material testing. Their sensitivity is much higher than that of other solid-state sensors such as magnetoresistors, magnetotransistors, Hall effect sensors and fibre-optical sensors. They measure also the field direction, unlike the resonance magnetometers.

The theory of the operation of the ring-core fluxgate is discussed in [2]. Basic information about the sensors may be found in review articles [3] and [4]. The sensor core made from soft magnetic material is periodically saturated by the AC excitation current so that the core permeability changes in each period. Therefore the measured DC magnetic field is modulated ("gated") and the voltage proportional to the magnitude of this field is induced in the pick-up (measuring) coil.

Sensors developed at CTU (ČVUT)

A number of fluxgate sensors have been developed at our department since the first open-core type from 1972 .The last generation of our sensor cores is produced by etching from permalloy or amorphous cobalt-based materials [5]. Standard sensor size is a ring with outer diameter of 22 mm. These sensors are used in magnetometers and variometers having 100 pT resolution. Miniature sensors used in paleomagnetic measurements have the diameter of 8 mm, but the sensitivity is lower and the resolution is about 1nT. Low-field sensors are of the race-track (oval) shape with 70 mm lenght. Our sensors are calibrated and tested in magnetic shieldings and magnetic vacuum system MAVACS [6] using 2-meter three-axis Helmholtz coil set.

Fig. 1 shows the output of the sensor RTVK-1 developed at our department in cooperation with Tesla Pardubice. Sensor core is made from Vitrokov 6116 produced by the Institute of Physics, Slovak Acad. Sci. Bratislava. The step of the calibration field was 200 pT. Rms noise of this type of sensor was below 10 pT (64 mHz to 10 Hz), peak-to-peak value about 50 pT, power spectral density was about 3.2 $pT/Hz^{1/2}$ at 1Hz. Fig. 2 shows the noise spectrum measured at the magnetic laboratory of the Danish Technical University using HP 3566A digital spectrum analyzer. The sensor was a part of the low-noise laboratory magnetometer described in [7]; the magnetometer noise was lower than 2pT rms (64 mHz..10Hz). The sensor itself was placed in five-layer magnetic shielding manufactured by Schonsted.

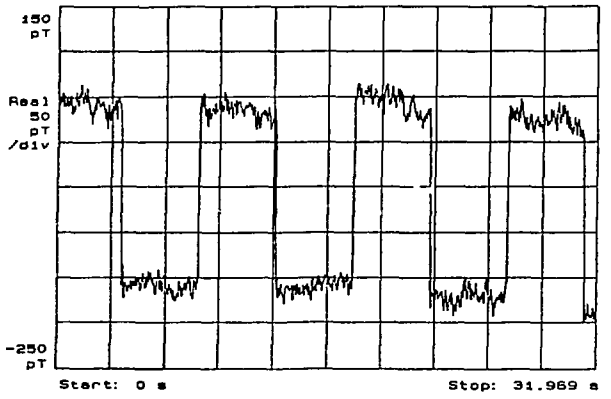

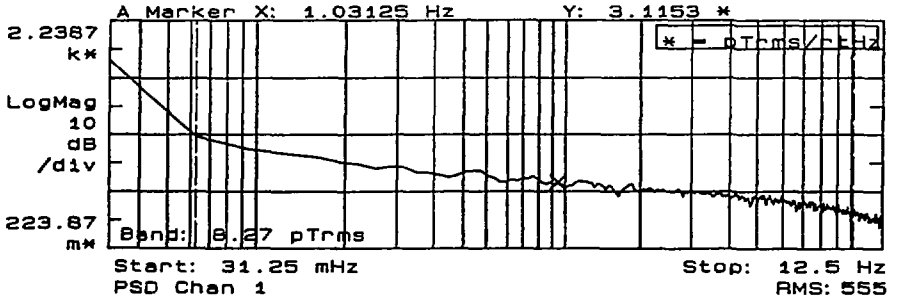

Conclusion:

The new technology allows the production of low-cost low-noise fluxgate sensors suitable for use in magnetometers with 10 pT resolution. Preliminary tests have shown that the sensor noise is comparable to that of permalloy ring-core sensors developed in Naval Ordnance Laboratories for NASA, which are considered to be the best ever reported.

References:

[1] P.Ripka, Improved Fluxgate for Compasses and Position Sensors, J.Magn.Magn., 83 (1990) 543-544.

[2] P.Ripka, Contribution to the Ring-Core Fluxgate Theory Physica Scripta, 40 (1989) 544-547.

[3] P.Ripka, Recent advances in fluxgate sensors to appear in Sensors and Actuators (1992)

[4] Ripka P., Draxler K.: Feromagnetické sondy a jejich použití (Fluxgate sensors and their applications), Slaboproudý obzor 48 (1987) 105-109.

[5] P.Ripka, F.Jireš and M.Macháček, Fluxgate Sensor with Increased Homogeneity, IEEE Trans.Magn., MAG-26 (1990) 2038-2041.

[6] K.Příhoda,M.Krs,B.Pešina,J.Bláha, "Mavacs - a new system creating a non-magnetic environment" Geol.Iber. 12/1988-89 p. 223.

[7] F.Primdahl, P.Ripka, J.R.Petersen, O.V.Nielsen, The Short-Circuited Fluxgate Sensitivity Parameters, Meas.Sci.Technol.,2 (1991),343.

A project on research of the fluxgate sensor noise was proposed for the competition for ČVUT research grants in 1992.

DETECTING AND PROCESSING OF THE TACTILE SIGNAL

J. Volf, V. Chalupa, H. Obrazová, D. Kunzová, P. Mrzena, S. Papežová, J. Vlček

Faculty of Mechanical Engineering, CTU, Technická 4, 166 07 Praha 6
Faculty of Electrical Engineering, CTU, Technická 2, 166 27 Praha 6

Key words : tactile sensors, transducer, information processing

Specific informations may be gained by means of transducers and sensors necessary for interaction between different objects and specimens. Large number of transducers, sensors and probes are being used as for instance micro-switches indicating the contact, sensors of gripping force or the sophisticated sensors substituting the touch.

In the course of the research tactile sensors and miniature transducers with different sensitivity to the acting force were designed. The sensors developed till the present operate on the basis of a semiconducting rubber. With these sensors resistance dependancy on the force acting for different electrode shapes and temperatures was investigated. Further the reproducibility of the measurement was tested [1]. The non-expensive production materials available in Czechoslovakia are suitable only in narrowly limited spheres. DYNACON is one of the foreign materials which are suitable too. Others semiconducting materials are being measured. Using the semiconducting elastic Material DYNACON with the thickness of 0.75 mm allows the shifting of the working region in the range from 2N to 1kN with miniature sensor size (ø 10 x 3 mm) and with the mass 0.4 to 6 g. The discrete transducers are able to switch in the range 0.62 to 200N. A large size sensor (50 x 50 x 4 mm) with 36 active points was elaborated.

The optical wave guide sensors take advantage of gaining a signal by affecting the properties of the optical wave guide by external influences.

At the Machinary Faculty of the Czech Technical University we are engaged in research of optical wave guides, at which the amplitude changes are raised by an external quantity [1]. There are sensors operating on the principle of microflexure or flexure loss, further sensors with the mutual optical wave guide coupling and sensors indicating the position change. The properties of the microflexure sensor and the mutual coupling may be considered as a good premise for designing and manufacturing a matrix optical sensor. At present a preparatory phase for measuring the properties of these optical wave guide sensors is performed.

In the sphere of distinguishing methods new ways were found making it possible to create a suitable description of the tactile image and so to obtain a tactile image and the following classification. It is the method of the testing triangle, variable angle, tolerancy zone with the VORO classification method. All given images investigated were classified correctly.

There is a further group of methods using the Helmholtz's equation [2].

1) using the eigen value of the matrix A of the image,
2) using the scalar charakteristic distribution of components matrix A of the image,
3) using the geometrical properties of the matrix A of the image.

Except for the method using the eigen value, all image matrices are operating in real time with the classification correctness of 80 to 100 % . The same method based on the discrimination analysis was launched. This method makes it possible to compare the methods for distinguishing the images one from the other on the basis of the criteria given. The mentioned way may be also applied for comparing arbitrary styles of projects, engines, installations and to select the best one enabling to suppress maximally the subjective advantageousness evaluation.

One of the perspective variants to solve the problem of distinguishing the tactile images is to use the neuron net. The reason for being that structure of the neuron net is suitable for performing some functions of the brain concerning the subject behaviour. It results from the accessible literature that the problematics of classificator materilizing the tactile images by aid of a neuron net was not yet solved anywhere. Therefore in this stage our attention was aimed at the study of the structures of neuron nets assigned for processing visual informations with the aim to transform the knowledge obtained in the sphere of the tactile information. It was especially the matter of Liusker's publications, which showed, that in a relatively simple structure of the neuron net synoptic images corresponding with the input information may be outstanding.

Furthermore the Grossberg's and Malsburg's model of neuron nets were studied. These models were originally projected for processing the visual information. It turned out that especially the Grossnerg's BCS model may be applied in the sphere of tactile information processing. The tactile images obtained by means of the discrete tactile sensors do not give total information on the characteristic outlines of the object and therefore it may be supposed that by applying the remote signs the information will be completed in those cases. The Fukushima's models were studied too.

The results of the research may be used in automation and robotization for controlling the gripping force, the right gripping and distinguishing the gripped object. Further applications may be used for terminal switches and safety switches also in explosive surroundings. They may be profitable for guarding buildings, lodgings, goods in department stores, galleries, museums, churches and elsewhere where it is necessary to indicate the lifting or misappropriating of an object or only its shifting along the sensor. These sensors may find their application also in medical diagnostic methods and in all other domains of human activities, where it is necessary to transform the acting force to an electric signal. The classification methods are suitable for distinguishing systems of robots and object classification eventually for scanning the motion of the object along the tactile sensor.

References:

[1] Volf, J. a kol.: Závěrečná výzkumná zpráva k úkolu č.III-8-4/06, FSI ČVUT Praha, 1990.

[2] Volf, J.: Metody zpracování taktilního obrazu s využitím Helmholtzovy rovnice. Acta Polytechnica 9(II,3), ČVUT Praha 1990

This research has been conducted at the Department of Electrical Engineering as a part of the research project "Method and Means of Detecting and processing tactile Information" and has been supported by Czech Technical University grant No.8007.

METHODS FOR MEASURING OF MECHANICAL QUANTITIES

J. Olmer, J. Kratochvíl, J. Záruba

Klokner Institute, CTU, Šolínova 7, 166 08 Praha 6

Key words: Methods, gages, calibration

A developement of methods of calibration of vibration pick-ups.

The method of determination of transverse sensitivity was suggested. The mechanical shaking tables of KI will be used along with the configuration of a set of vibrations sensors suggested to eliminate the parasit vibration of the tables. From the literature sources it is clear that the transverse sensitivity of vibration pick-ups reaches currently 3%, but also 20% (one at the Philips pick-ups).

The results of calibration of some modern pick-ups (Brüel & Kjaer, Philips, Peekel) demonstrate good agreement with the calibration parameters of the calibration equipment built in our institute. The parameters of the equipment were verified by the Czechoslovak metrological institute.

In our institute the technique FFT is used for calibration by means of non-periodic motion. This method was developed and published by J. Olmer. It is based on the theory of Fourier integral.

Methods of application of semiconductor strain gages in the measurement on structures.

In 1991, some cases of application of semiconductor strain gages were evaluated. There are the measurements of strain, acceleration and normal stresses under the foundation of a machine. There were dynamical measurements. It was necessary to suggest and produce an element, which is situated between the structure and the strain gage.

The best result was reached in 1986. A dynamical measurement of strain inside concrete was performed. The strain was of the order of $\epsilon = 10^{-10}$. It was proved that the semiconductor strain gage is an important element in the developement of a measuring technique for research on structures, especially because of its great sensitivity (gage factor K = 100 - 200). It makes possible the measurement of the static-dynamic deflection of bridges and high buildings. It will be necessary to prove a linear function between strain and deflection in important places of the structure.

Vibrating wire method of mechanical quantities' measuring.

Already in the 1950's , this method of measuring was founded by Ing. Miloš Petřík, CSc. in Klokner Institute in Czechoslovakia. A contemporary solution utilizes an innovative series of variable elements of vibrating wire sensors from a class of accuracy 0.02% (Awarded as the best solution RKS III - 3, ČSAV, in 1989).

In 1991, calibration equipment for vibrating wire tensometers was produced in the Klokner Institute. At the same time, a prototype of a 20 kN hanging loadcell for weighing and a sample of pore pressure's 500 kPa sensor with an increased endurance an aggressive environment were produced. While constructing a prototype of a 4 kN loadcell for measuring surface stability of concrete by a surface destructive method, a gage of a rainfall for ombrograf, a serial vibrating wire tensometer and a miniature pressure cell for soil humidity measuring are being prepared for production.

Although the development of the measuring method is focused mainly on application in civil engineering, it is also applied in another spheres (mining, geology, hydrometeorology, agriculture, etc.). The method is advantageous for use in conditions "in situ" and it can be successfully applied in solving tasks of ecology.

This research has been conducted at the Klokner Institute as a part of the research project "A development of methods for measuring of physical quantites in a civil engineering research" and has not been supported by a CTU grant.

Section 7

POWER ELECTROTECHNICS

PROTECTIONS IN A NETWORK OF POWER STATIONS, OWN CONSUPTION

F. Přibyl, A. Dočekal, J. Čermák, S. Bouček

Faculty of Electrical Engineering, CTU, Department of Electric Power Generation, Transmissioin and Distribution, Technická 2, 166 27 Praha 6

Key words: Power station, own consumption, setting protections, short circuits, voltage rates, current rates, auto-acceleration

The task "A complete analysis of setting protections in a network of power stations' own consumption in the nuclear power station Dukovany, with reference to section switchboards 0.4 kV" was solved on the basis of discussions between employees of the nuclear power station Dukovany and employees of the Faculty of Electrical Engineering, which is a part of the Czech Technical University (Department of Electric Power Generation, Transmission and Distribution).

In the recent period of the nuclear power station's operation, defects in a transformer station of the 1st main production unit were ocurring, in which crashes at section switchboards occurred at the low voltage level with consequent fires there, which were strongly influencing the nuclear safety of the power station Dukovany.

To solve the problem, a calculation scheme of supplying the 2nd reactor unit's own consumption, including a spear supplying its consumption from a transformer station 110 kV Slavětice, 110 kV Oslavany, from its own consumption of the 3rd and 4th reactor units (which belong to the 2nd main production unit) and from the transformer station "2CR" (0.4 kV), which is supplied from the 1st reactor unit (the 1st main production unit), was created upon the request of the power station's Dukovany employees. For all operational alternatives mentioned, calculations of short circuit rates with and without resistances, with consideration to motors in the network of both high and low voltage levels, were carried out. Furthermore the rates, when drives were auto-accelerated, were calculated. On the basis of the calculations mentioned, an analysis of setting protections with concrete recommendations and reminders to the present situation was carried out.

Following an agreement with an engager, a calculation of short circuit rates in its own consumption was made for the 2nd unit of the 1st main production unit of the nuclear power station Dukovany. With regard to a similar system of supplying in the entire power station, the results gained are valid also for other units. It is necessary to state that the problem mentioned was recently solved, for example, by Energoprojekt Praha.

Hitherto existing calculations of short circuits, made by Energoprojekt Praha, were processed by means of a programme considering the reaction reactants of scheme elements only - it is so called the approximate method, currently used for short circuit solving. It means that resistances of the scheme elements were not considered.

With regard to the fact that solvers were able to use an exact programme ZKR-T (worked out by Ing. Karel Pospíšil, CSc, FEI-CTU Praha), which respects both reactances and resistances of the scheme elements, they were enabled to model torse load (asynchronic motors are meant). These, initially, contribute toward the short circuit, which is why it was decided to create a similar scheme, where, excluding alternators, electrical power systems and transformators, all cables of both high and low voltages were respected.

Further, a calculation of voltage and electric current rates during auto-acceleration, mainly from the point of view of the right electric current establishment of protections, was made. But the calculation may also serve as a check of voltage decrease of the high voltage bus-bar of individual transformer stations and of the low voltage bus-bar of unit networks.

We carried out the calculation with the simple assumptions, that follow : we neglect resistance in the network, we calculate only with reactances of cables and transformers. We neglect resistances of asynchronic motors and we calculate, that starting in electric current is completely reactive, so $\cos \varphi z = 0$. In reality, starting in electric current of an asynchronic motor has also an active fraction, so $\cos \varphi z$ varies from 0.2 to 0.3.

To solve the problem, all necessary calculations have been made, with regard to the present situation in the power station's own consumption. At the same time, "Defect minutes", worked out in the power station [1], were studied in detail and all the major conclusions and recommendations were characterized by two standpoints :

1st : Reviewing of a protection selectivity

2nd : A suggestion of reliable turning off circuit breakers "AR" and "J2UX" during suspended short circuits.

From the point of view of the protection selectivity, the section switchboards were checked out and a sensitivity coefficient "K_c", respecting the least favourable defect states (minimum short circuit currents) was stated. At the same time, a safety coefficient "K_b", which respects a corresponding distinguishing ability, with regard to maximum operational currents (currents occuring during auto - acceleration) was calculated. An important conclusion performs also a suggestion of measures in a costruction of the section switchboards and at the circuit breakers "J2UX".

References:

[1] Defect minutes (Dukovany 1989-1991)

This research has been conducted at the Department of Electric Power Generation, Transmission and Distribution on the request of power station's Dukovany employees, engaged as "A complete analysis of establishing protection in a network of power stations' own consumption in the nuclear power station Dukovany, with reference to section switchboards 0.4 kV".

THE EVALUATION OF THE VOLTAGE FLUCTUATIONS

J. Tlustý and Z. Fejt

Faculty of Electrical Engineering, Department of Electric Power Generation and Distribution, Technická 2, 166 27 Praha 6

Key words: voltage fluctuation, disturbance, electromagnetic compatibility, flicker, flicker analysis

Electrical equipment with non-linear characteristics are sources of disturbance by harmonics,inter-harmonics, voltage fluctuations,voltage dips and supply interruptions and voltage unbalance.This report concerns voltage fluctuation due to load variation in supply systems. This phenomenon is strictly related to the sensitivity and the reaction of individuals.

Generally, since voltage fluctuations have an amplitude not exceeding 10%, most equipment is not disturbed by this type of disturbance. The main disadvantage which can be attributed to them is flicker, or fluctuation of luminosity of an incandescent lamp. The physiological discomfort associated with this phenomenon depends on the amplitude of the fluctuations the component frequencies, the rate of repetition for voltage changes and the duration of the disturbance. Fig.1 gives two examples in which the supply voltage at angular frequency 50 Hz is modulated by a voltage fluctuation.

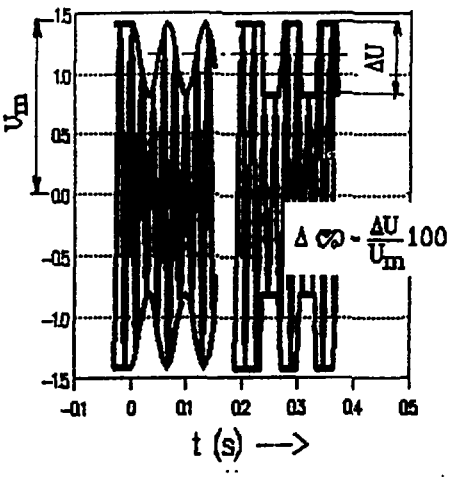

Fig. 1

The International Union for Electroheat (UIE) developed an internationally accepted flickermeter and criteria for the evaluation of flicker severity, using the experience available on the subject and carrying out the additional work required to establish a complete and widely accepted approach. The UIE flickermeter has gained approval from the IEC Technical Committee 77and the IEC issued Publication 868 that contains the specifica-tions for the instrument. Blocks of the flickermeter are: Input voltage adapter, quadratic demodulator,demodulation filter with weighing filter, non-linear variance estimator and statistical evaluation.

The flickermeter monitors a flicker occurrence in units of perceptivity and it is necessary to evaluate and display the severity level for regular and irregular types of flicker.The flickermeter simulates the process of physiological visual perception and gives a reliable indication of the reaction of an observer to any type of flicker indepedent of the source of the disturbance. In principle,therefore, the output of the instrument which is one unit at the threshold of perceptibility must be evaluated according to a procedure equally applicable to arc furnaces or household equipment.

When considering the development or the supply of equipment which is likely to cause voltage variation on an electricity distribution system, an equipment designer or an utility engineer must be mindful of the flicker limitations associated with the supply system.It's now possible to use the simplified prediction methods for simple and regular voltage fluctuation only. That's exactly why authors created a mathematic simulation algorithm.

Any chosen voltage fluctuation curves can be expressed as a series of polygonal segments and fed into the model. If required, a flickermeter model could also be used to analyse recorded data to replay the recording through a serial interface of the computer in use. The P_{st} value (short term perceptibility of voltage fluctuation severity) of the investigation interval (usually 10 min.) is obtained as an output signal. Fig.2 showes P_{st} values for some types of the voltage fluctuations.

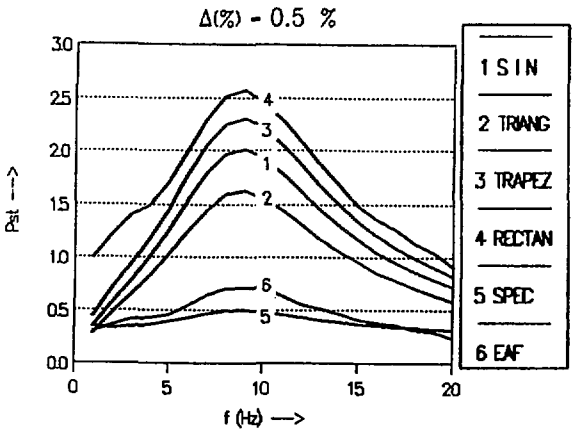

Fig. 2

of the electricity supply usage,so that the limitation of flicker severity has become a general problem at all levels of supply system. Authors' method using the mathematic model is very advanced. The results that can be obtained are necessarily approximated. This flicker predicting method can substitute a costly real time flickermeter in the operating supply system.

This report gives a new general method for increasing knowledge related to the disturbance of the voltage fluctuation.

The model contains a special block for fast flicker analysis too. For short intervals the periodic voltage fluctuations can be broken down into fundamental oscillation and subharmonics in the band from 0.5 to 30 Hz. Fig.3 gives an example of spectrum voltage fluctuation of the electrical arc furnace. Flicker predicting methods are very important because disturbing loads are steadily proliferating, due mainly to the heavy penetration of electronics in all sectors

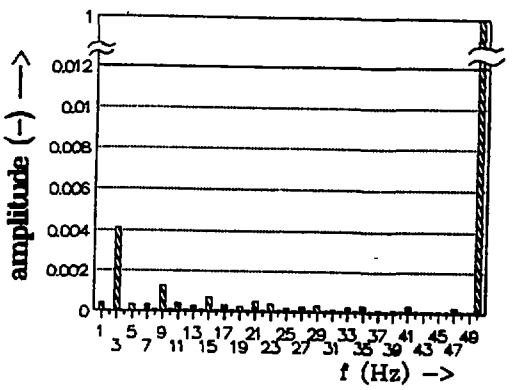

Fig. 3

This research has been conducted at the Department of Electric Power Generation and Distribution as a part of the research project of Electromagnetic compatibility and has not been supported by a grant of Czech Technical University.

COMPUTER–AIDED EVALUATION DISCHARGES ACTIVITY

K. Záliš

Czech Technical University, FEL, Technická 2, 166 27 Praha 6

Key words: High-voltage insulation, alternators, slot discharges, partial discharges, prophylaxis, computer program

While with the thermoplastic insulations the greatest problems were those with the hygroscopicity of the insulation and with partial discharges inside the dielectric, the thermoset insulations made on the basis of epoxy resins yield the greatest problems with vibrations and loosening of bars in slots, as well as with slot discharges, i.e. with discharges between the bar surface and the stator slot. That is why the need has considerably increased to measure PD with the aim of finding out the origin of slot discharges in the stator of the alternator. The method of global PD-measurement (off-line measurement across the entire stator or in one of its phases) is especially convenient for the orientation of PD-measurement in high-voltage alternators and for watching the general state of its insulation. In the High Voltage Laboratory of the Czech Technical University (Faculty of Electrical Engineering) the modified Dakin's method is used for global PD-measurement in the insulation of large alternators by using a PD-measuring instrument MUT8 produced by TuR Dresden. This method has been used for several years in collaboration with the purpose-established organization ORGREZ in prophylaxis of alternators. This method is a part of Czech Power Enterprises (ČEZ) Direction prophylactic measurement of alternators. The measurement is carried out with the alternator shut down (during its revision).

But these measurement require fast and quality evaluation computer support, because the "normal evaluation" of discharge activity is very slow and inaccurate. That's why the software for minicomputer Sinclair ZX Spectrum 48 kB was made for the evaluation and for saving the results. The computer program "CV-ALT" takes 39083 bytes of memory and it is used for the evaluation of the discharge activity by the prophylaxis measurement in high-voltage alternators. The computer program "CV v3.0" takes 38425 bytes of memory and it is used for the evaluation of the discharge activity in high-voltage insulation.

Both of the programs were based in BASIC language and do possible evaluation, editing and saving measured values of discharge activity including information and notes about the machine (the equipment, the sample of insulation) and measuring conditions. Input of measuring values can be done via the keyboard of a computer or directly from a tape recorder. The evaluation of entering data and the calculation of parameters (maximum apparent charge q and sum charge Q in a half-cycle of supply voltage, power of partial discharges) is performed automatically. Evaluated values can be corrected by several means. Output is displayed in the form of tables and graphs on the monitor of the computer or on the printer. The saving of values is performed on the tape.

This research has been conducted at the Department of Generation, Transmission and Distribution of Electrical Energy upon request and in collaboration with the purpose-established organization ORGREZ in prophylaxis of alternators. This research has not been supported by the grant of Czech Technical University.

SPACE VECTORS FOR TRANSIENTS ANALYSIS AND DISPLAY

Z. Čeřovský

Faculty of Electrical Engineering CTU, Technická 2, 166 27 Praha 6

Key words: Electrical m phase systems, electrical machines, transients, space vectors

The mathematical description of a m phase electrical system holds m phase voltages, m phase currents as time dependent variables and parameters of the system. The system of m phase variables can be substituted with a vector having m components.

In case of three phase machines these three components are collinear with the three phase axes of the machine. The vector addition of the components forms a singel space vector. The singel current space vector represents for example the singel mmf vector not only in its magnitude but also in its space orientation. The same holds for the magnetic flux and in the abstract about the voltage. The mathematical transformation is exact. The features of space vectors correspond to the features of physical quantities.

The space vectors represent the transient phenomena in electrical systems and enable one to form a clear image about what is happening in the physical process. This possibility is important not only for research but also for the teacher and students. To take full advantage of the space vector method computer technology has to be used.

At the Department of Electrical Machines, Apparatus and Drives computer technology is used both for science and for the teaching. The labs and classrooms at the Faculty of Electrical Engineering of CTU are provided with the appropriate computers which might enable the simulation of the transients using the space vector method in controlled electrical machines, in power electronics and microcomputer controlled drives or during different failers of this equipment as well. The results will be utilised in science and teaching as well. After computation they can be displayed as moving pictures of the space vectors at the screen of the computer. The same moving picture may be shown at the screen of the osciloscope measuring the transient phenomena.

As an example of the utility of the space vector method an electromechanical phenomenon in a voltage inverter fed induction motor by the loss of D.C. supply in the troley will be described.

In voltage inverters (see fig. 1.) a filtering capacitor with a considerable capacitance is connected to the terminals of the D.C. side of the inverter. The inverter consumes (supplies) energy from (to) the D.C. source the time dependence of which has a D.C. and an A.C. component. The filtering capacitor should consume and supply alternating components of the energy so that the D.C. source is loaded as far as possible only by the supplied D.C. component. After a sudden switching off of the D.C. source while the inverter continues its operation the filtering capacitor with the inverter and the induction machine form an independent system. The electrodynamic phenomenon appearing in this system can lead either to an extinction of the electromagnetic energy of the system or to an increase of the electromagnetic energy and endangering of the system by inadmissibly high overvoltages. This phenomenon can be practically used for a transition of the induction machine into a generator to brake the drive.

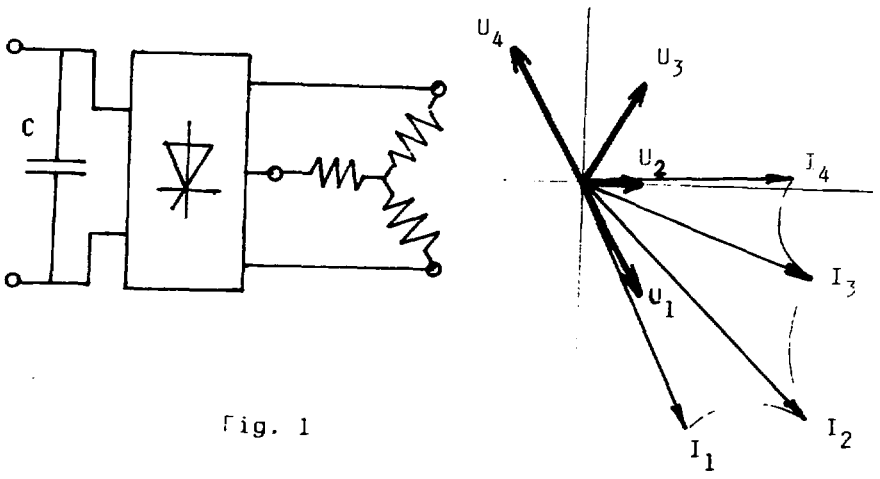

Fig. 1

A gradual change of the motor to the generator is shown on the fig. 1. The starting conditions are: The capacitor C has the starting voltage U(0). The frequency of the inverter is 50 Hz and the four pole machine rotates at 1575 rev./min., without any magnetic flux.

As soon as the inverter begins to operate the energy flows in the first intervals from the capacitor into the motor.The transmitted power is equal to the scalar prodact U.I. At the end of the first interval the scalar product U(1).I(1) is positive. The induction motor operates as a passive device and builds up its magnetic flux. At the end of the fourth interval the scalar product U(4).I(4) is negative. The capacitor is charged by the energy generated in the induction machine.

It is quite impossible to follow the whole transient phenomena in a static picture. The moving picture can bring fast results in research for different starting conditions. It can also be first rate help in teaching.

This research has been conducted at the Department of Electrical Machines, Apparatus and Drives. It has not been supported by a grant.

DIAGNOSTIC METHODS IN ELECTROTECHNOLOGY

J. Kuba and V. Benda

Faculty of Electrical Engineering, CTU, Technická 2, Prague 6

Key words: Technical diagnostic, semiconductors, deep levels

For further developments in elektrotechnology it is necessary to have maximum information about the behaviour and properties of materials and devices for their manufacture and use . The research project for the development of new diagnostic methods and their applications, connected with diagnostic of the power electrical insulation systems, dielectric, multilayer semiconductor structures, mechanical and magnetic parts of electrical appliances and elements was proposed by the Department of Elektrotechnology. These research projects have run for many years and have produced many significant developments. They have also given the possibility to use the special experimental equipment installed in our laboratories. The main goal of the research work is to contribute to the increase of technical and economical parameters of products. Thus the collaboration between the research team and selected electrotechnical producers is implemented or will be implemented in the future.

The significant results in the research of the properties of insulating materials at low temperatures and high frequencies and in the research of power semiconductor elements have been obtained in recent years. Some new information about the possibilities of characterisation of the concentration of deep level impurities in semiconductors are given in another text.

The most important parameters of power silicon devices (esp. bipolar devices) depend on the recombination rate of electrons and holes at local centres caused by impurities and crystal lattice defects and some centres may cause even deterioration of device reverse characteristics. Each local recombination centre may be described by one or more deep energy levels with characteristic capture cofficients for electrons and holes. The identification of deep impurities in silicon structures could be helpful for both technological optimization and location of sources of harmful impurities. For identification of the type of recombination centres in silicon structures, a number of diagnostic methods is used. For the deep level diagnostic in multilayer structures the method of thermally stimulated current (TSC) can be applied. The principle of the method is the following: at a high rate of temperature rise (from liquid nitrogen temperature to room temperature), ionisation of deep impurity levels of energy W_t occurs and creates a local maximum at the temperature T_m in the temperature dependence of the PN junction reverse current,

$$W_t = k \,.\, T_m \,.\, \ln \frac{k.T_m^4}{2W_t.\beta}$$

where

k is the Boltzmann constant,

β is the rate of temperature rise dT/dt,

B is a constant of the method which could be eliminated by measuring the sample at two or more different valves of dT/dt.

The TSC measuring consists of following steps:

- short circuit connection of sample electrodes
- cooling to liquid nitrogen temperature
- reverse voltage bias
- heating of the measured structure using a defined rate of temperature rise and measuring simultanously the reverse current and the sample temperature. When we developed the measuring equipment, we used experiment control by computer. The basic arrangement is shown in Fig.1.

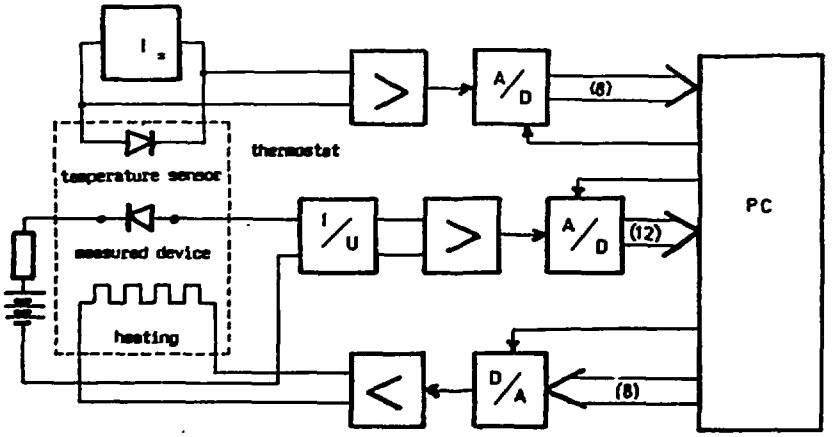

FIG. 1.

During the development of equipment, the following partial problems have been solved:

a) construction of the sample holder enables the use of a rate of temperature rise from 0.1 to 10 K/s.

b) construction of A/D converter measuring current up to 2 nA with the sensitivity of 1 pA/bit

c) construction of A/D converter for measuring the sample temperature

d) connection with a controlling computer

Individual parts of the measuring equipment were constructed. Using IBM-PC as a controlling computer, at present it is possible to measure deep level energy spectra on power semiconductor device structures of diameters up to 30 mm. The development of the measuring equipment will continue by optimization of the individual parts and preparation of a program containing a deep level centres database to be able to do deep level diagnostics in real semiconductor structures.

Besides the described TSC method, we are interested in development of two next independent measuring methods (DLTS, OCVD) and we expected to create a workplace being able to perform nondestructive and effective deep level diagnostics in power semiconductor structures.

Section 8

ARCHITECTURE, TOWN PLANNING, REGENERATION

REGENERATION OF RURAL SETTLEMENT IN THE BORDERLANDS

J. Horký, K. Maier, J.Němec

Faculty of Architecture, ČVUT, Thákurova 7, 16634 Praha 6

Keywords: Revitalization, Rural Settlement, Peripheral Regions, Environment

This stage of the research has been devoted to analysis of constraints and potentials, and to delimitation of particular regional systems within the Borderland area.

Czech and Moravian Borderlands (except Southern Moravia) have similar natural conditions: highlands or mountains with rather short vegetation periods and, consequently, substandard agricultural potentials and a greater portion of forests. The natural environment has been preserved in areas of restricted access at the Bavarian and Austrian borders, while more "open" Saxonian and Silesian borderlands suffer from heavy pollution.

Certain socio-economic characteristics are common for the Borderlands and stem from their recent history:

- Transfers of about 400 000 Czechs in 1938-1939 and 2.7 mil. Germans in 1945-1947 from the areas that had been temporarily annexed by Nazi Germany. Even with some 1.4 mil. new settlers from the Czech interior and abroad the total population of the area dropped from 3.6 mil. in 1930 to 2.2 mil. in 1947. The present population is 2.7 mil.
- The organization of military and border zones of limited access.
- Support of urban development at the expense of villages from the 1950s till the mid-1980s.

While the pre-war economy consisted of manifold and highly-specialized industrial production based on local natural resources and skilled and specialized labour, this tradition was disrupted as newcomers who had come mostly from rural areas were often unable to replace missing skilled workers. The percentage of jobs in industry in the Borderlands declined from 46.6% in 1930 to 45.3% in 1961, compared with the increase in the whole Czech Republic from 38.3% to 49.6%. The decline hit most small settlements, where local factories and trades vanished. While the resettlement policy succeeded in compensating the decline of population in medium and bigger towns by the 1980s, villages and small towns reached only 65.9% of the pre-war size in 1980 and they have been losing their productive population again. It is estimated that some 100 settlement units disappeared since 1950, about a half of them in the Bohemian Forest, where vast "empty" areas developed alongside the border and in military zones.

Despite efforts by the State to restore the Borderlands by the way of subsidies, the substantial cause for backwardness and steady decline remained until recently: peripheral location within the closed settlement and centralized economic management with almost negligible connections across the border. The general level of basic social services has been comparable with rural districts in the interior but the real magnitude of available jobs and accessibility of services, goods and facilities were not able to compete with other regions. As a result, a non-stabilized socio-economic structure developed, its viability being dependent on continuous external support from outside.

After the removal of the Iron Curtain and the withdrawal of most army troops, new potentials for development have emerged: tourism, quality food production through nature-saving agriculture, small-scale industry based on local resources, and international trade among regions.

The initial optimistic prospects for quick and easy revitalization can be compared now with the reality of the first two years after the opening of the borders. Although insufficent time has passed for precise conclusions, some insights are possible :

1. It is unfeasible and futile to re-create the original (pre-war) settlement system as a whole. Instead, settlements which have survived should be equipped with necessary infrastructure to become viable in the future. Only in the vast abandonned territories of former military zones some kind of settlement re-establishment should be considered.
2. Whereas all the borderland territory needs some sort of recovery and redevelopment, the actual situation, potentials and constraints are different with respect to particular regions. The distinctions among regions, sub-regions and their groupings may be expressed by:
   - exposure to the major transportation arterials crossing the border
   - accessibility of local towns and/or services and facilities
   - environmental quality and recreational attractivness of the area
   - extent and prospect of existing qualified and skilled jobs in the area
   - economic prosperity of the adjacent area across the border.

   On the local level of particular communities and municipalities, the future prospects also depend on strong and enlightened local leadership
3. Owing to different conditions of particular regions and sub-regions, no general prescriptions for recovery exist. The strategic objective for the regional policy should rest on reducing step-by-step the extent of areas that need some kind of state assistance. The existing subsidies for production, housing, social and other public services should be replaced gradually and with respect to local conditions by deliberate utilization and support of local resources (human, natural, and economic) for self-dependent and sustainable development.

Based on this knowledge, further research in this field is proposed, which should:

- intensify and deepen the existing knowledge on particular borderland regions and sub-regions, especially on the basise of the 1991 census
- propose the revitalization plans and procedures on the base of pilot projects and models on the sub-regional and local levels.

References

[1] K.Maier: Rural Settlement, Dissertation Paper, Faculty of Architecture CVUT 1990.

This research has been conducted at the Institutes of Urban Designing and Planning of the Faculty of Architecture and has been supported by the internal Faculty grant No 401.æ

REGENERATION OF HISTORIC TOWN CENTRES

Josef Pechar

Faculty of Architecture, Czech Technical University Tákurova 7, 166 34 Prague 6

Key words: pre-requisites and principles of regeneration

The regeneration of historic town centres is a world-wide problem today. The further life and identity of towns, of different sizes and types, depends on a rapid and successful solution to the problem. Historic town centres play an integrating role in town agglomerations as well centres play an integrating role in town agglomerations as well as in a broader context. The need for their regeneration has been raised by the imbalance in the development and the disintegration of towns, caused by extensive ways of life.

The pressure for the regeneration of towns in Czechoslovakia has been increased by the long-term one-sided orientation towards the construction of housing estates on open green-field sites on the outskirts of towns. At the same time, the development of centres has been neglected and the cores of historic towns have fallen into disrepair. It has not only cultural, social and demographic consequences, but there is also a lack of preparedness for regeneration in the field of legislation and in building. Historic towns have long traditions, a mature architectural culture and in many cases a compact historic core.

The problems of history, theory, methodology and conception in the regeneration of historic town centres have been confronted with contemporary processes of regeneration in Central and West European towns, with the following results:

- To understand the regeneration of town centres being a whole, continuous and cyclical process in the development of towns.
- To solve the social and demographic problems of the regeneration of town centres with regard to forthcoming changes in the way of life its inhabitants.
- To contribute to the social development and significance of town centres with the active participation of inhabitants, enterprises and institutions.
- To create legislative and economic conditions for the regene- ration of centres, to regulate developers' activities.
- To develop the theory of the social-spatial structure of town centres.
- To solve the regeneration of town centres in a broader regional context, to create a well-balanced multifunctional organism and spatial arrangement.
- To preserve the cultural, artistic and historical value of centres, which form the basis of the identity and continuity of the town/s development.
- Bearing in mind architectural and urban compositions and the relationship of the new and the old, not to affect the genius loci of a town, the function and character of a historic environment.
- To determine the level of historical value and preservation of urban units, spaces and buildings in the regeneration of town centres.
- To bring back the values of 19th century architecture and town planning in contemporary application, to preserve green spaces in town centres.

- To respect historic spatial structures in transport planning, to give priority to pedestrians and to reduce traffic loading in centres.
- *To preserve and use old spatial and typological structures, to apply the integration of* functions.
- To revive the application of traditional building techniques, materials and crafts. To develop methods for the evaluation of the structural and technical qualities of historic constructions.
- To improve the ecological situation and the quality of the environment through the technical modernization of centres and historic town cores.

This research has been conducted at the Faculty of Architecture as a part of the research project "Regeneration of Historic Town Centres" and has been supported by the Faculty of Architecture CVUT grant No.4O3.æ

ARCHITECTURAL CONDITIONS OF DEVELOPMENT FOR SMALL-MEDIUM FACTORIES

E. Hlaváček, F. Štědrý, J. Štěpaník, J. Attlová

Faculty of Architecture, CTU, Thákurova 7, 166 34 Praha 6

Key words: Architecture, small-medium industry, rentable factories

The first stage of research concentrates on the qualitative and quantitative definition of the notion small and medium-sized factories and on their characteristic features differing from large industrial factories, on the role they play in economically developed countries, as well as on the urban and architectural forms they take in such countries and on their possible application in this country.

Small and medium-sized enterprises represent an important part of economically developed countries, developing autonomously and existing together with large-scale industry. They enjoy some advantages, such as economic and organizational independence, flexibility and adaptability to demand, territorial dispersion and contact with the client, considerable responsibility in the hand of one person for the decisions concerning the selection of tools and forms of activity. Their work still includes some traces of craftmanship inherited from the past and adapted to the post-industrial era. They are a demonopolized field of enterprise activity which complements the work done by large-scale industry. Small factories (mostly with up to 50 workers) usually have an artisanal system of production, supported by electronics and information technology, whereas medium companies (with up to 500 workers) are a transitional type exhibiting some features typical of small factories (adaptability, independence) while, on the other hand, some principles and methods from the large industry are also applied.

The main impetus for the development of small and medium-sized industrial enterprises was the restructuring process in industrial production in western countries, accompanied by the application of new technologies, electronics and by the rising prestige of intellectual work, which is so widely represented in the work of small and medium-sized companies in technological centres and in multi-activity zones. The process of regeneration of CzechoslovakiaÝs national economy therefore includes the restoration of small-scale production and of the artisanal type of enterprise activity, which was practically destroyed in the recent past.

With the changing character of production efforts are made to restore a close relationship between home and the workplace. Part of this process is also a search for and a creation of new territorial, spacial and other conditions for such work. The search for a solution will always be confronted with particular situation of present settlements and with their particular type. For instance, the existing large-scale structure of industrial zones cannot easily be transformed and adapted to new use, new function and new territorial organization. An important aspect of this process will lie in the areas and buildings left unused after unprofitable production here has ceased.

In the central areas of towns this process will include a deliberate return to multi-layer vertical zoning as known to us from the medieval guild houses and streets and utilization of the old industrial buildings by small firms.

An optimum type of building for this type of activity is a versatile single- and multi-storey building for rent, which has proved very useful in Western Europe. The building either stands alone, or there is a group of buildings to let. The type exhibits a high level of flexibility which makes it possible to divide the rooms into several operation units of different sizes and to introduce permanent changes. The mixture of private and public zones in such buildings contributes to the visibility of working spaces and to their better integration in the town, particularly within the areas in the town outlined for renovation.

Buildings with rooms to let for small and medium-sized enterprises are advantageous for manufacturers as they need not construct and maintain buildings and can concentrate on the enter- prising and manufacturing work.

The regeneration of our settlements, including the creation of appropriate conditions for the activity of small and medium-sized enterprises will be complex, with a number of transitional stages that in the future will always remain open. New urban and architectural concepts should help develop this im- portant sector of the national economy by offering realistic spaces and functional possibilities, forms and opportunities.

Their formulation, in accordance with new laws being prepared and with the new economic and social conditions, will be the topic of the second stage of research to take place in 1992.

References

[1] F. Štědrý: Buildings for Industry and Crafts. Man-Work-Space. ČSAV, 1991

[2] F. Štědrý, J. Attlová, J. Štěpaník: Duchcov - Regulation Plan of Industrial Estate in Central Zone of Town

[3] F. Štědrý et al.: Regeneration of Industrial and Agriculture Area and Buildings in Reconstruction Zones

[4] E. Hlaváček et al.: Kladno - Rehabilitation of Old Industrial Town

This research has been conducted at the Department of production buildings and has been supported by CTU grant No. 8059.

RECONSTRUCTION OF FACTORIES FOR NEW PURPOSES

Tomas Senberger

Faculty of Architecture, CTU, Thákurova 7, 166 34 Praha 6

Key words: Factory, Reconstruction, Conversion, New Use

One of the reasons for the reconstruction of buildings is to correct the difference between the physical and moral wear of a building. This mainly applies to factories, where the character of production speeds up the need for renovation. In the worst cases, when a building loses its original manufacturing function, it can be demolished or used for an alternative, often provisional programme. But factories often prove to have material and moral value (architectural and technical qualities), which prevent them from being demolished or inproperly used. The main aim of this project is to study the reasons why factories lose their function and to examine their possibilities for future use.

Loss of a manufacturing function has various reasons, but it is always related to the restructuring of industry. At present we are standing at the beginning of such a stage. With analysis and prognosis, it is possible to assess which factories will probably be abandoned in the future. Not all the redundant factories will be suitable for further use. The original function of a building and its location will play a significant role. Multifunctional factories are the most convenient buildings for such purposes. Most of them were built during the 19th and 20th centuries. The location has an impact on their further use, especially in connection with the price of sites and the number of available estates on the market. The evalution of a factory that has lost its original function, with regard to its preservation and eventual new use, can be based on urban, architectural, economic and social considerations.

The new functions of a factory can be of a passive character, non-profit making (museums), or economically active. The most suitable economically active use for factories is probably for them to house newly formed small firms, or multifunctional combinations of activities. (The possibilities of new uses have been demonstrated in a number of cases abroad and proved by a series of students projects).

To preserve redundant factories by converting them for new purposes, several steps have to be taken at first, mainly in the field of adult education for local authorities and owners.

It is necessary to carry records of buildings under observation, using, for example, indexes. Another important task is to find people to initiate projects involving new uses for factories. An architect can play a significant role in the whole process. Thanks to his training, he should be able to put forward a programme, a result being that of which the converted factories could enrich the town with their individual character and provide adequate space for new functions.

Example of student project: Conversion of old flouer mill in Prague into the Visual Arts Center

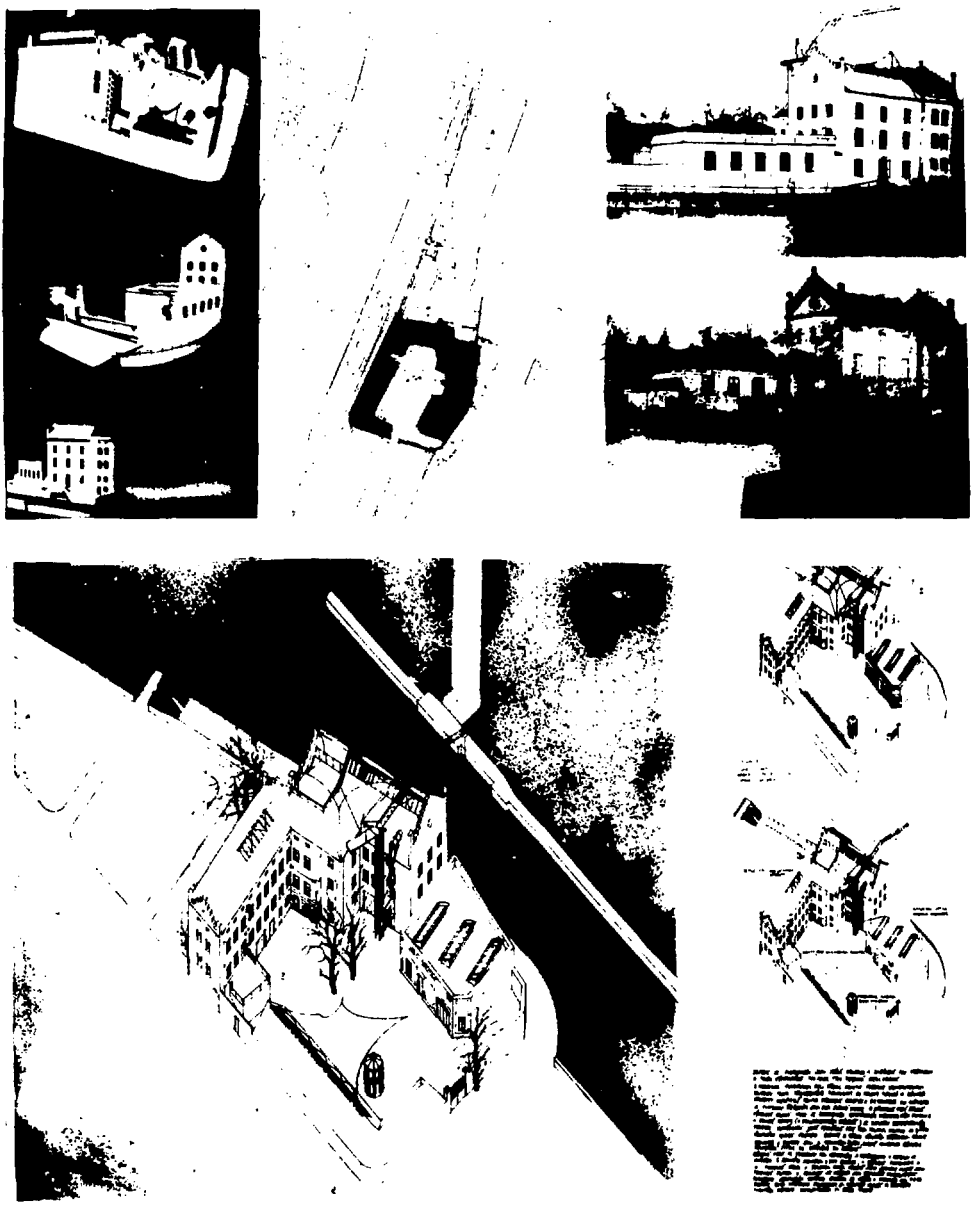

This research has been conducted at the Department of Production Building.

THE EXHIBITION "THE COMMUNITY HOUSE AND ITS ARTISTS"

R.Pošva

Faculty of Architecture, Czech Technical University Thákurova 7, 166 34 Prague 6

Through the exhibition "The Community House and its Artists" the Prague Cultural Institute, which has its offices there, intends to re-establish the tradition of exhibitions in this historic building, and before the planned restoration to remember the artists and architects who participated in its construction.

There is a relatively broad literature on the subject including a short monograph on the building (1), but the Community House has been mentioned above all in a number of publications referring to our art at the turn of the century (2).

From the time it was built, in 1911, the Community House and some of its wall paintings were the subject of several critical attacks, mainly from the generation of architects at the beginning of this century (3). Over the years, as views on the art of the beginning of this century have changed, the opinion concerning the building has become more moderate, but even today the building is still criticized for its rather untidy style. However, views on the work of the architects Balsanek and Polivka have not changed at all. Balsanek has been traditionally considered as the main architect, who designed the exterior of the building and the Smetana Hall, whereas Polivka was believed to be the author of remaining interiors.

But from the study of different sources during the preparation of the exhibition it has become clear that the contribution of each architect was different. The architect Polivka participated more in creating the building's exterior, mainly in its lay-out, the basic arrangement of the mass, and his contribution to the design of the two main porticos both in the and in the rear was significant.

There is no doubt today as to the contribution of artists who participated in the decoration of the Community House. The only question is which of the two architects played the main role in co-operating with the artists, such as Svabinsky, Spillar, Preisler, Mucha or the sculptors, such as Saloun, Maratka, F.Uprka and F.Novak. It seems that with the exception of Smetana Hall it was again the architect Polivka.

The architectural designs and studies of the Community House as well as the designs for its decoration will form the main part of the exhibition. A different view on the contribution of both architects will be expressed in the exhibition concept by showing the place of the Community House within its contemporary context. The purpose of the exhibition will be not only to show works of art of the Community House and to present the artists and architects involved, but also to elucidate more clearly the process or the development of the Community House itself.

References:

[1] J.Masin: The works of art of the Community House in Prague. Prague 1948

[2] Lately P.Wittlich: Czech Secession. Odeon Prague 1982 T.Vlcek: Prague 1900 Panorama Prague 1982

[3] e.g.O.Novotny: About the Ceremonial House of the Prague Community. Styl, year IV.(1912), p.38.39

The exhibiton has been prepared and financed as a grant-aided project of the Faculty of Architecture. Czech Technical University, Prague, in co-operation with the Prague Cultural Institute.

RESEARCH OF SERIOUS FAULTS FOR CHOICE OF REPAIR METHODS

T. Vaněk, V. Weiss, et. al.

Faculty of Civil Engineering, CTU,166 29 Praha 6, Thákurova 7

Key words: Building structure, fault, failure, damage, repair

Great experience was gained in investigations of several hundreds of failed or damaged building structures when several modes of repair were always recommended /1/. Worthwhile conclusions for consulters, contractors and users of buildings can be drawn from this work which is also accompanied by experiments in laboratories as well as by loading tests in situ.

Building codes and regulations based on the limit state approach consider the risk of failure or of damage due to permissible deviations from the design values on a very low probability level. All the failures and damages on various buildings yet observed have testified that the main cause always consisted in serious faults or mistakes during their design, execution or exploitation. Some recent examples of serious faults are briefly described below (for more details see e.g. /2/,/3/).

1. **Neglecting the volume changes in the design of watertight concrete or reinforced concrete tanks.** According to the classic theory, the permissible tensile stresses can not be exceeded but, nowadays, frequently only proof of ultimate load-bearing capacity is made and a rather weak and concentrated reinforcement is used and, consequently, cracks of up to several mm width are formed in the concrete. Sealing them with the aid of an elastic mastic is only a temporary solution. Full restoration requires either to span the crack by a tight adherent strip, or, for a great number of cracks, to form a continuous impermeable coating inside the tank.
2. **Bad control of real humidity of timber during fabrication of high glued girders.** Due to too fast drying of timber boards, their inner humidity exceeded the permissible value of 15 %. This was the main cause of a later debonding between numerous boards and of consequent excessive deflections of these girders supporting a great roof structure where the temperature frequently reached up to 50°C. The repair was made by the addition of steel columns, and where such a measure was impossible, by means of additional nailed timber boards.
3. **Confusion of vertical concrete panels in multi-storey house.** Instead of load-bearing panels containing a strong steel reinforcement, similar non-bearing panels were placed into some highly loaded position. Difficult reconstruction consisted of inserting activated steel struts into excavated vertical grooves.
4. **Overloading during exploitation.** Reinforced concrete columns were heavily damaged by numerous cracks and presented excessive deformations. The restoration together with additional strengthening was executed by steel confining holders of a great perimeter, the gaps up to 50 mm thick being grouted by cement mortar.
5. **Chemical attack due to air pollution and to bad discipline (leakage of aggressive liquids) in a chemical plant.** Concrete and particularly steel in

reinforced concrete floor were heavily corroded, the load bearing capacity was reduced to 50 or even to 30%. After removing of all corroded parts, the structure was strengthened by execution of additional reinforced concrete ribs and plates.

The data and knowledge gained in the course of the described activities will enable the forming of a rather extended database, and also the working out of a catalogue of suitable repair methods for individual structural elements as well as for whole structures and, eventually, will enable an attempt to try to establish an intelligent expert system for diagnosis of cause of failure or damage as well as for the choice of appropriate repair modes and processes to be used in solving similar problems in practice.

References:

[1] VANĚK, T.: Reconstruction of buildings (2.ed., in Czech), SNTL, Praha 1989.

[2] VANĚK, T.: Consequences of negligence at construction of precast timber and concrete structures. In: Lessons from structural failures, Aristocrat, Telč 1991, (pp. 115-122).

[3] WEISS, V.: Damages on concrete reservoires and cofferdams. In: ibid (pp. 145-151).

This research has been carried out by the Department of Concrete Structures and Bridges as a part of the research project "Reconstructions of concrete and masonry structures" and has been supported by the Faculty of Civil Engineering, CTU grant No. 1117.

RECONSTRUCTION OF THE URBAN NETWORKS

P. Šrytr, I. Vávra and coworkers

Department of Sanitary Engineering, Faculty of Civil Engin., CTU, Thákurova 7, 166 29 Praha 6, Czechoslovakia

Key words: reconstruction, urban network, pipe system,

The development of the urban infrastructure, especially the pipe systems, was undersized in the recent years. We are now facing the situation of renewal and modernization of the old, insufficient and damaged urban network systems. The situation is very similar to these of other parts of the urban infrastructure, e. g. transport systems, living standards etc. The previous methods do not satisfy all the requirements of the best, cheapest and most modern solution.

In comparison with the developed countries, the situation is worse due to the us of poor-quality good materials and technology, the neglect of maintenance and revision of the systems and the lack of coordination between responsible managers of particular urban networks systems. The solution of these problems is seen in the use of new technology (fig. 1) with a maximal effort to coordinate and unify methods.

The reconstruction of the urban networks was divided into several parts e.g. coordination of the technological solution, water supply systems, sewage systems, technology of reconstruction processes and economical evaluation of the methods used.

The coordination of technological solution is focused on the preparation of standards and standardization for newly developed and used patterns of urban networks construction and new approaches to the coordination of reconstruction works.

The part on water supply systems deals with the problems of new methods of dimensioning of the system, when more detailed hydraulic analysis and advanced statistical, probabilistic and deterministic methods of determining of the hydraulic load of the water supply system are applied. The intensification of the operation of the water supply network is also coverd by this part.

Among these methods the mathematical method of forecasting the daily drinking water demand is also developed./5/

The possibility of the use of the sewage system for other networks and the use of retention tanks on the sewage system is widely discussed.

Review of technologies and the companies which manufacture the special building equipment was prepared to enable the Czech building company to have the choice of the right technology at its fingertips.

All existing technology processes of reconstruction of urban networks, their evaluation and preparation of standards for their application in Czechoslovakia are also of concern in this research.

The economical evaluation of these reconstruction processes deals with a new method of evaluating the variants of the used technology use in the constructional solution.

The results of this research will be applied in future and development of the infrastructure of Czechoslovak towns, especially of the urban networks.

Fig. 1 - General conduit for cabels and pipe lines

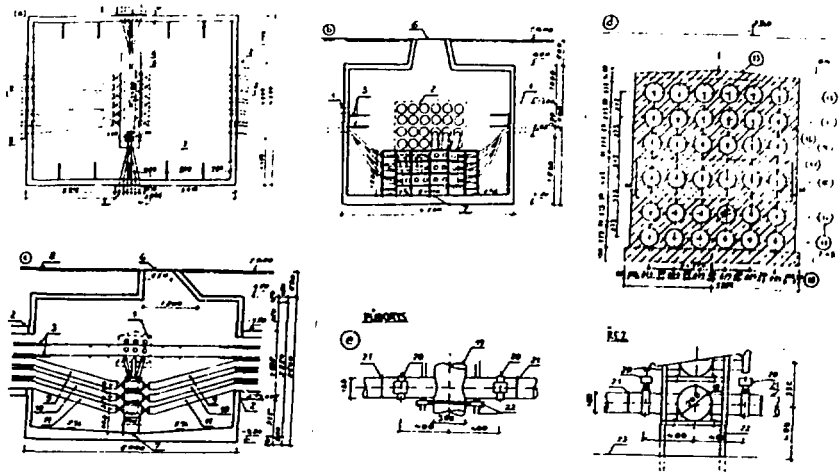

References:

[1] Srytr P. et al: Urban Networks, CTU, 1992, under publishing;

[2] Srytr P., Macek L.: Contribution to the intensification of the operation of the water supply sytem. Proc. Conf. STU, 1989, p. 71-81;

[3] Vávra I. et al: Technological processes of construction of the urban networks, CTU, 1992, under publishing;

[4] Srytr P. et al: Intensification of the water supply systems, CTU, 1989,

[5] Cihakova I. et al: Short term prognoses of water demand. Research report-Faculty of Civil.Eng., CTU, 1990.

This research has been conducted at the Depatrtment of Sanitary Engineering and has been supported by the grant of the Faculty of Civil Engineering, CTU, No. 1141.

ENERGY-SAVING IN THE ARCHITECTURE DESIGN OF BUILDINGS

M.Rejchl and L.Přibyl

Faculty of Architecture, CTU, Thákurova 7, 166 34 Praha 6

Key words: Energy-saving, Architecture Design, Residential buildings, Public buildings

A. Possible energy savings in design, construction and use of residential and public buildings.

a) possibilities b) means for architectural design

1. a) in the sitings of a building or group of buildings.
   b) protected and sheltered position, orientation towards the sun
2. a) in the arrangement of buildings in group.
   b) compact arrangement, buildings acting as barriers
3. a) in the design of individual buildings.
   b) minimalization of the volume of the building, of the mains recycling of energy
4. a) in the design of buildings,ss details
   b) insulation, avoidance of thermal bridges and heat accumulation
5. a) in choosing the main construction materials.
   b) maximum energy savings at optimum cost
6. a) in the production of the construction materials.
   b) minimum consumption of energy
7. a) in the production of the structural elements.
   b) maximum variability, minimum weight
8. a) in the construction of the building and the technical systems.
   b) economical mechanization
9. a) in the working of a building and a group of buildings
   b) the regulation of the system of temperature control day/night, winter/summer, frequent checks of all heating and electrical sources, rationalization of energy-saving measures

B. Thermal and electrical energy gain from relatively constant sources and the storage of this energy.

a) means b) consequences for architectural design

1. a) Fixed solar collectors - panels, lenses, focuses.

b) design and arrangement of spaces for and around this equipment

2. a) Thermal pumps gaining heat from water or the ground.
   b) accumulators increase the space of the building
3. a) Accumulatot walls, tanks, energy storages.
   b) influence on the interior and the layout of the building
4. a) Verandas, greenhouses, winter-gardens, solar conservatory
   b) influence on the form, volume, micro-climate of the building
5. a) Chemical collectors.
   b) inclination of the elements towards the sun
6. a) Photochemical units.
   b) flexible elements, accessibility for cleaning
7. a) Sinking of the building into the ground.
   b) considerstion of light when designing for the site and the window openings
8. a) Covering of the building with greenery.
   b) change of visual perception of the form of the building
9. a) Production of methane from biomass.
   b) special plants around the building
10. a) Exploitation of the dynamics of water-flow.
    b) need for larger and special building
11. a) Exploitation of wind.
    b) siting of rotor in reletion to the building

Survey of the examples on slides

1. Energy-gaining roof of the new building of the Centre of Planing Calculations at the Ministry of Economy of the Czech Republic, Praha 7 Architects: M.Rejchl, J.Pospíšil, A.Blahušek, K.Čermák, M.Perlík - 1982 to 1986 Building plan: Keramoprojekt Praha Realization: IPS Praha 1987-1992
2. Family house for two generations with a solar conservatory in Praha 6 Architect: M.Rejchl - 1986, realization: M.Bajer - 1991
3. Family house for country in Miřetice by Chrudim Architects: V.Řezníčkova, L.Přibyl, Martin Kraus
4. Family house in Žatec Architect: O.Hájek
5. Block of flats in Praha 4 Architect: O.Hájek
6. Linear conductor of light in METRO Praha Architect: P.Kotas

This research has been conducted at the Institut of Building Science Faculty of Architecture with co-operation Environmental Department of the Mechanical Engineering Faculty CTU Research grant of the Czech Technical University No 8003-502

Section 9

ENVIRONMENTAL ENGINEERING

PIXE SYSTEM FOR ENVIRONMENTAL SCIENCE

V. Potoček, Z. Nejedlý

Dept. of Physical Electronics, CTU (Faculty of Nuclear Science and Physical Engineering), V Holešovičkách 2, 180 00 Praha 8

Key words: PIXE, data processing, applications

About ten years ago the PIXE program was introduced at the ion beam laboratory of the Department of Physical Electronics, Faculty of Nuclear Science and Physical Engineering of the Czech Technical University. At present, the PIXE set-up is used in routine analyses and at the same time it is continuously completed with special parts to make it more effective, more accurate and more user-friendly for users.

PIXE (Particle-Induced X-Ray Emission) as an analytical method was first reported in 1970 from Lund, Sweden [1] and since that time it has rapidly grown. It is based on the spectral analysis of the characteristic X-rays emitted from the matter under its bombardment by energetic charged particles, in our case 1.5-2 MeV protons from Van de Graaff accelerator. It is a fast, non-destructive, multi-element and sensitive analytical tool which is almost ideal especially for an elemental analysis of aerosols and some types of biological samples. That is why the PIXE program was inspired with the needs of the Institute of Landscape Ecology of the Czechoslovak Academy of Sciences in mind in its beginning and why it is still directed to the application in environmental and biological science.

The actual state of the PIXE set-up is reported elsewhere [2] because its technical development has been the granted aim in the last several months. Nevertheless, to become a real analytical device, the PIXE system had be also completed with appropriate software and methodology. In 1991 the software for rapid and effective spectra procession and primary data evaluation in the applications for environmental science has been developed. At the same time, the program for data transfer between multichannel analyzer and computer and graphic program for spectra evaluation and presentation have been completed. More then 500 samples were analyzed to calibrate the system, confirm the power of the new software and test some types of analytical methodologies, mainly those suitable for aerosol analysis for air pollution investigation and blood analysis for medical purposes.

Experimental data (i.e. spectra of characteristic X-rays) are stored on floppy disks to be processed off-line. At first they are fitted by the program TROJAX which has been created on the principles of AXIL [3]. This program can process both binary and ASCII data by non-linear least-squares fitting to produce the intensities of separate spectral lines corrected for background, overlapping, pile-up effect and escape peaks. It generates for each spectrum the basic output (BAO file) and optionally also some other files for detailed information about the fitting process and the fitted spectra for the graphic presentation. Some of those optional files can also be generated independently from BAO if it is necessary.

Graphic software RBS4 enables to view, print and plot both binary and ASCII spectra in optional horizontal and vertical scales, colors and shape including 3-dimensional figure. Some simple operations as comparison of spectra, subtraction of a background, energy

calibration and integrals or peak areas determination in selected ranges of interest are also possible.

The BAO files from TROJAX can be directly read as input of the program TROCON. Other input files for this program contain the information about calibration parameters specific for our PIXE set-up, about the actual analytical conditions and about blank samples. These additional input files can be easy created from the old ones with the use of common editor. On the basis of input data and tabled physical parameters, TROCON generates the output files containing the amounts of separate elements either in nanograms per sample (for thin samples) or in relative mass contributions. Other software utilities then serve for their conversion to concentrations (for instance, in nanograms of elements detected in aerosol per cubic meter of the sampled air), for formatting to the presentation tables and to the input files for common presentation software, spreadsheets etc.

The software mentioned above has been completed under substantial influence of the PIXE software used at the University of Gent, Belgium. Moreover, the target holder which had originally been constructed for the samples in slide frames as in the PIXE laboratories in Lund, Sweden, and in Turku, Finland, has recently been adapted to become compatible also with the Gent target holder. It facilitates interlaboratory comparative analyses like those reported about a year ago [4].

The PIXE analytical system at our ion beam laboratory has been proved to be ready for analyses for the purposes of environmental and biological including medical research with good quality. Hundreds of samples per year can be analyzed non-destructively with average number of 10-15 elements detected. The unique feature of our device is the vertical external proton beam which enables the analysis of even liquid samples without drying (suppose the concentrations of elements to be detected are above ppm level). This potential should be turned to advantage.

References:

[1] T.B. Johansson, R. Akselsson, S.A.E. Johansson: X-Ray Analysis: Elemental Trace Analysis at the 10-12 g Level. Nucl. Instrum. Methods 84 (1970), 141

[2] J. Král, J. Voltr, R. Salomonovič, T. Bačíková: Equipment for PIXE Analysis with External Beam. Workshop '92

[3] P. Van Espen, H. Nullens, F.Adams: A Computer Analysis of X-Ray Fluorescence Spectra. Nucl. Instrum. Methods 142 (1977), 243

[4] V. Potoček, R. Brenner, F. Hodík, J. Voltr: Interlaboratory Simultaneous Multielement Analysis of Aerosol Samples from Šumava Mountains. J. Radioanal. Nucl. Chem., Articles 149 (1991), 205

A GIS APPROACH TO NATURAL ENVIRONMENT MAPPING

B. Veverka and L. Soukup

Department of Mapping and Cartography, CTU, Thakurova 7, 166 29 Praha 6

Key words: geographical information system (GIS), computer cartography, ARC/INFO, thematic mapping

In this abstract research activity of the Department of mapping and Cartography in the Czech Technical University is briefly described. The main topic of this research was focused on the creating of the thematic maps by means of GIS technology.

A Geographic Information System is a computerised system for the capture, storage, retrieval, analysis and display of spatial data describing the land attributes and environmental features (e.g. terrain elevation, land form, soil type, vegetation type, etc.) for a given geographic region, by using modern information technology. In recent years, there has been a strongly growing interest in the design of GIS systems, especially in the design of intelligent GIS systems.

Traditionally, a typical GIS system usually consists of three main objects - a data collection subsystem, a database subsystem and last but not least a data application subsystem where computer cartography has a significant role at present.

In Czechoslovakia there are many reasons for the increasing popularity of the use of GIS. Most importantly GIS are seen to be relevant to a huge range of practical management problems involving topographic and thematic spatial distributions. Domestically we have many skillful cartographers, geodesists, geographers, programmers and other professionals who use spatial information, but we still missed the technology specialising in GIS, computer cartography and remote sensing.

This poor situation was rapidly changed during the year 1991, when our Department of Mapping and Cartography acquired a progressive and world-wide known GIS system ARC/INFO. This software system was developed by ESRI (Environmental Systems Research Institute Inc., California, U.S.A.) and was provided for the educational and research needs of department free of charge.

The ARC/INFO system is intended for large computers and workstations, with the PC version being developed there also. The simpliest configuration requires PC AT/286 with math coprocessor and at least 25 Mbyte free space on HD.

The main functions of ARC/INFO are as follows:

- capturing of spatial data: digitizing and graphical editation,
- getting attribute data gaining the database files which consist of descriptional data related to the geographical features. The database files may be gained by creating under ARC/INFO or using existing files in the various formats.
- geographic analysis: composing the stored information to point out the spatialy related events which the user is interested in.
- presentation of the results of the analysis. Firstly, interactively where the situation is displayed on the screen and the user can interactively get the answer for his questions about various geographical features. Secondly, statically where the results of answers are fixed in the form of a thematic map or a tabular report.

All the operations with the system can be given by writing commands on the PC keyboard. More sophisticated operations are possible due to simple programming language SML (Simple Macro Language). It allows the user to create more complex statements and release them in more comfortable menue form.

The 3.4D version of PC ARC/INFO was installed at Department of Mapping and Cartography in April 1991.

The basic functions of the system were tested in the beginning.

In the second stage the devices for capturing and presentating the data were connected by using special in-home tailored software (PASCAL 5.5). Simultaneously a supporting software OCTOPUS was developed for solving of coordinate transformation between source maps and geodetic state coordination system S-JTSK, where map distortion is automatically eliminated.

The digitiser DGZ (ZPA Nový Bor) is used for digitising of source maps in both the on-line or off-line modes.

The Hewlett Packard DraftPro plotter is used for drawing the output maps.

The most crucial third stage covers building the special complex GIS project. The objective of this project is to identify the areas where the risk of groundwater contamination is significant. This project is a cooperative effort with AQUATEST Praha.

Several source thematic maps were digitized to represent the seep properties of the soil and to locate sources of pollution and depths of groundwater level.

The results of this work is a complex of various thematic maps showing total distribution of the groundwater pollution hazard. This complex of analytic and synthetic map will be used for the controlled planning of the water regime in the North Bohemian Region.

Results of the research until now clearly indicate that the GIS technology could be successfully and satisfactory used on a greater scale as a tool within education and research.

Related to this there will be time invested in further development of GIS technology, with the Department of Mapping and Cartography in cooperation with the State Institute for Regional Planning in Prague (TERPLAN Praha) and abroad with the GIS Mapping Section on the Department of Regional Planning of the County of Los Angeles.

This research has been conducted at the Department of Mapping and Cartography in CTU as a part of the research project "GIS - collecting and ellaboration of the localising information for purposes of State Information System" and has been supported by the CTU grant No. 8016.

MODEL OF THE ACIDIFICATION OF THE SURFACE WATER

M. Mach, L. Macek and A. Grunwald

Department of Sanitary Engineering, Faculty of Civil Engineering, CTU
Thákurova 7, 166 29 Praha 6

Key words: acid rain, acid deposition, acidification of water, modelling

The relationship between the acid depositions, the acidification of surface waters and the loss of biological resources has become an important regional environmental issue in our country. The question of whether the pH, acid neutralizing capacity ANC, content of calcium and magnesium, organic matters, heavy metals and other chemical attributes of surface waters have been affected by acidic inputs of antropogenic origin has been extensively reviewed, analyzed and discussed [1,2].

Models of acidification have been developed to evaluate the effects of atmospheric deposition of strong acids on lake watershed systems and surface water quality [3,4]. These models utilize thermodynamic relationships coupled with mass balance and electroneutrality constrains to predict pH and ANC as well as the speciation of Al, F-, SO_4^{2-}, organic matters and organic carbon. We have adopted the IIASA model in our work to predict pH changes in the water reservoir Souš (Protected Region of the Jizera Mountains). A simple IIASA model consists of several moduls e. g. hydrometeorologic, hydropedologic, soil chemistry, and lake response modul. Some of the input data used for the acidification model are listed in Tab. I.

The model of acidification of the surface water was tested using the data for the 1971 to 1986 period. The comparison of measured and computed values of pH are presented in Fig. 1. It can be seen that the presented model can be used as a good tool for prognosis of changes of the water quality in relation to the predicted evolution of acid deposition in specific region. The modelled plot of month averages of pH in the water of the Souš Reservoir shows, that its catchment is undergoing a slow acidification.

Fig. 1

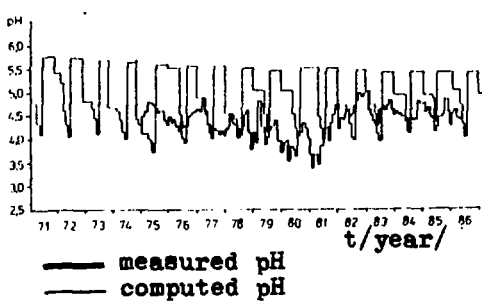

Tab. I Main input data

Area of catchment	m^2	17 542 000
Area of reservoir	m^2	1 020 000
Volume of reservoir	m^3	5 111 000
Soil thickness of layers A,B	m	0.5
Hydraulic conductivity	$m.mo^{-1}$	80
Saturation of soil	-	0.45
Total cation exchange capacity	$keq.ha^{-1}$	95.8
Silicate buffer rate	$keq.ha^{-1}.yr^{-1}$	0.029
Average concentration of SO_2 atmosphere	$\mu g.m^{-3}$	20
Average concentration of SO_4^{2-} in precip.	$mg.l^{-1}$	10

References:

[1] Mach M. et al: Study of the metal content in the waters of the Protected Region of the Jizera Mountains. Arch. Hydrobiol.Beih. 33,1989, p. 339;

[2] Macek L. et al: Model of the influence of acid depositions on the surface water quality, Vodní hospodářství 21, 1, 1991, p. 19;

[3] Johanessen M. et al: Chemistry of snow meltwater. Changes in concentration during melting. Water Resource Res. 14, 1978, 4, p.651-659;

[4] Kamari J., Posch M., Kauppi L: Development of a model analyzing surface water acidification on a regional scale. Proc. Workshop 16, Sept. 1984, Uppsala NHP, Rep. Nordic Hydrological Programmes, Copenhagen, p. 151-171.

This research has been conducted at the Dept. of Sanitary Engin. as a part of the research project "Hydrology of Small Catchment" and was supported by the Czech Hydrometeorol. Institute.

PROTECTION OF WATERS AGAINST URBAN RUNOFF

Z. Koníček and coworkers

Dep. of Sanitary Engineering, CTU, Thákurova 7, 166 29 Praha 6

Key words: Urban runoff, combined sewer system, source control, storm water catch basin, combined sewer overflow

To minimize the impact of combined sewer systems on the recipient two main lines were followed: 1. source control, addressing both water quantity and quality issues, 2. stormwater control of combined sewer overflows.

Source control includes reducing urban runoff flows and pollutant loads before they enter the drainage system. The removal of N compounds from wastewater prior to discharge into the water course is important. The problems resulting from controlled discharge of N-rich wastewater can range from eutrofication in receiving waters to high nitrate concentrations in drinking water, causing methemoglobinemia in infants and cardiac problems in adults [1]. N compounds in liquid exists in two forms: ammonium ions NH_4^+ and disolved ammonia NH_3. The distribution of NH_4^+ and NH_3 is pH dependent according to Eq. 1.

$$NH_3 + H_2O = NH_4^+ + OH \tag{1}$$

Under completely mixed conditions, the following equation is obtained:

$$(1-\beta)dN/dt = QN_0 - QN_e + (1-\beta)V(-KN_e) \tag{2}$$

where N_0 and N_e = influent and efluent NH_3-N concentrations [mgl^{-1}], V = pond volume [m^3], Q = influent flow rate [m^{3}d^{-1}]. The eq. 2. can be rearranged for the removal efficiency

$$N_e/N_0 = 1/[1 + K(1-\beta)\Theta] \tag{3}$$

where K = removal rate [d^{-1}], β = volume of biological sludge/pond volume, and Θ = hydraulic retention time [d].

With the cooperation between EAWAG Zurich and ČVUT the influence of the different sewer designs and their impact on the receiving water was tested. The real catchment of 120 ha (30 ha impervious areas) was chosen. The maximum overflow discharge Qmax of 800 rainfalls was used. The network with the stormwater catch basin (SCB), the network without SCB, and the sewer network without SCB and without water from roofs (infiltrated to the undergrounds) was examined and evaluated.

Because nitrification in SCB was insignificant, the ammonium ions were chosen as an indicator of the pollution. The relation between the inverse value of the flow periodicity p and Qmax is shown in the Fig. 1. The relation between the 1/p and the amount of NH_4^+ has the same form of the curves, and the values for the 1/p = 1 are: network with SCB 3.47 kg, without SCB 3.52 kg, and without SCB and outflow from roofs 3.05 kg of NH_4^+ per event.

The conclusions of the research show that it is necessary to use continual simulation for a lot of historical rains, and to investigate the statistical relationship between the effects (overflowing volume, overflowing discharge, and overflowing pollutants) to be able to design the overflow structures. It is not possible to use statistical rains for this task.

The transport of solid wastes (SW) during stormwater flow in combined sewer is caused by turbulent flow (fluidized SW) and by drag forces (block scour and deposition). Dimensional analysis of hydrodynamic forces acting on sediment particle leads to Shields criterion: $\tau_c/[(Ç_s - Ç)d] = f[(u_* d/\tau)]$, where τ_c = critical shear stress reqired to to induce particle motion , $Ç_s$, $Ç$ = density of particle and water, d = diameter of particle, u_* friction velocity = $\sqrt{\tau_c/Ç} = \sqrt{gRS}$, τ = kinematic viscosity of water, R = hydraulic radius of sewer, S = slope of energy line. The mathematical relationship combining dynamic flow conditions with mass transport are published elsewhere [2]. The hydraulic condition of the steady state distribution of polydispersed suspension in the turbulent flow could be expressed using the theory of Dobbins. Camp expressed sedimentation effect as a function of the particle settling velocity and hydraulic condition of the flow (3):

$$E = f\,[(v_s y)/(2\epsilon), (v_s A)/Q = (v_s l)/(v_t y) = v_s/v_u] \qquad (4)$$

On this mathematical model the storm overflow with the high overflow weir were developed to let the higher concentrations of SW near the bottom flow to the sewage treatment plant. The other system of overflows concentrators (O-C) were developed using the intensification of separating proces in cross-circulation flow conditions. Three types of O-C were tested in the laboratory conditions: The swirl and the vortex O-C are circular tanks with the tangent inlets near the bottom. The floatable material are caught by baffles situated before the peripherial spill weir. The outflow of concentrated wastes is situated on the centre of inverse conical bottom. For the model of helical bend O-C the US-EPA type with transition section invert level , suitable for exploitation of the storage capacity in the sewer network was used.

Fig. 1.

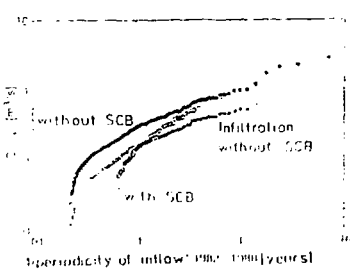

Fig. 2

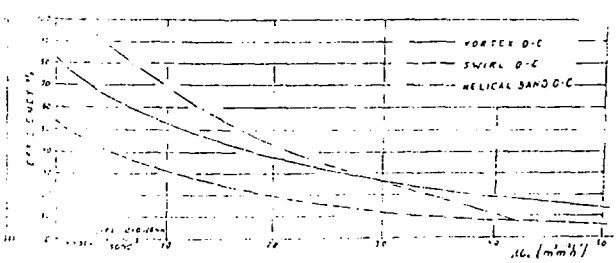

The separation efficiency of all three O-C types related to the hydraulic load of separators are presented in Fig. 2. With respect to the environmental protection the results proved also the great economical effect.

References:

[1] Shin H.K., Polprasert CH.: Ammonia Nitrogen Removal in Attached Growth Ponds, Journ.Env.Eng., ASCE, Aug. 1988., No.4.

[2] Ristenpart E., Wittenberg D.: Hydrodynamic Water Quality Simulation-An Aproximative Solution, Wat.Sci.Tech., Vol.24.,No.6. IAWPRC 1991.

[3] Koníček Z.: Usazovací nádrže, NČSAV, Praha 1956.

This research has been conducted at the Dept. of San.Eng. as a part of the project "ELBE" with the collaboration of EAWAG Zurich, and has been supported by CTU grant No. 8013.

MIGRATION OF POLLUTANTS IN FRESHWATER STREAMS AND SOILS

P.Beneš, K.Štamberg, M.Černík, A.Gosman, V.Spěváčková, D.Vopálka

Department of Nuclear Chemistry, CTU, Břehová 7, 115 19 Praha 1

Key words: Trace elements, radionuclides, migration, natural waters, soils, modelling

Freshwater streams and soils belong to the most important media for transporting and cumulating toxic trace elements and radionuclides and for incorporating these pollutants into food chains. Therefore the migration and speciation of the pollutants in freshwater streams and soils have been extensively studied. In the last decade mathematical models have been frequently used to describe or predict the migration and speciation. Despite the large effort devoted to these problems present knowledge of them is still insufficient for evaluating the effects of the pollutants on human health and the environment. Therefore we conducted research into these fields.

Migration of radiocesium, radiostrontium and radiocobalt has been studied in Dudváh River receiving waste waters from nuclear power plant in Jaslovské Bohunice. Three main approaches have been chosen: laboratory investigation of principal factors affecting the interaction of radionuclides with river sediments, which strongly influences the migration; development of mathematical model suitable for describing the effect of the interaction on the migration; analysis of the migration in the real river.

The laboratory investigation has shown that radiostrontium is adsorbed only very little in suspended sediments in Dudváh River. Much higher adsorption has been found for radiocesium and radiocobalt. The following factors significantly affect uptake and release of radiocesium and radiocobalt: contact time, solid-to-liquid ratio, temperature, composition of sediment, pH of water (only radiocobalt), composition of water (only radiocesium). The effect of the first three factors has to be explicitly included into migration models. For this purpose parameters of two-step kinetics of radionuclide interaction with sediments have been proposed which are suitable for inclusion into the models. The effects of solid-to-liquid ratio and of temperature on the parameters have been determined. The effects of other factors can hardly be described quantitatively and have to be considered in the form of variability of the interaction parameters. Therefore the parameters should be sought by laboratory experiments with repeatedly sampled natural water. This has been done for Dudváh River and a set of interaction parameters was obtained for radiocesium and radiocobalt.

Simple migration model has been constructed, based on the system of stirred reactors representing consecutive sections of a river. The model has been used for analysis and prediction of radiocesium migration in Dudváh River contaminated by accidental release of ^{137}Cs. The model has been calibrated and verified using data on distribution of radiocesium in bottom sediments of the river and in the river water. Satisfactory agreement between calculated and analytical data was achieved for activity of bottom sediments but significant errors were found if instantaneous distribution of radiocesium between dissolved and suspended forms was calculated using year-averaged input parameters for the model.

The study of pollutant migration in soil aims at obtaining a suitable migration model and input data for the model. The data include parameters necessary for description of

the uptake and release of the pollutant by solid phase in soil, dispersion coefficient of the pollutant in soil and speciation of the pollutant in the soil solution and soil solid phase. The study began in 1991 and it has been focused on the migration of lead, radiocesium and radiostrontium.

At first, suitable methods for studying the interaction of the pollutants with solid phase in soil and for measuring their diffusion in soil were sought. Then soil samples from a well characterized forested watershed were taken in collaboration with scientists of the Institute of Applied Ecology in Kostelec nad Černými lesy, who investigate the fluxes of trace elements in the watershed. The samples were characterized by total silicate, mineralogic and granulometric analyses and by determination of their pH and active aluminium. Their contents of heavy metals were determined by atomic absorption spectroscopy after acid leaching.

The samples were used for the study of the uptake of lead by laboratory experiments. Kinetic and equilibrium data for lead sorption on the selected samples were determined using batch reactor technique. The data were fitted with kinetic relations applicable for the so called "unreacted core kinetic model" and with equilibrium (nonlinear) Langmuir type isotherm, whereby kinetic and equilibrium parameters characterizing lead sorption were obtained. Furthermore, dispersion coefficients in the soils and sorption curves for lead were measured in columns filled with the soils. The sorption curves were also calculated using non-equilibrium dynamic sorption model and the parameters obtained from the batch experiments. Rather good agreement between the calculated and experimental sorption curves was found.

The data obtained and models proposed are useful for prediction and interpretation of the migration of radionuclides and trace elements studied in surface waters and soil. They will be used for interpretation of long term monitoring of fluxes of trace elements in the watershed mentioned above. It is desirable that the study be continued and extended to other pollutants.

This research has been conducted at the Department of Nuclear Chemistry as a part of the research projects "Transport of selected radionuclides in the hydrosphere affected by a nuclear power plant" and "Key factors and processes affecting the migration of trace elements and radionuclides in soils and surface waters of selected ecosystems" and has been supported by Czech Technical University grant No. 8050.

DESULPHURIZATION OF FLUE GASSES BY PRESSURE SWING ADSORPTION

I. Roušar, M.Čekal, K. Hoch and P. Ditl

Faculty of Mechanical Engineering, CTU, Technická 4, 166 07 Praha

Keywords: desulphurization, flue gas, adsorption, pressure swing.

The most serious air pollutant in Czechoslovakia is sulphur dioxide, mainly emitted through burning the high sulphur content (up to 10 wt.%) coal. The most common industrially used desulphurization technology is based on a limestone washing. The investment costs of this technology are 5010 Kčs per installed kW in 1991 prices [1]. The present investment costs of a competitive and very promising Bergbau-Forschung adsorption process are 13000 Kčs per kW in 1991 [2].

Classical adsorption processes reguire low temperatures. However, the gas separation process called Pressure Swing Adsorption (PSA) [3] might work even at high temperatures because it requires a low adsorption affinity which some components exhibit at temperatures of 150 to 200°C [4]. At present, most industrial PSA processes operate at ambient temperature and separate components with a low adsorption capacity [5].

This project is devoted to the estimation and evaluation of PSA capabilities to remove sulphur dioxide from the flue gas from 20 MW power station block, which is burning lignite having 5 wt.% of sulphur. This 20 MW block generates 23 m^3/s of flue gasses with the composition of 0.53% SO_2, 11.29% H_2O, 6.16% CO_2 , 76.86% N_2, 4.88% O_2 and 0.92% Ar by volume [6].

The high water content (12 vol.%) is the main obstacle of desulphurization by PSA. The classical adsorbents as synthetic zeolites are not resistant against wet sulphur dioxide. The important zeolite characteristic is the Si/Al content ratio. The adsorbent is stable in a wet sulphur dioxide environment if this ratio is higher than 500.

The choice of a suitable adsorbent was the first step. The two type of adsorbent with the Si/Al ratio of 600 has been experimentally tested. The volumetric apparatus was used to measure the constant of the linear adsorption isotherm at 30°C. The first adsorbent, synthetic zeolite NaZMS-5, takes the value of constant of 1.5 mg SO_2/g kPa and the constant of the second adsorbent, natural zeolite klinoptilolit, is 1.43 mg SO_2/g kPa. These adsorption capacities are not sufficient, because of the adsorbent capacity at the process temperature of 130°C will be low. However, there are still reserves in the adsorbent activation. Further calculations were performed for the adsorbent capacity of 1.43 mg SO_2/g kPa at the temperature 130°C [7].

In the adsorption step three components are adsorbed: water, carbon dioxide and sulphur dioxide. The other components behave as inert gasses. Adsorption is carried out in two columns connected in series. At the end of the adsorption step the first column contains water and carbon dioxide and at the second one carbon dioxide and sulphur dioxide. In the second step the each column is evacuated independently and counter-currently. The evacuated gas from the first column contains 68 mol.% H_2O, 29.1 mol.% CO_2, 0.01 mol.% SO_2 and the gas from the second column consists of 17.5 mol.% SO_2, 40.5 mol.% CO_2 and 39.1 mol.% N_2. The content of SO_2 is proportional to the

sulphur concentration in coal. The gas containing sulphur dioxide has to undergo further processing. One possibility is another PSA unit.

The whole PSA desulphurization unit consists of two vacuum compressors, one blower, two heat exchangers and four adsorption columns with total mass of adsorbent of 48 000 kg. The total investment costs are 130 mil Kčs which means 6500 Kčs/kW [7]. This is comparable to other desulphurization processes. However, it does not leave enough space for solving other problems like clogging of the fixed bed or uniformity of a gas flow through enormously large fixed beds.

This research showed new areas where PSA process can be succesfully employed. Our further research will be focused on desulphurization of output gasses from H_2SO_4 production plant. The dust free and dry gas containing 0.2% SO_2, 11% O_2 and the rest of N_2 can be succesfully treated by PSA processes.

References:

[1] Majer, P. et al.: Economic comparison of the possible alternatives of an electrical energy production in ČSFR, CTU-FEE,Prague, 1999 (in Czech).

[2] Macek, L., Raab, P.: Reduction of Sulphur Dioxide Emission, Prague, 1985 (in Czech).

[3] Skarström, C.W., U.S.Pat. 2,444,627 (1960).

[4] Breck, D.W., Zeolite molecular sieves, John Wiley & Sons, New York, 1974.

[5] Cassidy, R.T. a Holmes, E.S., AIChE Symp. Ser., Vol. 80, No. 233, 68 (1984).

[6] Černý, V. a kol.: Steam boiler and burning facilities, SNTL, Prague, 1975.

[7] Čekal, M., Roušar, I. and Ditl,P., Desulphurization of gas mixtures by PSA, conference CHISA'91, Seč, 1991 (in Czech).

This research has been conducted at the Department of Chemical and Food Process Equipment Design, Faculty of Mechanical Engineering CTU as a part of the research project "Desulphurization of Flue Gasses by Pressure Swing Adsorption" and has been supported by Czech Technical University grant No.8027.

ENVIRONMENTAL POLLUTION PROBLEM BY XRFA

T. Čechák

Faculty of Nuclear Sciences and Physical Engineering, CTU, Břehová 7, 115 19 Praha 1

Key words: X-Ray Fluorescence Analysis, Aerosol Samples, Environmental Problems

X-Ray Fluorescence Analysis (XRFA) is now a technique suitable for measurement and control of environmental pollution.The features of XRFA method, such as almost no sample preparation, simultaneous analysis of many elements in the sample, short analysis time, and nondestructive analysis procedure are just what is required for routine measurements of hundreds of environmental pollution samples. The chemical composition of the atmospheric aerosol together with its particle size distribution play key roles in determining air pollution effects. For example, the health hazard associated with airborne particles depends on the deposition size in the lungs, which is related to particle size, shape, density, and chemical composition. The paper presents some results of measurements and application from the point of view of environmental pollution. The particulate fraction of the atmosphere typically includes, in addition to dust of natural origin and smoke, trace amounts of compounds containing heavy elements. It is well known that a number of heavy elements are toxic at certain concentrations, but there is great uncertainty about their toxicity at the levels present in the atmosphere. These questions will only be answered through further research on the toxicology of heavy elements and by expanding the scope of air monitoring programmes to permit systematic surveys of heavy elements level. Air pollution studies in Czechoslovakia have been limited untill now. Only SO_2, NO_x and dust content are monitored. It is necessary to search quick and cheap method for determination such elements as As, Br, Pb etc.

In seeking a relatively uncomplicated and reliable method we have paid special attention to thin film procedures. The thin film approximation lays down limits within which inter - element interferences may be discounted. Within these limits we find that R_i, the fluorescent beam intensity for element i, is proportional to w_i, the mass/area for element i. A simple estimate of the limit of infinite thickness of a sample can be determined by assuming that primary beam is monochromatic. Then the relationship R_i that is proportional to w_i, holds within 1% provided that

$$1 - e^{-uw} \geq 0.99\, u\, w \qquad (1)$$

where $u = (u_p \operatorname{cosec} \tau_1 + u_s \operatorname{cosec} \tau_2)$, and w = mass/area of the sample. Here, u_p = mas absorbtion coefficient for the wave length of primary beam, u_s = mass absorbtion coefficient of the sample for the fluorescent wave lenght, τ_1 = angle between incident beam of radiation and the surface of the sample, τ_2 = take off angle of the fluorescent radiation.

The limiting condition for w is given by

$$u\, w_{lim} = 0.02 \qquad (2)$$

where w_{lim} is the limit of infinite thickness of the sample. This equation was a useful working rule for estimating w_{lim}. In the present investigation it was used to determine the limits for heavy element particulates and for filter material.

Samples of air particulates were collected as the solid deposit on SYMPOR7 filter paper by Institute of Hygiene and Epidemiology. Suspended particulate samples were measured directly from the filter paper on which they were collected. These were intended for the qualitative determination of various elements and the quantitative determination of part of them.

Standards were prepared by absorbing solution of known content on filter papers. These were evaporated to dryness. Filter paper of a thickness of the sample was chosen in order to minimalize possible absorbtion differences.

Two sources: 370 MBq ^{238}Pu annular source embedded in Sn hausing and Mo X-Ray tube was used for purpose of this work to excite characteristic X-Ray in the samples. A lithium drifted silicon diode was used for the detection. The energy resolution FWHM for K_α Mn was 175 eV. Typical spectra of different elements in ambient air sample contain the peaks of S, K, Ca, Cr, Mn, Fe, Ni, Cu, Zn, As, Pb, Br. The measured amounts of calcium are large in comparison with other Europian cities. The high level of iron may be due mainly to activities of the industry. Lead and bromine are usually associated with traffic activity. Other trace elements such as Zn, Mn, Ca, Ni, Cu are found in quantities characteristic of pollution arising from industrial activities. As content is believed to be associated with high content of As in some of our sorts of coal.

Detection limits depend on the type of the source and for the osotopic source on its activity. The detection limits based on 2σ statistics was for our apparature about $\mu g/cm^2$ (it depends on Z). Table 1 illustrates the amount of elements occuring in a representative air polution sample.

Table 1

Concentration ranges of elements occuring in a representative air pollution sample

Element	Concentration ranges $\mu g.m^{-3}$
Fe, K	10^2 - 10^5
Na, Zr, Br, Ni, Pb	10^2 - 10^4
Cr, As, Hg	10 - 10^2
Se, Sb, Co	1 - 10

All these elements can be determined by the XRFA method.

The aim of the work was to show the usefulness and versatility of the XRFA method in solving different environmental problems. Though the accuracy of XRFA is not as good as that of the widely-used atomic absorbtion, XRFA gives results without troublesome sample preparation and in a much shorter time. In Czechoslovakia, in the situation where only a few elements and oxides are monitored the XRFA method can widen the number of the elements to be measured.

LASER INDUCED FLUORESCENCE SPECTRUM OF CONIFERS

P.Gavrilov, A.Jančárek, V.Krajíček, J.Nováková and M.Vrbová

Faculty of Nuclear Science and Physical Engineering, CTU, Břehová 7, 115 19 Prague 1

Key words: Laser, fluorescence, luminescence, spectrum, plant vigor, conifer, environment, remote sensing, distant measurement

Spectral properties of the ultraviolet laser induced fluorescence (LIF) can be used for remote measurements of vegetation or other environmental object characteristics [1]. LIF allows one either to identify specific plants and minerals, to estimate the plant vigour or to judge the concentration of various polutants.

Our aim is to develop a method of use of the LIF for the airborne monitoring of forest vigor. For this purpose we have studied fluorescence spectral patterns of coniferous twigs under different conditions.

The fluorescence was induced by pulsed excimer laser radiation of energy of hundreds of millijoules in ten nanosecond pulses fired with repetition rate up to 50 Hz. The spectral analysis was done by a dual grating spectrometer equipped with a photomultiplier (with S20 photocathode). The experiments (laser trigger and grating position) were controlled by a computer. The laser pulse energy and fluorescent yields were measured and stored in the computer memory for each laser shot. All the experiments were done in a dark optical laboratory with samples (twigs) fixed to a stand on the optical bench. The detailed description of our experimental set-up was published recently in [2].

We would like to present here our current observations of spruce and pine LIF spectra, see Fig.1. The samples (twigs) were picked up from the young trees grown in the vicinity of our university building (north outskirts of Prague), on November 29th, 1991.

It is known [1],[2] that the fluorescent spectra of conifers induced by ultraviolet pulses and measured in the spectral range from 350 to 800 nm show three broad peaks at 450, 540 and 740 nm. The relative amplitudes of these peaks are different under different conditions, namely the amplitude ratio of the first to the second peaks, reflects the living activity of the sample.

Authors of [1] compared two different measurements with red Canadian spruce grown under different environmental conditions and ascribed the lower value of the peak ratio to the influence of acid rains in the appropriate region.

We have observed the decrease of the relative first peak amplitude during the experiments we performed. Consequently, the peak ratio decreases with the increasing time interval from the moment when the twig was broken off the tree. As it is seen from the Fig. 1 the amplitude of the first peak becomes approximately 1.4 times lower after 2.5 (3) hours for both spruce and pine tested. These measurements were repeated under different levels of the sample exposition from 1 to 50 mJ cm^{-2} and the results were reproducible.

Referring to our previous measurements [2] done in the summer of 91 we come to a conclusion the detailed shape of the LIF spectrum is not identical in summer and in winter. Further calibration measurements are needed.

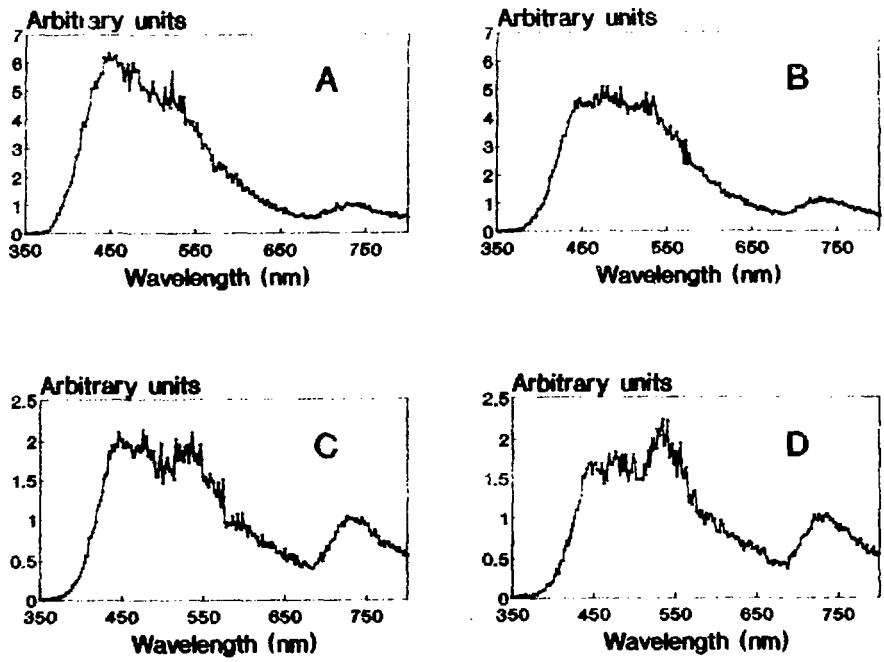

Fig. 1: Fluorescence spectra of coniferous twigs induced by XeCl laser (308 nm) measured with different time delays since being broken off; A - spruce, 1 hour delay, B - spruce, 2.5 hour delay, C - pine, 0.5 hour delay, D - pine, 3 hour delay

The theoretical interpretation of the effects observed is not plausible and is tightly correlated with the understanding of the dynamics of assimilation.

References:

[1] E.W.Chappelle, D.L.Williams, R.F.Nelson, J.E.McMurtrey, Laser Focus World, June 1989, p.595-600.

[2] P.Gavrilov, A.Jančárek, V.Krajíček, M.Svoboda, M.Vrbová: Laser Induced Fluorescence Spectrum of Spruce, European Quantum Electronics 27-30th August 1991, Edinburgh, U.K.

This research has been conducted at the Department of Physical Engineering as a part of the research project "Methods of applications of excimer lasers" and has been supported by the Faculty of Nuclear Science and Physical Engineering grant No: 4009.

DEVELOPMENT OF THE INFORMATION SYSTEM FOR MONITORING OF THE HYDROSPHERE IN CZECHOSLOVAKIA

E. Zeman, M. Kemel et. al.

Department of Civil Engineering, Division Hydraulics and Hydrology
Thakurova 7, Prague 6, Dejvice

Environmental care in the light of the recent development in Europe is regarded as one of the priority areas of cooperation among European countries. A smoothly functioning monitoring system enabling each of these countries to gain and evaluate all the necessary information, not only for taking measures on the local level but also for conveying information to neighboring and other involved European countries, is the fundamental precondition of fulfilling the above-mentioned task. Consequently, these systems should be compatible and should attain approximately the same technological standards in order to come up to the same degree of efficiency. Czechoslovakia ranks among those countries whose information system concerning the state of environment is considered to be far from advanced and, to a large extent, imperfect.

The present level of the air and water pollution in Czechoslovakia has created rapidly-growing national concern on environmental issues, that are further strengthened by international obligation and liabilities on cross-boundary water quality.

The present Czechoslovak Government is fully aware of its responsibility for resolving this unsatisfactory situation and has recently initiated activities aimed at catching up with the advanced European standards in the above area of monitoring individual environmental components as soon as possible.

To get a reliable picture on the development in time and space of all involved parameters affecting the human environment, an *Integrated Environmental Information System* for our country will be developed. The monitoring of the quality and quantity of the hydrospheric parameters plays a vital role in the stated activity. An adequate hydrological monitoring system is a prerequisite for proper planning, design and management of the human environment.

The main objectives of the monitoring system of the hydrosphere are :

1. real time data for
   - water management
   - flood protection and flood handling
   - navigation
2. regime data for
   - planning and preparation
   - design and maintenance

The hydrological monitoring systems in Czechoslovakia are run at the state level by the Czech and Slovak Hydrometeorological Institutes respectively. The systems cover the collection, transfer, processing and presentation of water quality and quantity data. Their activity includes forecasting of parameter changes due to the human impact.

The increased ecological awareness together with changed economical objectives and conditions have created differences in demands on the monitoring systems and will need reassessment of its objectives. The need for the value and cost of data may change. This results in consequences for types of parameters to be monitored, their measuring locations and frequency, data storage and processing and a new approach to hydrological methodology. In the future much more attention has to be given to the monitoring of aquatic systems in real time to register and/or record calamitous states and trends in our environment.

The accessibility of data is dependant on the system of storing and processing. The present data bases are rather rigid; the data are stored in 22 separate registers in Czechoslovakia. Those data are not mutually interlinked.

The working team at the Division Hydraulics and Hydrology deals with a database *HYMOS* that was recently developed in the Institute Delft Hydraulics. The first steps in preparation of a new methodology for data processing during the first year of the international project "Development of the information system for monitoring of the hydrosphere in Czechoslovakia" were taken. The software tools for data transformation into new database were developed. Based on suggestions given by members of research team a few elements of the Hymos database were changed and prepared for our specific condition. Several inputs were given to our partners concerning new approaches in handling the data.

The pilot basin (Otava) was selected and constant equidistant series were successfully converted into the system using the database. The longest time series being currently measured were statistically tested using *HYMOS* . A trend of time series was discovered in one or two cases but it was considered that most of the tested time series are independent. Cooperation with tools of *Hydroinformatics* (simulation tools for forecasting purposes) were tested and possible linkage with the Hymos database was considered.

All the above-mentioned activities are in line with the international project that is supported by both the Czechoslovak and the Netherland's governments. The international cooperation involves research and development activity on most of the elements of the ČSFR monitoring systems for the hydrosphere. Phase 1 of the project has already started this year. The pilot basins were selected. The cost-effectiveness analysis of the proposed monitoring systems has to be currently carried out on the Ohře and Otava river basins.

All works on the projects have been conducted at the Division of Hydraulics and Hydrology as a part of an international project. The transfer of the advanced technology from the Netherland has given an unique opportunity to the research group to be involved in the HI-TECH development. The activity of the group will contribute directly to the improvements in the environment, that might be seen within a period of a few years from now.

Section 10

POWER ENGINEERING

ECONOMICAL COMPARATION OF POSSIBLE POWER STATIONS IN ČSFR

Majer P., Handlíř K., Starý O.

The Department of Economics and Management of Power Engineering, Faculty of El. Engineering, CTU, Technická 2, 166 27 Praha 6.

Key words: economy, electrical energy, levelized production costs, power stations, fuel, investment, inflation, escalation of costs

All possible types of power generation plants, which can be built in ČSFR in the years 2000 - 2010, have been rated by using modern methods of economical analyses. This study has been ordered by the federal Ministry of Economy as one of the studies used to prepare the new governmental energy policy. The principal object of the study is to choose an economically optimal strategy from all available options with respect to new economical relations and privitization projects in the field of energy. The evaluation also includes ecological requirements.

The working team used the long-term research program currently operating at the department and an application of the UNIPEDE method. This is the same method which is used by industrialized countries and international power supply institutions. The basic principle of the method is in discounting costs which have been expended in different times. The criterion value is the levelized production costs. These costs are evaluated as a rate of discounted sums of all costs spent for construction, exploitation and dismantling and the discounted sum of the annual production of electrical energy.

First, the computation was made under a condition of constant macroeconomical inputs during the entire working period (computation in constant money). Second the dynamic features were implemented to the model, especially the escalation of costs and inflation.

The authors took into consideration all possible technologies which can be used in the future development of a power supply. Special attention was paid to the ecological requirements. The involved technologies are: nuclear power stations of world and European standards, advanced coal power stations with desulfurization and denitrification, combined gas cycles and cycles with gasification of coal. Also, possibilities and constrains of small gas engines were proved especially for the combined production of heat and electricity. Peripherally the authors explored possibilities of small water power stations in comparison with sources of big power supply.

The extent of the problem and the amount of the mathematical operations required using a computer. The program was developed using the spreadsheet QUATTRO PRO version 3.0. The program was written in a user-friendly format. This program is interactive and allows easy control of computation and also provides a great deal of sensitivity analysis. The program should be a powerful tool for top managers in ministries and power supply institutions.

The applied methods will work with a variety of organizational structures or as a way of privatizing power supply. The method is utilized in a market economy for basic information about the relative economical optimality of the project. This is the first step of the "feasibility study".

From the all considered options the most profitable is a nuclear power station in a based loading. The option of constructing an imported nuclear island with some of the world's best known companies (for instance ABB, Westinghouse or Siemens) and constructing the rest of the power station in cooperation with domestic companies is the best choice from the all nuclear options. This choice can also significantly help to solve the environmental problems in the region.

The most economically suitable option for covering top loading in the electrical grid (loading up to 3000 hours per year) is a combined gas cycle.

Under our circumstances due to the burning poor brown coal classic coal power stations have to be equipped with expensive ecological equipment . Their economics results are then relatively worse.

The conclusions were also confirmed by extended sensitivity analyses. Levelized production costs as a function of discount rate, load factor, exchange rate of CS koruna and US dollar and economic life were analyzed . Neither escalation of costs and fuel prices nor inflation changed results.

The results of the study were compared with similar studies of the French company Cogena and of the power supply division of the German company Siemens. The method and also the numeric outputs are fully in correspondence. Also the customer confirms the correspondence with similar foreign studies.

This research has been conducted at the Department of Economy and Management of Energy as a part of the research project "Economical comparation of possible power stations in ČSFR in the period 2000 - 2010" and has been supported by a grant of Federal Ministry of Economy.

IMPLEMENTATION OF MARKETING IN ENERGY SYSTEM

J. Zavřel and J. Knápek

Department of Economics and Management of Power Engineering, Faculty of Electrical Engineering, CTU, Zikova 2, 166 27 Praha 2

Key words: Marketing, Energy Systems, Ecology

In wider continuities marketing is understood as a kind of business philosophy. Some authors expound marketing as a comprehensive system that can explain human relations of all social systems and that appears to be a universal theory of human behavior. In market economies the so-called non-commercial marketing is generally implemented in private hospitals, museums, theatres and universities.

The above-outlined broader conception of marketing offers a sufficient number of incentives for the improvement of work and general accessibility of energy system problems to vast masses of population. The need for the implementation of marketing methods in the energy system does not result from the necessity of the struggle for customers but rather it results from the moral obligation towards the surrounding world.

Thus, for example, the Upper Austrian Power Joint-Stock Company (OKA) in addition to power generation also deals with development and publicity of energy saving programs and environment protection programs (the development of an electromobile, thermal pumps, utilization of non-conventional energy sources etc.). As a whole its activity can be described as offering complex services to the customers.

The task of publicity for the energy system is not product promotion but it aims at the work concerned with the general public, i.e.offering information on current objects of the energy system and its political, national-economy and business roles, as well as, for example the construction of new power plants, possibilities of purposeful energy utilization, environment protection, chances for non-convential energy sources and last but not least energy savings.

At present one of the most significant problems in the CSFR consists of the negative impact of the energy system (and its individual subsystems) on the environment. The decision-making process concerned with further development of the energy system must issue from the condition of "sustainable development" as well as the necessity of system approach towards the functioning of the energy system as a whole (respecting all relations of the energy system to the society and environment). At the same time it is necessary to create conditions for the general public acceptability of a selected strategy of the development of the energy system (particularly from the point of view of the environmental protection). In this field the marketing methods could be fully implemented.

Molding public opinion must issue from an objective scientific analysis of complex system impacts on the environment arising from the generation and consumption of a given energy form.

The substance of such a system approach consists in an effort to cover all negative impacts on the environment originating in the whole chain of generation and final consumption of a given energy form (e.g. electricity). In a simplified way this chain can

be understood as a series of consecutive energy processes from the primary energy sources gaining, through the generation of a given energy form, to its final consumption.

In the current situation of the ČSFR it is necessary to ensure the general acceptance of the energy system development. For this reason it's necessary to work out not only the complex system analysis of the negative environmental impacts resulting from the individual energy forms generation and utilization but also to use the appropriate marketing methods towards public opinion.

This proposal was made on the base of the suggested project for the year 1992.

ENERGY INFORMATION SYSTEM FOR EFFICIENT USE OF ENERGY

J. Dudorkin, V. Mařík*, B. Melichar*, V. Skurovec*, B.Duchoň*, J.Maroušek** and others*

* CTU, Faculty of El. Engineering, Technická 2, 16627 Prague 6
* The Energy Efficiency Center, Slezská 9, Prague 2

Key words: Energy saving and conservation, energy economy, environment, information systems, expert and knowledge systems.

Information concerning energy efficient technologies and measures, their environmental impact and their economical and financial evaluation is very dispersed in Czechoslovakia and difficult to obtain. This information is neither unified nor stored electronically. Data for the EIS are of a diverse quality - numerical, textual, graphical and audio-video data types are all used.

Difficulties in accessing this information obstructs implementation of energy efficient and environmentally clean technologies and obstructs progress in environmental protection in CSFR and its transition towards a modern economy.

Energy Information System (EIS) consists of information about energy efficient technologies and measures suitable for CSFR. Each technology and measure will have a unified description, environmental impact assessment and economical and financial evaluation and will be classified for easier future retrieval.

Targets of EIS-design and EIS-implementation are to accelerate and to enable the large implementation of advanced energy saving technologies, the mapping of appropriate energy saving potential and finally to improve through this system of the environmental protection in CSFR.

The EIS and its research covers the entire energy chain starting from the discovery of primary energy sources, through energy production (conversion) and transport and ending by final energy use. Complex multiobjective evaluation of energy-efficient technologies is based on careful systems analysis and synthesis and on approved methodological approaches.

The research covers an area of large information systems including multimedia databases and is focused on the use of artificial intelligence and the design of an expert or knowledge system. The fast and rational retrieval of information in EIS will be grounded on the hypertext retrieval approach with the key words and text fragments search possibilities. Free public access to the EIS is planned for at least two years.

Design and implementation of EIS is closely connected with different problems of optimal hardware configuration, data protection, networks and telecommunication architecture etc.

The research in 1992 is divided into the following parts:

1. Systems analysis and decomposition of the energy chain technologies area - discovery, production, conversion, storage, transport, distribution and use of different kinds of energy.

2. Methodology of complex evaluation of energy saving technologies from technical, economical and financial, social and environmental point of view.
3. Data model for unified description of energy efficient technologies with classification, codes etc.
4. Design of the architecture of a knowledge (expert) system for fast and user-friendly retrieval of information in multimedia bibliographic databases with heterogenous data.
5. Comaparative analysis of available national and international energy information systems and possibilities of connection. Technical aspects of EIS (networking, data protection etc.)

Focused results in 1992:

- Research report including EIS decomposition and systems analysis, information strategy of EIS development, technology and saving potential assessment methodology, data model, design of expert system architecture, comparative analysis of other EIS.
- Trial data base implementation for test case technology.
- Model description of representative energy efficient technologies.

Final result: Fully automated and integrated Energy Information System with user-friendly, rational and fast access in all of Czechoslovakia.

Supposed users: Governmental and Nongovernmental organizations, enterprises, companies, interested persons. Results are also supposed to be widely used in education at all levels.

Multidisciplinary research team was created initially by the staff from three departments of CTU:

1. Dpt. of Energy Economy and Management,
2. Dpt. of Control Engineering - Group of Artificial Intelligence and
3. Dpt. of Computer Science.

Participants in the team are: 2 Full Professors, 8 Associate Professors, 8 Assistant Professors, 6 Ph.D-students and 1 researcher. The team is fully qualified and has a vast experience in the above-mentioned problem areas (main implemented projects: Information system about Secondary Energy Sources and Appropriate Equipment for Federal Bureau of Statistics, expert system FEL-EXPERT, CAD-system TEPRO, computer networks for Faculty of Electrical Engineering).

The success in multidisciplinary research of EIS is based on large co-operation with other departments of CTU and with other institutions outside CTU, namely with the nonprofit agency SEVEn (Agency for Efficient Use of Energy) and by FAW Linz. The research is supposed to be continuously supervised by CS Federal Energy Agency.

CTU has free access to the supercomputer IBM 3090 (courtesy IBM) which is located in the CTU headquarters and is connected with the national and international computer network. Proposed research of EIS is a multidisciplinary research task in the area of energy savings, environmental protection, large information systems and artificial intelligence.

This research is conducted in the Department of Energy Economy and Management as a research project and hopes to be supported by the grant of the Czech Technical University for the year 1992.

COMPLEX CONTROL OF POWER SYSTEMS

J.Tůma, K.Pospíšil, J.Dudorkin, V. Skurovec, R. Povýšil

CTU, Technická 2, 16627 Praha 6

Key words: control of power system, environment, optimization, optimal power flow, multiobjective programming,.

The European continent is polluted with about 60-70 mil.t of gas mixtures every year and more than 90% of this amount represents the emissions of SO_2 and NO_x produced in coal-fired power stations. ČSFR takes part in this pollution with about 3 mil.t of SO_2 and 1 mil.t of NO_x. In our case the high level of gas mixtures are caused mainly by the structure of primary energy resources and by the excessive consumption of energy in all parts of national economy. More than 60% of electrical energy is produced in coal fired power stations and the coal used is of very poor quality.

The main goal of the optimal dispatching's: to meet all needs of consumers of electrical energy with maximal economy at all times; it is therefore necessary to comply with greater respect to ecological conditions. This is especially important during the most adverse meteorological situations, when the average 24 hours levels are higher than for 150 $\mu g.m^{-3}$ SO_2 and 100 $\mu g.m^{-3}$ for NO_x.

The methodology of solving optimal dispatching in power systems is collectively called Optimal Power Flow. For our purpose we decided to start with the OPF method based on Newton-Raphson approach. This method is formulated quite universally and it is possible to include all needed network elements and limiting conditions and at the same time it uses specific conditions of power systems in such a way that it is fully usable even for large power systems with large number of elements. The classical OPF deals with function of operational costs, such as the cost of active power or active losses in the transport of electrical energy. The system conditions and types of controls which the method must be able to accommodate include active powers of generators, transformer tap settings and phase shifter angles. Solution of OPF is formulated as a solving of a big (hundreds to thousands of equations) system of nonlinear equations, expressing the connections between power injections and bus voltages. This system of nonlinear equations can be replaced with two systems of linear equations, which can be solved iteratively with respect to all operating conditions applying for the network and the whole power system.

The need to take into account the adverse ecological effects brings changes into existing methods. In all cases it is necessary to keep the following basic rules.

- The balance of production and consumption of electrical energy must be kept even if production of some sources is forcibly decreased due to its adverse environmental impact.
- All technical constraints in the power system must be kept.
- The governmental rules for levels of emissions must be complied with.
- The method must provide give a possibility to change its objective function accordingly to the various conditions in the power system and to the meteorological conditions and predictions.

The knowledge of trade-off relations among conflicting economical and ecological objectives and knowledge of increased environmental marginal costs due to improved ecological impact are very important for operator and computer dispatch. It leads to the solution of a more complicated multiple objective dispatching problem: Minimization of total operating costs and minimization of total emissions under conditions of supply and demand balance, power output limits, emissions limits etc. The use of different approaches to the solution of this problem (penalty method, goal programming etc.) was studied. Further introduction of limits on ground level concentrations at defined locations or grid points needs a sophisticated and calibrated diffusion model (eg. Martin-Tikvart).

For the solution of so complex task for real power system in a reasonably short time with respect to stochastic character of the problem, the supercomputer IBM 3090 is used (courtesy of IBM under Academic Initiative). It enables very large simulation experiments using the Monte Carlo approach and detailed area modelling.

Task outlined in this article cannot be finished in one year. We suppose that it will take at least three years till the end product - practically usable methodology and software package-will be used in optimal control of the power system of ČSFR. In the year 1991 we have finished those steps:

- Study of accessible literature. We have prepared a large list of articles, mainly from internationally-accepted sources like IEEE-PAS or IEE Transactions. It seems that the theme is interesting, but up to now there are only a few approaches of this kind.
- Algorithmisation of the task. First approximation of algorithms used in the task is prepared.
- Load Flow model of power system. Full algorithm and computer program for necessary calculations of electrical networks is prepared and tested.
- Production and emission curves of main types of generators used in the power system of ČSFR are compiled and prepared for algorithmization.
- Method for optimization is selected. The methodology OPF (Tinney, Walker at all), modified with respect to ecological needs will be used. All the necessary modifications are prepared and now we are in the process of programming them.

This research has been conducted at the Department of Production and Transport of Electrical Energy and at the Department of Energy Economy and Management of Faculty of Electrical Engineering as a part of the research project "Complex control of Power Systems" and has been supported by Czech Technical University grant No.8038.

DECISION MODELS IN ENERGY SYSTEMS

V. Skurovec, J.Dudorkin, B.Duchoň

CTU, Faculty of Electrical Engineering, Technická 2, 16627 Prague 6

Key words: Energy Systems, Decision Support Systems, Investment Management, Optimization, Modelling, Databases

Combination of basic parts (dialogue management unit, data management unit and model management unit) into coherent, user-oriented and user-friendly decision support system (DSS) applied for decisions in energy fields is the main aim of the project. Connection of DSS units with parts of rule-based expert systems should extend the possibilities of these systems.

DSS will be created as modular architecture system (offering model techniques from different areas) enabling easy knowledge representation, knowledge extraction from real data, communication etc.

DSS will be prepared for real decision situations in energy systems (investment decisions, project evaluation, environmental protection, energy policy making etc.) based on analysis of user needs.

The principal target is to create a modern Decision Support Systems based on sophisticated software packages and mathematical models for managerial and educational purposes with applications in energy and power systems, electrical industry and education.

The research in the area of DSS in Department of Energy Economy and Management began some years ago. Created software products for Decision Support Systems were produced on PC computers in the Department during the last few years (programs for investment analysis, operations research, statistics etc.). These software products can be judged as a part of future DSS.

For prepared DSS it is possible to use research and scientific results gained in the area of Expert Systems by the Faculty of Electrical Engineering (knowledge representation, rule-based systems and uncertainty processing, knowledge acquisition, common-sense reasoning etc.). A family of rule-based diagnostic expert systems was also developed.

On the basis of successfully experiences in divers fields of applications it is possible to extend them to the area of energy and power systems and electrical industry. Parallels will be extended into implementations of several real applica- tions for Computer Aided Instruction purposes.

There are several expected gains of the research:

1. Development of useful DSS for scientific, educational and commercial purposes.
2. New scientific progress in the area of DSS and expert systems.
3. Incorporation of the research and educational groups from the Czech Technical University into similar groups in European countries and establishing close contacts among Universities and Companies from West Europe and the Czech Technical University in Prague (TU).

The activities in the future will be oriented towards the problems of a market economy. This competition environment influences the decision process of investors,

project engineers and customers (flexibility of demands, problems of financial resources etc.).

The author of the proposal was a member of team that solved the DSS problems in the past . The members of mentioned team presented a series of research works, articles and contributions in Czechoslovak and international magazines and at conferences.

Results of this project will be useful for project, investment and engineering and financial organisations and will be broadly used in educational field and will be connected to other systems (ecological, social, decision etc.).

This research is conducted in the Department of Energy Economy and Management as a research project and will be submitted for Czech Technical University grant consideration for the year 1992 æ

Section 11

ENERGY SAVING

ENERGY SAVINGS IN RESIDENTAL AND PUBLIC BUILDINGS

R. Nový and co-workers

Faculty of Mechanical Engineering CTU, Technická 4, Praha 6 Department of Environmental Engineering Department of Thermal and Nuclear Power Plants

Key words: energy saving, heating, ventilation

The energy consumption of our country, per unit of manufacture and per head of population, is amongst the highest in the world. A significant part of this goes into heating and ventilation of buildings. The present work is aimed at reducing energy requirements of heating systems.

The energy consumption for heating in time T, can be described as

$$E = eta \int_0^T \frac{Q_N \epsilon}{(t_i - t_e)_N} .(t_i - t_e) dT \tag{1}$$

where Q_N represents the total thermal loss of a building for a standard temperature gradient through the building envelope. Generally, the thermal loss at any moment of time can be expressed as a function of the average heat transfer coefficient k, the envelope surface, the thermal capacity of internal spaces, the size and number of windows, the length and quality of window joints or intensity of ventilation, the heat gains of the outer walls, the wind effects, the outer and inner temperatures etc.

Mathematically, the required heating capacity can be expressed as

$$Q = Q_0 + dQ \tag{2}$$

where Q_0 is the capacity at some steady - state, standard conditions under specific thermal conditions, the thermal load must change by dQ, given by partial differentials

$$dQ = (\frac{\partial Q}{\partial x_1})dx_1 + (\frac{\partial Q}{\partial x_2})dx_2 + ... + (\frac{\partial Q}{\partial x_n})dx_n \tag{3}$$

where x_1 to x_n are the above - mentioned conditions affecting the thermal state of the building. This method was used to evaluate the individual effects on the overall energy consumption in heating of buildings. Leaving aside the effects of insulation properties of the envelope surface, a problem currently studied by the civil engineering faculty, we can list the individual effects in the order of their importance, i.e. according to their absolute effect on the overall energy consumption.

The most serious is the problem of air infiltration into buildings and the thermal losses it causes, which in the recently built houses represents 20 - 30 % of the total thermal losses. The calculation methods for infiltration losses according to ČSN (Czechoslovak Standard) do not correctly shaw the actual situation. A new methodology was created therefore, to determine experimentally the infiltration losses directly in the field. This alows realatively accurate extimates of the level of thermal losses due to infiltration.

Another direction of research must be the stochastic effects of wind on the buildings, in realtion to the pressure distribution inside. This would improve the estimate of overall

infiltration of specific buildings under certain meteorological conditions. To carry out an experiment, it will be necessary to build a low - velocity aerodynamic tunnel.The dynamic changes in thermal conditions, caused by weather changes, have to be included in the mathematical models of heated building, where heat accumulation plays an important role. A solution to this problem is vital in relation to the control curves of a heating systems.

When additional insulation is applied, the existing heating systems will be seriously over - designed. It is, therefore, important to investigate this effect in relation to the overall efficiency of a heating system and, if necessary, to re - design the system.

Any new heating systems should be flexible, i.e. consist of components able to respond to rapid thermal changes in the surroundings. This necessitates research into dynamic properties of heating systems, particularly heat sources, pipeworks and heating radiators. The development of heating surfaces should follow this direction too. That would require creation of conditions for experimental work and testing of any newly - developed heating surfaces. The utilization of cheaper sources of energy will require further research in heat pumps for heating and air - conditioning and in effective ways of storing heat.

The research work carried out at the Department of Environemntal Engineering, in particular the design of one - pipe horizontal systems, shows the ways of distribution of heat meters in each apartment. This would greatly improve the interest of individuals in heat saving. The work on the so - called relative meters shows that these are not accurate and reliable. It has been shown that only about 30 particular unit can be detected that way.

In ventilation of residential buildings, heat recovery is much more effective in saving energy. Until recently, ventilation of apartments had been limited to local air extraction from the kitchen and the toilet. New findings in the area of "sick buildings" show that, in addition to the need for forced ventilation of residential spaces and when infiltration is reduced, it is necessary to equip any new apartment by an efficient ventilation system which would achieve hygienic limits of pollutants, as with radon and formaldehyde resin. In this respect, it will be necessary to develop new ventilation systems of low energy requirement which incorporate heat recovery.

This research has been conducted at the Department of Environmental Engineering as a part of a research project under the same name and has been supported by Czech Technical University, grant No. 8003.

ENERGY SAVINGS IN CIVIL ENGINEERING BUILDINGS

J. Witzany and cooperating group

Czech Technical University, Faculty of Civil Engineering
Thákurova 7, Praha 6, PSČ 166 29

Key words: energy consumption, energy savings, energy consumption optimization, choice of optimum building structures properties.

The starting point for energy savings considerations is to find the optimum strategy how to change the contemporary structure of energy consumption to get the model of its optimum distribution.

The quantitative analysis of contemporary energy losses are to be taken into consideration.

The following task is to propose a group of technical arrangements to decrease energy consumption via both new energy saving building methods applied to new building structures and/or complementary building adaptations applied to contemporary buildings.

The complex problematics of energy consumption in buildings during their service life is being solved through the grant "Energy savings in civil engineering buildings".

This problem is being solved from the point of view of interaction between particular building systems and subsystems taking into account the energy consumption.

The term energy service life consumption is in this case understood as the amount of energy necessary to insure required internal environment amenity.

The particular elements (technical means) that in collection determine the amenity of an internal environment are:

- heating system
- warm water supply
- air conditioning system
- artificial lightning
- recuperation and regeneration installation systems.

Its own building structure is the factor that has essential influence upon the selection process of components that insure the internal environment amenity.

The problem of an interaction between building structures and particular components from the point of view of an optimum energy consumption seems to be basic.

Relation and interaction between internal and external environment seems to be unomitable too.

The research of this interaction especially involvesan internal environment with a respect to type of building structures and technical means.

The solution is focused to choice of optimum properties and design of building structures, especially on:

- optimum thermal inertia of internal structures
- optimum thermal inertia of covering structures
- optimum thermal incomes of a building

and on choice of optimum technical means for internal environment amenity.

The solution involves possibilities of utilization of so-called non-traditional resources of energy in our conditions as well.

The estimated output of the task is going to determine criteria, boundary conditions and solution of optimization methods for optimization of energy consumption of buildings during their service life.

This research has been conducted at the Czech Technical University of Prague, Faculty of Civil Engineering, as a part of the research project "Energy Conservation" and has been supported by CTU grant No 8003.

Sborník příspěvků pracovního semináře ČVUT WORKSHOP 92, vydán nákladem 400 ks,
vydavatel ČVUT, vytisklo ediční středisko ČVUT, leden 1992, neprodejné.